Design and Synthesis of Novel Quinazoline-based EGFR kinase Inhibitors and Dual EGFR/NF-κB Inhibitors as potential anti-cancer drugs with enhanced efficacy

Dissertation

zur Erlangung des Grades
des Doktors der Naturwissenschaften
der Naturwissenschaftlich-Technischen Fakultät III
Chemie, Pharmazie, Bio- und Werkstoffwissenschaften
der Universität des Saarlandes

von
Master-Pharmazeut
Mostafa Mohamed Mostafa Hamed
Saarbrücken
2013

Tag des Kolloquiums: 13.08.2013

Dekan:	Prof. Dr. Volkhard Helms
Berichterstatter:	Prof. Dr. Rolf W. Hartmann
	Prof. Dr. Ashraf H. Abadi
Vorsitz:	Prof. Dr. Claus Jacob
Akad. Mitarbeiter:	Dr. Jessica Hoppstädter

Diese Arbeit entstand unter der Anleitung von Prof. Dr. R.W. Hartmann in der Fachrichtung 8.2 Pharmazeutische und Medizinische Chemie der Naturwissenschaftlich-Technischen Fakultät III der Universität des Saarlandes von Juni 2010 bis Juli 2013.

Acknowledgements

I would like to express my sincere gratitude to Prof. Dr. Rolf W. Hartmann, for giving me the opportunity to prepare my thesis as a member of his research group. His endless support has been a great help during these years.

I am deeply indebted to Prof. Dr. Ashraf Abadi, for partly suggesting the point of the research, constructive supervision, great support and valuable advices throughout the whole work. His guidance helped me all the time, I will always be grateful for that.

I am deeply grateful to Dr. Matthias Engel, for partly suggesting the point of the research, valuable guidance during the lab work, fruitful discussions, writing of scientific papers, and the endless support during these years.

I would like also to acknowledge Prof. Dr. Dalal Abou El Ella for the suggestions and help during the chemistry work.

I like to thank Prof. Dr. Gary Piazza, Dr. Adam Keeton and their group for performing part of the cellular assays.

I wish to thank also Dr. Jennifer Hermann for the help with some biological assays.

I would like to thank Nadja Weber and Tamara Paul for their great help and assistance in performing the biological tests, Dr. Joseph Zapp for the NMR measurements, Dr. Stefan Boettcher for running the mass experiments, Dr. Wolfgang Fröhner for the help during the chemistry work.

I would like to thank Mohammad Abdel-Halim, Ahmed Saad, and all the members of Prof. Hartmann group for their help and support.

I also wish to thank the laboratory staff, especially Martina Schwarz, Katrin Schmitt and Lothar Jager for their sympathy and their pleasant service.

Finally, I would like to thank my family, especially my mother, wife and my children for their support.

Abbreviations

$(CD_3)_2CO$	deuterated acetone
µM	micromolar
Abl	Abelson murine leukemia viral oncogene homolog
AKT	v-akt murine thymoma viral oncogene homolog
ALK	anaplastic lymphoma kinase
aPK	atypical protein kinase
AR	amphiregulin
ATP	adenosine triphosphate
BAFF	B-cell activating factor
Bcl-2	B-cell lymphoma 2
BSA	bovine serum albumin
BTC	betacellulin
CAMK	calcium/calmodulin dependent protein kinase
CD_3OD	deuterated methanol
$CDCl_3$	deuterated chloroform
CDKs	cyclin-dependent kinases
cGMP	cyclic guanosine monophosphate
CK1	casein kinase 1
CLK	CDK-like kinases
CML	chronic myelogenous leukemia
Cys (C)	cysteine
DM	double mutated (T790M/L858R) EGFR
DMEM	Dulbecco's modified Eagle's medium
DMF	dimethylformamide
DMSO	dimethylsulfoxide
DTT	dithiothreitol
DUB	deubiquitinating enzymes
EDTA	ethylenediaminetetraacetic acid
EGF	epidermal growth factor
EGFR	epidermal growth factor receptor "also named ErbB1"
ePK	conventional protein kinase
EPR	epiregulin
FADD	fas-associated protein with death domain
FBS	fetal bovine serum
FGF	fibroblast growth factor
GFP	green fluorescent protein
GIST	gastrointestinal stromal tumor
GPCR	G protein coupled receptors
GSK	glycogen synthase kinase
GTP	guanosine triphosphate
HB-EGF	heparin-binding EGF-like growth factor
HER (ErbB)	Human Epidermal Growth Factor Receptor
Hz	hertz

IAP	Inhibitors of apoptosis
IC_{50}	half maximal inhibitory concentration
IKK	IκB kinase
IL-1β	Interleukin-1 beta
IκB	Inhibitors of κB
JAK	janus kinase
JAMM	JAB1/MPN/Mov34 enzymes
Km	Michaelis constant
Lys	lysine
mabs	monoclonal antibodies
MAP	mitogen-activated protein
MAPK/ERK	mitogen-activated protein/extracellular-signal-regulated kinases
Met (M)	methionine
MHz	megahertz
MJD	Machado Joseph Disease proteases
MOE	molecular operating environment
MOPS	3-(N-morpholino)propanesulfonic acid
MTT	thiazolyl blue tetrazolium bromide
MVB	multivesicular bodies
NEMO	nuclear factor-kappa B essential modulator
NF-κB	nuclear factor kappa-light-chain-enhancer of activated B cells
NGF	nerve growth factor
NIK	NF-κB-inducing kinase
nM	nanomolar
NMR	nuclear magnetic resonance
NRTKs	non-receptor tyrosine kinases
NSCLC	non-small cell lung cancer
OUT	otubain proteases
PBS	phosphate-buffered saline
PDB	protein data bank
PDGF	platelet-derived growth factor
PDGFR	platelet-derived growth factor receptor
PDHK	pyruvate dehydrogenase kinase
PI3K	phosphoinositide 3-kinase
PIKK	phosphatidylinositol 3-kinase-related kinase
PKA	protein kinase A
PKC	protein kinase C
PKG	protein kinase G
ppm	part per million
PTKs	protein tyrosine kinases
PTMs	posttranslational modifications
RAS	rat sarcoma viral oncogene homolog
RET	rearranged during transfection
RGC	receptor guanylate cyclases
RHD	Rel homology domain

RIO	right open reading frame
rt	room temperature
RTKs	receptor tyrosine kinases
SDS	sodium dodecyl sulphate
Syk	spleen tyrosine kinase
TEA	triethylamine
TGFα	transforming growth factor alpha
Thr (T)	threonine
TK	tyrosine kinase
TKIs	tyrosine kinase inhibitors
TKL	tyrosine kinase-like kinases
TNF	tumor necrosis factor
TNFR	tumor necrosis factor receptor
TNF-α	tumor necrosis factor alpha
TRADD	tumor necrosis factor receptor type 1-associated death domain
TRAF2	TNF receptor-associated factor 2
TRAF3	TNF receptor-associated factor 3
Ub	ubiquitin
UBC	ubiquitin-conjugating enzyme
Ubl	ubiquitin-like
UCHs	ubiquitin C-terminal hydrolases
ULPs	Ubl-specific proteases
UPS	ubiquitin/proteasome system
USPs	ubiquitin specific proteases
VEGF	vascular endothelial growth factor
VEGFR	vascular endothelial growth factor receptor
Wt	wild-type

Abstract

The inhibition of signal transduction pathways, e.g. of EGFR kinase signaling, is a proven strategy in the treatment of cancers with several drugs clinically approved. Treatment with EGFR inhibitors suffers some limitations such as that certain cancers are originally insensitive or mutations emerge that cause drug resistance. The NF-κB pathway is also known to play a role in cell proliferation and survival and therefore, the inhibition of the NF-κB activation could be used in the treatment of cancer. Herein, a new class of quinazoline derivatives have been designed and synthesized to realize two strategies to overcome the above mentioned drawbacks. The first strategy included structural modifications which resulted in compounds that retain potency towards mutant EGFR. In addition, several compounds were identified to be more potent than Gefitinib towards cancer cell lines with wild-type and mutant EGFR. The second strategy involved the synthesis of compounds with dual inhibitory activity towards the EGFR and the NF-κB pathway. These compounds act as potent anticancer agents that are able to overcome the problem of cancers which are insensitive or resistant to the EGFR inhibitors. Several derivatives were obtained with enhanced potency towards both targets. The main structural requirements essential for activity for each target has been identified and the cellular mechanism of action was discovered for one of the potent compounds. The presented inhibitors open up new approaches to overcome the limitations associated with clinically approved EGFR inhibitors.

Zusammenfassung

Die Hemmung von Signaltransduktionswegen, z.B. der EGFR-Kinase-Signalweges, ist eine bewährte Strategie für die Krebstherapie und hat bereits einige klinisch zugelassene Medikamente hervorgebracht. Die Behandlung mit EGFR-Inhibitoren stößt oft an ihre Grenzen, so sprechen z.B. nicht alle Tumore an und einige werden aufgrund von Mutationen resistent. Der NF-kB-Signalweg spielt ebenfalls eine wichtige Rolle bei Zellproliferation und –überleben, so dass er ebenfalls ein vielversprechender Angriffspunkt bei Krebs sein könnte. In dieser Arbeit wurde eine neue Klasse von Chinazolinderivaten entworfen und synthetisiert, um zwei neue Strategien zur Überwindung der o.g. Nachteile umzusetzen. Die erste Strategie zielte auf die Einführung von Modifikationen ab, die auf eine Steigerung der Hemmaktivität gegenüber mutierter EGFR-Kinase abzielten. Dieses Ziel wurde erreicht, und zusätzlich wurde im Vergleich zu Gefitinib eine potentere Hemmung des Wachstums von Krebszellen mit Wildtyp- und mutierter EGFR-Kinase beobachtet. Die zweite Strategie beinhaltete die Synthese von Derivaten mit dualer Hemmwirkung sowohl auf den EGFR- als auch auf den NF-kB-Signalweg. Diese neuen Verbindungen versprechen eine gesteigerte Anti-Tumor-Wirkung und sind möglicherweise in der Lage, auch die gegen reine EGFR-Inhibitoren unempfindlichen oder resistenten Tumore zu bekämpfen. Einige Derivate mit verbesserter Wirksamkeit bei beiden Targets konnten entwickelt werden. Die wichtigsten strukturellen Voraussetzungen für die Aktivität bei jedem Target konnten identifiziert und der zelluläre Wirkmechanismus für eines der Derivate nachgewiesen werden. Die vorgestellten Inhibitoren könnten neue Wege zur Überwindung der eingeschränkten Wirksamkeit der bisherigen EGFR-Hemmstoffe aufzeigen.

Table of Contents

1 Introduction

1.1 Kinases

A kinase is a type of enzyme that catalyze the transfer of phosphate groups from high-energy donor molecules, such as ATPs to specific substrates, a process referred to as phosphorylation.[1, 2] Kinases are part of the larger family of phosphotransferases which is a subclass of transferases.[2] Kinases are used extensively to transmit signals and control complex processes in cells. One of the largest groups of kinases is protein kinases, which act on and modify the activity of specific proteins. Various other kinases act on small molecules such as lipids, carbohydrates, amino acids, and nucleotides, either for signaling or to prime them for metabolic pathways. Kinases are often named after their substrates.[1, 3]

1.2 Protein Kinases

A protein kinase is a kinase enzyme that catalyze the transfer of the γ phosphate of a purine nucleotide triphosphate (i.e. ATP and GTP) to the protein substrate[4] (Figure 1)[5]. Protein kinases mediate most of the signal transduction in eukaryotic cells and also control many other cellular processes, including metabolism, transcription, cell cycle progression, cytoskeletal rearrangement and cell movement, apoptosis, and differentiation. Protein phosphorylation also plays a critical role in intercellular communication during development, in physiological responses and in homeostasis, and in the functioning of the nervous and immune systems.[6] They are among the largest families of genes in eukaryotes[6-10] with more than 500 members within the human genome.[3, 6] Mutations and dysregulation of protein kinases play fundamental roles in human disease, therefore, protein kinases is a very attractive target class for therapeutic interventions in many disease states such as cancer, diabetes, inflammation, and arthritis.[11] Accordingly, targeting the protein kinases could be used successfully in disease therapy[3, 6, 11, 12] with over a hundred different protein kinase inhibitor already entered clinical trials.[13]

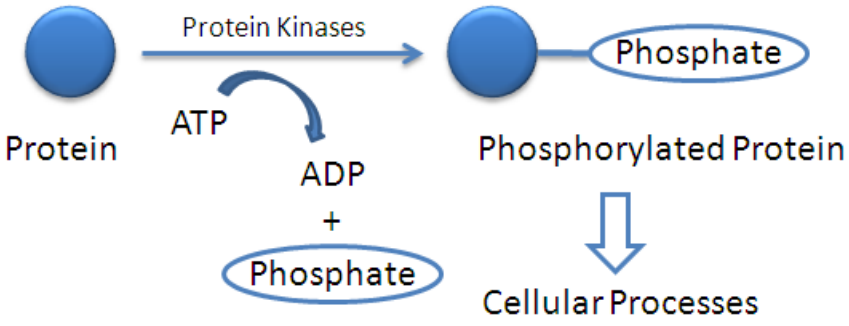

Figure 1: Protein phosphorylation (taken from Ref.[5]).

1.2.1 Protein Kinase Groups

The protein kinases are generally classified depending on the receiving amino acid of their substrates into serine/threonine or tyrosine or dual substrate kinases.[14] Also, the eukaryotic protein kinase superfamily could be split into two groups: "conventional" (ePK) and "atypical" protein kinases (aPKs). The largest group are the ePKs which have been further sub-classified into 8 groups by examining sequence similarity between catalytic domains, the presence of accessory domains, and by considering any known modes of regulation[15] (Figure 2)[8].

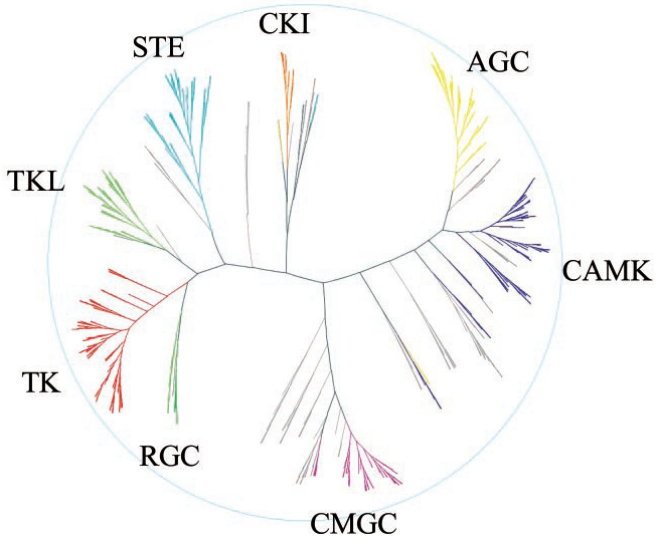

Figure 2: Conventional protein kinase groups (taken from Ref.[8])

1.2.1.1 Conventional Protein Kinases

The 8 ePK groups are:[15]

i) **AGC:** Named after the Protein Kinase A, G, and C families (PKA, PKC, PKG).[16, 17]

ii) **CAMK:** Best known for the Calmodulin/Calcium regulated kinases (CAMK) in CAMK1 and CAMK2 families, this also has several families of non-calcium regulated kinases.[17, 18]

iii) **CK1:** Casein kinases are named after the use of casein as a convenient substrate for experimental examination of kinase activity. The CK1s represent a typically small but essential ePK group found in all eukaryotes.[19]

iv) **CMGC:** The CMGC including cyclin-dependent kinases (CDKs), mitogen-activated protein kinases (MAP kinases), glycogen synthase kinases (GSK) and CDK-like kinases (CLK) are an essential and typically large group of kinases found in all eukaryotes.[20-23]

v) **RGC:** Receptor Guanylate Cyclases. This small group contains an active guanylate cyclase domain, which generates the cGMP second messenger, and

a catalytically inactive kinase domain, which appears to have a regulatory function.[24]

vi) **STE:** The STE group includes many protein kinases involved in MAP kinase cascades, transducing signals from the surface of the cell to the nucleus.[17, 25]

vii) **TK:** Tyrosine Kinase (TK) group members phosphorylate tyrosine residues specifically and so are different from dual specificity kinases which phosphorylate serine/threonine as well as tyrosine.[26, 27]

viii) **TKL:** Tyrosine kinase-like kinases are serine-threonine protein kinases named so because of their close sequence similarity to tyrosine kinases.[28, 29]

ix) **Other:** This group consists of several families, and some unique kinases that are clearly ePKs but do not fit into the other ePK groups.

1.2.1.2 Atypical Protein Kinases

The aPKs are a small set of protein kinases that do not share clear sequence similarity with ePKs. To date, four groups of aPKs have been shown to display protein kinase activity,[15] and these groups are:[6, 11]
alpha,[30] PIKK (phosphatidyl inositol 3-kinase-related kinases),[31] PDHK (pyruvate dehydrogenase kinases)[32] and RIO (right open reading frame).[33]

1.2.2 Protein Kinase Inhibitors

Protein kinases have now become the second most important group of drug targets, after G-protein-coupled receptors, and this increased the interest in developing orally active protein kinase inhibitors.[11]

Small-molecule inhibitors of protein kinases typically prevent either autophosphorylation of the kinase or subsequent phosphorylation of other protein substrates.[13] Protein kinases have well formed binding sites for adenosine triphosphate (ATP), the phospho-donor for the phosphorylation of protein substrates, and this contributed to their high druggability.[13] In the beginning, the discovery of small molecules that inhibit protein kinase through targeting the ATP site was criticized regarding their ability to achieve cellular potency and target selectivity.[13] The first argument was that the inhibitor at the ATP binding site would not be able to potently block the protein kinase activity and signal transduction due to the ineffective competition against the high intracellular ATP concentration.[13] This was based on the fact of the great intracellular concentration of ATP (around 1-2 mM), whereas most protein kinases have affinities for ATP in the 10-300 μM range.[13] The second argument was the difficulty of development of a selective ATP-competitive inhibitor due to the overall sequence homology for the amino acid residues within the kinase ATP binding sites.[13]

Development of the first protein kinase inhibitors took place in the early 1980's and they were naphthalene sulphonamides such as N-(6-aminohexyl)-5-chloro-1-naphthalenesulphonamide (W7).[11, 34] These derivatives were already developed as

antagonists of the calcium-binding protein calmodulin, and were also found to inhibit several protein kinases at higher concentrations.[11] It was seen that replacing the naphthalene ring by isoquinoline caused the derivatives to lose their calmodulin antagonistic activity, while retained the protein kinases inhibitory activity such as in compound "H8" (Figure 3).[11] Fasudil hydrochloride (Figure 3) is an isoquinolinesulphonamide that progressed to human clinical trials in the early 1990s although being of relatively low potency and inhibit several protein kinases.[11]

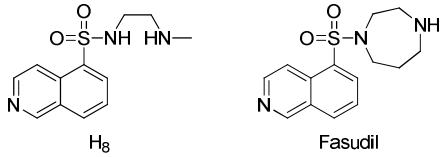

Figure 3: Isoquinoline derivatives as protein kinase inhibitors

The bisindolyl maleimide derivatives have been of great interest after the discovery that staurosporine (Figure 4)[13] was a nanomolar inhibitor of PKC.[11, 35] Staurosporine is a natural antifungal agent that is produced by bacteria of the genus Streptomyces. Although, several bisindolyl maleimides were shown to lack specificity, and inhibited several other protein kinases,[36, 37] yet some have progressed to human clinical trials.[11] Other staurosporine-derived kinase inhibitors that are in clinical testing include 7-hydroxystaurosporine (UCN-01; Figure 4) and N-benzoyl staurosporine (PKC412; Figure 4).[11, 13]

Other examples of natural products that are potent inhibitors of protein kinases include the alkaloid the flavonoid rohitukine,[13, 38] the purine olomoucine,[13, 39] and their structurally related cyclin-dependent kinases inhibitors flavopiridol[13, 40] and R-roscovitine[13, 41] (Figure 4).[13]

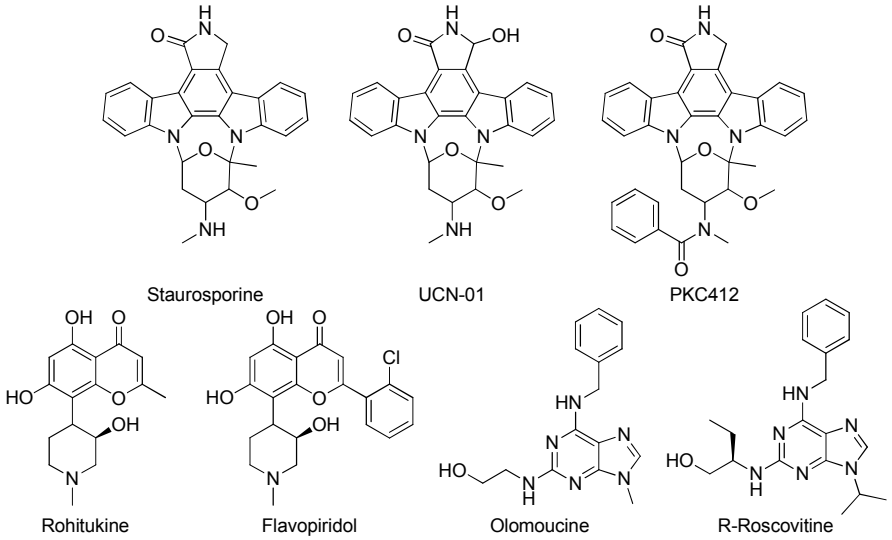

Figure 4: Natural product based protein kinase inhibitors.[13]

To date, thirteen small-molecule therapeutic protein kinase inhibitors have been FDA approved within the US[4] (Figure 5). All are indicated for the treatment of oncological

diseases. These compounds can be generally classified depending on the protein kinase that they target which include BCR-ABL fusion protein kinase (an oncogene for chronic myeloid leukemia), EGFR (human epidermal growth factor receptor tyrosine kinases),[13] VEGFR (vascular endothelial growth factor receptor tyrosine kinase), ALK (anaplastic lymphoma kinase), B-Raf and JAK (Janus kinase) (Table 1).[4] Some of the compounds also inhibit other kinases in addition to those described above (Table 1). Understanding of how these drugs bind to their target kinases has facilitated their discovery and many other kinase inhibitors in clinical development.[13]

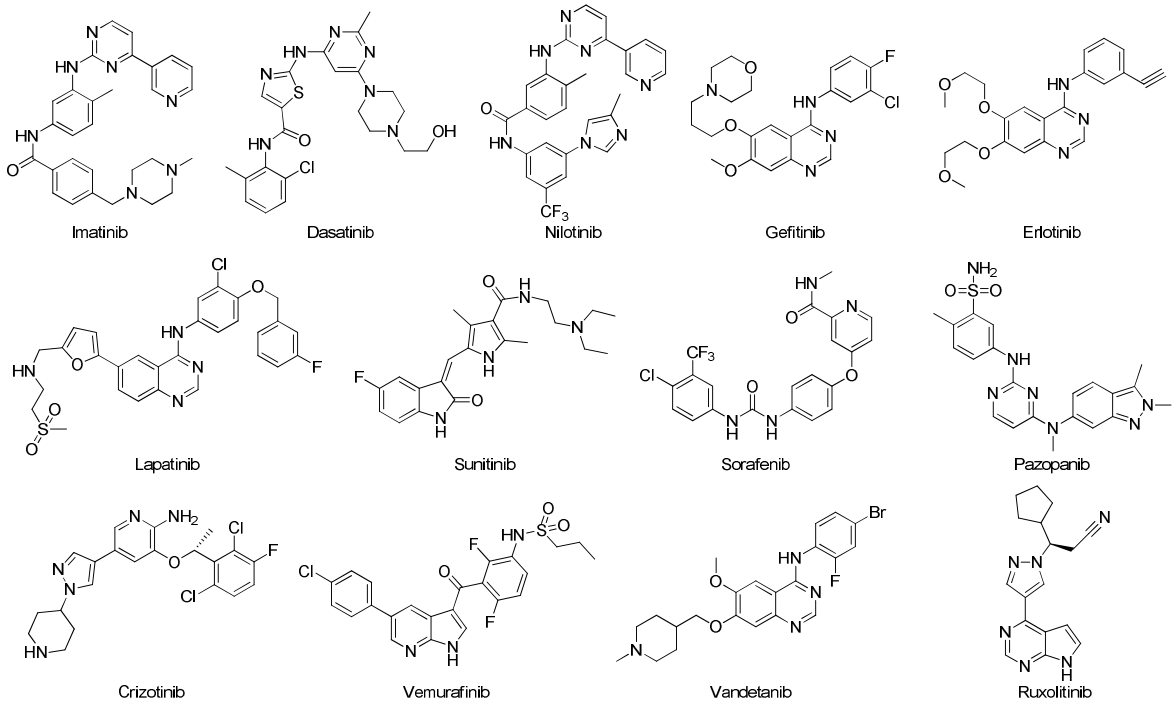

Figure 5: US FDA-approved, small-molecule protein kinase inhibitors.

Table 1: US FDA-approved direct kinase inhibitors by competing for the ATP-binding pocket.[4]

Agents	Target for therapeutic activity	US FDA-approved indication
Imatinib	BCR–ABL, PDGFR and KIT	CML and GIST
Dasatinib	BCR–ABL	CML
Nilotinib	BCR–ABL	CML
Gefitinib	EGFR	Non-small cell lung cancer
Erlotinib	EGFR	Non-small cell lung cancer and pancreatic cancer
Lapatinib	EGFR and ErbB2	Breast cancer
Sunitinib	VEGFR2, PDGFR and KIT	Renal cell carcinoma, GIST, pancreatic cancer
Sorafenib	VEGFR2 and PDGFR	Renal cell carcinoma and hepatocellular carcinoma
Pazopanib	VEGFR2, PDGFR and KIT	Renal cell carcinoma
Crizotinib	ALK/c-MET	Non-small cell lung cancer
Vemurafenib	BRAF	Melanoma
Vandetanib	VEGFR-2, EGFR, and RET	Medullary thyroid cancer
Ruxolitinib	JAK1/JAK2	Myelofibrosis

1.2.3 Classification of Protein Kinase Inhibitors

Small-molecule protein kinase inhibitors can be categorized into three classes according to their binding mode: type I, type II, and type III.[42-45]

1.2.3.1 Type I inhibitors:

Type I inhibitors are ATP-competitive compounds targeting the ATP binding site in the active form of a kinase. Type I inhibitors bind to the hinge region through at least one hydrogen bond donor or acceptor group (Figure 6).[45, 46] Although, type I inhibitors usually face problems to achieve high selectivity yet some selectivity is gained by targeting the hydrophobic back pocket whose access is controlled by the gatekeeper residue. Examples of marked drugs which are type I inhibitors include gefitinib, erlotinib, sunitinib, and dasatinib (Figure 5).[45]

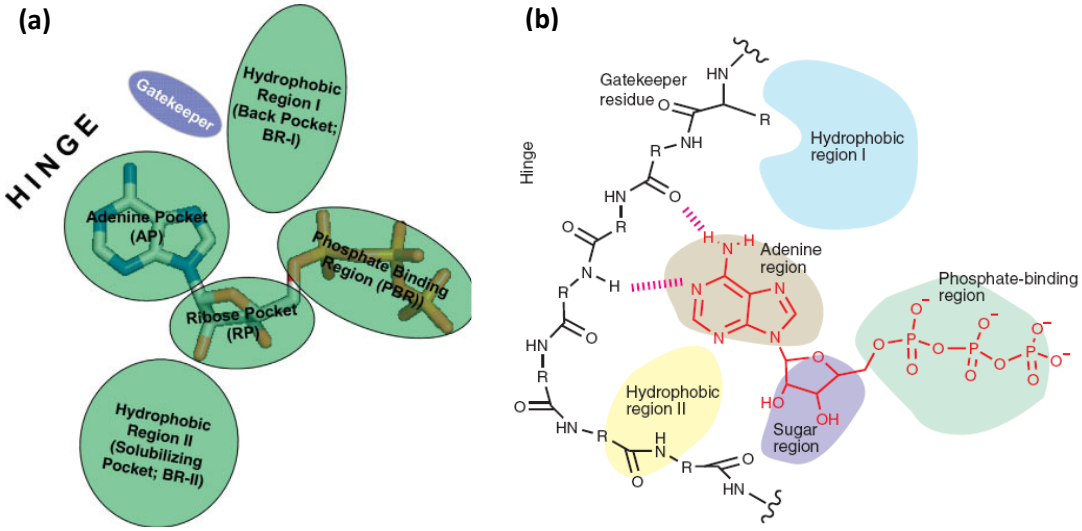

Figure 6: (a) Pharmacophore model for type I inhibitors shown with ATP in the PKA binding site (PDB 1ATP) (taken from Ref.[45]). (b) Schematic representation showing the binding of ATP to the hinge region and the ATP binding site divided into subregions (taken from Ref.[44]).

1.2.3.2 Type II inhibitors:

Type II inhibitors are ATP-competitive compounds which also target the ATP binding site but in the inactive form of a kinase. Binding to the hinge region in type II inhibitors is not essential.[47] All type II compounds target an extended hydrophobic deep pocket created by conformational changes in the protein which is not available in an activated kinase (Figure 7).[45]

Type II inhibitors can achieve higher selectivity than type I compounds, since the deep pocket is only known so far in few kinases. A type II inhibitor can act as type I inhibitor in another kinase, such as with imatinib which acts as a type II inhibitor of Abl kinase, and as a type I inhibitor for Syk.[48] Examples of marked drugs which are type II inhibitors include imatinib, sorafenib, and nilotinib (Figure 5).[45]

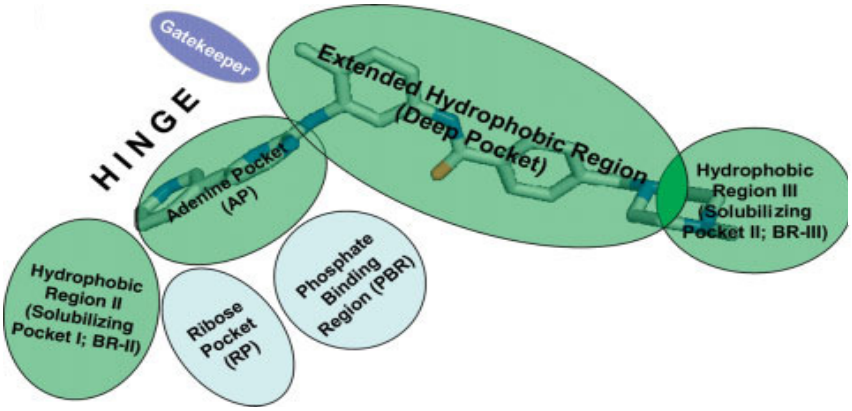

Figure 7: Pharmacophore model for type II inhibitors shown with Imatinib (Figure 5) in the binding site of Abl kinase (PDB 1IEP) (taken from Ref.[45]).

1.2.3.3 Type III inhibitors:

Type III inhibitors are allosteric inhibitors which are not ATP-competitive since they bind to binding sites that are far from the ATP binding site. Type III inhibitors bind to the kinase despite its activation state and don't target the hinge region.[45] High selectivity and potency is expected with type III inhibitors due to the high specificity of the allosteric sites for a certain kinase. Only few examples of type III inhibitors are known since only few kinases may have allosteric binding sites.[45, 49-51]

1.3 Protein Tyrosine Kinases

Protein tyrosine kinases (PTKs) are a class of enzymes involved in tyrosine phosphorylation through the transfer of the γ-phosphate of ATP to tyrosine residues on protein substrates.[52, 53] PTKs activity is essential in multiple cellular signaling pathways that are responsible for critical functions in the cell such as growth, proliferation, migration, synthesis and apoptosis.[52] Tyrosine phosphorylation modulates enzymatic activity and creates binding sites to be engaged in downstream signaling proteins. The cells include two classes of PTKs which are the transmembrane receptor PTKs and the nonreceptor PTKs.[53]

1.3.1 Receptor tyrosine kinases (RTKs)

Receptor tyrosine kinases (RTKs) are cell surface glycoproteins which play an important role in transmitting the extracellular signal to the cytoplasm.[52, 53] RTKs require binding of their cognate ligands to be activated.[53] The activation takes place on two stages; the first stage involves a dimerization of the receptor leading to conformational changes. This is followed by tyrosine phosphorylation on the receptors themselves (autophosphorylation).[52] These processes will further initiate a cascade of phosphorylations which activate successive proteins until the signal reaches the nucleus leading to the expression of the specific genes[52] (Figure 8)[54]. Several fundamental cellular processes are controlled by RTKs including cell cycle, cell migration, cell

metabolism and survival, as well as cell proliferation and differentiation.[55] The RTK family includes the receptors for insulin and for many growth factors, such as epidermal growth factor (EGF), fibroblast growth factor (FGF), platelet-derived growth factor (PDGF), vascular endothelial growth factor (VEGF), and nerve growth factor (NGF).[53] RTKs can be divided into 20 subfamilies sharing a domain for the catalytic tyrosine kinase function.[56, 57] In all the RTKs, the extracellular portion is separated from the intracellular tyrosine kinase region through a single transmembrane domain.[57, 58]

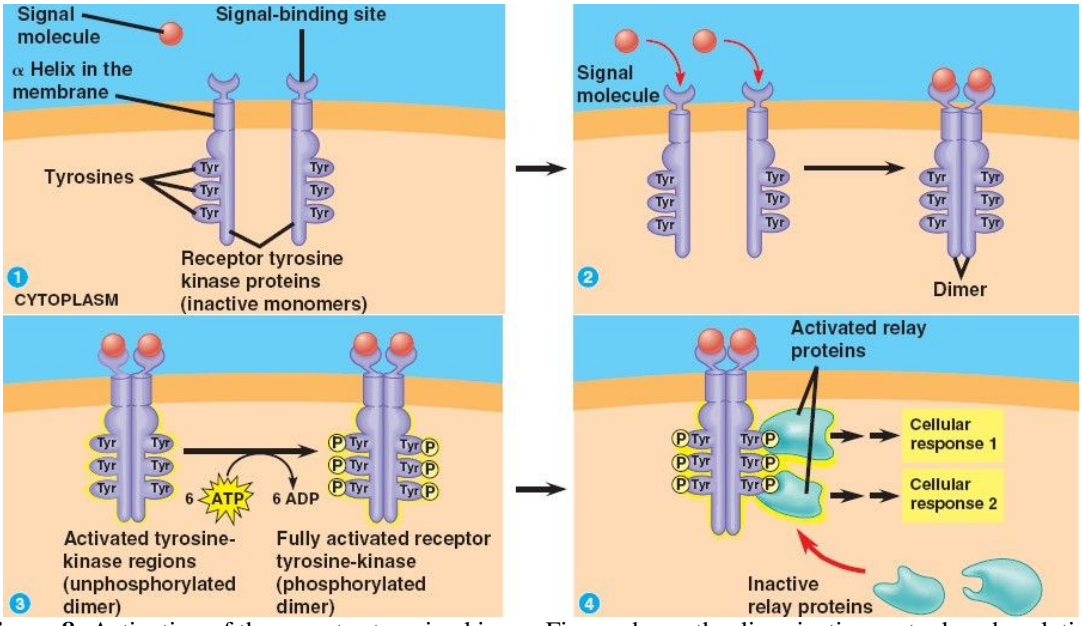

Figure 8: Activation of the receptor tyrosine kinase. Figure shows the dimerization, autophosphorylation and then initiation of signaling cascades to finally produce a cellular response (taken from Ref.[54]).

1.3.2 Nonreceptor tyrosine kinases (NRTKs)

The NRTKs are cytoplasmic enzymes which are essential components of the signaling cascades triggered by cell surface receptors such as RTKs, G protein-coupled receptors and immune system receptors. NRTK's includes several kinases such as Src, the Janus kinases (JAKs) and Abl.[53]

1.4 Epidermal growth factor receptor (EGFR) family

The epidermal growth factor receptor (EGFR) family is a RTK which comprises four members: the EGFR/ErbB1 (the first molecularly cloned RTK),[59] HER2/ErbB2, HER3/ErbB3 and HER4/ErbB4. All receptors have a two cysteine-rich domains extracelluarly and a tail of long C-terminal having nearly all the autophosphorylation sites in the intracellular portion.[57] EGFR family receptors can form various homo- or heterodimers, depending on the activating ligand, to generate a complex signal transduction network.[57, 60, 61] Examples of EGF-related growth which activate the EGFR family include EGF, transforming growth factor-α (TGFα), epiregulin (EPR), betacellulin

(BTC), heparin-binding EGF-like growth factor (HB-EGF), amphiregulin (AR) and the large family of alternatively-spliced neuregulins.[57, 62] The different growth factors have diverse binding specificities and affinities to EGFR, HER3 and HER4, with no identified ligand for HER2 yet[57] (Figure 9)[63].

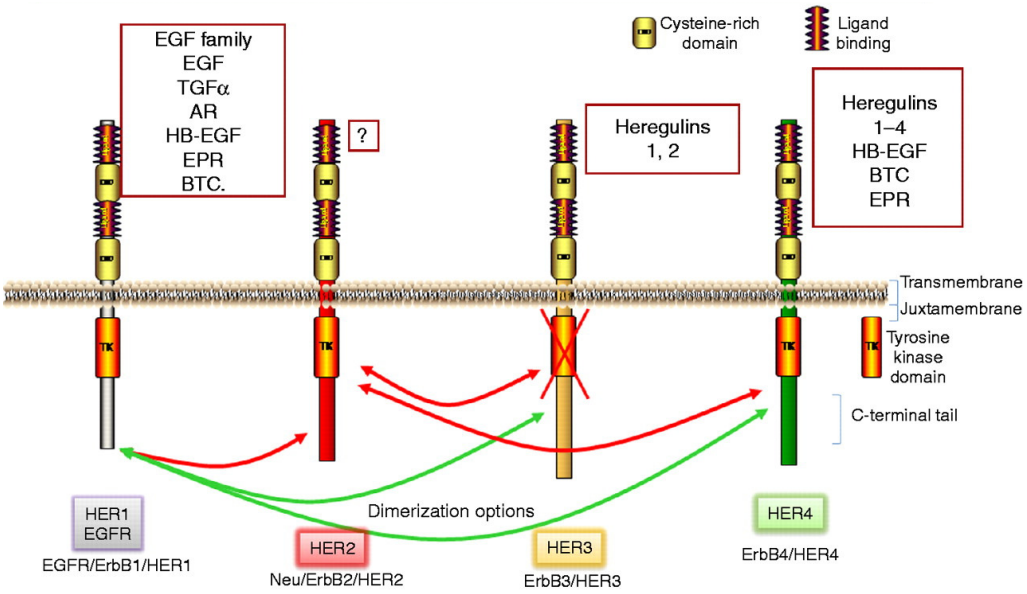

Figure 9: The 4 members of the ErbB receptor family with their activating ligands. Green and red arrows show the possible different dimers formed between the family members during the activation (taken from Ref.[63]**).**

1.4.1 EGFR

The epidermal growth factor receptor (EGFR) which is also known as HER-1 or ErbB-1, was the first member of the EGFR family.[64] EGFR is involved in signal transduction pathways concerned with various processes, including cell cycle progression, inhibition of apoptosis, tumor cell motility and invasion[65] (Figure 10)[66].

EGFR is a glycoprotein of 170-kd and with a normal expression range in cells from 40,000 to 100,000 receptors per cell.[64, 67] EGFR tyrosine kinase function is present in the intracellular domain, alongside EGFR also consists of an extracellular domain and a transmembrane region.[64] The most important ligands that bind and activate the EGFR are the epidermal growth factor (EGF) and the transforming growth factor–α. Other ligands which also bind to EGFR include amphiregulin, heparin-binding EGF, and betacellulin.[64, 68] Receptor homo- or heterodimerization at the cell surface results from ligand binding with EGFR, this is followed by internalization of the dimerized receptor and then autophosphorylation of the intracytoplasmic EGFR tyrosine kinase domains.[64, 69] Phosphorylated tyrosine kinase residues will then stimulate intracellular signal transduction cascade by acting as binding sites for signal transducers and activators of intracellular substrates such as Ras.[64]

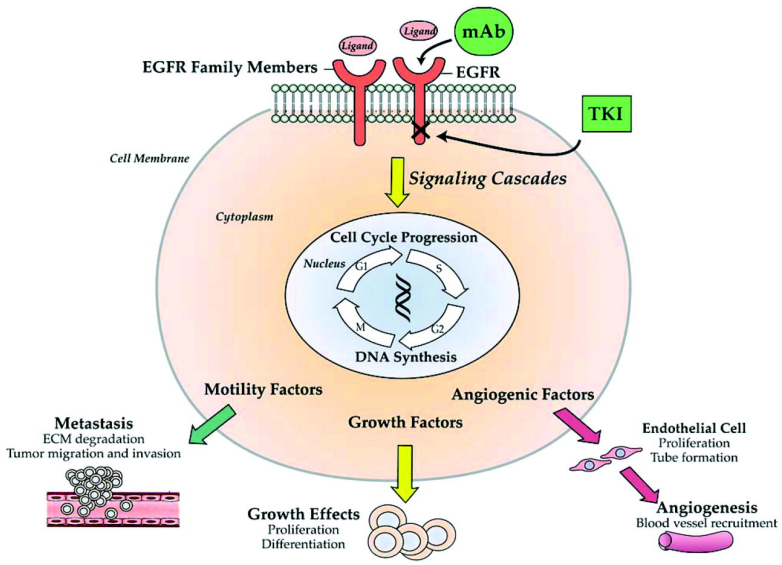

Figure 10: Schematic representation showing the involvement of EGFR in the transmission of signals regulating cell growth and metastasis. Green boxes indicate the different methods for inhibition of EGFR either by mAb "monoclonal antibodies" or TKI "Tyrsoine kinase inhibitors" (taken from Ref.[66]).

1.4.1.1 EGFR mutation

It was discovered in 2004 that a group of somatic mutations take place in the EGFR kinase domain which results in higher possibility of response to TKIs which was observed in a subpopulation of NSCLC patients.[70-72]

Patients with EGFR mutations was found to respond favorably to EGFR TKIs beside having clinically remarkable results, with rapid, nearly complete reduction of their cancers. EGFR mutations were more common in TKI-responsive NSCLC patients, i.e., females, never-smokers, Asians, and those with adenocarcinoma histology.[70, 73, 74]
Nearly 90% of the EGFR mutations observed were of either types:[70-72, 75, 76] (Figure 11)
1) small, inframe deletions in exon 19 clustered around the catalytic site of the receptor.
2) the single point mutation L858R, which lies within the TK activation loop in exon 21.

Mutations were seen to preserve the ligand dependence of receptor activation while modifying the downstream signaling pattern. Whereas, the antiapoptotic downstream activation signals (via Akt) is greatly enhanced in EGFR mutated cells with minimal effect on proliferative signals (via MAPK/ERK).[70, 77, 78]

Enhanced inhibition of biochemical signaling by small molecule TKIs is seen in NSCLC cells with mutated EGFR than with wild type receptors.[70, 78, 79] This is because the mutations taking place in critical residues of the catalytic domain near the ATP binding site, causes change in the physical structure and enhanced drug binding.[70, 80] Clinical significance appears since low doses of TKIs are needed for complete suppression of the mutated EGFR signaling, in contrast to the wild type receptor which needs higher plasma drug levels.[70]

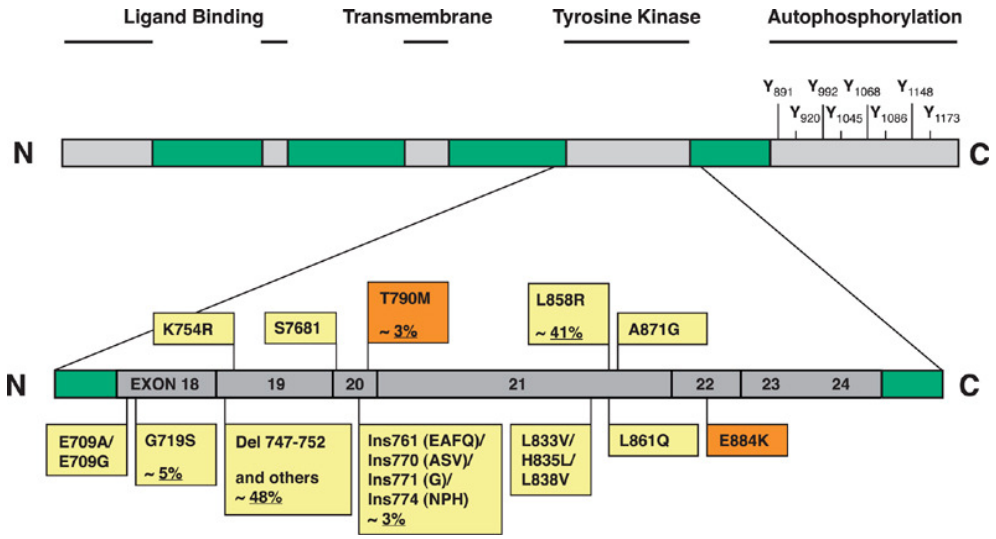

Figure 11: Different EGFR kinase domain mutations in NSCLC with frequencies indicated (taken from Ref.[81]).

Other reported rare types of mutations in EGFR TK domain, which is not clear yet if they are TKI-sensitizing as the common types, include exon 20 insertions, exon 18 point mutations, and exon 20 point mutations. On the contrary, at least some of the minor mutations are associated with resistance to TKI agents.[70, 82, 83]

The mechanism by which EGFR mutations cause rapid and remarkable responses to EGFR TKI therapy include at least two hypotheses.

1) The "oncogene addiction" hypothesis states that the cancer with mutated receptor and constantly transducing high levels of antiapoptotic (prosurvival) signals, become solely dependent on this signaling and loses its flexibility to adapt to signaling via other parallel pathways.[70, 84, 85] Accordingly, sudden interruption of EGFR signaling by TKIs for EGFR mutated cells that are "addicted" to EGFR prosurvival signaling, causes massive cell death.[70]

2) The "oncogenic shock" hypothesis states that some quantity of EGFR-generated proapoptotic signals are still present even if prosurvival signals dominate in cells.[70, 86] Accordingly, both signals are inhibited when TKIs block the receptor signaling. Since the prosurvival signals decay much more rapidly than proapoptotic signals, a proapopotic signaling predominate temporarily leading to irreversible apoptotic cascade causing cell death.[70]

1.4.1.2 EGFR resistance

Most of the patients responding to EGFR TKI treatments will eventually develop resistance and suffer a clinical relapse. Nearly 50% of the acquired TKI resistance cases are attributed to a secondary EGFR mutation, the point mutation T790M in exon 20 at the "gatekeeper" threonine residue.[70, 82, 87] Mutations at the gatekeeper threonine residue usually lead to kinase-targeted drug resistance.[70, 88] In the T790M EGFR mutation, there is an exchange of a threonine residue by a bulkier methionine residue which causes steric

hindrance and blocking of the ATP-catalytic pocket for the binding of gefitinib or erlotinib (Figure 12).[89]

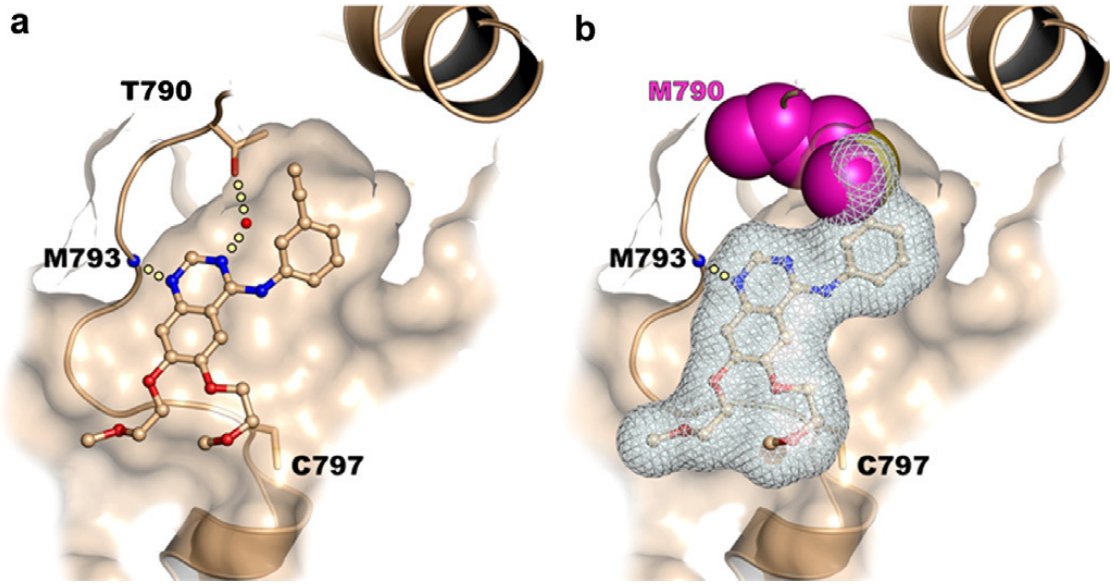

Figure 12: Crystal structure of wild type EGFR complexed with the reversible ATP competitive drug Erlotinib (PDB 1M17).[90] (a) Show hydrogen bonds (dotted lines) formed between the quinazoline core of the drug and the enzyme. (b) Modeled drug resistance mutation T790M (magenta) showing steric clash with the drug. The T to M mutation prevented the formation of the water-mediated hydrogen bond between N3 of the quinazoline and the side chain (taken from Ref.[89]).

A second mechanism of EGFR TKI resistance is the MET amplification which offers a comparable pathway for activation of intracellular proliferation signals and so can prevent the blocking effect of the EGFR TKI.[70, 91] Other mechanisms proposed to be involved in developing TKIs resistance include signaling via parallel redundant pathways, constitutive activation of downstream mediators, altered receptor trafficking, efflux of the drug from the cell, and mutation of the drug target itself.[70, 92, 93]

1.4.1.3 EGFR and cancer

EGFR overexpression was observed in many solid tumors such as breast cancer (up to 2 x 10^6 EGFR molecules per cell),[64, 94, 95] head-and-neck cancer, non–small-cell lung cancer (NSCLC), renal cancer, ovarian cancer, and colon cancer.[64, 96] Smaller percentage of bladder cancers, pancreatic cancers, and gliomas were also found to overexpress EGFR.[64, 68] EGFR overexpression results in more aggressive growth and invasiveness characteristics of cells due to intense signal generation and activation of downstream signaling pathways.[64, 97] EGFR overexpression is found in about 40-80% of the NSCLC cases.[64] It is also reported that 84% of squamous cell tumors,[69] 68% of large cell and 65% of adenocarcinomas are positive for EGFR.[64]

Generally, EGFR overexpression is associated with late stage of disease progression and is usually correlated with high metastatic rate, poor tumor differentiation, and increased rate of tumor proliferation.[57, 64 98, 99] The main mechanism leading to EGFR

overexpression is the gene amplification with more than 15 copies per certain tumor cell.[57, 100]

Tumorigenic mutations can change the EGFR activity through receptor activation without ligand binding. Human cancer mutations have seen to cause EGFR deletions leading to change in the extracellular receptor ligand binding domain which result in a constantly active EGFR kinase function.[57, 101]

Autocrine stimulation via growth factor loops is a potent mechanism for constitutive EGFR activation in several cancers. TGFα is the main ligand involved in the activation of the autocrine growth receptor.[57, 102, 103] Glioblastomas and squamous cell carcinomas of the head and neck were found to coexpress the TGFα and EGFR which is correlated with poor prognosis.[57, 104]

EGFR transactivation and EGFR-related signaling in cancer cells was found to take place through G protein-coupled receptor (GPCR)-induced cleavage of EGF-like growth factors.[57, 105] This takes place through a metalloprotease activation by GPCR stimulation leading to the cleavage of a transmembrane EGF-like ligand precursor allowing EGFR transactivation by the released growth factor.[57, 106]

1.4.1.4 EGFR as a target for anti-cancer therapies

EGFR is considered as an excellent target for anti-cancer therapy since abnormal EGFR signaling is implicated in many cancers and appears to be correlated with poor prognosis.[57, 107] Inhibition of the oncogenic EGFR tyrosine kinase activity takes place by two main approaches. The first one is the use of monoclonal antibodies “mabs” which is directed to block the extracellular receptor domain. The second approach is the use of small-molecule compounds which inhibit the intracellular EGFR tyrosine kinase activity (TKI; also known as “nibs”) through interacting with the ATP-binding domain[52, 64] (Figure 10).

Cetuximab (IMC-C225) is an example of anti-EGFR monoclonal antibody which binds to the EGFR and prevents the receptor tyrosine kinase activation, thus causing an antiproliferative effect on several cancer cells including pancreatic, renal and breast carcinomas.[57, 64, 108, 109] The most important small-molecule EGFR inhibitors that block EGFR activation are ATP analogues of the quinazoline and pyridopyrimidine family.[57, 110, 111] Gefitinib (Iressa) is an example of a quinazoline derivative showing significant anti-tumor effect on human breast and colon cancer cells.[57, 112]

1.4.1.5 Development of small molecule EGFR Inhibitors

In 1995 a SAR study was conducted on a series of compounds derived from ten-membered nitrogen-containing bicyclic scaffolds and it concluded that the quinazoline nucleus was the best scaffold for developing EGFR inhibitors.[113, 114] It was found that any modification in the nitrogen substitution pattern in the bicyclic ring resulted in less active compounds, especially when the quinazoline (**I**) is replaced by a quinoline (**II**) ring which resulted in 200-fold drop in affinity (Figure 13).[113, 114] This was explained by a hypothesis based on modeling studies that there is water-mediated hydrogen bond formed between

the N3 of the quinazoline and the side chain of the gatekeeper Thr790 residue of EGFR[113, 115] (Figure 14a). This provided a rationale for the importance of the N3 of the quinazoline core for activity and helped in the development of another series of compounds where the quinazoline N3 is replaced by C-CN group (**III**, Figure 13).[113, 116] This modification replaced the hypothetical water molecule and acted as a hydrogen bond acceptor for the Thr790 hydroxyl group (Figure 14b).[113]

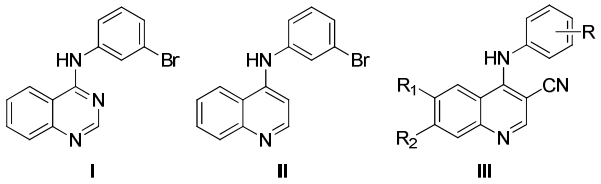

Figure 13:[113] Replacing the quinazoline nucleus in **I** by the quinoline nucleus in **II** resulted in 200-fold drop in affinity of the EGFR inhibitory activity. While replacing the quinazoline **II** by a 3-cyanoquinoline **III** results in equipotent compounds.

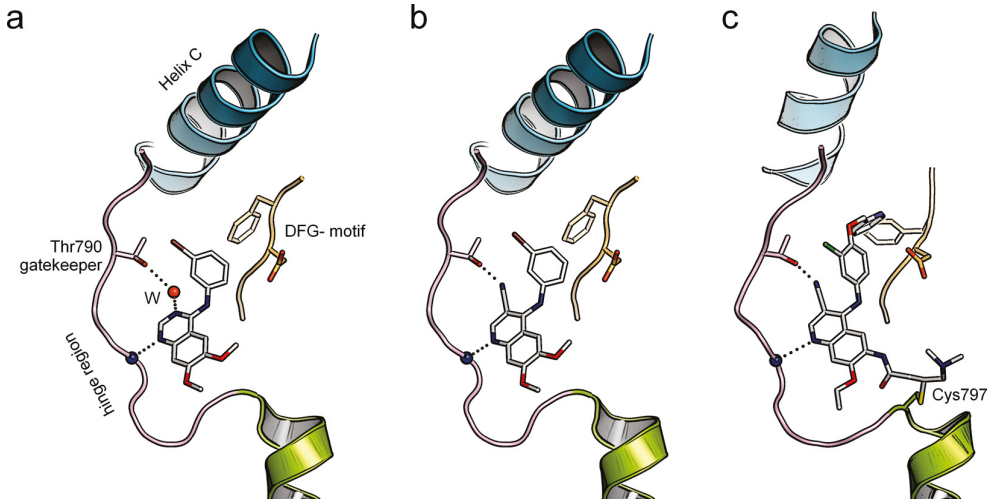

Figure 14: Binding modes of 4-anilinoquinazoline- and 3-quinolinecarbonitriles-based EGFR inhibitors. (a) Proposed binding mode of a 4-anilinoquinazoline to the ATP-binding site of EGFR showing hydrogen bonding interactions (dotted lines) of the inhibitor with the hinge region and via a mediated water molecule (W). (b) Binding mode of 3-quinolinecarbonitriles to displace the proposed water molecule and to form a direct hydrogen bond to the side chain of gatekeeper residue (Thr790). (c) The irreversible inhibitor Neratinib in complex with drug resistant EGFR-T790M (PDB code: 2JIV). The compound forms a covalent bond with the side chain of Cys797 of the ATP pocket (taken from Ref.[113]).

A second generation of EGFR TKIs has then been developed to overcome the resistance caused by T790M mutation and other acquired resistance mechanisms to gefitinib and erlotinib. At least one of two strategies is employed by the second generation EGFR TKIs to achieve better effectiveness over the first generation compounds which include:

1) Introduce in the compounds certain groups that are able to form covalent, irreversible bonds with EGFR which will prolong the inhibition of EGFR signaling resulting in an enhanced efficacy.[70] Cells with acquired resistance to first generation TKIs were effectively killed by using the irreversible TKIs.[70, 117]

2) The use of drugs able to target several kinases and block multiple signaling pathways in the cancer cell by using either a combination of agents or a single multitargeted drug.[70, 118] Cells are flexible in having a variety of possible signal transduction routes but in the same time, this could help the appearance of resistant clones that could bypass the inhibited receptor in case of cancer cells treated with targeted anticancer agents.[70, 117] HER-2 and vascular endothelial growth factor receptor (VEGFR) are secondary targets combined with EGFR inhibition by novel NSCLC drugs.[70]

1.5 NF-κB signaling in health and disease

1.5.1 Introduction to NF-κB protein family

Nuclear factor kappa beta (NF-κB) is a protein family consisting of five members of highly regulated dimeric transcription factors. The five proteins are Rel (c-Rel), RelA (p65), RelB, NF-κB1 (p50), and NF-κB2 (p52) and all of them share a common Rel homology domain (RHD)[119] (Figure 15)[120]. NF-κB exists in an inactive form and are activated through homo-[119, 121] and hetero-dimerization[119, 122] in response to pro-inflammatory stimuli such as tumor necrosis factor-α (TNF-α) and interleukin-1β (IL-1β).[123] The active transcription factors are able to bind to DNA at specific promoter sequences.[119]

The NF-κB nuclear translocation is blocked in the cytosol of unstimualted cells since the inactive dimers of NF-κB are held in complex with inhibitors of κB (IκB).[119, 124] Seven members of the IκB family are identified which are IκBα, IκBβ, Bcl-3, IκBε, IκBζ and the precursor proteins p100 and p105 (Figure 15)[120]. Post translational processes of the large proteins p105 and p100 results in the formation of p50 and p52 proteins respectively.[119] The release and translocation of active NF-κB into nucleus takes place when an outside signaling induces IκB degradation, phosphorylation, and polyubiquitination[123, 125-129] (Figure 16). The actively translocated NF-κB transcribes then the sets of genes according to the activated NF-κB dimer.[130]

NF-κB play critical roles in response to inflammation and in immunological reactions[131-134] as well as being involved in regulating cell proliferation, apoptosis and migration.[135-138]

On the other hand, several inflammatory disorders, such as bowel disease, psoriasis, asthma, rheumatoid arthritis, and sepsis can result from the excessive activation of NF-κB.[123, 139-141] In addition, the constitutive activation of NF-κB has been involved in cancer.[119]

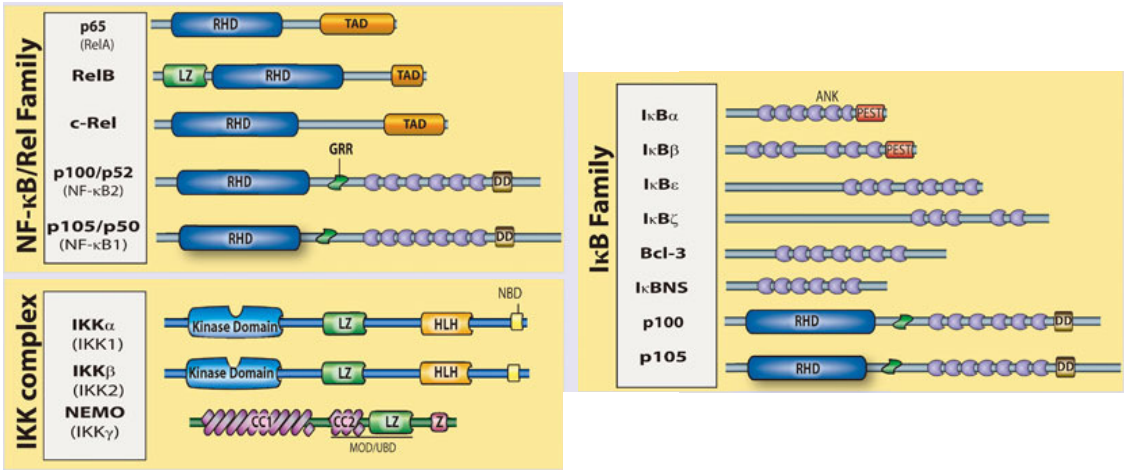

Figure 15: The mammalian protein families of NF-κB, IκB and IKK with their relevant domains and alternative nomenclatures (provided in parenthesis). The precursor proteins p100 and p105 function as family member of both IκB and NF-κB (after proteasomal processing) (taken from Ref.[120]).

1.5.2 The NF-κB signaling pathways

Activation of NF-κB can take place mainly through two signaling pathways known as the canonical pathway (or classical) and the non-canonical pathway (or alternative pathway)[142-145] depending on whether activation involves IκB degradation or p100 processing.[146] Upon stimulation, both pathways will induce phosphorylation of the IκB kinase (IKK) complex, consisting of two catalytically active kinases, IKKα and IKKβ, and the regulatory subunit IKKγ (NEMO) "NF-kappa B essential modulator". This is followed by the phosphorylation of IκB proteins which are targets for ubiquitination and proteasomal degradation, leading to the translocation of the NF-κB dimers to the nucleus to stimulate the expression of the target gene (Figure 16).[147] Post translational modifications (PTMs) further regulate transcriptional activity of nuclear NF-κB.[147, 148]
In the canonical pathway, which is the predominant NF-κB signaling pathway,[146] upon stimulation by binding of certain ligands, signaling pathways will cause the activation of the IKKβ which leads to the phosphorylation, polyubiquitination and degradation of IκB proteins.[147, 148]

In the non-canonical pathway, which operates mainly in B-cells,[146] activation of NF-κB through this pathway occurs by fewer stimuli such as BAFF (B cell activating factor) and lymphotoxin-β.[147, 148] Upon stimulation, the protein kinase NIK is activated which in turns activate the IKKα complex through phosphorylation which then phosphorylates p100 causing its processing and the liberation of p52/RelB active heterodimer.[147, 148]

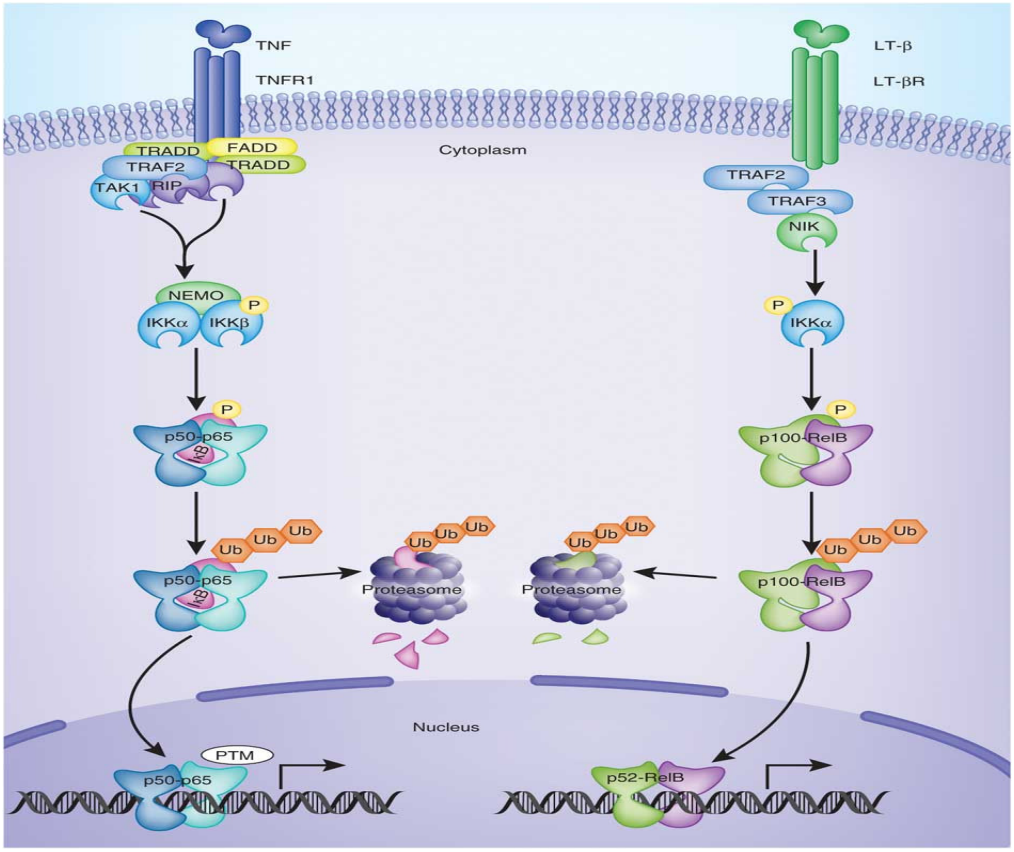

Figure 16: The canonical and non-canonical NF-κB pathways. In the canonical pathway, the IKK complexes containing NEMO are activated which in turn leads to the phosphorylation and degradation of IκBα releasing NF-κB dimers (including p65/p50). In the non-canonical pathway, NEMO-independent activation of IKKα through the kinase NIK. IKKα induces the phosphorylation and processing of p100 to p52 resulting in the activation of predominantly p52/RelB complexes.[120] (diagram taken from Ref.[147]).

1.5.3 The Ubiquitin/Proteasome System (UPS)

Addition of ubiquitin (Ub) and ubiquitin-like (Ubl) modifiers to proteins helps to modulate function and is considered a key step in protein degradation, epigenetic modification and intracellular localization.[149] Ubiquitination regulates several steps in the NF-κB pathway, where the ubiquitin–proteasome pathway plays a crucial role in both the canonical and non-canonical pathways of NF-κB activation. Ubiquitin targets IκB for degradation, processing of NF-κB precursors, p105 and p100, by proteasome to the mature forms and activation of the IκB kinase (IKK).[146] In addition, recent studies revealed that ubiquitination play a key role in activating protein kinases in the NF-κB pathway through a degradation-independent mechanism.[146, 150, 151]

Ubiquitination is a reversible covalent modification that is catalysed by three enzymatic steps. In the first step, an ATP-dependent reaction takes place where the ubiquitin is activated by a ubiquitin-activating enzyme (E1). In the second step, transferring of the activated ubiquitin to a ubiquitin-conjugating enzyme (E2 or UBC) takes place to form an E2-Ub thioester. Finally, the ubiquitin-protein ligase (E3) mediates the attachment of ubiquitin to a target protein through an isopeptide bond formed

between the ubiquitin C terminus and the ε-amino group of a lysine residue in the target protein[146] (Figure 17)[152]. Ubiquitin contains seven lysine residues that can be attached to other ubiquitins to form a polyubiquitin chain.[146] A polyubiquitin chain that targets a protein for degradation by the proteasome is linked mainly through Lys 48 and Lys 11 of ubiquitin. While, Lys-63-linked polyubiquitin chains function as scaffolds to assemble signaling complexes participating in diverse cellular processes ranging from DNA repair to activation of NF-κB signaling (Figure 17).[152]

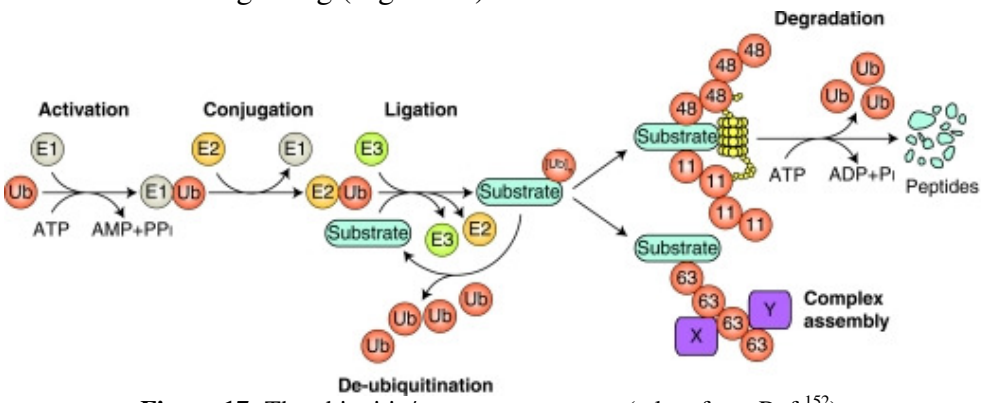

Figure 17: The ubiquitin/proteasome system (taken from Ref.[152]).

1.5.4 Deubiquitinating enzymes (DUB)

Protein ubiquitination and subsequent degradation by the proteasome require the participation of both ubiquitinating enzymes and deubiquitinating enzymes.[153] Deubiquitinating enzymes (DUBs) and Ubl-specific proteases (ULPs) are proteases that counteract Ub/Ubl ligases and serve to deconjugate the Ub/Ubl-modified substrates.[149] The DUBs encoded by the human genome are approximately 100 and can be grouped based on their sequence homology within the catalytic domain into five classes. These include 4 classes of cysteine proteases: the Ubiquitin C-terminal Hydrolases (UCHs; 4 members), the Ubiquitin Specific Proteases (USPs; 57 members), the Machado Joseph Disease proteases (MJD; 4 members), and the Otubain proteases (OTU; 13 members). The fifth class is composed of the JAB1/MPN/Mov34 enzymes (JAMM; 8 members), which are metalloproteases.[154] DUBs function at multiple steps in the ubiquitin system: (1) DUBs are required to generate free Ub monomers from ubiquitin precursors, (2) DUBs counter the action of ubiquitin ligases, (3) DUBs function at the proteasome to edit ubiquitin chains, to remove ubiquitin prior to substrate degradation in the proteasome, and to recycle monomeric ubiquitin, and (4) DUBs function at the MVB to promote recycling of monomeric ubiquitin by removing ubiquitin prior to internalization of substrates into the MVB[154, 155] (Figure 18)[154].

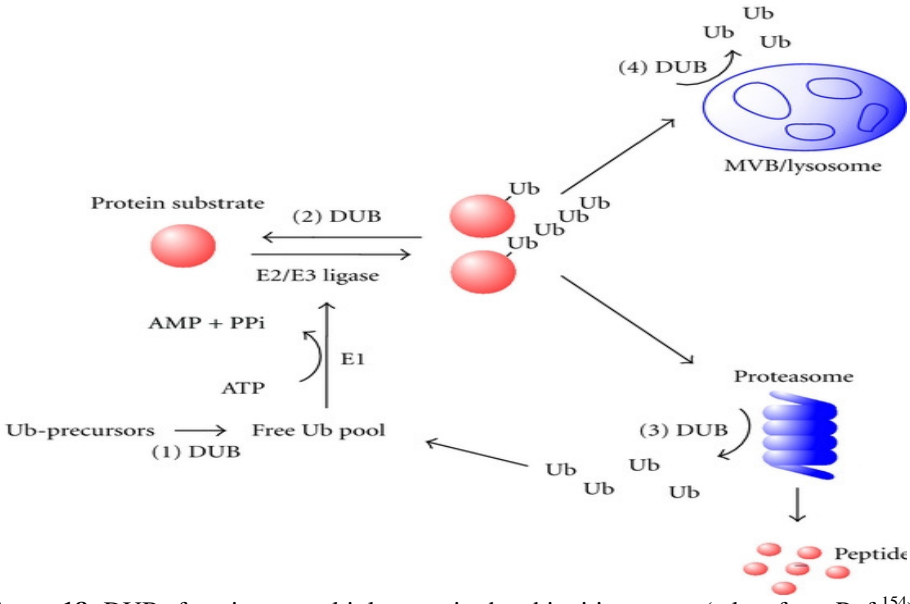

Figure 18: DUBs function at multiple steps in the ubiquitin system (taken from Ref.[154]).

Recently, several studies revealed the involvement of deubiquitinating enzymes in cancers as well as in other diseases. Several types of deubiquitinating enzymes were found to be upregulated in cancer cells.[153] In addition, certain DUBs mutation in cases of human cancers demonstrates their involvement as true oncogenes and tumor supressors.[156]

The ubiquitination-proteasome pathway play vital role in cancer development and progression due to its proteolytic involvement in the regulation of protein turnover.[153] It has been reported that the ubiquitination-proteasome pathway play a critical role in the pathogenesis of breast cancer by affecting the downregulation of growth factor receptors, such as EGFR/ErbB-1, Neu/ErbB-2, and ErbB- 3/HER3.[153, 157] Also, the Nuclear factor-kappa B (NF-κB) plays a pivotal role in many aspects of tumor development, progression, and therapy, and its activation relies primarily on the ubiquitination-mediated degradation of its inhibitor IκB.[153, 158]

1.5.5 NF-κB role in cancer

NF-κB-dependent transcription regulates key cellular processes such as cell growth, proliferation, and survival, therefore dysregualtion of NF-κB pathways could result in cancer.[159] It has been reported that some cancer cells such as breast, liver, prostate, pancreatic and gastric cancer have been found to involve constitutive activation of NF-κB.[135, 160-164]

The role of NF-κB in cancer is thought to be related to the transcription control of key antiapoptotic genes that encode B-cell lymphoma-2 (Bcl-2) and inhibitor of apoptosis (IAP) family proteins.[119, 165] These antiapoptic genes upon overexpression can prevent the tumor cells from undergoing programmed cell death and as a result contribute in

tumorigenesis and resistance to therapies.[119, 166] In addition, NF-κB is also involved in the regulation of proliferation through cyclins and growth factors.[159]

1.5.6 NF-κB inhibition

Inhibition of the NF-κB activity is through several strategies which could be direct or indirect. Direct strategies are to prevent the function of one or more of the NF-κB family proteins by inhibitors which may prevent the NF-κB family members dimerization or DNA binding. Indirect strategies include the inhibitors that affect NF-κB function such as molecules upstream of NF-κB e.g. IKK, cytokines and cytokine receptors or prevent NF-κB degradation, such as proteasome inhibitors.[119, 167]

Certain chemical classes such as the triazine, coumarin, and quinazoline are known to possess an NF-κB inhibitory activity which is predicted to be due to preventing DNA binding through direct interaction with p50.[119, 168-170]

1.5.7 Small molecules as NF-κB inhibitors

Several compounds have been reported to have inhibitory activities toward NF-κB-mediated transcriptional activation. Low-molecular-weight compounds, such as MG-132 (1),[171, 172] BAY 11-7085 (2),[173] and an indane derivative (3), as well as natural products, such as caffeic acid phenylethyl ester (4)[174] and the sesquiterpene lactone helenalin (5),[175, 176] have been shown to inhibit NF-κB activation (Figure 19).[170] This was followed by Tobe et al.[170] reporting quinazoline derivatives (6) as new structural class of NF-κB activation inhibitors.[170]

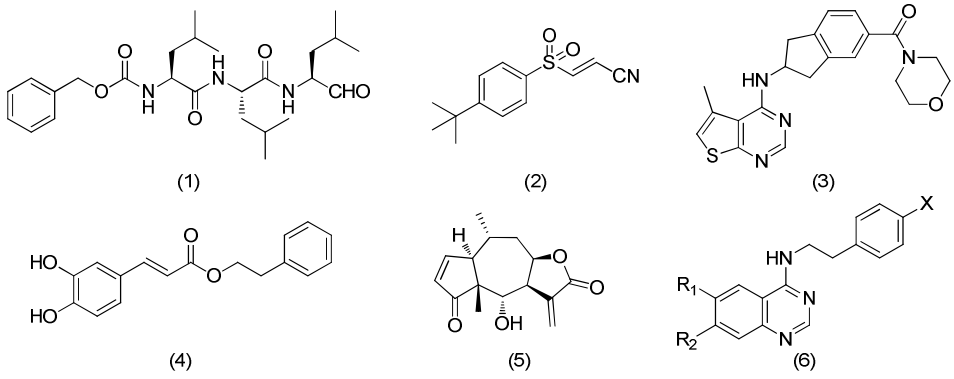

Figure 19:[170] Some low molecular weight compounds shown to inhibit NF-κB activation.

1.6 Combination Therapy for cancer

Targeted anticancer therapy which specifically targets key molecules of cancer cells, was successfully developed with an aim of achieving tumor selectivity and limiting non-specific toxicities.[65, 177]

However, an important overall limitation of target-based monotherapy is that the strict specificity of agents used can be overcome by alternative hyper-activated survival pathways in cancer cells.[177, 178] Accordingly, monotherapy treatment could sometimes be

hindered by patient insensitivity and development of resistance.[177, 179] Therefore, research now also supports combinations of agents as significant cancer treatments to overcome resistance and synergistically produce a greater and more durable degree of response for more cancer patients.[177, 180-182]

1.7 Link between EGFR and NF-κB pathway

A number of studies demonstrated a link between the EGFR receptors and the NF-κB activation pathway in different types of cancer.[183-185] The activation of EGFR receptors leads to the activation of downstream signalling cascades including the RAS/extracellular signal regulated kinase (ERK) pathway, the phosphatidylinositol 3-kinase/AKT (PI3K/AKT) pathway and the Janus kinase/Signal transducer and activator of transcription (JAK/ STAT) pathway (Figure 20).[186] Accordingly, it has been reported that EGFR can activate NF-κB through the PI3K/Akt pathway which leads to the phosphorylation of IκBα.[184]

It has also been reported that using a combination of specific inhibitors of NF-κB and the EGFR family receptors blocks proliferation synergistically at concentrations which are ineffective when used individually.[183, 187] This significantly demonstrates the major advantage that would be achieved in the cancer therapy through inhibiting both pathways simultaneously.

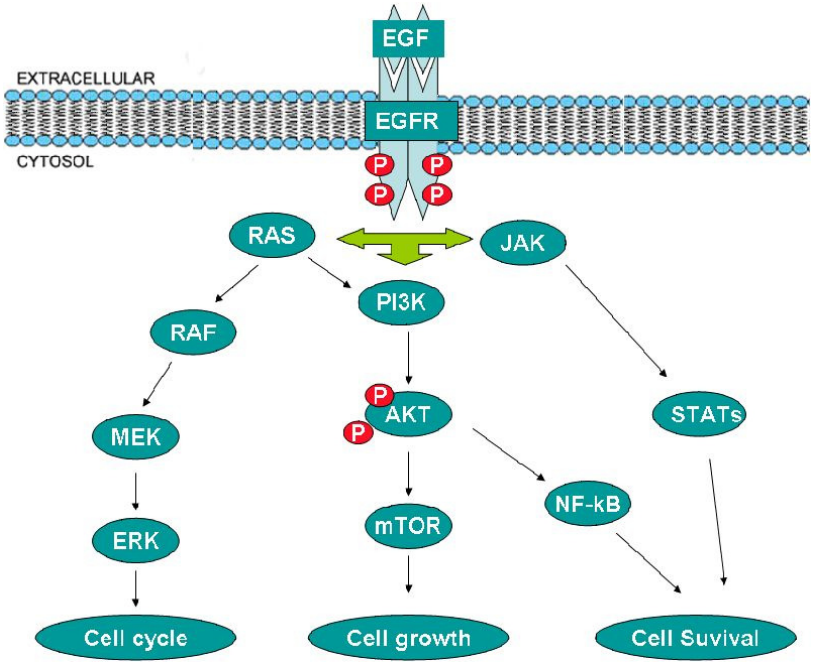

Figure 20: Activation of the the EGFR receptors leads to the activation of downstream signalling cascades which involves the NF-κB activation (taken from Ref.[186]).

2 Outline of this thesis

2.1 Scientific goal

Targeted cancer therapy is a type of cancer treatment which interferes with specific targeted key molecules needed for tumorigenesis, cancer progression and metastasis. Targeted therapy was applied to decrease the side effects on the normal cells than the traditional chemotherapy. Epidermal growth factor receptor was among the first receptors proposed for targeted cancer therapy as being involved in cancer cell proliferation and found to be overexpressed in several types of cancer. Although several EGFR inhibitors such as Gefitinib and Erlotinib have been clinically approved in the treatment of cancer, yet several limitations such as the development of resistance due to mutations or being originally insensitive may hinder their application.

It is also generally accepted that simultaneous blocking of two major signaling pathways would have synergistic anti-tumor effects and might decrease the development of mutations. Accordingly, co-application of EGFR inhibitors with other specific agents having identified complementary cancer pathways, such as NF-κB, would enhance the efficacy of clinically approved EGFR inhibitors even towards previously insensitive tumor cells. While co-administration of anti-tumor therapeutics has proven to be beneficial in several cases, yet could still suffer from certain limitations such as increased toxic side effects and individual pharmacokinetic properties of the drugs. Therefore, a single molecule with dual inhibitory activity is considered more beneficial and advantageous in treatment of several types of cancers.

Accordingly, the main goal of this thesis was the development of new potent anticancer agents that could be effective against cancers that are originally insensitive or resistant to the clinically approved EGFR inhibitors. This was achieved through applying two general strategies.

2.2 Working Strategy

The first strategy (**A**) was to introduce structural modifications to the molecules which were expected to result in more potent EGFR inhibitors, especially towards the mutant EGFR. This strategy will help mainly to overcome the problem of cancers that have or develop resistance towards the EGFR inhibitors due to mutation.

The second strategy (**B**) was through seeking additional target sites such as the NF-κB signaling pathway besides the EGFR kinase activity. The resulting dual inhibitory activity would lead to the suppression of two major complementary signaling pathways in cancer cells at the same time. This would have significant clinical advantage in producing a synergistic potent anticancer activity towards several types of cancer that are originally insensitive or resistant to the clinically approved EGFR inhibitors.

A) The first strategy was applied by making structural modifications that were expected to result in enhanced activity towards the mutant EGFR. To begin, we started the modifications from the 6-substitued 4-anilinoquinazoline scaffold (**I**) which was known to possess a significant EGFR inhibitory activity. This first strategy involved two parts: 1) Variation of the position 4 substituents and the quinazoline nucleus. 2) Modification of the position 6 side chain.

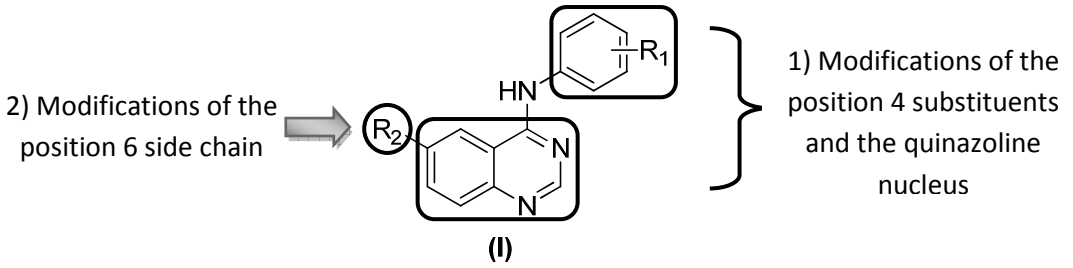

(I)

A.1) Modifications of the position 4 substituents and the main nucleus (Chapter 3.I)

The first part of the work included the synthesis of irreversible inhibitors by adding to scaffold (**I**) a Michael acceptor group in position 6 (R_2= acrylamide) while doing several modifications in position 4 (**II**). The acrylamide group was known to form a covalent interaction with the enzyme. The compounds were then tested against wild-type and mutant EGFR containing cancer cell lines. This part of the work also included testing the effect of replacing the main quinazoline core with the tetrahydropyridothieno[2,3-*d*]pyrimidine nucleus (**III**).

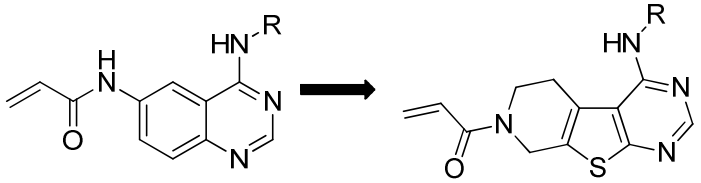

(II) **(III)**

A.2) Modifications of position 6 side chain (Chapter 3.II)

The second part of the work included the modifications in the position 6 side chain of the quinazoline while using a *m*-bromo aniline in position 4 (**IV**). These modifications were done with an intention to offer chances for extra possible interactions that could take place with the mutant enzyme

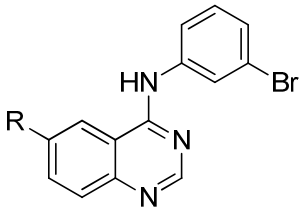

(IV)

B) The second strategy was to seek an additional inhibitory activity towards the NF-κB pathway beside the EGFR kinase activity. To reach this goal we started by screening most of the previously synthesized compounds for an additional activity towards the NF-κB using the U937 cells reporter gene assay.

Hit identification, Hit optimization and trials for identification of the exact molecular target for the inhibition of the NF-κB pathway (Chapter 3.III)

This part of the work included screening of most of our synthesized compounds for the NF-κB inhibitory activity which resulted in a Hit compound. The Hit compound was the benzylthiourea derivative (**V**) which showed a 97% inhibition at 10μM for the NF-κB pathway in addition to an IC_{50} of 17.2nM towards the EGFR enzyme. Further optimization was done to the Hit compound guided by the NF-κB activity. The optimization included 3 parts: 1) Modification of the substituents on the 4 anilino ring while keeping the benzylthiourea moiety. 2) Replacing the thiourea linker with a urea. 3) Modification of the benzyl part linked to the thiourea through removal of the methylene spacer, varying the substituents on the aromatic ring and the use of different heterocyclic rings. Several trials were also done to identify the molecular target for the inhibition of the NF-κB pathway which included testing against different kinases or steps involved in the pathway.

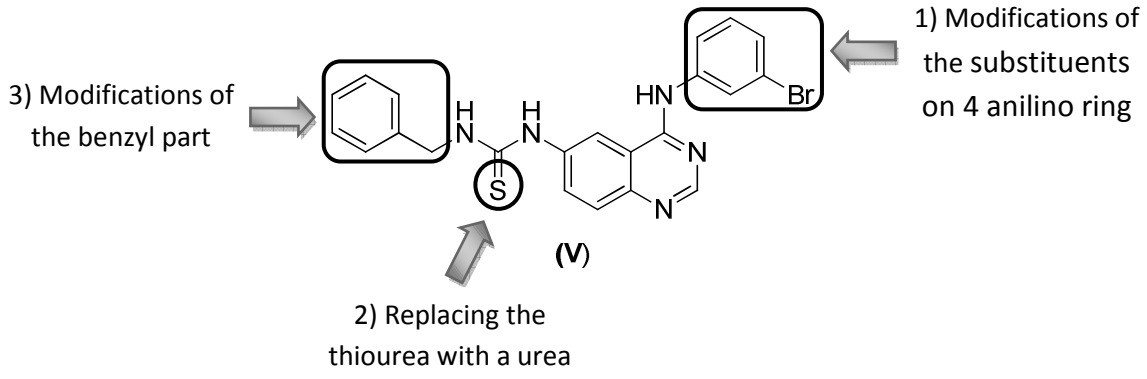

(V)

3 Results

3.I Quinazoline and tetrahydropyridothieno[2,3-d]pyrimidine derivatives as irreversible EGFR tyrosine kinase inhibitors: influence of the position 4 substituent

Mostafa M. Hamed, Dalal A. Abou El Ella, Adam B. Keeton, Gary A. Piazza, Matthias Engel, Rolf W. Hartmann, Ashraf H. Abadi

This manuscript has been accepted as a consice article in *MedChemComm*, (**2013**), DOI: 10.1039/C3MD00118K

Paper I

Abstract

Herein, we describe new quinazoline and tetrahydropyridothieno[2,3-*d*]pyrimidine derivatives with an acrylamido group at positions 6 and 7 respectively; and with variable anilino, sulfonamido and cycloalkylamino substituents at position 4. The lipophilic and steric properties of the position 4 substituent seem crucial for activity. Several compounds were more active than gefitinib in inhibiting the wild type EGFR enzyme, the autophosphorylation of the mutant EGFR expressing cell line (H1975), and the growth of cell lines with wild type and mutant EGFR tyrosine kinase. Moreover, novel synthesis of the quinazoline nucleus from the formimidate derivative is described.

Introduction

Members of the epidermal growth factor receptor (EGFR) family were found to play a vital role in lung tumorigenesis being overexpressed in 40-80% of non-small cell lung carcinoma (NSCLC) tumors.[1-4] A series of downstream signaling events results from EGFR activation and can mediate cancer cell growth, proliferation, motility, adhesion, invasion, apoptosis inhibition and metastasis as well as resistance to chemotherapy. Accordingly, EGFR inhibitors would be valuable in cancer treatment.[1, 2] Gefitinib, erlotinib, and lapatinib (Figure 1) are examples of small molecules, acting as kinase inhibitors, that have been approved in cancer treatment.[5] They are used clinically in the treatment of EGFR/HER2-dependent tumors which occur in non-small cell lung cancer (NSCLC) or breast cancer.[6] They belong to a class of compounds known as 4-anilinoquinazolines which are designed mainly to target the ATP binding pocket of the kinase domain.[6]

The quinazoline core is reported to be among the best scaffolds for the development of EGFR inhibitors.[7] This was justified by a hypothesis explaining the importance of the quinazoline N3 in the formation of a water-mediated hydrogen bond to the side chain of the gatekeeper Thr790 of EGFR.[8, 9] This aided successfully in designing reversible and irreversible EGFR and HER2 kinase inhibitors.[10-13] The tetrahydropyridothieno[2,3-*d*]pyrimidine nucleus is also among the scaffolds showing EGFR inhibitory activity.[4] The 4-(phenylamino) quinazoline core have also been used to develop several irreversible EGFR inhibitors by introducing a Michael acceptor functional group such as the acrylamide group attached at the C-6 or C-7 positions, e.g. **I** & **II** (Figure 1). These groups form a covalent linkage with the sulfhydryl group of the Cys797 of EGFR and these compounds proved to be potent inhibitors of tumor growth relying on overexpression of EGFR.[14-15]

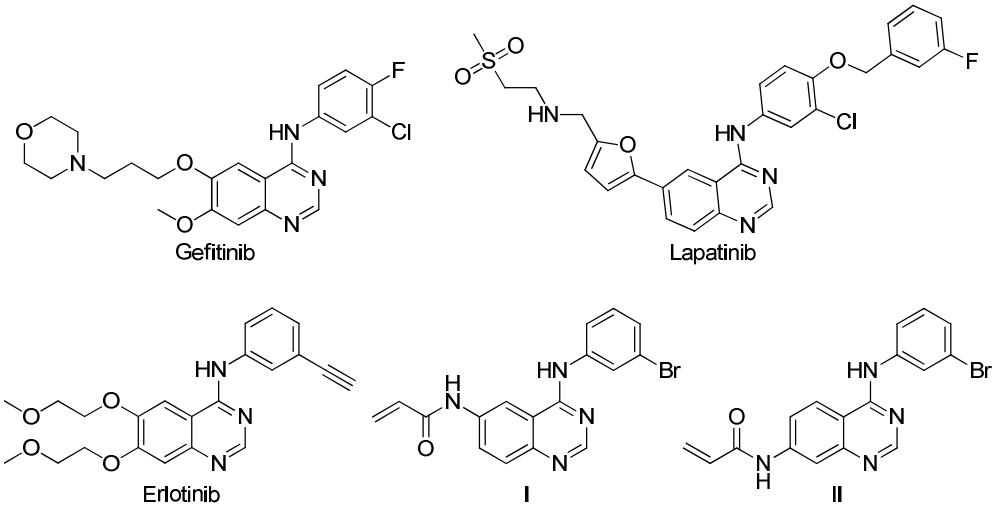

Figure 1. Reversible and irreversible EGFR tyrosine kinase inhibitors

Drug resistance was found to develop in approximately half of NSCLC cases that showed an initial response to reversible EGFR tyrosine kinase inhibitors. This was associated with the emergence of a secondary mutation leading to the substitution of a single amino acid threonine 790 by methionine (T790M) in the ATP binding pocket of EGFR.[16-18] Several other mechanisms of resistance to reversible EGFR inhibitors have also been reported.[19, 20] The Thr790 residue in EGFR is present at the entrance of the deep hydrophobic pocket of the ATP binding site. Therefore, its substitution with the bulkier methionine residue caused resistance towards the reversible tyrosine kinase inhibitors such as gefitinib and erlotinib and this had been attributed to an increased enzyme affinity for ATP.[21] Several studies reported that the irreversible inhibitors[22-24] are able to overcome this mutation-associated drug resistance.[18, 25-28]

Although the T790M mutation takes place in the Thr790 which is present in the deep pocket that is occupied mainly by the position 4 substituents of quinazoline derivatives, yet the introduction of a Michael acceptor group in position 6 of the quinazoline has proven to overcome this mutation-associated drug resistance. While, the role of the

Michael acceptor groups in overcoming this resistance is justified and clear, yet the significant role of the position 4-substituents in the inhibition of the mutant EGFR in presence of Michael acceptor groups is still not clear.

Therefore, we strived to investigate the effect of position 4 substituents on the potency of our potential irreversible inhibitors. In this study we aimed to provide a better understanding about the significant role, nature and size of the position 4 substituents - that can be attached to a quinazoline scaffold in the presence of a potential covalent interaction - on the inhibition of the mutant as well as the wild type EGFR kinase. In addition, the importance of the quinazoline core was also tested by replacing it with a tetrahydropyridothieno[2,3-*d*]pyrimidine nucleus. Accordingly, to apply our study we synthesized quinazoline derivatives having an acrylamido substituent at position 6 and with diverse substituents at position 4. The acrylamido substituent is intended to potentially alkylate cysteine (C797) in the ATP binding site of EGFR, to help in overcoming the mutation-associated drug resistance. Varied substituents at position 4 were added, namely haloanilines, alicyclic amines, alkylanilines, alkoxyanilines, and sulfonamide containing aniline derivatives **4a-4o**. Furthermore, a new cost-effective modification for the synthesis of quinazoline nucleus is described. In addition, another series of compounds **10a-10f** was synthesized by replacing the quinazoline nucleus with a tetrahydropyridothieno[2,3-*d*]pyrimidine scaffold with also the same acrylamido substituent at position 7 while keeping the position 4 substituents showing potent inhibitory activity with the quinazoline nucleus. All acrylamido derivatives **4a-4o** and **10a-10f** have been tested for their inhibitory activity on the recombinant wild type EGFR kinase as well as cell growth inhibition versus cancer cell lines, with mutant EGFR (H1975) and with wild type (SKBR3). In addition, cell based autophosphorylation inhibition was done for selected compounds.

Chemistry

Synthesis of the quinazoline nucleus started by refluxing of 2-amino-5-nitrobenzonitrile with triethyl orthoformate in presence of drops of acetic anhydride to yield the formimidate derivative **1** (Scheme 1). Compound **1** was confirmed from its IR spectrum showing a band at 2228.6 cm^{-1} indicating the existence of the (C≡N) group. 1H-NMR spectrum of **1** in DMSO-d_6 revealed signals at 8.22 ppm (N=CH-) as singlet, quartet at 4.36 ppm (CH2) and triplet at 1.35 ppm (CH3).

The second step in scheme 1 shows a novel modification for the synthesis of the quinazoline nucleus, whereby the formimidate derivative **1**, was refluxed in acetic acid with different amines to yield the nitroquinazoline derivatives **2a-2o** and the cyclization was confirmed from the IR spectrum by the disappearance of the band for the cyano group. This novel modification is cost-effective since the quinazoline nucleus is synthesized from the formimidate derivative which is prepared from the much cheaper triethyl orthoformate instead of the usual N,N-dimethylformimidamide derivative prepared from the more expensive DMF-dimethyl acetal.[29]

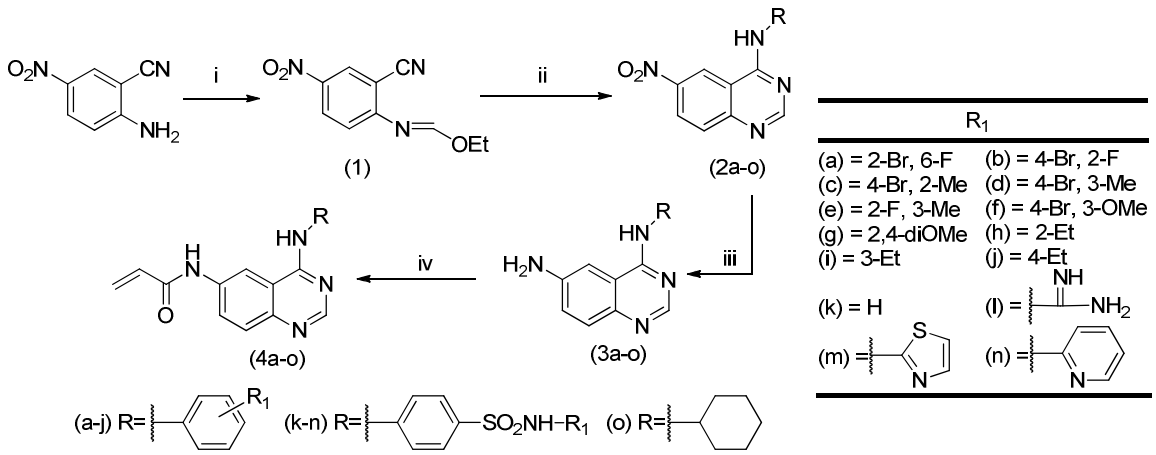

Scheme 1. Reagents and conditions: (i) TEOF, $(Ac)_2O$, reflux, 24h; (ii) R-NH_2, CH_3COOH, reflux, 1h; (iii) $SnCl_2$, MeOH, reflux, 1h; (iv) CH_2=CHCOCl, $NaHCO_3$, acetone or DMF, 0°C, 30 min.

The suggested mechanism for the formation of the quinazoline nucleus from the formimidate derivative **1** is described in scheme 2 as reported in literature for a similar derivative.[30] It is assumed that the aromatic amines or the cyclohexylamine firstly attacks the carbon of the ethoxy resulting into ejection of the ethoxy group. An amidine intermediate is then formed which cyclizes into the quinazoline skeleton via Dimroth rearrangement where the endocyclic and exocyclic nitrogen atoms switched place to afford the 4-substituted aminoquinazoline.

Reduction of the nitroquinazoline derivatives was done by refluxing with $SnCl_2$ in methanol to yield the aminoquinazoline derivatives **3a-3o**, which were then reacted with acryloyl chloride in acetone or DMF at 0º C in the presence of $NaHCO_3$ to yield the acrylamide derivatives **4a-4o** (Scheme 1).

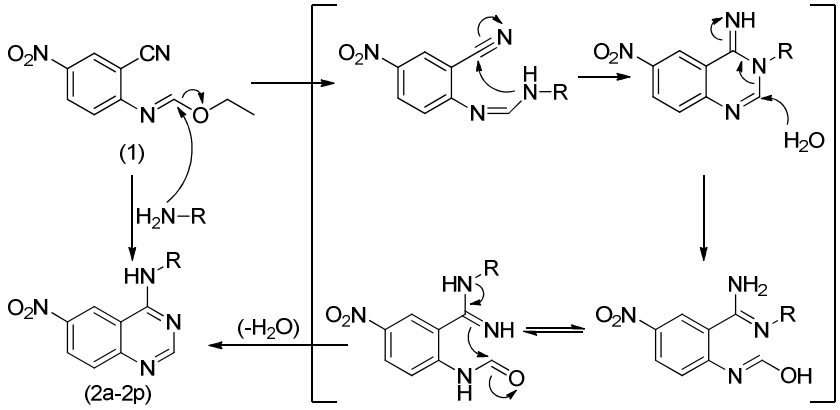

Scheme 2. Suggested mechanism for the formation of the quinazoline nucleus

Synthesis of the tetrahydropyridothieno[2,3-*d*]pyrimidine derivatives is outlined in scheme 3 according to the reported procedure.[4] It started by condensing the 4-oxo-piperidine-1-carboxylic acid *tert*-butyl ester with ethyl cyanoacetate under basic conditions followed by cyclization through a Gewald reaction[31] to construct the thiophene core. The construction of the thieno[2,3-*d*]pyrimidine ring system **6** was done

using a modified Niementowski quinazoline synthesis by condensation of **5** with formamidine acetate. This was followed by chlorination of pyrimidone **6** with phosphorus oxychloride which gave the intermediate **7**. Nucleophilic reaction of **7** with appropriate amines gave **8 a-f**, which were then subjected to Boc deprotection using TFA resulting in the intermediates **9 a-f**. The desired compounds **10 a-f** were obtained by reacting the intermediates **9 a-f** with acryloyl chloride in acetone at 0º C in the presence of sodium bicarbonate to yield the acrylamide derivatives **10 a-f**.

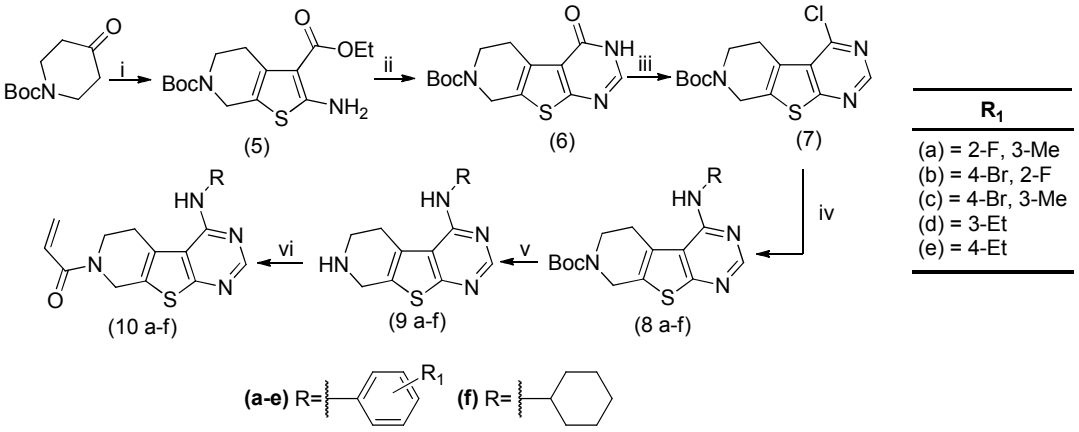

Scheme 3. Reagents and conditions: (i) $NCCH_2COOEt$, S_8, Et_3N, rt, 16h; (ii) formamidine acetate, DMF, 100 °C, 16h; (iii) $POCl_3$, Et_3N, 60°C, 3h; (iv) R-NH_2, EtOH, reflux, 8h; (v) TFA, CH_2Cl_2, 0°C→rt, 2h; (vi) CH_2=CHCOCl, $NaHCO_3$, acetone, 0°C, 30min.

Biological Results and Discussion

All synthesized acrylamide derivatives **4a-4o** and **10a-10f** were tested for their ability to inhibit isolated recombinant wild type EGFR kinase. This was followed by testing the cell growth inhibitory activity on cancer cell lines with wild type EGFR (breast cancer cell line SKBR3) and the gefitinib-resistant (H1975) NSCLC cell line harboring the L858R and T790M mutations. In addition, to correlate the cell growth inhibition with the mutant EGFR kinase inhibition, selected compounds were tested for their ability to inhibit EGFR autophosphorylation in mutant EGFR expressing cell line (H1975) (Table 1).

From the results, it can be seen that several compounds show significant inhibitory activity on the wild type as well as the mutant EGFR kinase which is correlated to the cell growth inhibition. Compounds like **4a**, **4b** and **4f** were the most potent versus both cancer cell lines having mutant and wild type EGFR.

Concerning the inhibitory activity on the recombinant wild type EGFR enzyme, it was generally observed that the potent activity was accompanied with di-substitution on the 4-aniline ring, either with dihalo or alkyl halo groups as in **4a**, **4b** and **4e**. In addition, it is the first time to report that replacing the usual aniline derivatives with a cyclohexyl amine as in compound **4o** resulted in an active and potent compound on the wild type EGFR.

Table 1. IC_{50} for the inhibition of recombinant EGFR (active) kinase, cell growth inhibitory activity, EGFR autophosphorylation inhibition in mutant EGFR-expressing cell line.[a]

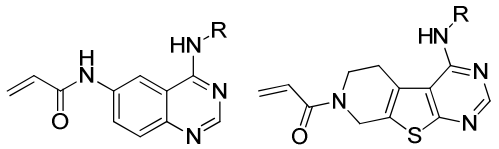

Cpd.	IC_{50} (nM)	IC_{50} (µM) Growth inhibition		IC_{50} (µM) Autophosphorylation inhibition
	Recombinant EGFR kinase	SKBR3 cells	H1975 cells	Mutant EGFR (H1975)
4a	2.2	0.23	0.26	N.D.
4b	2.1	0.51	0.28	0.036
4c	2.2	0.63	1.86	N.D.
4d	2.3	1.42	1.82	N.D.
4e	1.5	1.86	0.39	0.111
4f	2.5	0.36	0.40	N.D.
4g	53.6	6.89	13.87	0.931
4h	18.9	7.70	15.96	2.0
4i	2.7	2.82	0.68	0.275
4j	3.2	1.14	15.69	N.D.
4k	76.5	2.50	>40	N.D.
4l	53.3	>40	>40	N.D.
4m	43.7	4.00	>40	N.D.
4n	9.8	0.39	>40	4.39
4o	3.4	0.40	>40	2.8
10a	3.95	1.4	33.8	0.28
10b	3.71	2.3	>40	N.D.
10c	4.40	>40	>40	N.D.
10d	8.73	3.2	23.8	N.D.
10e	7.38	6.2	15.2	0.13
10f	>150	>40	>40	>5.0
Gefitinib	4	5.36	11.39	13.98
I	3.5	0.20	0.44	0.028

[a]SE ≤ 5%, N.D.: Not determined.

It has also been found that *ortho* substitution on the 4-phenyl ring with fluorine is tolerable as in **4b** and **4e** which are the most potent compounds. Bulkier groups like "Br" or "Me" in the *ortho* position, as in **4a** and **4c**, is still also tolerable while the potency decreased by further increasing the chain length like with the ethyl or methoxy groups, as

in **4h** and **4g**. In addition, extended substituents in the *para* position like ethyl, methoxy, sulfonamide or substituted sulfonamide generally lead to decrease in activity. This indicates that steric hindrance is a limiting factor to substituents at the *ortho* or *para* positions. Similarly, compounds with a sole ethyl substitution at the *meta* position, gave a more potent compound than in the *para* or *ortho* position.

Polar substituents such as the sulfonamide group was found to significantly decrease the activity, but when substituted with heterocylic rings such as the pyridine, the activity increased and resulted in highly potent compound. Furthermore, replacing the quinazoline nucleus with tetrahydropyridothieno[2,3-*d*]pyrimidine nucleus resulted in less potent compounds.

Concerning the activity on the mutant EGFR, several substituents significantly enhanced the activity such as dihalo in **4a** and **4b**, fluoro methyl in **4e**, bromo methoxy in **4f** and *m*-ethyl in **4i**. Some other substituents were found to affect the mutant EGFR potency and should be avoided. This includes substituents such as sulfonamide or substituted sulfonamide anilines as well as the cyclohexylamine which destroy the activity, while bulky substitutents in the *para* or *ortho* positions such as 2,4-dimethoxy, *p*-ethyl or *o*-ethyl as well as the tetrahydropyridothieno[2,3-*d*]pyrimidine derivatives significantly decrease the activity towards the mutant EGFR.

Generally, concerning the cell growth inhibitory activity, it was found that the dihalo substituted anilines at position 4 as **4a** and **4b** are the most potent compounds. Also it was clear that replacing the methyl group in **4d** by methoxy group in **4f** enhanced the activity on the cellular level against both cell lines. The 3-ethyl group in **4i** was also optimum in producing potent compound towards mutant EGFR-expressing cell line.

Docking of the most active compounds **4a**, **4b**, **4e** together with gefitinib and compound **I**, was done to give a better understanding about their binding modes in the ATP binding site of the double mutated and wild type EGFR. Figure 2 clearly demonstrates that gefitinib as well as the most active compounds exhibit a similar binding mode as the co-crystallized ligand **I** towards the wild type EGFR. The 4-anilino substituent of all compounds accommodates the deep hydrophobic pocket of the ATP-binding site. The Michael acceptor group at position 6 of **4a**, **4b**, **4e** and **I** form a covalent interaction with the Cys797, while the side chain of gefitinib extends towards the surface of the pocket.

Figure 3 shows that compounds **4a**, **4b**, **4e** and **I,** having a Michael acceptor group that can potentially form a covalent interaction with Cys797, exhibit a similar binding mode while gefitinib exhibit a totally different binding mode which could explain being very less active towards the double mutated EGFR. The figure also demonstrates that in the presence of a covalent interaction the 4-anilino substituent can still accommodate the back hydrophobic pocket of the mutated EGFR which was not the case with gefitinib.

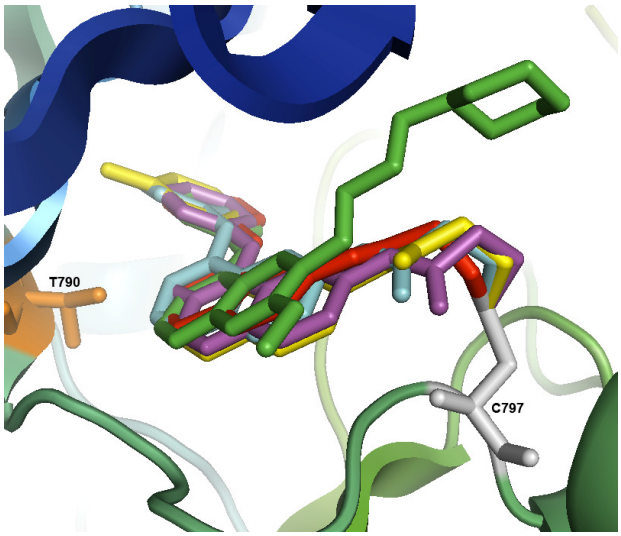

Figure 2. Docked pose of compounds **4a** "cyan", **4b** "magenta", **4e** "yellow", gefitinib "green" and the co-crystallized ligand **I** "red" in the ATP binding site of wild type EGFR (PDB entry 2J5F). All compounds exhibit a similar binding mode as the co-crystallized ligand **I.** The 4-anilino moiety of all compounds accommodates the deep hydrophobic pocket of the ATP-binding site of wild type EGFR. The position 6 side chain of compounds **4a**, **4b**, **4e** and **I** form a covalent interaction with residue Cys797 "grey" while that of gefitinib extends to the surface of the pocket.

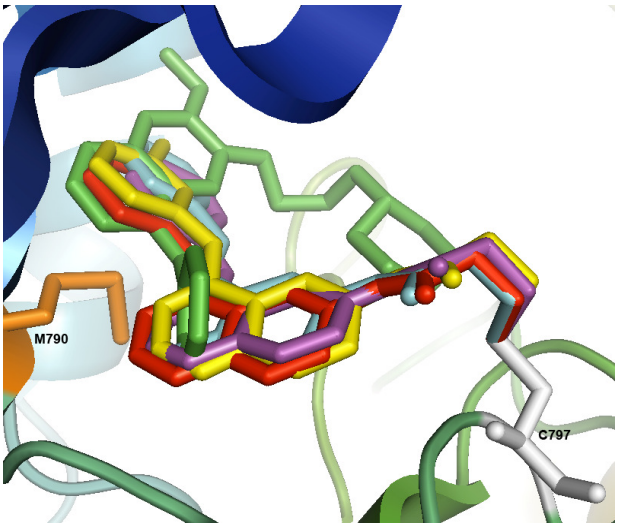

Figure 3. Docked pose of compounds **4a** "cyan", **4b** "magenta", **4e** "yellow", gefitinib "green" and the co-crystallized ligand **I** "red" in the ATP binding site of double mutated EGFR (PDB entry 3W2P). All compounds with a Michael acceptor group **4a**, **4b**, **4e**, **I**, and potentially form a covalent interaction with Cys797 "grey" exhibit a similar binding mode while gefitinib exhibits a totally different binding mode. The 4-anilino moiety of all Michael acceptor group containing compounds accommodate the deep hydrophobic pocket of the ATP-binding site of the double mutated EGFR, while this didn't take place in case of gefitinib.

Conclusions

A series of 6-acrylamide-4-substituted quinazoline derivatives and a series of 7-acrylamide-4-substituted tetrahydropyridothieno[2,3-*d*]pyrimidine derivatives have been

synthesized. Several potent compounds were obtained and were able to overcome the mutation associated drug resistance. Compounds **4a**, **4b** and **4f** were the best compromise showing potent growth inhibitory activities towards cancer cells with mutant or wild type EGFR kinase. Although it is clear that the presence of a potential covalent interaction is the limiting factor and responsible for retaining the activity towards the mutant EGFR, yet the modifications in the substituents on position 4 still have significant influence towards this inhibitory activity which should be taken into consideration to achieve highly potent compounds. Several substituents showed potent inhibitory activity against both mutant and wild type EGFR containing cancer cell lines. While, others seemed to be more potent towards either cell lines such as the *m*-ethyl in **4i** or fluoro methyl in **4e** were more potent towards mutant EGFR expressing cell line. Among the new findings is that substituents like the cyclohexyl amine in **4o** as well as the pyridyl sulfonamide aniline in **4n** resulted in active and potent compounds towards the wild type EGFR while they were not active towards the mutant EGFR. The quinazoline nucleus still remains to be among the best scaffolds since replacing it with a tetrahydropyridothieno[2,3-*d*]pyrimidine scaffold didn't seem to be beneficial towards the EGFR inhibitory activity.

Supporting information

Experimental

Chemistry

Solvents and reagents were obtained from commercial suppliers and used as received. ^{1}H and ^{13}C NMR spectra were recorded on a Bruker DRX 500 spectrometer. Chemical shifts are referenced to the residual protonated solvent signals. The purities of the tested compounds 4a-4p and 10a-10e were determined by HPLC coupled with mass spectrometry and were higher than 95% in all cases. Mass spectrometric analysis (HPLC-ESI-MS) was performed on a TSQ quantum (Thermo Electron Corporation) instrument equipped with an ESI source and a triple quadrupole mass detector (Thermo Finnigan). The MS detection was carried out at a spray voltage of 4.2 kV, a nitrogen sheath gas pressure of 4.0 x 10^5 Pa, an auxiliary gas pressure of 1.0 x 10^5 Pa, a capillary temperature of 400 ºC, a capillary voltage of 35 V, and a source CID of 10 V. All samples were injected by an autosampler (Surveyor, Thermo Finnigan) with an injection volume of 10 μL. An RP C18 NUCLEODUR 100-3 (125 x 3 mm) column (Macherey-Nagel) was used as the stationary phase. The solvent system consisted of water containing 0.1% TFA (A) and 0.1% TFA in acetonitrile (B). HPLC-Method: flow rate 400 μL/min. The percentage of B started at an initial of 5%, was increased up to 100% during 16 min, kept at 100% for 2 min, and flushed back to 5% in 2 min. Melting points are uncorrected and were determined on Buchi melting point apparatus (B-540). The IR spectra were measured on Nicolet 380 FT-IR spectrometer.

Ethyl *N*-(2-cyano-4-nitrophenyl)formimidate (1). 5g (30.6 mmol) of 2-amino-5-nitrobenzonitrile was refluxed in 50ml of triethyl orthoformate for 24 hours in the presence of 10 drops of acetic anhydride. The reaction was then concentrated under vacuum and the remaining residue was poured on ice water where a precipitate has been formed. The ppt. was filtered under vacuum and left to dry to give compound **1**. Yield 82% (5.5 g, solid); IR: 2228.6 cm^{-1} (C≡N); ^{1}H NMR (500 MHz, DMSO-d_6): δ 8.67 (d, *J* = 2.6 Hz, 1H), 8.43 (dd, *J* = 8.9, 2.7 Hz, 1H), 8.22 (s, 1H), 7.46 (d, *J* = 8.9 Hz, 1H), 4.36 (q, *J* = 7.0 Hz, 2H), 1.35 (t, *J* = 7.1 Hz, 3H).

General procedure for the synthesis of *N*-(substituted)-6-nitroquinazolin-4-amine (2a-2o). Compound **1** (5 mmol) was refluxed for 1 hour with the respective amine derivative (5 mmol) in 8ml glacial acetic acid. A precipitate is formed during the reaction which is filtered on hot and the precipitate is then washed with diethyl ether to give the corresponding nitroquinazoline derivatives **2a-2o**. If a precipitate is not formed, the solution is poured on ice water and the formed precipitate is filtered followed by washing with diethyl ether to give the corresponding nitroquinazoline derivative.

***N*-(2-bromo-6-fluorophenyl)-6-nitroquinazolin-4-amine (2a)**. Yield 67% (1.21 g, solid); ^{1}H NMR (500 MHz, DMSO-d_6): δ 10.70 (s, 1H), 9.49 (s, 1H), 8.56 (dd, *J* = 8.9, 1.7 Hz, 2H), 7.90 (s, 1H), 7.78 (dd, *J* = 8.2, 6.1 Hz, 1H), 7.46 (s, 1H), 7.16 (s, 1H). LC/MS (+ESI): m/z = 362.75 (M + H).

***N*-(4-bromo-2-fluorophenyl)-6-nitroquinazolin-4-amine (2b).** Yield 71% (1.28 g, solid); ^{1}H NMR (500 MHz, $(CD_3)_2CO$): δ 9.71 (s, 1H), 9.38 (d, *J* = 1.6 Hz, 1H), 8.70 (s, 1H), 8.60 (dd, *J* = 9.2, 2.1 Hz, 1H), 8.01 (d, *J* = 9.1 Hz, 1H), 7.83 (t, *J* = 8.3 Hz, 1H), 7.54 (d, *J* = 10.0 Hz, 1H), 7.48 (d, *J* = 8.5 Hz, 1H). ^{13}C NMR (126 MHz, $(CD_3)_2CO$) δ 160.60, 158.60, 157.48 (d, $^1J_{C-F}$ = 254.2 Hz), 154.40, 146.12, 131.02, 129.90, 128.47 (d, $^4J_{C-F}$ = 3.4 Hz), 127.45, 120.90, 120.28 (d, $^2J_{C-F}$ = 23.3 Hz), 119.47, 118.37 (d, $^3J_{C-F}$ = 9.2 Hz). 115.26. LC/MS (+ESI): m/z = 362.99 (M + H).

***N*-(4-bromo-2-methylphenyl)-6-nitroquinazolin-4-amine (2c).** Yield 62% (1.11 g, solid); ^{1}H NMR (500 MHz, $(CD_3)_2CO$) δ 9.61 (s, 1H), 9.35 (d, *J* = 1.7 Hz, 1H), 8.58 (dd, *J* = 9.2, 2.4 Hz, 2H), 7.97 (d, *J* = 9.2 Hz, 1H), 7.54 (s, 1H), 7.48 – 7.32 (m, 2H), 2.32 (s, 3H). ^{13}C NMR (126 MHz, $(CD_3)_2CO$): δ 161.08, 158.93, 154.46, 153.48, 145.91, 138.83, 138.82, 134.16, 130.83, 130.82, 130.21, 127.24, 120.95, 115.20, 18.22. LC/MS (+ESI): m/z = 359.02 (M + H).

***N*-(4-bromo-3-methylphenyl)-6-nitroquinazolin-4-amine (2d)**. Yield 65% (1.16 g, solid); ^{1}H NMR (500 MHz, DMSO-d_6) δ 10.41 (s, 1H), 9.61 (d, *J* = 2.4 Hz, 1H), 8.70 (s, 1H), 8.52 (dd, *J* = 9.2, 2.4 Hz, 1H), 7.90 (d, *J* = 9.2 Hz, 1H), 7.81 (d, *J* = 2.4 Hz, 1H), 7.69 (dd, *J* = 8.6, 2.5 Hz, 1H), 7.58 (d, *J* = 8.7 Hz, 1H), 2.37 (s, 3H). ^{13}C NMR (126

MHz, DMSO-d_6) δ 158.53, 157.48, 152.96, 144.50, 138.02, 137.21, 131.95, 129.34, 126.56, 124.87, 122.02, 120.74, 118.81, 114.39, 22.59. LC/MS (+ESI): m/z = 358.86 (M + H).

***N*-(2-fluoro-3-methylphenyl)-6-nitroquinazolin-4-amine (2e).** Yield 67% (0.99 g, solid); ^{1}H NMR (500 MHz, DMSO-d_6) δ 10.49 (s, 1H), 9.58 (s, 1H), 8.61 (s, 1H), 8.55 (dd, J = 9.2, 2.4 Hz, 1H), 7.93 (d, J = 9.1 Hz, 1H), 7.35 (t, J = 6.4 Hz, 1H), 7.24 (t, J = 6.9 Hz, 1H), 7.16 (t, J = 7.7 Hz, 1H), 2.30 (s, 3H). ^{13}C NMR (75 MHz, DMSO-d_6) δ 159.85, 157.94, 155.39 (d, $^1J_{C\text{-}F}$ = 245.9 Hz), 152.95, 144.50, 129.48, 129.40 (d, $^4J_{C\text{-}F}$ = 4.8 Hz), 126.68, 125.87, 125.24 (d, $^3J_{C\text{-}F}$ = 7.8 Hz), 125.05 (d, $^2J_{C\text{-}F}$ = 11.2 Hz), 123.80 (d, $^4J_{C\text{-}F}$ = 4.5 Hz), 120.94, 113.94, 14.22 (d, $^4J_{C\text{-}F}$ = 4.0 Hz). LC/MS (+ESI): m/z = 298.95 (M + H).

***N*-(4-bromo-3-methoxyphenyl)-6-nitroquinazolin-4-amine (2f)**. Yield 75% (1.4 g, solid); ^{1}H NMR (500 MHz, DMSO-d_6) δ 10.39 (s, 1H), 9.62 (d, J = 2.4 Hz, 1H), 8.74 (s, 1H), 8.54 (dd, J = 9.2, 2.4 Hz, 1H), 7.93 (d, J = 9.2 Hz, 1H), 7.67 (d, J = 2.0 Hz, 1H), 7.58 (d, J = 8.6 Hz, 1H), 7.55 (dd, J = 8.6, 2.1 Hz, 1H), 3.89 (s, 3H). ^{13}C NMR (126 MHz, DMSO-d_6) δ 158.59, 157.46, 155.19, 152.99, 144.55, 139.35, 132.37, 130.59, 129.57, 129.36, 126.62, 120.67, 115.88, 107.08, 56.14. LC/MS (+ESI): m/z = 374.73 (M + H).

***N*-(2,4-dimethoxyphenyl)-6-nitroquinazolin-4-amine (2g)**. Yield 70% (1.14 g, solid); ^{1}H NMR (500 MHz, DMSO-d_6): δ 10.12 (s, 1H), 9.57 (d, J = 2.4 Hz, 1H), 8.52 (dd, J = 9.1, 2.6 Hz, 2H), 7.88 (d, J = 9.2 Hz, 1H), 7.29 (d, J = 8.6 Hz, 1H), 6.70 (d, J = 2.6 Hz, 1H), 6.59 (dd, J = 8.6, 2.7 Hz, 1H), 3.81 (s, 3H), 3.76 (s, 3H). ^{13}C NMR (126 MHz, DMSO-d_6): δ 160.40, 159.11, 158.16, 155.24, 153.04, 144.24, 129.24, 128.88, 126.40, 120.90, 119.02, 114.01, 104.62, 99.24, 55.60, 55.40. LC/MS (+ESI): m/z = 327.15 (M + H).

***N*-(2-ethylphenyl)-6-nitroquinazolin-4-amine (2h).** Yield 66% (0.97 g, solid); ^{1}H NMR (500 MHz, DMSO-d_6) δ 10.38 (s, 1H), 9.58 (s, 1H), 8.54 (dd, J = 9.2, 2.4 Hz, 1H), 8.50 (s, 1H), 7.90 (d, J = 9.2 Hz, 1H), 7.37 (d, J = 6.7 Hz, 1H), 7.31 (dd, J = 8.2, 3.5 Hz, 1H), 7.28 (d, J = 3.7 Hz, 2H), 2.56 (q, J = 7.6 Hz, 2H), 1.09 (t, J = 7.6 Hz, 3H). ^{13}C NMR (126 MHz, DMSO-d_6): δ 160.51, 158.20, 153.07, 144.49, 140.91, 135.94, 129.40, 128.90, 128.29, 127.43, 126.70, 126.55, 120.98, 114.02, 24.11, 14.35.

***N*-(3-ethylphenyl)-6-nitroquinazolin-4-amine (2i)**. Yield 69% (1.01 g, solid); ^{1}H NMR (500 MHz, $(CD_3)_2CO$) δ 9.70 (s, 1H), 9.37 (d, J = 2.3 Hz, 1H), 8.74 (s, 1H), 8.56 (dd, J = 9.2, 2.4 Hz, 1H), 7.96 (d, J = 9.2 Hz, 1H), 7.80 (dd, J = 8.1, 1.2 Hz, 1H), 7.75 (t, J = 1.6 Hz, 1H), 7.32 (t, J = 7.8 Hz, 1H), 7.05 (dd, J = 7.6, 0.6 Hz, 1H), 2.68 (q, J = 7.6 Hz, 2H), 1.25 (t, J = 7.6 Hz, 3H). ^{13}C NMR (126 MHz, $(CD_3)_2CO$): δ 159.95, 158.71, 154.53,

145.94, 145.60, 139.63, 130.90, 129.40, 127.13, 125.00, 122.80, 120.90, 120.67, 115.60, 29.48, 15.97.

***N*-(4-ethylphenyl)-6-nitroquinazolin-4-amine (2j).** Yield 67% (0.98 g, solid); ^{1}H NMR (500 MHz, DMSO-d_6): δ 10.35 (s, 1H), 9.58 (d, J = 2.4 Hz, 1H), 8.62 (s, 1H), 8.49 (dd, J = 9.2, 2.4 Hz, 1H), 7.86 (d, J = 9.2 Hz, 1H), 7.67 (d, J = 8.4 Hz, 2H), 7.23 (d, J = 8.5 Hz, 2H), 2.60 (q, J = 7.6 Hz, 2H), 1.19 (t, J = 7.6 Hz, 3H). ^{13}C NMR (126 MHz, DMSO-d_6): δ 158.88, 157.83, 153.12, 144.48, 140.30, 136.00, 129.44, 127.85, 126.57, 123.15, 120.86, 114.40, 27.81, 15.74.

4-((6-nitroquinazolin-4-yl)amino)benzenesulfonamide (2k). Yield 78% (1.34 g, solid); ^{1}H NMR (500 MHz, DMSO-d_6): δ 10.61 (s, 1H), 9.67 (d, J = 2.4 Hz, 1H), 8.78 (s, 1H), 8.57 (dd, J = 9.2, 2.4 Hz, 1H), 8.07 (d, J = 8.8 Hz, 2H), 7.96 (d, J = 9.2 Hz, 1H), 7.88 (d, J = 8.8 Hz, 2H), 7.32 (s, 2H). ^{13}C NMR (126 MHz, DMSO-d_6): δ 158.72, 157.40, 153.03, 144.68, 141.53, 139.28, 129.63, 126.76, 126.30, 122.17, 120.83, 114.44. LC/MS (+ESI): m/z = 346.09 (M + H).

***N*-carbamimidoyl-4-((6-nitroquinazolin-4-yl)amino)benzenesulfonamide (2l).** Yield 75% (1.45 g, solid); ^{1}H NMR (500 MHz, DMSO-d_6) δ 10.58 (s, 1H), 9.66 (d, J = 1.9 Hz, 1H), 8.77 (s, 1H), 8.56 (dd, J = 9.2, 2.5 Hz, 1H), 8.00 (d, J = 8.6 Hz, 2H), 7.95 (d, J = 9.2 Hz, 1H), 7.83 – 7.81 (m, 1H), 7.81 – 7.79 (m, 1H), 6.72 (s, 4H). ^{13}C NMR (126 MHz, DMSO-d_6) δ 158.71, 158.13, 157.47, 153.04, 144.66, 141.00, 139.86, 129.62, 126.77, 126.23, 122.07, 120.87, 114.46. LC/MS (+ESI): m/z = 387.87 (M + H).

4-((6-nitroquinazolin-4-yl)amino)-*N*-(thiazol-2-yl)benzenesulfonamide (2m). Yield 73% (1.56 g, solid); ^{1}H NMR (500 MHz, DMSO-d_6) δ 12.72 (s, 1H), 10.60 (s, 1H), 9.66 (d, J = 2.2 Hz, 1H), 8.77 (s, 1H), 8.55 (dd, J = 9.2, 2.4 Hz, 1H), 8.06 (d, J = 8.7 Hz, 2H), 7.95 (d, J = 9.2 Hz, 1H), 7.88 – 7.86 (m, 1H), 7.86 – 7.84 (m, 1H), 7.26 (d, J = 4.6 Hz, 1H), 6.84 (d, J = 4.6 Hz, 1H). ^{13}C NMR (126 MHz, DMSO-d_6) δ 168.80, 158.66, 157.40, 153.04, 144.69, 141.82, 137.32, 129.66, 126.80, 126.55, 124.51, 122.06, 120.87, 114.47, 108.19. LC/MS (+ESI): m/z = 428.79 (M + H).

4-((6-nitroquinazolin-4-yl)amino)-*N*-(pyridin-2-yl)benzenesulfonamide (2n). Yield 75% (1.58 g, solid); ^{1}H NMR (500 MHz, DMSO-d_6): δ 11.90 (s, 1H), 10.59 (s, 1H), 9.66 (d, J = 2.3 Hz, 1H), 8.78 (s, 1H), 8.56 (dd, J = 9.2, 2.4 Hz, 1H), 8.07 (d, J = 8.8 Hz, 2H), 8.03 (dd, J = 5.5, 1.1 Hz, 1H), 7.96 (d, J = 9.2 Hz, 1H), 7.95 – 7.91 (m, 2H), 7.73 (ddd, J = 8.9, 7.2, 1.9 Hz, 1H), 7.19 (d, J = 8.7 Hz, 1H), 6.88 (ddd, J = 7.0, 5.5, 0.9 Hz, 1H). ^{13}C NMR (126 MHz, DMSO-d_6): δ 158.64, 157.35, 153.03, 144.70, 141.98, 140.23, 140.21, 136.69, 136.67, 129.65, 127.35, 126.79, 121.94, 120.84, 115.72, 114.48, 113.65. LC/MS (+ESI): m/z = 423.09 (M + H).

***N*-cyclohexyl-6-nitroquinazolin-4-amine (2o)**. Yield 55% (0.74 g, solid); ^{1}H NMR (500 MHz, $(CD_3)_2CO$): δ 9.10 (d, *J* = 2.5 Hz, 1H), 8.60 (s, 1H), 8.47 (dd, *J* = 9.2, 2.5 Hz, 1H), 7.84 (d, *J* = 9.2 Hz, 1H), 4.51 – 4.15 (m, 1H), 2.16 – 2.10 (m, 2H), 2.09 (s, 1H), 1.86 – 1.79 (m, 2H), 1.73 – 1.67 (m, 1H), 1.50 – 1.41 (m, 4H), 1.29 – 1.18 (m, 1H). ^{13}C NMR (126 MHz, $(CD_3)_2CO$) δ 160.76, 159.34, 154.42, 145.33, 130.43, 126.73, 120.63, 115.20, 51.30, 33.05, 26.39, 26.04. LC/MS (+ESI): m/z = 273.17 (M + H).

General procedure for the synthesis of compunds (3a-3o). According to the reported procedure,[1] a mixture of the respective nitroquinazoline derivative **2a-2o** (3 mmol) and stannous chloride (15 mmol) in MeOH (20 ml) was stirred at reflux for 1 h under nitrogen atmosphere. The excess MeOH was removed under reduced pressure; the remaining residue was dissolved in ethyl acetate (200 ml) and basified with aqueous $NaHCO_3$ solution. The resulting mixture was filtrated under vacuum followed by separation of the organic phase from the aqueous phase. The aqueous phase was extracted with ethyl acetate (2 x 20 ml), these organic fractions were combined, dried over anhydrous $MgSO_4$ and concentrated under reduced pressure to obtain the corresponding aminoquinazoline derivatives **3a-3o.**

***N*^{4}-(2-bromo-6-fluorophenyl)quinazoline-4,6-diamine (3a)**. Yield 75% (0.75 g, solid); ^{1}H NMR (500 MHz, DMSO-d_6): δ 9.19 (s, 1H), 8.18 (s, 1H), 7.72 (dd, *J* = 8.8, 6.0 Hz, 1H), 7.65 (s, 1H), 7.50 (d, *J* = 7.8 Hz, 1H), 7.23 (d, *J* = 15.8 Hz, 2H), 7.04 (d, *J* = 6.7 Hz, 1H), 5.66 (s, 2H). LC/MS (+ESI): m/z = 332.85 (M + H).

***N*^{4}-(4-bromo-2-fluorophenyl)quinazoline-4,6-diamine (3b).** Yield 78% (0.78 g, solid); ^{1}H NMR (300 MHz, DMSO-d_6) δ 9.29 (s, 1H), 8.22 (s, 1H), 7.61 (dd, *J* = 9.9, 2.2 Hz, 1H), 7.55 (dd, *J* = 8.7, 6.4 Hz, 2H), 7.43 (dd, *J* = 8.6, 1.3 Hz, 1H), 7.27 (d, *J* = 2.2 Hz, 1H), 7.24 (s, 1H), 5.63 (s, 2H). ^{13}C NMR (75 MHz, DMSO-d_6) δ 156.47, 156.39 (d, $^{1}J_{C-F}$ = 251.5 Hz), 149.85, 147.34, 142.55, 128.89 (d, $^{5}J_{C-F}$ = 2.4 Hz), 128.61, 127.35 (d, $^{4}J_{C-F}$ = 3.5 Hz), 126.97 (d, $^{3}J_{C-F}$ = 11.8 Hz), 123.87, 119.12 (d, $^{2}J_{C-F}$ = 23.7 Hz), 116.95 (d, $^{3}J_{C-F}$ = 9.2 Hz). 116.35, 100.82. LC/MS (+ESI): m/z = 332.84 (M + H).

***N*^{4}-(4-bromo-2-methylphenyl)quinazoline-4,6-diamine (3c).** Yield 78% (0.77 g, solid); ^{1}H NMR (500 MHz, $(CD_3)_2CO$): δ 8.28 (s, 1H), 8.26 (s, 1H), 7.60 (t, *J* = 8.4 Hz, 2H), 7.47 (d, *J* = 1.8 Hz, 1H), 7.39 (dd, *J* = 8.5, 2.1 Hz, 1H), 7.34 – 7.29 (m, 2H), 5.12 (s, 2H), 2.31 (s, 3H). ^{13}C NMR (126 MHz, $(CD_3)_2CO$): δ 157.84, 151.60, 148.04, 144.58, 138.37, 137.05, 133.76, 130.29, 129.87, 128.81, 124.41, 118.54, 117.41, 101.75, 18.21. LC/MS (+ESI): m/z = 329.0 (M + H).

***N*^{4}-(4-bromo-3-methylphenyl)quinazoline-4,6-diamine (3d).** Yield 80% (0.79 g, solid); ^{1}H NMR (500 MHz, DMSO-d_6) δ 9.34 (s, 1H), 8.35 (s, 1H), 7.86 (d, *J* = 2.4 Hz, 1H), 7.71 (dd, *J* = 8.7, 2.6 Hz, 1H), 7.54 (d, *J* = 6.7 Hz, 1H), 7.52 (d, *J* = 6.5 Hz, 1H), 7.35 (d,

J = 2.3 Hz, 1H), 7.25 (dd, *J* = 8.9, 2.4 Hz, 1H), 5.57 (s, 2H), 2.36 (s, 3H). ^{13}C NMR (126 MHz, DMSO-d_6): δ 155.80, 149.68, 147.26, 142.65, 139.54, 136.84, 131.74, 128.67, 123.79, 123.68, 120.98, 116.91, 116.68, 100.96, 22.68.

***N*^{4}-(2-fluoro-3-methylphenyl)quinazoline-4,6-diamine (3e).** Yield 82% (0.66 g, solid); ^{1}H NMR (500 MHz, DMSO-d_6) δ 9.17 (s, 1H), 8.21 (s, 1H), 7.52 (d, *J* = 8.8 Hz, 1H), 7.40 (td, *J* = 7.5, 2.1 Hz, 1H), 7.27 (d, *J* = 2.2 Hz, 1H), 7.24 (dd, *J* = 8.8, 2.4 Hz, 1H), 7.15 – 7.07 (m, 2H), 5.59 (s, 2H), 2.27 (d, *J* = 1.9 Hz, 3H). ^{13}C NMR (126 MHz, DMSO-d_6) δ 156.88, 155.13 (d, $^1J_{C-F}$ = 245.4 Hz), 150.11, 147.20, 142.48, 128.57, 127.85 (d, $^4J_{C-F}$ = 4.6 Hz), 126.92 (d, $^3J_{C-F}$ = 12.7 Hz), 125.26, 124.61 (d, $^2J_{C-F}$ = 16.2 Hz), 123.66, 123.49 (d, $^4J_{C-F}$ = 4.2 Hz), 116.34, 101.00, 14.28 (d, $^4J_{C-F}$ = 4.0 Hz). LC/MS (+ESI): m/z = 268.97 (M + H).

***N*^{4}-(4-bromo-3-methoxyphenyl)quinazoline-4,6-diamine (3f).** Yield 83% (0.86 g, solid); ^{1}H NMR (500 MHz, DMSO-d_6) δ 9.97 (s, 2H), 8.48 (s, 1H), 7.95 (s, 1H), 7.70 (d, *J* = 2.1 Hz, 1H), 7.61 (d, *J* = 8.9 Hz, 1H), 7.55 (d, *J* = 8.6 Hz, 1H), 7.52 (dd, *J* = 8.6, 2.1 Hz, 1H), 7.46 (d, *J* = 2.3 Hz, 1H), 7.33 (dd, *J* = 8.9, 2.4 Hz, 1H), 3.86 (s, 3H). ^{13}C NMR (126 MHz, DMSO-d_6) δ 156.48, 155.17, 148.32, 148.12, 140.05, 138.45, 132.28, 126.07, 124.36, 116.33, 115.63, 106.92, 104.50, 101.23, 56.09. LC/MS (+ESI): m/z = 344.88 (M + H).

***N*^{4}-(2,4-dimethoxyphenyl)quinazoline-4,6-diamine (3g).** Yield 80% (0.70 g, solid); ^{1}H NMR (500 MHz, DMSO-d_6): δ 8.53 (s, 1H), 8.18 (s, 1H), 7.66 (d, *J* = 8.7 Hz, 1H), 7.49 (d, *J* = 9.3 Hz, 1H), 7.26 – 7.15 (m, 2H), 6.68 (d, *J* = 2.6 Hz, 1H), 6.56 (dd, *J* = 8.7, 2.6 Hz, 1H), 5.53 (s, 2H), 3.80 (s, 3H), 3.79 (s, 3H). ^{13}C NMR (126 MHz, DMSO-d_6): δ 157.45, 156.80, 153.54, 150.29, 147.10, 142.16, 128.58, 126.49, 123.24, 121.01, 116.26, 104.29, 100.56, 99.01, 55.72, 55.33. LC/MS (+ESI): m/z = 297.19 (M + H).

***N*^{4}-(2-ethylphenyl)quinazoline-4,6-diamine (3h).** Yield 79% (0.62 g, solid); ^{1}H NMR (500 MHz, DMSO-d_6): δ 9.10 (s, 1H), 8.09 (s, 1H), 7.49 (d, *J* = 8.8 Hz, 1H), 7.33 – 7.26 (m, 3H), 7.26 – 7.19 (m, 3H), 5.52 (s, 2H), 2.55 (q, *J* = 7.5 Hz, 2H), 1.08 (t, *J* = 7.5 Hz, 3H). ^{13}C NMR (126 MHz, DMSO-d_6): δ 157.69, 150.40, 147.01, 142.17, 140.61, 137.17, 128.47, 128.39, 128.18, 126.27, 126.11, 123.36, 116.07, 101.16, 24.08, 14.09.

***N*^{4}-(3-ethylphenyl)quinazoline-4,6-diamine (3i).** Yield 77% (0.61 g, solid); ^{1}H NMR (300 MHz, DMSO-d_6) δ 9.27 (s, 1H), 8.32 (s, 1H), 7.73 (d, *J* = 8.1 Hz, 1H), 7.66 (s, 1H), 7.52 (d, *J* = 8.9 Hz, 1H), 7.37 (d, *J* = 2.3 Hz, 1H), 7.27 (d, *J* = 7.5 Hz, 1H), 7.22 (d, *J* = 2.4 Hz, 1H), 6.91 (d, *J* = 7.5 Hz, 1H), 5.57 (s, 2H), 2.62 (q, *J* = 7.6 Hz, 2H), 1.21 (t, *J* = 7.6 Hz, 3H). ^{13}C NMR (75 MHz, DMSO-d_6) δ 156.08, 149.93, 147.22, 143.85, 142.55, 139.93, 128.64, 128.24, 123.54, 122.42, 121.06, 119.27, 116.72, 101.16, 28.34, 15.63. LC/MS (+ESI): m/z = 265.02 (M + H).

***N*⁴-(4-ethylphenyl)quinazoline-4,6-diamine (3j)**. Yield 78% (0.62 g, solid); ^{1}H NMR (500 MHz, DMSO-d_6) δ 9.25 (s), 8.29 (s), 7.73 (d, *J* = 8.5 Hz), 7.51 (d, *J* = 8.8 Hz), 7.36 (d, *J* = 2.3 Hz), 7.23 (dd, *J* = 8.9, 2.4 Hz), 7.18 (d, *J* = 8.5 Hz), 5.53 (s), 2.59 (q, *J* = 7.6 Hz), 1.19 (t, *J* = 7.6 Hz). ^{13}C NMR (126 MHz, DMSO-d_6): δ 156.09, 149.95, 147.10, 142.51, 138.35, 137.51, 128.57, 127.53, 123.43, 121.95, 116.61, 101.16, 27.66, 15.78.

4-((6-aminoquinazolin-4-yl)amino)benzenesulfonamide (3k). Yield 82% (0.77 g, solid); ^{1}H NMR (500 MHz, DMSO-d_6): δ 9.63 (s, 1H), 8.40 (s, 1H), 8.07 (d, *J* = 8.7 Hz, 2H), 7.80 (d, *J* = 8.8 Hz, 2H), 7.57 (d, *J* = 8.9 Hz, 1H), 7.37 (d, *J* = 2.2 Hz, 1H), 7.28 (dd, *J* = 8.9, 2.2 Hz, 1H), 7.23 (s, 2H), 5.64 (s, 2H). ^{13}C NMR (126 MHz, DMSO-d_6): δ 155.64, 149.45, 147.46, 143.17, 142.82, 137.43, 128.73, 126.24, 123.98, 120.52, 116.82, 100.81. LC/MS (+ESI): m/z = 316.15 (M + H).

4-((6-aminoquinazolin-4-yl)amino)-N-carbamimidoylbenzenesulfonamide (3l). Yield 85% (0.91 g, solid); ^{1}H NMR (500 MHz, DMSO-d_6): δ 9.56 (s, 1H), 8.39 (s, 1H), 8.00 (d, *J* = 8.8 Hz, 2H), 7.73 (d, *J* = 8.9 Hz, 2H), 7.56 (d, *J* = 8.9 Hz, 1H), 7.36 (d, *J* = 2.3 Hz, 1H), 7.27 (dd, *J* = 8.9, 2.4 Hz, 1H), 6.68 (s, 4H), 5.62 (s, 2H). ^{13}C NMR (126 MHz, DMSO-d_6): δ 158.04, 155.66, 149.52, 147.40, 142.82, 142.60, 138.03, 128.73, 126.12, 123.90, 120.41, 116.81, 100.86.

4-((6-aminoquinazolin-4-yl)amino)-N-(thiazol-2-yl)benzenesulfonamide (3m). Yield 79% (0.94 g, solid); ^{1}H NMR (500 MHz, DMSO-d_6): δ 9.67 (d, *J* = 4.9 Hz, 1H), 8.39 (s, 1H), 8.04 (d, *J* = 8.8 Hz, 2H), 7.85 (s, 1H), 7.80 – 7.75 (m, 2H), 7.56 (d, *J* = 8.9 Hz, 1H), 7.35 (d, *J* = 2.3 Hz, 1H), 7.24 (d, *J* = 4.6 Hz, 1H), 6.85 – 6.82 (m, 1H), 6.81 (d, *J* = 4.6 Hz, 1H), 5.64 (s, 2H). ^{13}C NMR (126 MHz, DMSO-d_6): δ 155.60, 149.36, 147.48, 144.70, 135.47, 128.61, 126.49, 124.41, 124.00, 122.07, 121.54, 120.47, 116.83, 108.00, 100.82.

4-((6-aminoquinazolin-4-yl)amino)-N-(pyridin-2-yl)benzenesulfonamide (3n). Yield 83% (0.97 g, solid); ^{1}H NMR (500 MHz, DMSO-d_6) δ 11.73 (s, 1H), 9.66 (s, 1H), 8.40 (s, 1H), 8.06 (d, *J* = 1.8 Hz, 1H), 8.05 (d, *J* = 5.2 Hz, 2H), 7.88 – 7.83 (m, 2H), 7.71 (ddd, *J* = 8.7, 7.2, 1.9 Hz, 1H), 7.56 (d, *J* = 8.9 Hz, 1H), 7.34 (d, *J* = 2.3 Hz, 1H), 7.28 (dd, *J* = 8.9, 2.4 Hz, 1H), 7.17 (dt, *J* = 8.6, 0.9 Hz, 1H), 6.88 (ddd, *J* = 7.1, 5.4, 0.9 Hz, 1H), 5.68 (s, 2H). ^{13}C NMR (126 MHz, DMSO-d_6) δ 155.56, 152.86, 149.34, 147.54, 143.71, 142.72, 139.89, 134.51, 128.66, 127.42, 124.07, 122.00, 120.39, 116.88, 116.06, 113.31, 100.79. LC/MS (+ESI): m/z = 392.92 (M + H).

***N*⁴-cyclohexylquinazoline-4,6-diamine (3o).** Yield 80% (0.58 g, solid); ^{1}H NMR (500 MHz, $(CD_3)_2CO$): δ 8.23 (d, *J* = 42.6 Hz, 1H), 7.44 (dd, *J* = 42.8, 8.8 Hz, 1H), 7.13 (td, *J* = 33.1, 16.5 Hz, 2H), 6.49 (d, *J* = 32.5 Hz, 1H), 4.84 (d, *J* = 36.6 Hz, 2H), 4.21 (s, 1H),

2.02 – 1.94 (m, 2H), 1.82 – 1.57 (m, 3H), 1.48 – 1.27 (m, 4H), 1.25 – 1.08 (m, 1H). ^{13}C NMR (126 MHz, $(CD_3)_2CO$): δ 158.45, 152.40, 147.24, 143.95, 129.83, 123.51, 102.34, 84.10, 50.28, 33.49, 26.52, 26.09. LC/MS (+ESI): m/z = 243.21 (M + H).

General procedure for the synthesis of compounds (4a-4j, 4o). A mixture of the corresponding aminoquinazoline derivative **3a-3j, 3o** (1 mmol) and $NaHCO_3$ (1.3 mmol) was stirred at 0°C in acetone (10 ml) under nitrogen atmosphere. This is then followed by dropwise addition of acryloyl chloride (1.3 mmol) and then was stirred for 30 min. at 0°C. Excess solvent was then removed under reduced pressure and the remaining residue was neutralized using $NaHCO_3$ solution. The formed solid was then filtered and the purified using column chromatography with ethylacetate as eluent.

General procedure for the synthesis of compounds (4k-4n).
Same above procedure except that the solvent used in the reaction was DMF instead of acetone and the eluent in column chromatography was Dichloromethane:Methanol 100:5.

***N*-(4-((2-bromo-6-fluorophenyl)amino)quinazolin-6-yl)acrylamide (4a).** Yield 56% (0.21 g, solid); m.p. 303-304°C; ^{1}H NMR (500 MHz, DMSO-d_6): δ 10.52 (s, 1H), 9.78 (s, 1H), 8.81 (s, 1H), 8.46 (s, 1H), 7.92 (d, *J* = 8.3 Hz, 1H), 7.85 – 7.72 (m, 2H), 7.63 (s, 1H), 7.14 (s, 1H), 6.53 (dd, *J* = 16.5, 10.4 Hz, 1H), 6.34 (d, *J* = 16.9 Hz, 1H), 5.83 (d, *J* = 10.1 Hz, 1H). LC/MS (+ESI): m/z = 386.99 (M + H).

***N*-(4-((4-bromo-2-fluorophenyl)amino)quinazolin-6-yl)acrylamide (4b).** Yield 58% (0.22 g, solid); m.p. 234-236°C; ^{1}H NMR (500 MHz, DMSO-d_6): δ 10.50 (s, 1H), 9.91 (s, 1H), 8.81 (s, 1H), 8.40 (s, 1H), 7.89 (dd, *J* = 8.9, 2.1 Hz, 1H), 7.77 (d, *J* = 8.5 Hz, 1H), 7.67 – 7.57 (m, 1H), 7.49 (s, 1H), 7.45 (dd, *J* = 8.3, 1.6 Hz, 1H), 6.52 (dd, *J* = 17.0, 10.1 Hz, 1H), 6.34 (dd, *J* = 17.0, 1.9 Hz, 1H), 5.83 (dd, *J* = 10.1, 1.9 Hz, 1H). LC/MS (+ESI): m/z = 386.99 (M + H).

***N*-(4-((4-bromo-2-methylphenyl)amino)quinazolin-6-yl)acrylamide (4c).** Yield 59% (0.22 g, solid); m.p. 261-262°C; ^{1}H NMR (500 MHz, DMSO-d_6): δ 10.46 (s, 1H), 9.66 (s, 1H), 8.78 (d, *J* = 2.1 Hz, 1H), 8.36 (s, 1H), 7.87 (dd, *J* = 9.0, 2.2 Hz, 1H), 7.76 (d, *J* = 8.9 Hz, 1H), 7.53 (d, *J* = 1.9 Hz, 1H), 7.42 (dd, *J* = 8.4, 2.1 Hz, 1H), 7.29 (d, *J* = 8.4 Hz, 1H), 6.53 (dd, *J* = 17.0, 10.2 Hz, 1H), 6.34 (dd, *J* = 17.0, 1.9 Hz, 1H), 5.83 (dd, *J* = 10.1, 1.9 Hz, 1H), 2.17 (s, 3H). ^{13}C NMR (126 MHz, DMSO-d_6): δ 163.29, 158.44, 153.60, 146.55, 137.62, 137.14, 136.40, 132.77, 131.59, 129.38, 128.96, 128.33, 127.29, 126.93, 118.41, 115.00, 112.28, 17.77. LC/MS (+ESI): m/z = 383.03 (M + H).

***N*-(4-((4-bromo-3-methylphenyl)amino)quinazolin-6-yl)acrylamide (4d)**. Yield 63% (0.24 g, solid); m.p. 296-297°C; ^{1}H NMR (500 MHz, DMSO-d_6): δ 10.47 (s, 1H), 9.83 (s, 1H), 8.80 (d, *J* = 2.0 Hz, 1H), 8.54 (s, 1H), 7.89 (dd, *J* = 9.0, 2.2 Hz, 1H), 7.82 (d, *J* = 2.4

Hz, 1H), 7.79 (d, *J* = 8.9 Hz, 1H), 7.66 (dd, *J* = 8.6, 2.5 Hz, 1H), 7.56 (d, *J* = 8.7 Hz, 1H), 6.53 (dd, *J* = 17.0, 10.2 Hz, 1H), 6.35 (dd, *J* = 17.0, 1.9 Hz, 1H), 5.84 (dd, *J* = 10.1, 1.9 Hz, 1H), 2.37 (s, 3H). ^{13}C NMR (126 MHz, DMSO-d_6): δ 163.30, 157.37, 153.23, 146.73, 138.97, 136.96, 136.51, 131.81, 131.55, 128.43, 127.39, 127.15, 124.57, 121.71, 117.73, 115.44, 112.38, 22.65. LC/MS (+ESI): m/z = 383.05 (M + H).

***N*-(4-((2-fluoro-3-methylphenyl)amino)quinazolin-6-yl)acrylamide (4e).** Yield 65% (0.21 g, solid); m.p. 229-231°C; ^{1}H NMR (500 MHz, DMSO-d_6): δ 10.48 (s, 1H), 9.75 (s, 1H), 8.81 (d, *J* = 1.8 Hz, 1H), 8.42 (s, 1H), 7.88 (dd, *J* = 9.0, 2.1 Hz, 1H), 7.78 (d, *J* = 8.9 Hz, 1H), 7.37 (t, *J* = 7.0 Hz, 1H), 7.17 (t, *J* = 6.7 Hz, 1H), 7.12 (t, *J* = 7.7 Hz, 1H), 6.53 (dd, *J* = 17.0, 10.1 Hz, 1H), 6.34 (dd, *J* = 17.0, 1.8 Hz, 1H), 5.83 (dd, *J* = 10.2, 1.8 Hz, 1H), 2.29 (s, 3H). ^{13}C NMR (126 MHz, DMSO-d_6) δ 163.31, 158.37, 155.30 (d, $^{1}J_{C\text{-}F}$ = 246.1 Hz), 153.57, 146.55, 136.47, 131.58, 128.41, 128.36, 127.32, 126.96, 126.49 (d, $^{3}J_{C\text{-}F}$ = 12.7 Hz), 125.46, 124.72 (d, $^{2}J_{C\text{-}F}$ = 16.1 Hz), 123.56 (d, $^{4}J_{C\text{-}F}$ = 4.1 Hz). 115.06, 112.22, 14.25 (d, $^{4}J_{C\text{-}F}$ = 3.9 Hz). LC/MS (+ESI): m/z = 323.18 (M + H).

***N*-(4-((4-bromo-3-methoxyphenyl)amino)quinazolin-6-yl)acrylamide (4f).** Yield 62% (0.25 g, solid); m.p. 268-269°C; ^{1}H NMR (500 MHz, DMSO-d_6): δ 10.49 (s, 1H), 9.85 (s, 1H), 8.81 (d, *J* = 2.1 Hz, 1H), 8.58 (s, 1H), 7.91 (dd, *J* = 9.0, 2.2 Hz, 1H), 7.80 (d, *J* = 8.9 Hz, 1H), 7.69 (d, *J* = 2.0 Hz, 1H), 7.56 (dd, *J* = 8.7, 2.1 Hz, 1H), 7.54 (d, *J* = 8.6 Hz, 1H), 6.53 (dd, *J* = 17.0, 10.2 Hz, 1H), 6.35 (dd, *J* = 17.0, 1.9 Hz, 1H), 5.84 (dd, *J* = 10.1, 1.9 Hz, 1H), 3.87 (s, 3H). ^{13}C NMR (126 MHz, DMSO-d_6): δ 163.33, 157.28, 155.13, 153.16, 146.74, 140.38, 136.58, 132.22, 131.53, 128.49, 127.45, 127.18, 115.50, 115.35, 112.27, 106.60, 103.98, 56.04. LC/MS (+ESI): m/z = 399.02 (M + H).

***N*-(4-((2,4-dimethoxyphenyl)amino)quinazolin-6-yl)acrylamide (4g)**. Yield 68% (0.24 g, solid); m.p. 178-180°C; ^{1}H NMR (500 MHz, DMSO-d_6): δ 10.45 (s, 1H), 9.13 (s, 1H), 8.68 (d, *J* = 2.0 Hz, 1H), 8.36 (s, 1H), 7.89 (dd, *J* = 9.0, 2.2 Hz, 1H), 7.73 (d, *J* = 8.9 Hz, 1H), 7.49 (d, *J* = 8.6 Hz, 1H), 6.69 (d, *J* = 2.6 Hz, 1H), 6.57 (dd, *J* = 8.7, 2.7 Hz, 1H), 6.52 (dd, *J* = 17.0, 10.2 Hz, 1H), 6.33 (dd, *J* = 17.0, 1.9 Hz, 1H), 5.82 (dd, *J* = 10.1, 1.9 Hz, 1H), 3.80 (s, 3H), 3.77 (s, 3H). ^{13}C NMR (126 MHz, DMSO-d_6): δ 163.32, 158.46, 158.10, 154.31, 153.77, 146.38, 136.29, 131.62, 128.28, 127.40, 127.25, 126.68, 120.47, 115.04, 111.94, 104.41, 99.13, 55.68, 55.35. LC/MS (+ESI): m/z = 351.18 (M + H).

***N*-(4-((2-ethylphenyl)amino)quinazolin-6-yl)acrylamide (4h)**. Yield 61% (0.19 g, solid); m.p. 148-150°C; ^{1}H NMR (500 MHz, DMSO-d_6) δ 10.49 (s, 1H), 9.66 (s, 1H), 8.73 (s, 1H), 8.31 (s, 1H), 7.90 (dd, *J* = 8.9, 1.8 Hz, 1H), 7.74 (d, *J* = 8.9 Hz, 1H), 7.33 (d, *J* = 4.3 Hz, 1H), 7.26 (d, *J* = 4.1 Hz, 3H), 6.52 (dd, *J* = 17.0, 10.2 Hz, 1H), 6.33 (dd, *J* = 17.0, 1.5 Hz, 1H), 5.82 (dd, *J* = 10.2, 1.4 Hz, 1H), 2.55 (q, *J* = 7.5 Hz, 2H), 1.08 (t, *J* = 7.5 Hz, 3H). ^{13}C NMR (126 MHz, DMSO-d_6): δ 163.84, 159.56, 154.32, 146.90, 141.22,

137.33, 136.77, 132.01, 129.05, 128.68, 127.89, 127.42, 127.11, 126.70, 115.38, 112.90, 112.87, 24.54, 14.60. LC/MS (+ESI): m/z = 319.21 (M + H).

***N*-(4-((3-ethylphenyl)amino)quinazolin-6-yl)acrylamide (4i)**. Yield 65% (0.21 g, solid); m.p. 216-217°C; ^{1}H NMR (500 MHz, DMSO-d_6): δ 10.45 (s, 1H), 9.74 (s, 1H), 8.79 (d, *J* = 2.1 Hz, 1H), 8.52 (s, 1H), 7.90 (dd, *J* = 8.9, 2.2 Hz, 1H), 7.77 (d, *J* = 8.9 Hz, 1H), 7.69 (dd, *J* = 8.1, 1.1 Hz, 1H), 7.63 (t, *J* = 1.6 Hz, 1H), 7.28 (t, *J* = 7.8 Hz, 1H), 6.97 (dd, *J* = 7.6, 0.5 Hz, 1H), 6.53 (dd, *J* = 17.0, 10.2 Hz, 1H), 6.35 (dd, *J* = 17.0, 1.9 Hz, 1H), 5.83 (dd, *J* = 10.1, 1.9 Hz, 1H), 2.63 (q, *J* = 7.6 Hz, 2H), 1.22 (t, *J* = 7.6 Hz, 3H). ^{13}C NMR (126 MHz, DMSO-d_6): δ 163.28, 157.56, 153.41, 146.71, 143.88, 139.34, 136.36, 131.58, 128.34, 128.22, 127.32, 127.05, 123.03, 121.68, 119.88, 115.45, 112.58, 28.23, 15.50. LC/MS (+ESI): m/z = 319.19 (M + H).

***N*-(4-((4-ethylphenyl)amino)quinazolin-6-yl)acrylamide (4j)**. Yield 63% (0.20 g, solid); m.p. 229-230°C; ^{1}H NMR (500 MHz, DMSO-d_6) δ 10.45 (s, 1H), 9.74 (s, 1H), 8.77 (d, *J* = 1.3 Hz, 1H), 8.48 (s, 1H), 7.89 (dd, *J* = 8.9, 1.8 Hz, 1H), 7.76 (d, *J* = 8.9 Hz, 1H), 7.70 (d, *J* = 8.3 Hz, 2H), 7.21 (d, *J* = 8.3 Hz, 2H), 6.53 (dd, *J* = 17.0, 10.2 Hz, 1H), 6.34 (dd, *J* = 17.0, 1.5 Hz, 1H), 5.83 (dd, *J* = 10.2, 1.5 Hz, 1H), 2.61 (q, *J* = 7.5 Hz, 2H), 1.20 (t, *J* = 7.6 Hz, 3H). ^{13}C NMR (126 MHz, DMSO-d_6): δ 163.28, 157.59, 153.44, 146.68, 139.05, 136.95, 136.32, 131.58, 128.31, 127.58, 127.31, 127.00, 122.60, 115.40, 112.56, 27.67, 15.71. MS (+ESI): m/z = 319.2 (M + H).

***N*-(4-((4-sulfamoylphenyl)amino)quinazolin-6-yl)acrylamide (4k).** Yield 59% (0.22 g, solid); m.p. 269-271°C; ^{1}H NMR (500 MHz, DMSO-d_6): δ 10.52 (s, 1H), 10.09 (s, 1H), 8.84 (d, *J* = 1.9 Hz, 1H), 8.61 (s, 1H), 8.04 (d, *J* = 8.8 Hz, 2H), 7.93 (dd, *J* = 9.0, 2.1 Hz, 1H), 7.83 (d, *J* = 8.7 Hz, 3H), 7.27 (s, 2H), 6.53 (dd, *J* = 17.0, 10.1 Hz, 1H), 6.35 (dd, *J* = 17.0, 1.7 Hz, 1H), 5.85 (dd, *J* = 10.1, 1.7 Hz, 1H). ^{13}C NMR (126 MHz, DMSO-d_6): δ 163.38, 157.32, 153.06, 146.86, 142.61, 138.19, 136.72, 131.50, 128.54, 127.52, 127.32, 126.23, 121.40, 115.57, 112.24. LC/MS (+ESI): m/z = 370.09 (M + H).

***N*-(4-((4-(*N*-carbamimidoylsulfamoyl)phenyl)amino)quinazolin-6-yl)acrylamide (4l).** Yield, 55% (0.23 g, solid); m.p. 282-284°C; ^{1}H NMR (500 MHz, DMSO-d_6): δ 10.51 (s, 1H), 10.03 (s, 1H), 8.82 (d, *J* = 1.8 Hz, 1H), 8.59 (s, 1H), 7.97 (d, *J* = 8.7 Hz, 2H), 7.94 (dd, *J* = 9.0, 2.0 Hz, 1H), 7.82 (d, *J* = 8.9 Hz, 1H), 7.75 (d, *J* = 8.7 Hz, 2H), 6.69 (s, 4H), 6.54 (dd, *J* = 17.0, 10.1 Hz, 1H), 6.35 (dd, *J* = 17.0, 1.7 Hz, 1H), 5.84 (dd, *J* = 10.2, 1.7 Hz, 1H). ^{13}C NMR (126 MHz, DMSO-d_6): δ 163.35, 158.07, 157.32, 153.11, 146.84, 142.02, 138.80, 136.68, 131.53, 128.50, 127.46, 127.28, 126.11, 121.28, 115.55, 112.30. LC/MS (+ESI): m/z = 412.10 (M + H).

***N*-(4-((4-(*N*-(thiazol-2-yl)sulfamoyl)phenyl)amino)quinazolin-6-yl)acrylamide (4m).** Yield 60% (0.27 g, solid); m.p. 279-280°C; ^{1}H NMR (500 MHz, DMSO-d_6): δ 10.29 (s,

2H), 9.86 (s, 2H), 8.62 (s, 2H), 8.38 (s, 2H), 7.81 (d, *J* = 8.3 Hz, 4H), 7.71 (dd, *J* = 9.2, 2.2 Hz, 3H), 7.60 (d, *J* = 8.8 Hz, 6H), 7.03 (s, 4H), 6.30 (dd, *J* = 17.0, 10.1 Hz, 2H), 6.12 (dd, *J* = 17.0, 1.7 Hz, 2H), 5.62 (dd, *J* = 10.2, 1.7 Hz, 2H). ^{13}C NMR (126 MHz, DMSO-*d*$_6$): δ 163.36, 162.27, 157.31, 153.04, 146.86, 142.64, 138.18, 136.74, 131.52, 128.54, 127.48, 127.30, 126.23, 121.39, 116.20, 116.17, 115.59, 112.28. LC/MS (+ESI): m/z = 453.13 (M + H).

***N*-(4-((4-(*N*-(pyridin-2-yl)sulfamoyl)phenyl)amino) quinazolin-6-yl)acrylamide (4n)**. Yield 63% (0.28 g, solid); m.p. 210-212°C; ^{1}H NMR (500 MHz, DMSO-*d*$_6$): δ 8.78 (s, 1H), 8.57 (s, 1H), 8.04 (d, *J* = 8.7 Hz, 2H), 8.01 (d, *J* = 5.4 Hz, 1H), 7.95 (d, *J* = 8.8 Hz, 2H), 7.82 – 7.76 (m, 2H), 7.75 – 7.69 (m, 1H), 7.28 (d, *J* = 8.7 Hz, 1H), 6.90 (t, *J* = 6.3 Hz, 1H), 6.50 (s, 1H), 6.49 – 6.47 (m, 1H), 5.85 (dd, *J* = 8.4, 3.4 Hz, 1H). ^{13}C NMR (126 MHz, DMSO-*d*$_6$): δ 166.25, 159.27, 154.50, 147.75, 144.40, 144.22, 141.75, 141.69, 138.32, 137.38, 132.07, 129.07, 128.90, 128.79, 128.44, 122.63, 117.20, 117.03, 115.83, 112.73. LC/MS (+ESI): m/z = 447.14 (M + H).

***N*-(4-(cyclohexylamino)quinazolin-6-yl)acrylamide (4o)**. Yield 68% (0.20 g, solid); m.p. 182-184°C; ^{1}H NMR (500 MHz, DMSO-*d*$_6$) δ 10.34 (s, 1H), 8.49 (d, *J* = 2.1 Hz, 1H), 8.37 (s, 1H), 7.83 – 7.78 (m, 2H), 7.64 (d, *J* = 8.9 Hz, 1H), 6.50 (dd, *J* = 17.0, 10.1 Hz, 1H), 6.31 (dd, *J* = 17.0, 1.9 Hz, 1H), 5.80 (dd, *J* = 10.1, 1.9 Hz, 1H), 4.24 – 4.13 (m, 1H), 1.92 (d, *J* = 12.2 Hz, 2H), 1.77 (d, *J* = 12.9 Hz, 2H), 1.65 (d, *J* = 12.8 Hz, 1H), 1.46 – 1.32 (m, 4H), 1.21 – 1.14 (m, 1H). ^{13}C NMR (126 MHz, DMSO-*d*$_6$): δ 163.13, 158.25, 154.10, 146.21, 135.58, 131.62, 127.94, 127.06, 126.52, 114.99, 112.82, 49.35, 31.89, 25.37, 25.07. LC/MS (+ESI): m/z = 297.21 (M + H).

6-*tert*-butyl 3-ethyl 2-amino-4,5-dihydrothieno[2,3-*c*]pyridine-3,6(7*H*)-dicarboxylate (5). According to the reported procedure.[2]

***tert*-butyl 4-oxo-3,4,5,6-tetrahydropyrido[4',3':4,5]thieno[2,3-*d*]pyrimidine-7(8*H*)-carboxylate (6).** According to the reported procedure.[2]

***tert*-butyl 4-chloro-5,6-dihydropyrido[4',3':4,5]thieno[2,3-*d*]pyrimidine-7(8*H*)-carboxylate (7).** According to the reported procedure.[2]

General procedure for the synthesis of compounds (8a-8f).

A mixture of **7** (3 mmol) and the corresponding amine (3.2 mmol) in 1ml ethanol was refluxed for 8 h. The reaction mixture was concentrated, and the residue was partitioned between water and dichloromethane; the organic layer separated, dried over anhydrous $MgSO_4$, and concentrated. The crude product was purified by silica gel column chromatography using a mixture of Dichloromethane:Methanol (100:3) to give compounds **8a-8e**.

***tert*-butyl 4-((2-fluoro-3-methylphenyl)amino)-5,6-dihydropyrido[4',3':4,5]thieno[2,3-*d*]pyrimidine-7(8*H*)-carboxylate (8a).** Yield 53% (0.66 g, solid); LC/MS (+ESI): m/z = 414.65 (M + H).

***tert*-butyl 4-((4-bromo-2-fluorophenyl)amino)-5,6-dihydropyrido[4',3':4,5]thieno[2,3-*d*]pyrimidine-7(8*H*)-carboxylate (8b).** Yield 50% (0.72 g, solid); ^{1}H NMR (300 MHz, $CDCl_3$) δ 8.61 (t, *J* = 8.7 Hz, 1H), 8.57 (s, 1H), 7.35 (s, 1H), 7.34 – 7.27 (m, 2H), 4.72 (s, 2H), 3.87 (t, *J* = 5.7 Hz, 2H), 3.15 (t, *J* = 5.4 Hz, 2H), 1.51 (s, 9H). LC/MS (+ESI): m/z = 478.62 (M + H).

***tert*-butyl 4-((4-bromo-3-methylphenyl)amino)-5,6-dihydropyrido[4',3':4,5]thieno[2,3-*d*]pyrimidine-7(8*H*)-carboxylate (8c).** Yield 46% (0.65 g, solid); ^{1}H NMR (300 MHz, DMSO-d_6) δ 8.42 (s, 1H), 8.20 (s, 1H), 7.61 (s, 1H), 7.51 (d, *J* = 1.2 Hz, 2H), 4.67 (s, 2H), 3.69 (t, *J* = 5.4 Hz, 2H), 3.20 (s, 2H), 2.34 (s, 3H), 1.45 (s, 9H). LC/MS (+ESI): m/z = 474.61 (M + H).

***tert*-butyl 4-((3-ethylphenyl)amino)-5,6-dihydropyrido[4',3':4,5]thieno[2,3-*d*]pyrimidine-7(8*H*)-carboxylate (8d).** Yield 48% (0.59 g, solid); ^{1}H NMR (500 MHz, DMSO-d_6) δ 8.40 (s, 1H), 8.15 (s, 1H), 7.53 (dd, J = 8.1, 1.2 Hz, 1H), 7.25 (t, *J* = 7.8 Hz, 1H), 6.95 (dd, *J* = 7.6, 0.5 Hz, 1H), 4.67 (s, 2H), 3.69 (s, 2H), 3.21 (t, *J* = 5.6 Hz, 2H), 2.61 (q, *J* = 7.6 Hz, 2H), 1.45 (s, 9H), 1.20 (t, *J* = 7.6 Hz, 3H). LC/MS (+ESI): m/z = 410.67 (M + H).

***tert*-butyl 4-((4-ethylphenyl)amino)-5,6-dihydropyrido[4',3':4,5]thieno[2,3-*d*]pyrimidine-7(8*H*)-carboxylate (8e).** Yield 47% (0.57 g, solid); ^{1}H NMR (500 MHz, $CDCl_3$) δ 8.49 (s, 1H), 7.50 (d, *J* = 8.4 Hz, 2H), 7.23 (d, *J* = 8.5 Hz, 2H), 6.92 (s, 1H), 4.71 (s, 2H), 3.85 (t, *J* = 5.6 Hz, 2H), 3.14 (s, 2H), 2.66 (q, *J* = 7.6 Hz, 2H), 1.51 (s, 9H), 1.25 (t, *J* = 7.6 Hz, 3H). LC/MS (+ESI): m/z = 410.72 (M + H).

***tert*-butyl 4-(cyclohexylamino)-5,6-dihydropyrido[4',3':4,5]thieno[2,3-*d*]pyrimidine-7(8*H*)-carboxylate (8f).** Yield 42% (0.49 g, solid); ^{1}H NMR (300 MHz, $CDCl_3$) δ 8.39 (s, 1H), 5.07 (d, *J* = 7.0 Hz, 1H), 4.65 (s, 2H), 4.28 – 4.08 (m, 1H), 3.80 (t, *J* = 5.7 Hz, 2H), 2.99 (s, 2H), 2.15 – 1.97 (m, 2H), 1.83 – 1.60 (m, 4H), 1.50 (s, 9H), 1.35 – 1.17 (m, 4H). LC/MS (+ESI): m/z = 388.66 (M + H).

General procedure for the synthesis of compounds (9a-9f).

To a mixture of the corresponding intermediate **8a-8f** (1.5 mmol) in dichloromethane (2mL) at 0°C was added trifluoroacetic acid (TFA) (1mL) and then warmed to room temperature. The reaction mixture was stirred for 2 h, removed the solvent under vacuum, and neutralized the residue by slow addition of sodium bicarbonate solution and then

extracted with ethyl acetate. The organic layer separated, dried over anhydrous $MgSO_4$, and concentrated to give **9a-9f** and they were used directly for the next step without further purification.

Compound	**9a**	**9b**	**9c**	**9d**	**9e**	**9f**
% Yield	89	82	86	94	83	85
Amount (g)	0.42	0.46	0.48	0.43	0.38	0.36
Physical State	solid	solid	solid	solid	solid	solid
LC/MS(+ESI): m/z (M + H)=	314.80	378.48	374.59	310.80	310.89	288.97

General procedure for the synthesis of compounds (10a-10f).

A mixture of the corresponding intermediate **9a-9f** (1 mmol) and $NaHCO_3$ (1.3 mmol) was stirred at 0°C in acetone (10 ml) under nitrogen atmosphere. This is then followed by dropwise addition of acryloyl chloride (1.3 mmol) and then was stirred for 30 min. at 0°C. Excess solvent was then removed under reduced pressure and the remaining residue was neutralized using $NaHCO_3$ solution. The formed solid was then filtered and the purified using column chromatography using a mixture of dichloromethane:methanol (100:1) as eluent.

1-(4-((2-fluoro-3-methylphenyl)amino)-5,6-dihydropyrido[4',3':4,5]thieno[2,3-*d*]pyrimidin-7(8*H*)-yl)prop-2-en-1-one (10a). Yield 25% (92 mg, solid); m.p. 189-190°C; ^{1}H NMR (500 MHz, $CDCl_3$) δ 8.56 (s, 1H), 8.45 (d, *J* = 7.6 Hz, 1H), 7.31 (d, *J* = 23.4 Hz, 1H), 7.08 (t, *J* = 7.8 Hz, 1H), 6.92 (t, *J* = 7.3 Hz, 1H), 6.74 – 6.53 (m, 1H), 6.45 – 6.29 (m, 1H), 5.81 (d, *J* = 9.6 Hz, 1H), 4.90 (d, *J* = 44.8 Hz, 2H), 4.04 (d, *J* = 49.4 Hz, 2H), 3.23 (s, 2H), 2.32 (d, *J* = 2.0 Hz, 3H). LC/MS (+ESI): m/z = 368.73 (M + H).

1-(4-((4-bromo-2-fluorophenyl)amino)-5,6-dihydropyrido[4',3':4,5]thieno[2,3-*d*]pyrimidin-7(8*H*)-yl)prop-2-en-1-one (10b). Yield 28% (121 mg, solid); m.p. 231-233°C; ^{1}H NMR (500 MHz, $CDCl_3$) δ 8.60 (s, 1H), 8.57 (s, 1H), 7.36 – 7.30 (m, 2H), 7.22 (s, 1H), 6.78 – 6.52 (m, 1H), 6.38 (t, *J* = 14.4 Hz, 1H), 5.82 (d, *J* = 9.5 Hz, 1H), 4.91 (d, *J* = 44.8 Hz, 2H), 4.05 (d, *J* = 44.3 Hz, 2H), 3.22 (s, 2H). LC/MS (+ESI): m/z = 432.46 (M + H).

1-(4-((4-bromo-3-methylphenyl)amino)-5,6-dihydropyrido[4',3':4,5]thieno[2,3-*d*]pyrimidin-7(8*H*)-yl)prop-2-en-1-one (10c). Yield 30% (128 mg, solid); m.p. 216-218°C; ^{1}H NMR (500 MHz, $CDCl_3$) δ 8.52 (s, 1H), 7.51 (d, *J* = 8.6 Hz, 1H), 7.48 (d, *J* = 2.4 Hz, 1H), 7.37 (s, 1H), 6.87 (d, *J* = 38.4 Hz, 1H), 6.73 – 6.53 (m, 1H), 6.37 (t, *J* = 14.2 Hz, 1H), 5.81 (d, *J* = 10.4 Hz, 1H), 4.90 (d, *J* = 45.1 Hz, 2H), 4.03 (d, *J* = 43.8 Hz, 2H), 3.20 (s, 2H), 2.42 (s, 3H). LC/MS (+ESI): m/z = 428.63 (M + H).

1-(4-((3-ethylphenyl)amino)-5,6-dihydropyrido[4',3':4,5]thieno[2,3-*d*]pyrimidin-7(8*H*)-yl)prop-2-en-1-one (10d). Yield 22% (80 mg, solid); m.p. 105-107°C; ^{1}H NMR (500 MHz, $CDCl_3$) δ 8.51 (s, 1H), 7.49 (s, 1H), 7.38 (s, 1H), 7.31 (t, *J* = 7.8 Hz, 1H), 7.01 (dd, *J* = 7.6, 0.6 Hz, 1H), 6.92 (d, *J* = 37.2 Hz, 1H), 6.75 – 6.53 (m, 1H), 6.44 – 6.27 (m, 1H), 5.80 (d, *J* = 10.6 Hz, 1H), 4.90 (d, *J* = 45.0 Hz, 2H), 4.03 (d, *J* = 46.7 Hz, 2H), 3.21 (s, 2H), 2.68 (q, *J* = 7.6 Hz, 2H), 1.27 (t, *J* = 7.6 Hz, 3H). LC/MS (+ESI): m/z = 364.70 (M + H).

1-(4-((4-ethylphenyl)amino)-5,6-dihydropyrido[4',3':4,5]thieno[2,3-*d*]pyrimidin-7(8*H*)-yl)prop-2-en-1-one (10e). Yield 26% (94 mg, solid); m.p. 201-202°C; ^{1}H NMR (500 MHz, $CDCl_3$) δ 8.49 (s, 1H), 7.49 (d, *J* = 7.9 Hz, 2H), 7.22 (d, *J* = 8.3 Hz, 2H), 6.89 (d, *J* = 36.7 Hz, 1H), 6.74 – 6.52 (m, 1H), 6.44 – 6.27 (m, 1H), 5.80 (d, *J* = 10.8 Hz, 1H), 4.89 (d, *J* = 44.7 Hz, 2H), 4.02 (d, *J* = 45.9 Hz, 2H), 3.19 (s, 2H), 2.65 (q, *J* = 7.6 Hz, 2H), 1.25 (t, *J* = 7.6 Hz, 3H). LC/MS (+ESI): m/z = 364.75 (M + H).

1-(4-(cyclohexylamino)-5,6-dihydropyrido[4',3':4,5]thieno[2,3-*d*]pyrimidin-7(8*H*)-yl)prop-2-en-1-one (10f). Yield 23% (78 mg, solid); m.p. 150-152°C; ^{1}H NMR (500 MHz, MeOD) δ 8.24 (s, 1H), 6.86 (ddd, *J* = 38.8, 16.8, 10.6 Hz, 1H), 6.28 (dd, *J* = 16.6, 9.3 Hz, 1H), 5.83 (t, *J* = 11.9 Hz, 1H), 4.95 – 4.67 (m, 2H), 4.16 – 4.07 (m, 1H), 4.01 (t, *J* = 5.6 Hz, 2H), 3.15 (d, *J* = 25.2 Hz, 2H), 2.04 (d, *J* = 9.6 Hz, 2H), 1.80 (dd, *J* = 9.4, 3.3 Hz, 2H), 1.68 (d, *J* = 12.6 Hz, 1H), 1.47 – 1.40 (m, 4H), 1.32 – 1.27 (m, 2H). LC/MS (+ESI): m/z = 342.95 (M + H).

Biological screening

Cell Culture and Plating

Cancer cell lines cultured included cell lines with wild type EGFR (SKBR-3 mammary carcinoma) and with mutant EGFR (H1975). Both cell lines were maintained in RPMI-1640 media supplemented with 10% fetal bovine serum in a 37°C humidified incubator with 5% CO_2 and subcultured twice weekly. Only cultures exhibiting greater than 95% viability were used in any experiment (determined by trypan blue exclusion). Cells were seeded in 96-well standard assay plates at a density of 5,000 cells/well for growth assays and 10,000 cells/well in optical quality PerkinElmer ViewPlate for immunofluorescence, then allowed to acclimate overnight before compound addition or stimulation with EGF.

Cytoblot Assay[3]

Serial dilutions of each compound were added to at least 3 replicate wells each 30 min prior to EGF stimulation (200 ng/mL). Each plate included a positive control (Iressa, 20μm) and negative control (DMSO). Cytoblot assays were conducted in H1975 (EGF mutant) cell line. Phosphorylated EGFR was specifically detected (Cell Signaling Technology anti-PY1068 rabbit monoclonal antibody) to quantify the level of receptor

autophosphorylation in response to EGF stimulation. Secondary goat anti-rabbit conjugate labeled with horseradish peroxidase enzyme was added, followed by addition of enhanced chemiluminescence reagent (ECL; Pierce Pico West). The resulting luminescence was quantitated using a Molecular Devices Paradigm multilabel microplate reader. Raw luminescence data were plotted to generate dose response curves and IC_{50} values.

Growth Assay

SKBR3 and H1975 cells were treated with 8 concentrations of inhibitors ranging from 50 µM to 8 nM (specifically, the doses tested were 50uM, 25uM, 10uM, 5uM, 1uM, 0.2uM, 0.04uM, and 0.008uM) followed by EGF stimulation (100 ng/mL) 1 h later. Cells were incubated for an additional 72 h at 37°C. Relative cell growth was determined by addition of Promega CellTiter Glo luciferase-based measure of ATP content, and the resulting luminescence was measured using a Molecular Devices Spectramax Paradigm microplate reader in luminescence mode. Growth inhibition data were analyzed using DMSO as a baseline (negative control equal to 0% growth inhibition) with GraphPad Prism curve fitting software. IC_{50} values are representative of the results at least two independent concentration-response experiments with three replicates per concentration.

EGFR kinase phosphorylation assay

Phosphorylation assays were performed in a final volume of 20 µl containing 8 mM MOPS (pH 7.0), 0.2 mM EDTA, 10 mM MnCl2, 200 µM substrate peptide, 0.25 mM DTT, 0.1 mg/ml BSA, 10 ng EGFR-Kinase (Cat. No. 40187, BPS Bioscience), 10 mM magnesium acetate, 100 µM γ–[32P]ATP, and inhibitors at different concentrations or DMSO control (1.25% v/v). Reactions were started by the addition of the magnesium acetate/ATP mixture. After 30 min incubation at 30°C, 5 µl of each reaction was spotted on phosphocellulose P81 paper (Whatman). The P81 paper was then washed 5 times with 50 mM phosphoric acid for 15 min, dried and exposed to a phosphorimager screen, which was scanned and densitometrically analyzed the next day. The sequence of the substrate peptide was derived from phospholipase C-γ1 and had the sequence "KHKKLAEGSAYEEV", according to Fry *et al.*[4]

Molecular modeling

The proteins used for the docking was downloaded from the protein data bank (PDB 2J5F, 3W2P). The proteins were first prepared for docking using MOE software where the proteins were protonated and saved for docking. The ligands were drawn on MOE and energy minimized and then saved as "mol2" file. Docking was done using GOLD software, where the proteins are first prepared by removing the water molecules and extracting the co-crystallized ligands. The docking of the compounds included a covalent interaction which was done by specifying the atoms in the ligand and the protein that will covalently bind together and then docking was done using CHEMPLP as the scoring

function and Goldscore as a rescoring function. The viewing of the results was done using PyMOL software and the side chains from the docked molecules were hidden to facilitate the viewing process.

References of the supporting information

1. Madapa, S.; Tusi, Z.; Mishra, A.; Srivastava, K.; Pandey, S. K.; Tripathi, R.; Puri, S. K.; Batra, S., Search for new pharmacophores for antimalarial activity. Part II: synthesis and antimalarial activity of new 6-ureido-4-anilinoquinazolines. *Bioorg Med Chem* **2009,** 17, (1), 222-34.

2. Wu, C. H.; Coumar, M. S.; Chu, C. Y.; Lin, W. H.; Chen, Y. R.; Chen, C. T.; Shiao, H. Y.; Rafi, S.; Wang, S. Y.; Hsu, H.; Chen, C. H.; Chang, C. Y.; Chang, T. Y.; Lien, T. W.; Fang, M. Y.; Yeh, K. C.; Chen, C. P.; Yeh, T. K.; Hsieh, S. H.; Hsu, J. T.; Liao, C. C.; Chao, Y. S.; Hsieh, H. P., Design and synthesis of tetrahydropyridothieno[2,3-d]pyrimidine scaffold based epidermal growth factor receptor (EGFR) kinase inhibitors: the role of side chain chirality and Michael acceptor group for maximal potency. *J Med Chem* **2010,** 53, (20), 7316-26.

3. Chiosis, G.; Keeton, A. B., Assay for isolation of inhibitors of her2-kinase expression. *Methods Mol Biol* **2009,** 486, 139-49.

4. Fry, D. W.; Kraker, A. J.; McMichael, A.; Ambroso, L. A.; Nelson, J. M.; Leopold, W. R.; Connors, R. W.; Bridges, A. J., A specific inhibitor of the epidermal growth factor receptor tyrosine kinase. *Science* **1994,** 265, (5175), 1093-5.

References of the manuscript

1. Charpidou, A.; Blatza, D.; Anagnostou, V.; Syrigos, K. N., Review. EGFR mutations in non-small cell lung cancer--clinical implications. *In Vivo* **2008,** 22, (4), 529-36.

2. da Cunha Santos, G.; Shepherd, F. A.; Tsao, M. S., EGFR mutations and lung cancer. *Annu Rev Pathol* **2011,** 6, 49-69.

3. Sharma, S. V.; Bell, D. W.; Settleman, J.; Haber, D. A., Epidermal growth factor receptor mutations in lung cancer. *Nat Rev Cancer* **2007,** 7, (3), 169-81.

4. Wu, C. H.; Coumar, M. S.; Chu, C. Y.; Lin, W. H.; Chen, Y. R.; Chen, C. T.; Shiao, H. Y.; Rafi, S.; Wang, S. Y.; Hsu, H.; Chen, C. H.; Chang, C. Y.; Chang, T. Y.; Lien, T. W.; Fang, M. Y.; Yeh, K. C.; Chen, C. P.; Yeh, T. K.; Hsieh, S. H.; Hsu, J. T.; Liao, C. C.; Chao, Y. S.; Hsieh, H. P., Design and synthesis of tetrahydropyridothieno[2,3-d]pyrimidine scaffold based epidermal growth factor receptor (EGFR) kinase inhibitors: the role of side chain chirality and Michael acceptor group for maximal potency. *J Med Chem* **2010,** 53, (20), 7316-26.

5. Backes, A. C.; Zech, B.; Felber, B.; Klebl, B.; Muller, G., Small-molecule inhibitors binding to protein kinase. Part II: the novel pharmacophore approach of type II and type III inhibition. *Expert Opin. Drug Discovery* **2008,** 3, 1427-1449.

6. Pao, W.; Miller, V.; Zakowski, M.; Doherty, J.; Politi, K.; Sarkaria, I.; Singh, B.; Heelan, R.; Rusch, V.; Fulton, L.; Mardis, E.; Kupfer, D.; Wilson, R.; Kris, M.; Varmus, H., EGF receptor gene mutations are common in lung cancers from "never smokers" and are associated with sensitivity of tumors to gefitinib and erlotinib. *Proc Natl Acad Sci U S A* **2004,** 101, (36), 13306-11.

7. Rewcastle, G. W.; Denny, W. A.; Bridges, A. J.; Zhou, H.; Cody, D. R.; McMichael, A.; Fry, D. W., Tyrosine kinase inhibitors. 5. Synthesis and structure-activity relationships for 4-[(phenylmethyl)amino]- and 4-(phenylamino)quinazolines as potent adenosine 5'-triphosphate binding site inhibitors of the tyrosine kinase domain of the epidermal growth factor receptor. *J Med Chem* **1995,** 38, (18), 3482-7.

8. Wissner, A.; Berger, D. M.; Boschelli, D. H.; Floyd, M. B., Jr.; Greenberger, L. M.; Gruber, B. C.; Johnson, B. D.; Mamuya, N.; Nilakantan, R.; Reich, M. F.; Shen, R.; Tsou, H. R.; Upeslacis, E.; Wang, Y. F.; Wu, B.; Ye, F.; Zhang, N., 4-Anilino-6,7-dialkoxyquinoline-3-carbonitrile inhibitors of epidermal growth factor receptor kinase and their bioisosteric relationship to the 4-anilino-6,7-dialkoxyquinazoline inhibitors. *J Med Chem* **2000,** 43, (17), 3244-56.

9. Michalczyk, A.; Kluter, S.; Rode, H. B.; Simard, J. R.; Grutter, C.; Rabiller, M.; Rauh, D., Structural insights into how irreversible inhibitors can overcome drug resistance in EGFR. *Bioorg Med Chem* **2008,** 16, (7), 3482-8.

10. Hennequin, L. F.; Allen, J.; Breed, J.; Curwen, J.; Fennell, M.; Green, T. P.; Lambert-van der Brempt, C.; Morgentin, R.; Norman, R. A.; Olivier, A.; Otterbein, L.; Ple, P. A.; Warin, N.; Costello, G., N-(5-chloro-1,3-benzodioxol-4-yl)-7-[2-(4-methylpiperazin-1-yl)ethoxy]-5- (tetrahydro-2H-pyran-4-yloxy)quinazolin-4-amine, a novel, highly selective, orally available, dual-specific c-Src/Abl kinase inhibitor. *J Med Chem* **2006,** 49, (22), 6465-88.

11. Rachid, Z.; Brahimi, F.; Qiu, Q.; Williams, C.; Hartley, J. M.; Hartley, J. A.; Jean-Claude, B. J., Novel nitrogen mustard-armed combi-molecules for the selective targeting of epidermal growth factor receptor overexperessing solid tumors: discovery of an unusual structure-activity relationship. *J Med Chem* **2007,** 50, (11), 2605-8.

12. Wissner, A.; Fraser, H. L.; Ingalls, C. L.; Dushin, R. G.; Floyd, M. B.; Cheung, K.; Nittoli, T.; Ravi, M. R.; Tan, X.; Loganzo, F., Dual irreversible kinase inhibitors: quinazoline-based inhibitors incorporating two independent reactive centers with each targeting different cysteine residues in the kinase domains of EGFR and VEGFR-2. *Bioorg Med Chem* **2007,** 15, (11), 3635-48.

13. Wissner, A.; Mansour, T. S., The development of HKI-272 and related compounds for the treatment of cancer. *Arch Pharm (Weinheim)* **2008,** 341, (8), 465-77.

14. Wissner, A.; Johnson, B. D.; Floyd, M. B.; Kitchen, D. B., Preparation of 4-Aminoquinazolines as EGFR inhibitors. *US Patent* **1998,** 5,760,041.

15. Fry, D. W.; Bridges, A. J.; Denny, W. A.; Doherty, A.; Greis, K. D.; Hicks, J. L.; Hook, K. E.; Keller, P. R.; Leopold, W. R.; Loo, J. A.; McNamara, D. J.; Nelson, J. M.; Sherwood, V.; Smaill, J. B.; Trumpp-Kallmeyer, S.; Dobrusin, E. M., Specific, irreversible inactivation of the epidermal growth factor receptor and erbB2, by a new class of tyrosine kinase inhibitor. *Proc Natl Acad Sci U S A* **1998,** 95, (20), 12022-7.

16. Engelman, J. A.; Janne, P. A., Mechanisms of acquired resistance to epidermal growth factor receptor tyrosine kinase inhibitors in non-small cell lung cancer. *Clin Cancer Res* **2008,** 14, (10), 2895-9.

17. Kobayashi, S.; Boggon, T. J.; Dayaram, T.; Janne, P. A.; Kocher, O.; Meyerson, M.; Johnson, B. E.; Eck, M. J.; Tenen, D. G.; Halmos, B., EGFR mutation and resistance of non-small-cell lung cancer to gefitinib. *N Engl J Med* **2005,** 352, (8), 786-92.

18. Pao, W.; Miller, V. A.; Politi, K. A.; Riely, G. J.; Somwar, R.; Zakowski, M. F.; Kris, M. G.; Varmus, H., Acquired resistance of lung adenocarcinomas to gefitinib or erlotinib is associated with a second mutation in the EGFR kinase domain. *PLoS Med* **2005,** 2, (3), e73.

19. Camp, E. R.; Summy, J.; Bauer, T. W.; Liu, W.; Gallick, G. E.; Ellis, L. M., Molecular mechanisms of resistance to therapies targeting the epidermal growth factor receptor. *Clin Cancer Res* **2005,** 11, (1), 397-405.

20. Engelman, J. A.; Settleman, J., Acquired resistance to tyrosine kinase inhibitors during cancer therapy. *Curr Opin Genet Dev* **2008,** 18, (1), 73-9.

21. Yun, C. H.; Mengwasser, K. E.; Toms, A. V.; Woo, M. S.; Greulich, H.; Wong, K. K.; Meyerson, M.; Eck, M. J., The T790M mutation in EGFR kinase causes drug resistance by increasing the affinity for ATP. *Proc Natl Acad Sci U S A* **2008,** 105, (6), 2070-5.

22. Bikker, J. A.; Brooijmans, N.; Wissner, A.; Mansour, T. S., Kinase domain mutations in cancer: implications for small molecule drug design strategies. *J Med Chem* **2009,** 52, (6), 1493-509.

23. Mukherji, D.; Spicer, J., Second-generation epidermal growth factor tyrosine kinase inhibitors in non-small cell lung cancer. *Expert Opin Investig Drugs* **2009,** 18, (3), 293-301.

24. Zhang, J.; Yang, P. L.; Gray, N. S., Targeting cancer with small molecule kinase inhibitors. *Nat Rev Cancer* **2009,** 9, (1), 28-39.

25. Kobayashi, S.; Ji, H.; Yuza, Y.; Meyerson, M.; Wong, K. K.; Tenen, D. G.; Halmos, B., An alternative inhibitor overcomes resistance caused by a mutation of the epidermal growth factor receptor. *Cancer Res* **2005,** 65, (16), 7096-101.

26. Kwak, E. L.; Sordella, R.; Bell, D. W.; Godin-Heymann, N.; Okimoto, R. A.; Brannigan, B. W.; Harris, P. L.; Driscoll, D. R.; Fidias, P.; Lynch, T. J.; Rabindran, S. K.; McGinnis, J. P.; Wissner, A.; Sharma, S. V.; Isselbacher, K. J.; Settleman, J.; Haber, D.

A., Irreversible inhibitors of the EGF receptor may circumvent acquired resistance to gefitinib. *Proc Natl Acad Sci U S A* **2005,** 102, (21), 7665-70.

27. Carter, T. A.; Wodicka, L. M.; Shah, N. P.; Velasco, A. M.; Fabian, M. A.; Treiber, D. K.; Milanov, Z. V.; Atteridge, C. E.; Biggs, W. H., 3rd; Edeen, P. T.; Floyd, M.; Ford, J. M.; Grotzfeld, R. M.; Herrgard, S.; Insko, D. E.; Mehta, S. A.; Patel, H. K.; Pao, W.; Sawyers, C. L.; Varmus, H.; Zarrinkar, P. P.; Lockhart, D. J., Inhibition of drug-resistant mutants of ABL, KIT, and EGF receptor kinases. *Proc Natl Acad Sci U S A* **2005,** 102, (31), 11011-6.

28. Godin-Heymann, N.; Ulkus, L.; Brannigan, B. W.; McDermott, U.; Lamb, J.; Maheswaran, S.; Settleman, J.; Haber, D. A., The T790M "gatekeeper" mutation in EGFR mediates resistance to low concentrations of an irreversible EGFR inhibitor. *Mol Cancer Ther* **2008,** 7, (4), 874-9.

29. Tsou, H. R.; Mamuya, N.; Johnson, B. D.; Reich, M. F.; Gruber, B. C.; Ye, F.; Nilakantan, R.; Shen, R.; Discafani, C.; DeBlanc, R.; Davis, R.; Koehn, F. E.; Greenberger, L. M.; Wang, Y. F.; Wissner, A., 6-Substituted-4-(3-bromophenylamino)quinazolines as putative irreversible inhibitors of the epidermal growth factor receptor (EGFR) and human epidermal growth factor receptor (HER-2) tyrosine kinases with enhanced antitumor activity. *J Med Chem* **2001,** 44, (17), 2719-34.

30. Foucourt, A.; Dubouilh-Benard, C.; Chosson, E.; Corbière, C.; Buquet, C.; Iannelli, M.; Leblond, B.; Marsais, F.; Besson, T., Microwave-accelerated Dimroth rearrangement for the synthesis of 4-anilino-6-nitroquinazolines. Application to an efficient synthesis of a microtubule destabilizing agent. *Tetrahedron* **2010,** 66, (25), 4495-4502.

31. Gewald, K.; Schinke, E.; Böttcher, H., Heterocyclen aus CH-aciden Nitrilen, VIII. 2-Amino-thiophene aus methylenaktiven Nitrilen, Carbonylverbindungen und Schwefel. *Chemische Berichte* **1966,** 99, (1), 94-100.

3.II 6-aryl and heterocycle quinazoline derivatives as potent EGFR inhibitors with improved activity toward Gefitinib-sensitive and -resistant tumor cell lines

Mostafa M. Hamed, Dalal A. Abou El Ella, Adam B. Keeton, Gary A. Piazza, Ashraf H. Abadi, Rolf W. Hartmann, Matthias Engel

This manuscript has been accepted as a full paper in
ChemMedChem, (**2013**), DOI: 10.1002/cmdc.201300147

Paper II

Abstract

A group of novel anilinoquinazoline derivatives, with variable aryl and heterocyclic substituents at position 6, have been synthesized and tested for their EGFR inhibitory activity. The aryl and heterocyclic rings have been attached to the quinazoline scaffold through different linkages such as an imine, amide and thiourea. Most of the aryl and heterocyclic derivatives showed potent inhibition of wild-type EGFR with IC_{50}'s in the low nanomolar range. Among these, the thiourea derivatives **6a**, **6b** and compound **10b** retained significant activity also towards the Gefitinib-insensitive $EGFR^{T790M/L858R}$ mutant, displaying an up to 24-fold stronger potency than Gefitinib. In addition, cell growth inhibitory activity has been tested versus cancer cell lines with wild-type (KB cells) and mutant EGFR (H1975). Several compounds such as **6a**, **11e**, **11i** and **11j** were more potent than the reference compound Gefitinib towards both cell lines, and **10b** towards H1975 cells. Hence, in particular **6a** and **10b** might serve as new leads for the development of inhibitors effective against wild-type EGFR and Gefitinib-resistant mutants.

Introduction

The epidermal growth factor receptor (EGFR) is a membrane bound tyrosine kinase involved in cellular signaling transduction pathways that regulate essential functions such as proliferation, differentiation and apoptosis.[1] EGFR was observed to be overexpressed in several types of cancers such as the non-small cell lung carcinoma (NSCLC) which is among the most common causes of cancer-related death.[2, 3] Therefore, EGFR inhibition has been approved as an important target in cancer therapy.[4-6]

Several small molecules inhibiting the EGFR kinase activity such as Gefitinib, Erlotinib and Lapatinib (Figure 1), were designed to bind to the ATP binding pocket and have been used in cancer therapy.[7] These molecules belong to the 4-anilinoquinazoline class,[8, 9] along with 4-anilino-3-quinolinecarbonitrile scaffold are the best known classes for the

development of EGFR inhibitors.[10, 11] In addition, several irreversible inhibitors having a Michael acceptor functional group such as **I** (Figure 1) were designed to bind covalently with the sulfhydryl group of the Cys 797 of EGFR.[12, 13] Although some irreversible kinase inhibitors have been advanced to clinical studies, the clinical usefulness of these compounds has been hampered mainly by toxicity and pharmacokinetic problems.[14] Also, the emergence of resistant EGFR mutants limits their efficacy. Therefore, the search of new potent inhibitors which retain activity towards mutated EGFR kinase remains an important and challenging goal.

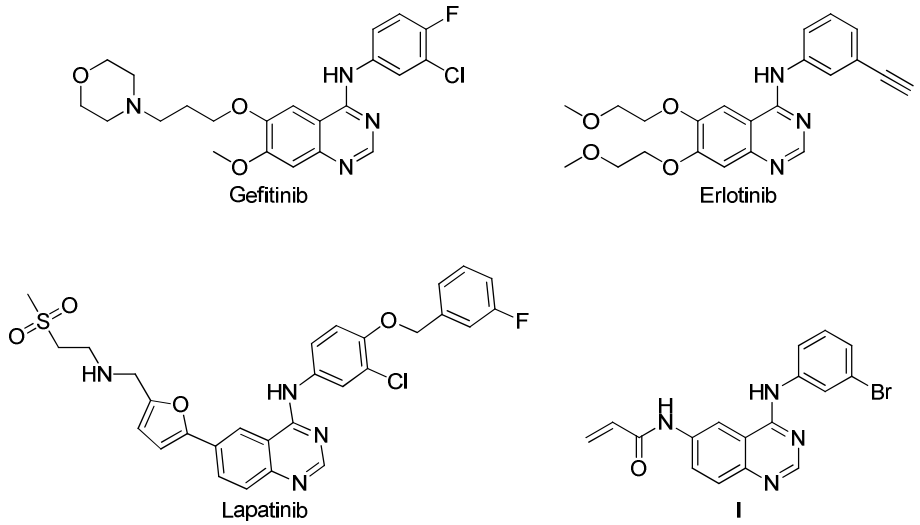

Figure 1. Reversible and irreversible EGFR tyrosine kinase inhibitors

In order to develop EGFR inhibitors with improved efficacy, we designed and synthesized novel quinazoline derivatives with several modifications in the position 6 side chain. These modifications included the introduction of different aryl and heterocyclic rings with different linkages to the 4-anilinoquinazoline scaffold. The different linker types included the imine, amide and thiourea function. We aimed at testing the effect of different aryl groups attached to the linkers at position 6 on the efficacy in EGFR -wild-type and -mutant tumor cell lines and towards the corresponding recombinant EGFR kinases.

Results and Discussion

Chemistry

Synthesis of the quinazoline nucleus was done through the formimidate derivative **1** which was obtained by refluxing of 2-amino-5-nitrobenzonitrile with triethyl orthoformate in the presence of drops of acetic anhydride (Scheme 1). Compound **1** was confirmed from its IR spectrum showing a band at 2228.6 cm^{-1} indicating the existence of the (C≡N) group.

The formimidate derivative **1**, was refluxed in acetic acid with 3-bromoaniline to yield the nitroquinazoline derivative **2**. The cyclization was confirmed from the IR spectrum by the disappearance of the (C≡N) group. The suggested mechanism for the formation of the quinazoline nucleus from the formimidate derivative **1** is through Dimroth rearrangement as reported for a similar derivative.[15] Reduction for the nitroquinazoline derivative **2** was done by refluxing it with stannous chloride in methanol to yield the aminoquinazoline derivative **3** (Scheme 1).

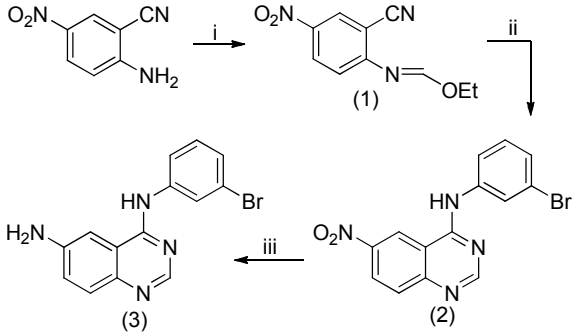

Scheme 1. Reagents and conditions: (i) TEOF, $(Ac)_2O$, reflux, 24h; (ii) 3-bromoaniline, CH_3COOH, reflux, 1h; (iii) $SnCl_2$, MeOH, reflux, 1h.

Different side chains have been introduced to position 6 of the quinazoline scaffold through different linkages. Several imine derivatives were synthesized by refluxing different aryl aldehydes with compound **3** in ethanol. A precipitate was formed during the reaction which was filtered while hot, yielding compounds **4a-4e**. Reaction of compound **3** with thiophosgene gave the isothiocyanate derivative **5** which was stirred in DMF with different amines to give compounds **6a** and **6b** (Scheme 2).

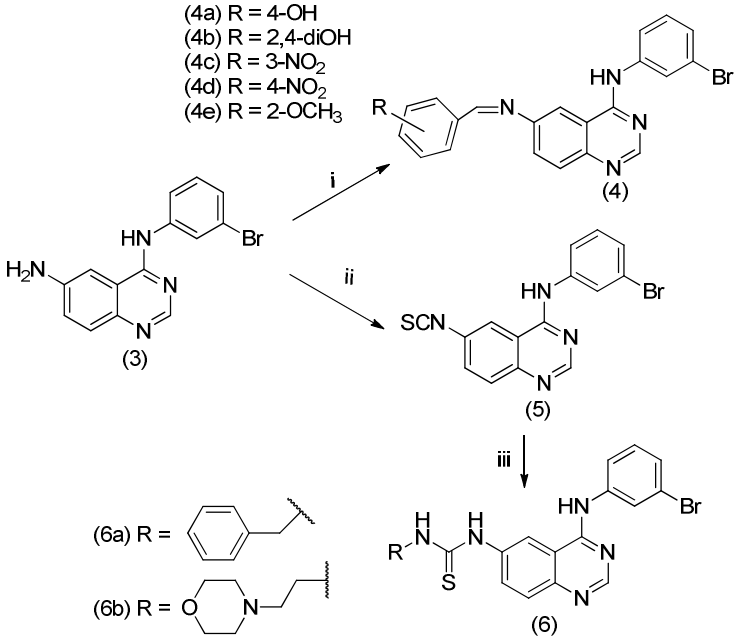

Scheme 2. Reagents and conditions: (i) Ar-CHO, Ethanol, reflux, 8h; (ii) $S=C(Cl)_2$; (iii) R-NH_2, DMF, rt, 16h.

Upon stirring of compound **3** with chloroacetyl chloride or chloropropionyl chloride in acetone at 0°C, the intermediates **7** or **8**, respectively, were formed. Compounds **9a-b** were obtained upon refluxing compound **7** in methanol with the respective amine, while compounds **10a-b** were synthesized by refluxing the intermediate **8** in ethanol with the respective amine in presence of TEA. In addition, different amide derivatives **11a-k** were obtained by stirring of the respective aryl or heterocyclic acid chloride with compound **3** in acetone at 0°C. (Scheme 3)

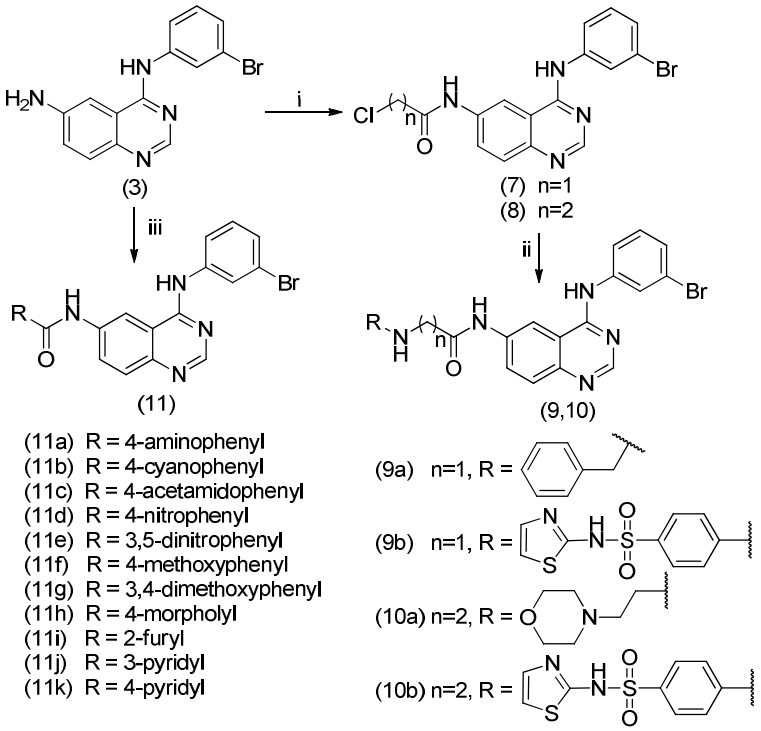

Scheme 3. Reagents and conditions: (i) $ClCH_2COCl$ or $Cl(CH_2)_2COCl$, $NaHCO_3$, acetone, 0°C, 30 min; (ii) R-NH_2, MeOH or EtOH, TEA, reflux, 8h; (iii) R-COCl, NaHCO3, acetone, 0°C, 30 min.

Biological screening

All final compounds **4a-4e, 6a-b, 9a-b, 10a-b** and **11a-k** were tested for their inhibitory potency towards isolated recombinant wild-type and double mutated (T790M/L858R) EGFR kinase as well as towards cell lines growing dependent on either wild-type EGFR (KB cells) or the same double mutant EGFR (H1975 cells). The new compounds were screened at 150 nM towards the recombinant wild-type EGFR kinase, and IC_{50}s were determined for compounds showing more than 85% inhibition in the primary screening. In the case of the Gefitinib-insensitive mutant, the primary screening concentration had to be raised to 8 µM. The primary screening dose versus the cell lines was 40 µM, and compounds reaching more than 60% inhibition were selected for the determination of exact IC_{50} values.

From the results in Table 1, it can be seen that the presence of aryl or heterocylic rings in the side chain at position 6 of the quinazoline can give rise to potent EGFR

inhibitors. Concerning the wild-type cell free assay for the aryl imine derivatives, it was observed that *ortho* and *meta* substitutions on the phenyl ring gave slightly more potent derivatives than those having a *para* substitution, as exemplified by the *o*-methoxy **4e** and the *m*-nitro-compound **4c**. However, the structure-activity relationships (SAR) of the substitution pattern in the cell free assay were found to be rather flat for this compound class; interestingly, though, there were substantial differences in the cell-based assays (Table 2 and see below).

Table 1. IC_{50} for the % inhibition of recombinant wild-type and double mutated EGFR (active) kinase.[a]

Comp.	Recombinant wild-type EGFR kinase		Recombinant double mutated (T790M/L858R) EGFR kinase	
	% inhibition at 150 nM [b]	IC_{50} (nM) [c]	% inhibition at 8 μM [b]	IC_{50} (nM) [c]
4a	92.2	15.3	9.6	N.D.
4b	90.9	17	10.3	N.D.
4c	90.4	13.3	13.5	N.D.
4d	91.8	16.2	10.2	N.D.
4e	91	10.7	1.9	N.D.
6a	86.1	17.2	95.3	290
6b	91.8	10.7	86.4	1020
9a	96	5.2	14.8	N.D.
9b	64.2	N.D.	0	N.D.
10a	91	11.8	22.0	N.D.
10b	90.1	23.1	93.1	480
11a	93.5	11.9	0	N.D.
11b	84.5	N.D.	0	N.D.
11c	92.6	12.8	3.7	N.D.
11d	85.6	61.8	0	N.D.
11e	80.9	N.D.	0	N.D.
11f	83.8	N.D.	0	N.D.
11g	88.7	19.5	0	N.D.
11h	89.6	25.3	0.9	N.D.
11i	96.9	8.4	6.4	N.D.
11j	88.7	19.8	0	N.D.
11k	91.1	17.5	0	N.D.
Gefitinib	93.2	4	53.6	7200

[a] IC_{50} values are representative of at least two independent concentration-response experiments performed in triplicate per concentration. [b] S.E. ≤ 7%. [c] S.E. ≤ 5%. [d] N.D.: Not determined.

For the amide derivatives **11a-k**, it was found that the most potent was the 5-membered heterocyclic furyl derivative **11i**; however, phenyl derivatives with polar substituents were also tolerated with only little loss of potency toward the purified

enzyme (cf. **11a** and **11c**). The 6-membered heterocyclic derivatives showed further reduced potency while the least active were the heterocylcoalkyl **11h** and the phenyl derivatives with rather lipophilic substituents **11d-f**.

Table 2. IC_{50} for the cell growth inhibitory activity.

Comp.	Cell Growth Inhibition IC_{50} (μM)[a]	
	KB cells	H1975 cells
4a	17.8 ±1.3	16 ± 1.1
4b	50.4% ± 4.5% @ 25 μM[b]	>40
4c	66.7% ± 11.6% @ 50 μM[b]	>40
4d	>40	>40
4e	47.2% ± 4.6% @ 50 μM[b]	>40
6a	9.02 ± 1.03	18 ± 1.1
6b	29.8 ± 1.2	35 ± 1.1
9a	14.6 ± 1.1	27.9 ± 1.2
9b	24.8 ± 1.1	>40
10a	N.D.[c]	N.D.[c]
10b	33.6 ± 1.2	20.8 ± 1.1
11a	16.4 ± 1.2	>40
11b	26.02 ± 1.3	>40
11c	39.9 ± 1.1	>40
11d	26.2 ± 1.1	>40
11e	14.7 ± 1.0	17.9 ± 1.1
11f	>40	>40
11g	>40	>40
11h	>40	>40
11i	12.3 ± 1.1	14.3 ± 1.2
11j	12.04 ± 1.1	22.35 ± 1.1
11k	19.8 ± 1.2	>40
Gefitinib	19.5 ± 1.1	31.2 ± 1.0

[a] IC_{50} values (± S.D.) are representative of the results at least two independent concentration-response experiments performed in triplicate per concentration. [b] Full curves could not be established. Maximum % inhibition ± S.D. [c] N.D.: Not determined.

By introducing some extensions at the position 6 side chain through the thiourea linkage, it became evident that the heterocycloalkyl derivative **6b** was more potent than the aryl derivative **6a** in the biochemical testing. Furthermore, the amino alkyl amide linker type was very well accepted by the enzyme in spite of its increased length; in this

compound class, the unsubstituted benzyl derivative **9a** was the most potent followed by the heterocycloalkyl derivative **10a** and finally the substituted aryl derivatives **9b** and **10b**.

Next we wanted to test whether the high potencies against wild-type EGFR observed for some of the new compounds in the biochemical assay would also translate in a corresponding inhibition of cell-growth. Indeed, as can be seen from Table 2, the presence of aryl or heteroaryl groups in the position 6 side chain resulted in compounds showing higher potency than Gefitinib towards both the EGFR wild-type (KB) and the double mutant cancer cell line (H1975). This was clearly observed with the amide derivatives having heterocyclic rings such as **11i** and **11j**, the nitrophenyl amide derivative **11e** and the benzylthiourea derivative **6a**. It was generally observed that in spite of sometimes comparable cell free potencies, both the type of the linker and the aryl or heterocycle in the position 6 side chain greatly determined the activity in the EGFR wild-type and the mutant cancer cell line. Of note, we were able to identify combinations which led to efficient growth inhibition of both cell lines; with respect to the linker, the amide and thiourea function yielded those inhibitors which preserved best their cell free potencies even in the EGFR mutant cell line (cf. **6a**, **11i** and **11j**). However, the nature of the aryl or heterocyclic ring was at least equally important, as it controlled the cellular activity in general but also the ratio of growth inhibition between the wild-type and mutant cell line (compare **4a** with **4c**, **11a** with **11i**). The most favorable scaffolds with respect to cell growth inhibition in both cell lines comprised the amide derivatives linked to heterocyclic rings (**11i** and **11j**).

Since it was an important goal of the present study to identify novel lead compounds which preserve efficacy against Gefitinib-insensitive mutated EGFR as a major biological activity, we screened all compounds against recombinant $EGFR^{L858R/T790M}$ double mutant. In agreement with earlier findings,[16] a considerable loss of potency was noted for Gefitinib towards this clinically relevant mutant; under the conditions of our kinase assay, the IC_{50} increased from 4 nM to more than 7 µM (Table 1). Since our diversification at the quinazoline 6-position was expected to provide additional functions to interact with residues outside the ATP-binding site or with hydrophobic areas within (cf. docking results below), we anticipated that the potency of at least some compounds would be less strongly affected by the T790M mutation. It turned out that the activity screening against the EGFR double mutant functioned as a highly stringent filter, clearly identifying the most promising modifications of the quinazoline scaffold. These comprised both thiourea derivatives (**6a** and **6b**), and **10b**, which carried a thiazole sulfonamide moiety (Table 1). Although **6a** exhibited a 17-fold reduction of potency towards the double mutated EGFR relative to the wild-type, this was moderate compared to the 1800-fold reduction observed with Gefitinib. Consistent with the relative potencies of the three active compounds towards the purified $EGFR^{L858R/T790M}$ double mutant, **6a** conserved best the growth inhibitory activity in the H1975 cells, closely followed by **10b** (Table 2). **6b** was clearly less potent than its congener **6a** in this cell line, but since this

was also observed before in the EGFR wild-type cells, it might be attributable to a lower cell permeability of **6b**. Altogether, the preliminary SAR clearly suggest that modifications in the position 6 side chain can have a significant role in modulating the activity towards the mutant enzyme. The thiourea linker was more effective in retaining the activity when bound to the benzyl group (**6a**) than to the hydrophilic morpholine (**6b**) (Table 1), which suggests that hydrophobic interactions involving this molecule part could contribute to the binding affinity. In addition, **10b**, possessing a more hydrophilic side chain which might reach to other interaction sites, might represent an interesting alternative scaffold.

However, it became also evident that all other compounds of our series were nearly inactive towards the double mutated EGFR kinase, suggesting that inhibition of H1975 cell growth by some compounds such as **4a** and **11i** is due to off-target effects. The targets remain to be identified but might comprise e.g. further kinases. It might be the goal of future studies to identify the potentially interesting biological activity spectrum of these compounds which enables inhibition of cancer cell growth independent of the EGFR mutation status.

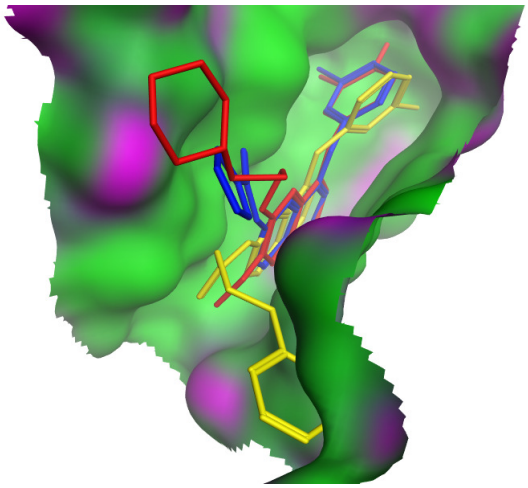

Figure 2. 3D Molecular surface map showing the docked poses of the most active compounds **9a** (yellow) and **11i** (blue) in the wild-type EGFR complexed with the reversible ATP competitive drug Gefitinib (red) (PDB entry 2ITY). All compounds show a similar binding mode for the 4-anilino quinazoline core. While the 4-anilino substituent is accommodated by the deep hydrophobic pocket, the position 6 side chain is interacting with hydrophobic regions at the exterior border of the ATP binding site. Surface color codes: green, hydrophobic areas; pink, hydrophilic regions.

An *in silico* docking of the most potent compounds **9a** and **11i** in the active site of the wild-type EGFR complexed with the reversible ATP competitive drug Gefitinib (PDB entry 2ITY)[17] predicted that the compounds might exhibit a binding conformation similar to that of Gefitinib (Figure 2). Thus it seems clear that the presence of aryl or heterocyclic rings in the position 6 side chain is tolerable and does not affect the binding mode of the quinazoline-based compounds while offering chances for additional

hydrophobic interactions with hydrophobic and/ or polar regions extending to the surface of the pocket.

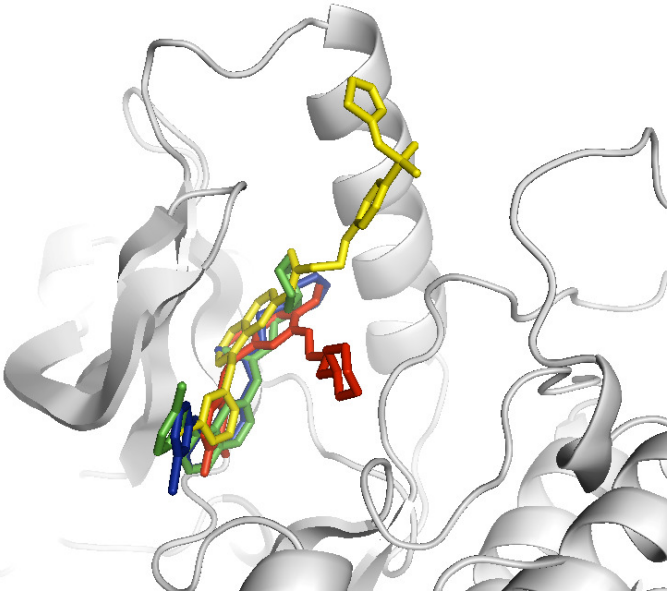

Figure 3. Docked poses of the most active compounds **6a** (blue), **6b** (green), **10b** (yellow) and Gefitinib (red) in the active site of the double mutated EGFR (PDB entry 3W2O). The docking results suggest that in particular **6a** and **6b** exhibit binding modes different from that obtained with wild-type EGFR.

Furthermore, comparative docking studies were also performed with compounds **6a**, **6b** and **10b**, which had shown markedly higher activities than Gefitinib towards the mutant EGFR kinase. The goal was to investigate whether this particular property could be explained by distinct binding modes. Firstly, using the wild-type EGFR kinase crystal structure, similar poses as with **9a** and **11i** were obtained (data not shown). In contrast, when the docking simulation was repeated using the 3D structure of the $EGFR^{L858R/T790M}$ double mutant, all three compounds exhibited binding modes different from those obtained with the wild-type EGFR kinase. In the binding poses of **6a** and **6b,** the molecules seemed to flip in a way that the entire structures including the side chains were placed much deeper in the pocket (Figure 3). This could be facilitated by the wider ATP binding cleft in the mutated enzyme which is due to a conformational shift of the N-lobe in the mutated EGFR catalytic domain. This shift is necessary to accommodate the bulky side chain of M790 adjacent to the regulatory αC-helix, in addition to a slight outward shift of the αC-helix.[18] It should be noted that essentially the same poses were consistently obtained for **6a** and **6b** in all docking runs with the EGFR double mutant, while in the case Gefitinib, no preferred binding mode was observed; poses were either similar to that in Figure 3 (red molecule) or to that in wild-type EGFR. Compound **10b** (Figure 3, yellow molecule) was docked more similarly to the Gefitinib pose shown in Figure 3 with respect to the bromophenylamino quinazoline part, while the side chain at position 6 contacted regions outside the ATP-binding pocket as anticipated.

The simulated binding poses provided a preliminary clue that in the $EGFR^{L858R/T790M}$ double mutant, compounds **6a** and **6b** might exploit an additional hydrophobic cleft which is only formed in the presence of the ^{T790M} mutation; further studies involving co-crystallography are required to experimentally confirm the potentially interesting binding mode.

Conclusion

We designed and synthesized new quinazoline derivatives having aryl and heterocyclic substituents at position 6 linked through an imine, amide or thiourea to the quinazoline nucleus. Many of the new compounds inhibited wild-type EGFR kinase with IC_{50}'s in low nanomolar range. Among these, **6a**, **11i** and **11j** were equally effective towards two model cell lines which grow dependent on wild-type and mutant EGFR, respectively, and displayed a more potent cell growth inhibition than the reference compound Gefitinib. However, at least in the case of **11i** and **11j**, the enhanced potency towards the H1975 cells harboring the $EGFR^{L858R/T790M}$ double mutant might be due to biological activities unrelated to EGFR kinase, because these compounds were inactive towards the purified double mutant. However, our diversification strategy at position 6 yielded two novel derivatives of quinazoline-based EGFR kinase inhibitors which retained significant activity towards the clinically relevant $EGFR^{L858R/T790M}$ mutant, one of which (compound **6a)** displayed a 24-fold stronger potency than Gefitinib. Because **6a** also retained a higher activity than Gefitinib in the H1975 cells, it represents the most promising lead compound of this study. Since our SAR clearly indicated that the cyclic substituent at the position 6 side chain is crucial for the biological activity of all linker chemotypes, replacement of the benzyl in **6a** by substituted derivatives or five- and six-membered heterocycles would likely result in optimized EGFR kinase inhibitors which are equally potent towards the wild-type enzyme and Gefitinib-resistant mutants.

Experimental Section

Solvents and reagents were obtained from commercial suppliers and used as received. ^{1}H and ^{13}C NMR spectra were recorded on a Bruker DRX 500 spectrometer. Chemical shifts are referenced to the residual protonated solvent signals. The purities of the tested compounds **4a-4e, 6a-b, 9a-b, 10a-b** and **11a-k** were determined by HPLC coupled with mass spectrometry and were higher than 97.5% except when mentioned. Mass spectrometric analysis (HPLC-ESI-MS) was performed on a TSQ quantum (Thermo Electron Corporation) instrument equipped with an ESI source and a triple quadrupole mass detector (Thermo Finnigan). The MS detection was carried out at a spray voltage of 4.2 kV, a nitrogen sheath gas pressure of 4.0×10^5 Pa, an auxiliary gas pressure of 1.0×10^5 Pa, a capillary temperature of 400 ºC, a capillary voltage of 35 V, and a source CID of 10 V. All samples were injected by an autosampler (Surveyor, Thermo Finnigan) with an injection volume of 10 μL. An RP C18 NUCLEODUR 100-3

(125 x 3 mm) column (Macherey-Nagel) was used as the stationary phase. The solvent system consisted of water containing 0.1% TFA (A) and 0.1% TFA in acetonitrile (B). HPLC-Method: flow rate 400 μL/min. The percentage of B started at an initial of 5%, was increased up to 100% during 16 min, kept at 100% for 2 min, and flushed back to 5% in 2 min. Melting points are uncorrected and were determined on Buchi melting point apparatus (B-540). The IR spectra were measured on Nicolet 380 FT-IR spectrometer. The elemental analysis was measured using an analyzer Model: Euro EA 3000 (Italy) done in the Regional Center for Mycology and Biotechnology, Al Azhar University, Cairo, Egypt.

Ethyl *N*-(2-cyano-4-nitrophenyl)formimidate (1). 5g (30.6 mmol) of 2-amino-5-nitrobenzonitrile was refluxed in 50ml of triethyl orthoformate for 24 hours in the presence of 10 drops of acetic anhydride. The reaction was then concentrated under vacuum and the remaining residue was poured on ice water where a precipitate has been formed. The ppt. was filtered under vacuum and left to dry to give compound **1**. Yield 82% (5.5 g, yellow solid); ^{1}H NMR (500 MHz, [D$_6$]DMSO): δ = 1.35 (t, J = 7.1 Hz, 3H), 4.36 (q, J = 7.0 Hz, 2H), 7.46 (s, J = 8.9 Hz, 1H), 8.22 (s, 1H), 8.43 (dd, J = 8.9, 2.7 Hz, 1H), 8.67 ppm (d, J = 2.6 Hz, 1H); ^{13}C NMR (126 MHz, [D$_6$]DMSO): δ = 13.87, 63.65, 114.95, 115.56, 122.20, 128.84, 130.58, 143.50, 156.08, 156.31 ppm; IR: $\tilde{\nu}$ = 2228.6 cm^{-1} (C≡N).

***N*-(3-bromophenyl)-6-nitroquinazolin-4-amine (2).**[19] Compound **1** (5 mmol) was refluxed for 1 hour with 3-bromo aniline (5 mmol) in 8ml glacial acetic acid. A precipitate is formed during the reaction which is filtered on hot and the precipitate is then washed with diethyl ether to give the corresponding nitroquinazoline derivative **2**.

***N*^{4}-(3-bromophenyl)quinazoline-4,6-diamine (3).**[19] According to the reported procedure,[20] a mixture of the nitroquinazoline derivative **2** (5 mmol) and stannous chloride (25 mmol) in MeOH (20 ml) was stirred at reflux for 1 h under nitrogen atmosphere. The excess MeOH was removed under reduced pressure; the remaining residue was dissolved in ethyl acetate (200 ml) and basified with aqueous $NaHCO_3$ solution. The resulting mixture was filtrated under vacuum followed by separation of the organic phase from the aqueous phase. The aqueous phase was extracted with ethyl acetate (2 x 20 ml), these organic fractions were combined, dried over anhydrous $MgSO_4$ and concentrated under reduced pressure to obtain the corresponding aminoquinazoline derivative **3**.

General procedure for the synthesis of compounds (4a-4e). A mixture of compound **3** (0.65 mmol) and the corresponding benzaldehyde derivative (0.65 mmol) were refluxed for 8h in ethanol (15 ml). The precipitate formed was filtered while hot and washed with ethanol to give the corresponding imine derivatives **4a-4e**.

4-(((4-((3-bromophenyl)amino)quinazolin-6-yl)imino)methyl)phenol (4a). Yield 42% (115 mg, yellow solid); m.p. 264-266 °C; ^{1}H NMR (500 MHz, [D$_6$]DMSO) δ = 6.91 – 6.95 (m, 2H), 7.29 (ddd, *J* = 8.0, 1.9, 1.0 Hz, 1H), 7.35 (t, *J* = 8.0 Hz, 1H), 7.81 (dd, *J* = 8.8, 1.9 Hz, 1H), 7.82 – 7.83 (m, 1H), 7.83 – 7.88 (m, 2H), 7.97 (ddd, *J* = 8.2, 2.0, 1.0 Hz, 1H), 8.28 (t, *J* = 2.0 Hz, 1H), 8.34 (d, *J* = 1.4 Hz, 1H), 8.64 (d, *J* = 2.3 Hz, 2H), 9.82 (s, 1H),10.23 ppm (s, 1H); ^{13}C NMR (126 MHz, [D$_6$]DMSO) δ = 113.44, 115.65, 115.82, 120.45, 121.21, 123.94, 125.86, 127.31, 127.67, 128.92, 130.39, 130.94, 141.07, 147.96, 150.08, 153.32, 157.37, 161.01, 161.37 ppm; Anal. calcd for $C_{21}H_{15}BrN_4O$: C 60.16, H 3.61, N 13.36, found: C 60.28, H 3.68, O 13.49.

4-(((4-((3-bromophenyl)amino)quinazolin-6-yl)imino)methyl)benzene-1,3-diol (4b). Yield 39% (110 mg, orange solid); m.p. 241-243 °C; ^{1}H NMR (500 MHz, [D$_6$]DMSO) δ = 6.35 (d, *J* = 2.3 Hz, 1H), 6.46 (dd, *J* = 8.5, 2.3 Hz, 1H), 7.31 (ddd, *J* = 7.9, 1.7, 0.9 Hz, 1H), 7.37 (t, *J* = 8.0 Hz, 1H), 7.51 (d, *J* = 8.6 Hz, 1H), 7.86 (d, *J* = 8.9 Hz, 1H), 7.95 (ddd, *J* = 5.5, 2.8, 1.5 Hz, 2H), 8.25 (t, *J* = 1.9 Hz, 1H), 8.47 (d, *J* = 2.1 Hz, 1H), 8.64 (s, 1H), 8.97 (s, 1H), 9.85 (s, 1H), 10.40 (s, 1H), 11.89 ppm (s, 1H); ^{13}C NMR (126 MHz, [D$_6$]DMSO) δ = 102.46, 108.19, 112.12, 114.64, 115.63, 120.61, 121.19, 124.09, 126.01, 126.81, 129.18, 130.39, 134.47, 140.90, 146.35, 148.30, 153.69, 157.39, 162.84, 162.95, 163.32 ppm; MS (+ESI): m/z = 434.55 (M^+); Anal. calcd for $C_{21}H_{15}BrN_4O_2$: C 57.95, H 3.47, N 12.87, found: C 57.98, H 3.52, O 13.02.

***N*^{4}-(3-bromophenyl)-*N*^{6}-(3-nitrobenzylidene)quinazoline-4,6-diamine (4c).** Yield 23% (47 mg, pale yellow solid); m.p. 238-239 °C; ^{1}H NMR (500 MHz, [D$_6$]DMSO) δ = 7.23 – 7.27 (m, 1H), 7.33 (t, *J* = 8.0 Hz, 1H), 7.83 (d, *J* = 8.8 Hz, 1H), 7.84 – 7.90 (m, 2H), 7.92 (dd, *J* = 8.8, 2.2 Hz, 1H), 8.22 (t, *J* = 1.9 Hz, 1H), 8.38 – 8.44 (m, 2H), 8.49 (d, *J* = 2.1 Hz, 1H), 8.59 (s, 1H), 8.78 – 8.86 (m, 1H), 9.01 (s, 1H), 9.89 ppm (s, 1H); ^{13}C NMR (126 MHz, [D$_6$]DMSO) δ = 114.01, 115.69, 116.37, 120.78, 121.16, 122.57, 124.20, 125.38, 125.82, 126.48, 128.83, 130.26, 130.67, 134.79, 137.46, 147.79, 148.29, 148.88, 154.19, 157.71, 159.44 ppm; Anal. calcd for $C_{21}H_{14}BrN_5O_2$: C 56.27, H 3.15, N 15.62, found: C 56.33, H 3.19, O 15.74.

***N*^{4}-(3-bromophenyl)-*N*^{6}-(4-nitrobenzylidene)quinazoline-4,6-diamine (4d).** Yield 35% (100 mg, pale yellow solid); m.p. 254-255 °C; ^{1}H NMR (500 MHz, [D$_6$]DMSO) δ = 7.29 (d, *J* = 8.1 Hz, 1H), 7.35 (t, *J* = 8.0 Hz, 1H), 7.87 (d, *J* = 8.8 Hz, 1H), 7.89 – 8.00 (m, 2H), 8.26 (d, *J* = 8.9 Hz, 3H), 8.41 (d, *J* = 8.8 Hz, 2H), 8.51 (d, *J* = 2.1 Hz, 1H), 8.64 (s, 1H), 9.00 (s, 1H), 9.91 ppm (s, 1H); ^{13}C NMR (126 MHz, [D$_6$]DMSO) δ = 115.42, 115.85, 120.65, 121.18, 124.11, 124.16, 125.78, 126.86, 129.02, 129.73, 130.35, 141.29, 141.50, 148.17, 148.86, 149.00, 154.09, 157.63, 159.89 ppm; Anal. calcd for $C_{21}H_{14}BrN_5O_2$: C 56.27, H 3.15, N 15.62, found: C 56.37, H 3.19, O 15.76.

***N*^{4}-(3-bromophenyl)-*N*^{6}-(2-methoxybenzylidene)quinazoline-4,6-diamine (4e).** Yield 29% (82 mg, pale yellow solid); m.p. 263-264 °C; ^{1}H NMR (500 MHz, [D$_6$]DMSO) δ =

3.93 (s, 3H), 7.11 (t, *J* = 7.5 Hz, 1H), 7.21 (d, *J* = 8.3 Hz, 1H), 7.26 (d, *J* = 8.5 Hz, 1H), 7.33 (t, *J* = 8.0 Hz, 1H), 7.51 – 7.61 (m, 1H), 7.73 – 7.83 (m, 2H), 7.90 (d, *J* = 8.0 Hz, 1H), 8.10 (dd, *J* = 7.7, 1.7 Hz, 1H), 8.22 (s, 1H), 8.35 (d, *J* = 1.6 Hz, 1H), 8.59 (s, 1H), 9.03 (s, 1H), 9.88 ppm (s, 1H); ^{13}C NMR (126 MHz, [D_6]DMSO) δ = 55.80, 112.11, 113.43, 116.12, 116.19, 117.32, 120.76, 121.14, 123.71, 124.18, 125.50, 126.88, 127.64, 128.78, 130.26, 133.57, 148.31, 149.82, 153.69, 156.48, 157.58, 159.43 ppm; Anal. calcd for $C_{22}H_{17}BrN_4O$: C 60.98, H 3.95, N 12.93, found: C 61.12, H 3.94, O 13.02.

N-(3-bromophenyl)-6-isothiocyanatoquinazolin-4-amine (5). Compound **3** (2 mmol) was added to a water solution (20ml) upon which conc. HCl (1 ml) was then added and stirred at 0ºC. Thiophosgene (2.2 mmol) was then added dropwise to the stirred solution and left stirring for 3 hours after which the formed precipitate is filtered and washed with diethyl ether to give compound **5**. Yield 81% (580 mg, yellow solid); ^{1}H NMR (500 MHz, [D_6]DMSO) δ = 7.46 (d, *J* = 8.0 Hz, 1H), 7.51 (ddd, *J* = 8.0, 1.9, 1.1 Hz, 1H), 7.78 (ddd, *J* = 8.0, 2.0, 1.1 Hz, 1H), 7.99 (d, *J* = 8.9 Hz, 1H), 8.06 (t, *J* = 1.9 Hz, 1H), 8.32 (dd, *J* = 9.0, 2.1 Hz, 1H), 8.88 (d, *J* = 2.0 Hz, 1H), 8.95 (s, 1H),11.29 ppm (s, 1H); ^{13}C NMR (126 MHz, [D_6]DMSO) δ = 113.97, 118.78, 120.53, 121.17, 123.39, 126.99, 128.96, 130.59, 130.64, 134.52, 138.59, 139.28, 150.55, 159.32, 181.28 ppm; MS (+ESI): m/z = 357.03 (M + H).

General procedure for the synthesis of compounds (6a and 6b). A mixture of compound **5** (0.7 mmol) and the corresponding amine derivative (0.7 mmol) were stirred at room temperature for 16h in DMF (10 ml). The solution was then poured on iced water where a precipitate was formed which was then filtered. The solid was then purified using column chromatography using (Ethylacetate/Hexane 8:2) as eluent to give compounds **6a** and **6b**.

1-benzyl-3-(4-((3-bromophenyl)amino)quinazolin-6-yl)thiourea (6a). Yield 52% (168 mg, pale brown solid); purity 95.73%; m.p. 197-198 °C; ^{1}H NMR (500 MHz, [D_6]DMSO) δ = 4.79 (d, *J* = 5.1 Hz, 2H), 7.25 (t, *J* = 7.1 Hz, 1H), 7.30 (ddd, *J* = 7.9, 1.9, 1.0 Hz, 1H), 7.31 – 7.38 (m, 5H), 7.78 (d, *J* = 8.9 Hz, 1H), 7.85 (dd, *J* = 8.9, 2.1 Hz, 1H), 7.93 (ddd, *J* = 8.2, 1.9, 0.9 Hz, 1H), 8.25 (t, *J* = 1.9 Hz, 1H), 8.42 (s, 1H), 8.47 (d, *J* = 1.3 Hz, 1H), 8.64 (s, 1H), 9.83 (s, 1H), 9.91 ppm (s, 1H); ^{13}C NMR (126 MHz, [D_6]DMSO) δ = 47.51, 115.26, 117.77, 120.43, 121.21, 123.89, 125.86, 126.83, 127.41, 128.21, 130.41, 131.80, 131.83, 136.98, 139.00, 141.07, 147.51, 153.66, 157.11,181.56 ppm; MS (+ESI): m/z = 464.09 (M + H); Anal. calcd for $C_{22}H_{18}BrN_5S$: C 56.90, H 3.91, N 15.08, found: C 56.97, H 3.95, O 15.16.

1-(4-((3-bromophenyl)amino)quinazolin-6-yl)-3-(2-morpholinoethyl)thiourea (6b). Yield 52% (175 mg, pale yellow solid); m.p. 149-151 °C; ^{1}H NMR (500 MHz, $(CD_3)_2CO$)) δ = 2.41 (s, 4H), 2.58 (s, 2H), 3.47 (s, 4H), 3.71 (s, 2H), 7.29 (ddd, *J* = 7.9, 1.6, 1.1 Hz, 1H), 7.34 (t, *J* = 8.0 Hz, 1H), 7.44 (s, 1H), 7.83 – 7.89 (m, 2H), 7.95 (ddd, *J*

= 8.0, 1.8, 1.0 Hz, 1H), 8.32 – 8.41 (m, 2H), 8.68 ppm (s, 1H), 9.15 (s, 2H); ^{13}C NMR (126 MHz, [D$_6$]DMSO) δ = 40.94, 53.06, 56.34, 66.14, 115.21, 117.13, 120.44, 121.18, 123.90, 125.87, 128.33, 130.39, 131.49, 136.92, 141.01, 147.40, 153.64, 157.04, 180.71 ppm; MS (+ESI): m/z = 487.16 (M + H); Anal. calcd for $C_{21}H_{23}BrN_6OS$: C 51.75, H 4.76, N 17.24, found: C 51.87, H 4.80, O 17.41.

General procedure for the synthesis of compounds (7 and 8). A mixture of intermediate **3** (2 mmol) and $NaHCO_3$ (2.2 mmol) was stirred at 0ºC in acetone (10 ml) under nitrogen atmosphere. This is then followed by dropwise addition of choroacetyl chloride (2.2 mmol) or chloropropionyl chloride (2.2 mmol) and then was stirred for 30 min. at 0ºC to give compounds **7** and **8**, respectively. Excess solvent was then removed under reduced pressure and the remaining residue was neutralized using $NaHCO_3$ solution. The formed solid was then filtered and the purified using column chromatography with ethylacetate as eluent.

N-(4-((3-bromophenyl)amino)quinazolin-6-yl)-2-chloroacetamide (7). Yield 75% (590 mg, yellow solid); ^{1}H NMR (400 MHz, [D$_6$]DMSO) δ = 4.43 (s, 2H), 7.43 (t, *J* = 7.9 Hz, 1H), 7.48 (dt, *J* = 8.0, 1.4 Hz, 1H), 7.70 – 7.78 (m, 1H), 7.96 (d, *J* = 9.0 Hz, 1H), 8.02 (t, *J* = 1.9 Hz, 1H), 8.06 (dd, *J* = 9.0, 2.1 Hz, 1H), 8.84 (s, 1H), 8.98 (d, *J* = 2.0 Hz, 1H), 11.15 (s, 1H),11.27 ppm (s, 1H); ^{13}C NMR (101 MHz, [D$_6$]DMSO) δ = 43.41, 112.99, 114.43, 121.14, 122.71, 123.16, 126.73, 128.46, 129.07, 130.58, 137.88, 138.13, 139.12, 150.57, 159.13, 165.28 ppm; MS (+ESI): m/z = 391.05 (M + H).

***N*-(4-((3-bromophenyl)amino)quinazolin-6-yl)-3-chloropropanamide (8)** Yield 79% (640 mg, yellow solid); ^{1}H NMR (500 MHz, [D$_6$]DMSO) δ = 2.92 (t, *J* = 6.2 Hz, 2H), 3.94 (t, *J* = 6.2 Hz, 2H), 7.26 – 7.30 (m, 1H), 7.34 (t, *J* = 8.0 Hz, 1H), 7.80 (d, *J* = 8.9 Hz, 1H), 7.87 (dt, *J* = 10.3, 5.2 Hz, 2H), 8.16 (s, 1H), 8.58 (d, *J* = 4.3 Hz, 1H), 8.72 (d, *J* = 1.6 Hz, 1H), 9.93 (s, 1H), 10.42 ppm (s, 1H); ^{13}C NMR (126 MHz, [D$_6$]DMSO) δ = 39.11, 40.66, 111.76, 115.46, 120.88, 121.08, 124.31, 125.82, 127.09, 128.49, 130.25, 136.65, 141.18, 146.68, 153.03, 157.29, 168.21 ppm; MS (+ESI): m/z = 405.02 (M + H).

General procedure for the synthesis of compounds (9a and 9b). A mixture of the intermediate **7** (0.5 mmol) and the corresponding amine derivative (0.6 mmol) were refluxed for 8h in methanol (15 ml) in the presence of 5 drops triethyl amine. Excess solvent was then removed under reduced pressure and the remaining residue was purified using column chromatography with (Dichloromethane/Methanol 100:5) as eluent to yield compounds **9a** and **9b**.

2-(benzylamino)-*N*-(4-((3-bromophenyl)amino)quinazolin-6-yl)acetamide (9a). Yield 50% (115 mg, pale brown solid); purity 96.02%; m.p. 189-191 °C; ^{1}H NMR (500 MHz, [D$_6$]DMSO) δ = 3.36 (s, 2H), 3.81 (s, 2H), 7.25 (t, *J* = 7.3 Hz, 1H), 7.27 – 7.38 (m, 5H), 7.40 (d, *J* = 7.4 Hz, 2H), 7.79 (d, *J* = 8.9 Hz, 1H), 7.88 (d, *J* = 7.8 Hz, 1H), 8.06 (d,

J = 8.9 Hz, 1H), 8.18 (s, 1H), 8.58 (s, 1H), 8.65 (d, *J* = 1.5 Hz, 1H), 9.86 (s, 1H),10.12 ppm (s, 1H); ^{13}C NMR (126 MHz, [D$_6$]DMSO) δ = 51.87, 52.64, 111.70, 115.40, 120.77, 121.12, 124.21, 125.83, 126.76, 126.98, 128.05, 128.22, 128.45, 130.30, 136.48, 140.14, 141.14, 146.59, 153.00, 157.18, 170.39 ppm; MS (+ESI): m/z = 462.13 (M + H); Anal. calcd for $C_{23}H_{20}BrN_5O$: C 59.75, H 4.36, N 15.15, found: C 59.86, H 4.39, O 15.21.

***N*-(4-((3-bromophenyl)amino)quinazolin-6-yl)-2-((4-(*N*-(thiazol-2-yl)sulfamoyl) phenyl)amino)acetamide (9b).** Yield 40% (120 mg, pale orange solid); purity 96%; m.p. 297-298 °C; ^{1}H NMR (500 MHz, [D$_6$]DMSO) δ = 4.90 (s, 2H), 5.81 (s, 2H), 6.45 – 6.55 (m, 2H), 6.85 (d, *J* = 4.7 Hz, 1H), 7.28 (ddd, *J* = 8.0, 1.8, 1.1 Hz, 1H), 7.33 (t, *J* = 8.0 Hz, 1H), 7.38 (d, *J* = 4.7 Hz, 1H), 7.40 – 7.44 (m, 2H), 7.81 (d, *J* = 2.0 Hz, 2H), 7.83 – 7.87 (m, 1H), 8.16 (t, *J* = 1.9 Hz, 1H), 8.59 (s, 1H), 8.72 (s, 1H), 9.93 (s, 1H), 10.73 ppm (s, 1H); ^{13}C NMR (126 MHz, [D$_6$]DMSO) δ = 49.67, 105.50, 111.68, 112.37, 115.47, 120.97, 121.06, 124.40, 125.86, 126.86, 127.39, 127.78, 128.68, 129.01, 130.23, 136.20, 141.13, 146.81, 152.30, 153.17, 157.30, 164.82, 166.05 ppm; MS (+ESI): m/z = 610.08 (M + H); Anal. calcd for $C_{25}H_{20}BrN_7O_3S_2$: C 49.18, H 3.30, N 16.06, found: C 49.22, H 3.28, O 16.22.

General procedure for the synthesis of compounds (10a and 10b). A mixture of the intermediate **8** (0.5 mmol) and the corresponding amine derivative (0.6 mmol) were refluxed for 8h in ethanol (15 ml) in the presence of 5 drops triethyl amine. Excess solvent was then removed under reduced pressure and the remaining residue was purified using column chromatography with (Dichloromethane/Methanol 100:5) as eluent to yield compounds **10a** and **10b**.

***N*-(4-((3-bromophenyl)amino)quinazolin-6-yl)-3-((2-morpholinoethyl)amino) propanamide (10a)** Yield 64% (160 mg, semisolid); purity 95.42%; ^{1}H NMR (500 MHz, [D$_6$]DMSO) δ = 1.77 (s, 1H), 2.34 (s, 4H), 2.38 (t, *J* = 6.4 Hz, 2H), 2.53 (t, *J* = 6.6 Hz, 2H), 2.65 (t, *J* = 6.4 Hz, 2H), 2.87 (t, *J* = 6.6 Hz, 2H), 3.50 – 3.53 (m, 4H), 7.27 (d, *J* = 8.0 Hz, 1H), 7.33 (t, *J* = 8.0 Hz, 1H), 7.76 (d, *J* = 9.0 Hz, 1H), 7.92 (d, *J* = 8.1 Hz, 1H), 7.96 – 8.03 (m, 1H), 8.22 (s, 1H), 8.56 (s, 1H), 8.83 (s, 1H), 9.96 (s, 1H), 10.72 ppm (s, 1H); MS (+ESI): m/z = 499.02 (M + H); Anal. calcd for $C_{23}H_{27}BrN_6O_2$: C 55.32, H 5.45, N 16.83, found: C 55.39, H 5.48, O 17.01.

***N*-(4-((3-bromophenyl)amino)quinazolin-6-yl)-3-((4-(*N*-(thiazol-2-yl)sulfamoyl) phenyl)amino)propanamide (10b).** Yield 67% (210 mg, yellow solid); m.p. 262-264 °C; ^{1}H NMR (500 MHz, [D$_6$]DMSO) δ = 2.88 (t, *J* = 6.7 Hz, 2H), 4.21 (t, *J* = 6.7 Hz, 2H), 5.85 (s, 2H), 6.57 (d, *J* = 8.6 Hz, 2H), 6.81 (d, *J* = 4.7 Hz, 1H), 7.29 (d, *J* = 8.2 Hz, 1H), 7.31 – 7.37 (m, 2H), 7.48 (d, *J* = 8.6 Hz, 2H), 7.79 (d, *J* = 8.9 Hz, 1H), 7.84 (dd, *J* = 14.5, 5.4 Hz, 2H), 8.17 (t, *J* = 1.8 Hz, 1H), 8.58 (s, 1H), 8.65 (d, *J* = 1.6 Hz, 1H), 9.87 (s, 1H),10.41 ppm (s, 1H); ^{13}C NMR (126 MHz, [D$_6$]DMSO) δ = 34.12, 43.76, 105.96, 112.10, 112.44, 115.40, 120.81, 121.10, 124.25, 125.82, 127.30, 127.32, 127.91, 128.48,

128.64, 130.28, 136.46, 141.15, 146.69, 152.31, 153.07, 157.25, 165.22, 168.58 ppm; MS (+ESI): m/z = 624.04 (M + H); Anal. calcd for $C_{26}H_{22}BrN_7O_3S_2$: C 50.00, H 3.55, N 15.70, found: C 50.14, H 3.59, O 15.82.

General procedure for the synthesis of compounds (11b-k). A mixture of intermediate **3** (0.65 mmol) and $NaHCO_3$ (0.8 mmol) was stirred at 0ºC in acetone (10 ml) under nitrogen atmosphere. This is then followed by dropwise addition of corresponding acid chloride derivative (0.8 mmol) and then was stirred for 30 min. at 0ºC to yield compounds **11b-k**. Excess solvent was then removed under reduced pressure and the remaining residue was neutralized using $NaHCO_3$ solution. The formed solid was then filtered and the purified using column chromatography with ethylacetate as eluent.

4-amino-*N*-(4-((3-bromophenyl)amino)quinazolin-6-yl)benzamide (11a). Compound **11a** was synthesized from its nitro derivative **11d** through the same procedure of compound **3**. Yield 30% (84 mg, yellow solid); m.p. 288-289 °C; ^{1}H NMR (500 MHz, [D_6]DMSO) δ = 5.81 (s, 2H), 6.64 (d, *J* = 8.7 Hz, 2H), 7.28 (ddd, *J* = 8.0, 1.7, 0.9 Hz, 1H), 7.34 (t, *J* = 8.0 Hz, 1H), 7.80 (t, *J* = 8.5 Hz, 3H), 7.87 – 7.92 (m, 1H), 8.02 (dd, *J* = 9.0, 2.2 Hz, 1H), 8.21 (t, *J* = 1.9 Hz, 1H), 8.59 (s, 1H), 8.86 (d, *J* = 2.0 Hz, 1H), 9.87 (s, 1H), 10.12 ppm (s, 1H); ^{13}C NMR (126 MHz, [D_6]DMSO) δ = 112.63, 112.96, 115.36, 120.45, 120.66, 121.11, 124.12, 125.71, 128.04, 128.36, 129.42, 130.28, 137.55, 141.26, 146.49, 152.40, 152.86, 157.21, 165.31 ppm; MS (+ESI): m/z = 433.99 (M + H); Anal. calcd for $C_{21}H_{16}BrN_5O$: C 58.08, H 3.71, N 16.13, found: C 58.21, H 3.79, O 16.26.

***N*-(4-((3-bromophenyl)amino)quinazolin-6-yl)-4-cyanobenzamide (11b).** Yield 27% (77 mg, white solid) ; m.p. 347-349 °C; ^{1}H NMR (500 MHz, [D_6]DMSO) δ = 7.46 (t, *J* = 8.0 Hz, 1H), 7.52 (ddd, *J* = 8.0, 1.9, 1.0 Hz, 1H), 7.75 (ddd, *J* = 8.0, 1.9, 1.0 Hz, 1H), 8.02 (t, *J* = 1.9 Hz, 1H), 8.05 – 8.09 (m, 3H), 8.24 – 8.27 (m, 2H), 8.29 (dd, *J* = 9.1, 2.1 Hz, 1H), 8.94 (s, 1H), 9.24 (d, *J* = 2.0 Hz, 1H), 11.25 (s, 1H),11.61 ppm (s, 1H); ^{13}C NMR (126 MHz, [D_6]DMSO) δ = 114.01, 114.35, 114.64, 118.20, 120.89, 121.13, 123.62, 127.22, 128.71, 129.05, 130.62, 130.76, 132.60, 136.12, 137.89, 138.52, 138.60, 149.96, 159.62,164.41 ppm; MS (+ESI): m/z = 444.08 (M + H); Anal. calcd for $C_{22}H_{14}BrN_5O$: C 59.47, H 3.18, N 15.76, found: C 59.61, H 3.14, O 15.82.

4-acetamido-*N*-(4-((3-bromophenyl)amino)quinazolin-6-yl)benzamide (11c). Yield 25% (76 mg, pale yellow solid); m.p. 338-340 °C; ^{1}H NMR (500 MHz, [D_6]DMSO) δ = 2.10 (s, 3H), 7.29 (d, *J* = 8.6 Hz, 1H), 7.35 (t, *J* = 8.0 Hz, 1H), 7.76 (d, *J* = 8.7 Hz, 2H), 7.83 (d, *J* = 8.9 Hz, 1H), 7.90 (d, *J* = 8.1 Hz, 1H), 7.99 – 8.07 (m, 3H), 8.21 (s, 1H), 8.61 (s, 1H), 8.90 (d, *J* = 1.8 Hz, 1H), 9.93 (s, 1H), 10.24 (s, 1H),10.49 ppm (s, 1H); ^{13}C NMR (126 MHz, [D_6]DMSO) δ = 24.12, 113.52, 115.33, 117.54, 118.21, 120.71, 121.12, 124.17, 125.78, 128.21, 128.42, 128.64, 130.29, 136.98, 141.20, 142.52, 146.80, 153.14, 157.28, 164.96,168.79 ppm; MS (+ESI): m/z = 476.1 (M + H); Anal. calcd for $C_{23}H_{18}BrN_5O_2$: C 58.00, H 3.81, N 14.70, found: C 58.13, H 3.79, O 14.84.

***N*-(4-((3-bromophenyl)amino)quinazolin-6-yl)-4-nitrobenzamide (11d).** Yield 62% (188 mg, orange solid); purity 95.77%; m.p. 310-312 °C; ^{1}H NMR (500 MHz, [D$_6$]DMSO) δ = 7.36 – 7.47 (m, 2H), 7.79 (dt, *J* = 7.0, 2.0 Hz, 1H), 7.96 (d, *J* = 9.0 Hz, 1H), 8.08 (d, *J* = 1.8 Hz, 1H), 8.19 (dd, *J* = 9.0, 2.1 Hz, 1H), 8.27 – 8.34 (m, 2H), 8.36 – 8.45 (m, 2H), 8.81 (s, 1H), 9.10 (d, *J* = 2.0 Hz, 1H), 10.94 (s, 1H),11.18 ppm (s, 1H); ^{13}C NMR (126 MHz, [D$_6$]DMSO) δ = 114.39, 114.51, 121.14, 122.55,123.67, 126.10, 127.87, 129.35, 129.84, 130.51, 137.64, 139.57, 139.69, 146.99, 149.41, 151.30, 158.70, 160.05, 164.10 ppm; MS (+ESI): m/z = 464.08 (M + H); Anal. calcd for $C_{21}H_{14}BrN_5O_3$: C 54.33, H 3.04, N 15.08, found: C 54.36, H 3.10, O 15.21.

***N*-(4-((3-bromophenyl)amino)quinazolin-6-yl)-3,5-dinitrobenzamide (11e).** Yield 51% (167 mg, yellow solid); m.p. 351-352 °C; ^{1}H NMR (500 MHz, [D$_6$]DMSO) δ = 7.43 (t, *J* = 8.0 Hz, 1H), 7.48 (ddd, *J* = 8.0, 1.8, 1.1 Hz, 1H), 7.78 (ddd, *J* = 7.9, 1.9, 1.1 Hz, 1H), 8.02 – 8.10 (m, 2H), 8.33 (dd, *J* = 9.0, 2.1 Hz, 1H), 8.91 (s, 1H), 9.02 (t, *J* = 2.1 Hz, 1H), 9.18 (d, *J* = 2.0 Hz, 1H), 9.27 (d, *J* = 2.1 Hz, 2H), 11.54 (s, 1H),11.68 ppm (s, 1H); ^{13}C NMR (126 MHz, [D$_6$]DMSO) δ = 114.12, 115.15, 121.11, 121.43, 121.62, 123.33, 126.87, 128.19, 128.70, 130.52, 136.59, 137.81, 138.83, 139.55, 148.13, 149.55, 150.41, 159.34, 161.72 ppm; MS (+ESI): m/z = 509.05 (M + H); Anal. calcd for $C_{21}H_{13}BrN_6O_5$: C 49.53, H 2.57, N 16.50, found: C 49.61, H 2.52, O 16.73.

***N*-(4-((3-bromophenyl)amino)quinazolin-6-yl)-4-methoxybenzamide (11f).** Yield 62% (180 mg, yellow solid); purity 95.12%; m.p. 331-333 °C; ^{1}H NMR (500 MHz, TFA-D) δ = 4.15 (s, 3H), 7.31 (d, *J* = 8.9 Hz, 2H), 7.58 (t, *J* = 8.1 Hz, 1H), 7.70 (d, *J* = 9.0 Hz, 1H), 7.81 (d, *J* = 8.1 Hz, 1H), 7.95 (s, 1H), 8.15 (d, *J* = 8.9 Hz, 2H), 8.23 (d, *J* = 9.0 Hz, 1H), 8.33 (dd, *J* = 9.1, 1.7 Hz, 1H), 9.11 (s, 1H), 9.81 ppm (d, *J* = 1.4 Hz, 1H); ^{13}C NMR (126 MHz, TFA-D) δ = 57.61, 116.27, 116.59, 117.24, 123.63, 125.85, 126.43, 126.92, 131.06, 132.36, 133.57, 134.05, 135.38, 136.73, 137.23, 142.34, 151.54, 162.02, 166.22,172.54 ppm; MS (+ESI): m/z = 449.08 (M + H); Anal. calcd for $C_{22}H_{17}BrN_4O_2$: C 58.81, H 3.81, N 12.47, found: C 58.89, H 3.88, O 12.55.

***N*-(4-((3-bromophenyl)amino)quinazolin-6-yl)-3,4-dimethoxybenzamide (11g).** Yield 46% (143, yellow solid); purity 95.54%; m.p. 257-258 °C; ^{1}H NMR (500 MHz, TFA-D) δ = 4.22 (s, 3H), 4.23 (s, 3H), 7.33 (d, *J* = 8.6 Hz, 1H), 7.62 (t, *J* = 8.1 Hz, 1H), 7.74 (ddd, *J* = 8.0, 2.0, 0.8 Hz, 1H), 7.80 (d, *J* = 2.1 Hz, 1H), 7.85 (ddd, *J* = 8.1, 1.8, 0.9 Hz, 1H), 7.91 (dd, *J* = 8.5, 2.1 Hz, 1H), 8.00 (t, *J* = 1.9 Hz, 1H), 8.20 (d, *J* = 9.0 Hz, 1H), 8.31 (dd, *J* = 9.0, 2.1 Hz, 1H), 9.08 (s, 1H), 9.83 ppm (d, *J* = 2.0 Hz, 1H); ^{13}C NMR (126 MHz, TFA-D) δ = 55.76, 56.02, 111.73, 114.29, 114.60, 116.52, 121.46, 122.88, 123.79, 124.41, 125.16, 129.06, 131.52, 131.86, 133.26, 134.96, 135.50, 140.12, 149.24, 149.84, 154.06, 160.60, 170.37 ppm; MS (+ESI): m/z = 479.09 (M + H); Anal. calcd for $C_{23}H_{19}BrN_4O_3$: C 57.63, H 4.00, N 11.69, found: C 57.76, H 4.03, O 11.85.

***N*-(4-((3-bromophenyl)amino)quinazolin-6-yl)morpholine-4-carboxamide (11h).** Yield 24% (65 mg, pale brown solid); purity 95.33%; m.p. 281-283 °C; ^{1}H NMR (500 MHz, [D$_6$]DMSO) δ = 3.46 – 3.54 (m, 4H), 3.61 – 3.69 (m, 4H), 7.27 (ddd, *J* = 7.9, 1.8, 0.9 Hz, 1H), 7.33 (t, *J* = 8.0 Hz, 1H), 7.73 (d, *J* = 8.9 Hz, 1H), 7.84 (dd, *J* = 9.0, 2.2 Hz, 1H), 7.88 (d, *J* = 7.9 Hz, 1H), 8.19 (s, 1H), 8.50 (d, *J* = 2.0 Hz, 1H), 8.56 (s, 1H), 8.91 (s, 1H), 9.81 ppm (s, 1H); ^{13}C NMR (126 MHz, [D$_6$]DMSO) δ = 44.14, 66.01, 112.12, 115.37, 120.60, 121.11, 124.05, 125.67, 127.78, 128.16, 130.27, 138.45, 141.27, 145.71, 152.43, 155.09,157.05 ppm; MS (+ESI): m/z = 428.05 (M + H); Anal. calcd for $C_{19}H_{18}BrN_5O_2$: C 53.28, H 4.24, N 16.35, found: C 53.37, H 4.22, O 16.52.

***N*-(4-((3-bromophenyl)amino)quinazolin-6-yl)furan-2-carboxamide (11i).** Yield 43% (115 mg, white solid); m.p. 334-336 °C; ^{1}H NMR (500 MHz, [D$_6$]DMSO) δ = 6.76 (dd, *J* = 3.5, 1.7 Hz, 1H), 7.46 (t, *J* = 8.0 Hz, 1H), 7.52 (ddd, *J* = 8.0, 1.9, 1.0 Hz, 1H), 7.59 (dd, *J* = 3.5, 0.7 Hz, 1H), 7.74 (ddd, *J* = 8.0, 1.9, 1.0 Hz, 1H), 7.99 – 8.03 (m, 2H), 8.05 (d, *J* = 9.0 Hz, 1H), 8.31 (dd, *J* = 9.1, 2.1 Hz, 1H), 8.93 (s, 1H), 9.18 (d, *J* = 2.0 Hz, 1H), 10.93 (s, 1H),11.61 ppm (s, 1H); ^{13}C NMR (126 MHz, [D$_6$]DMSO) δ = 112.32, 113.99, 114.37, 115.78, 120.62, 121.13, 123.64, 127.24, 129.08, 130.63, 130.66, 135.62, 138.43, 138.57, 146.42, 146.85, 149.71, 156.43,159.62 ppm; MS (+ESI): m/z = 408.99 (M + H); Anal. calcd for $C_{19}H_{13}BrN_4O_2$: C 55.76, H 3.20, N 13.69, found: C 55.80, H 3.24, O 13.78.

***N*-(4-((3-bromophenyl)amino)quinazolin-6-yl)nicotinamide (11j).** Yield 50% (135 mg, pale brown solid); purity 96.52%; m.p. 280-281 °C; ^{1}H NMR (500 MHz, [D$_6$]DMSO) δ = 7.29 (ddd, *J* = 8.0, 1.8, 1.0 Hz, 1H), 7.35 (t, *J* = 8.0 Hz, 1H), 7.62 (ddd, *J* = 8.0, 4.8, 0.8 Hz, 1H), 7.85 (d, *J* = 8.9 Hz, 1H), 7.90 (ddd, *J* = 8.2, 1.9, 1.0 Hz, 1H), 8.02 (dd, *J* = 9.0, 2.2 Hz, 1H), 8.20 (t, *J* = 1.9 Hz, 1H), 8.34 – 8.42 (m, 1H), 8.62 (s, 1H), 8.81 (dd, *J* = 4.8, 1.6 Hz, 1H), 8.92 (d, *J* = 2.1 Hz, 1H), 9.21 (dd, *J* = 2.3, 0.7 Hz, 1H), 9.95 (s, 1H),10.80 ppm (s, 1H); ^{13}C NMR (126 MHz, [D$_6$]DMSO) δ = 113.75, 115.31, 120.80, 121.12, 123.62, 124.26, 125.88, 128.33, 128.42, 130.07, 130.30, 135.44, 136.41, 141.13, 147.07, 148.70, 152.39, 153.37, 157.34, 164.16 ppm; MS (+ESI): m/z = 420.05 (M + H); Anal. calcd for $C_{20}H_{14}BrN_5O$: C 57.16, H 3.36, N 16.66, found: C 57.28, H 3.33, O 16.78.

***N*-(4-((3-bromophenyl)amino)quinazolin-6-yl)isonicotinamide (11k).** Yield 35% (94 mg, white solid); m.p. 255-256 °C; ^{1}H NMR (500 MHz, [D$_6$]DMSO) δ = 7.27 – 7.32 (m, 1H), 7.35 (t, *J* = 8.0 Hz, 1H), 7.86 (d, *J* = 8.9 Hz, 1H), 7.89 (d, *J* = 8.0 Hz, 1H), 7.95 (dd, *J* = 4.4, 1.6 Hz, 2H), 8.02 (dd, *J* = 8.9, 2.1 Hz, 1H), 8.20 (s, 1H), 8.63 (s, 1H), 8.84 (dd, *J* = 4.4, 1.6 Hz, 2H), 8.92 (d, *J* = 1.7 Hz, 1H), 9.96 (s, 1H), 10.86 ppm (s, 1H); ^{13}C NMR (126 MHz, [D$_6$]DMSO) δ = 114.02, 115.29, 120.82, 121.12, 121.50, 124.28, 125.90, 128.38, 128.45, 130.31, 136.15, 141.11, 141.42, 147.18, 150.43, 153.47, 157.35, 164.07 ppm; MS (+ESI): m/z = 420.02 (M + H); Anal. calcd for $C_{20}H_{14}BrN_5O$: C 57.16, H 3.36, N 16.66, found: C 57.25, H 3.37, O 16.80.

Biological screening

Cell Culture and Plating

Cancer cell lines cultured included cell line with wild-type EGFR (KB-HeLa variant), and (H1975) with mutant EGFR. Both cell lines were maintained in RPMI-1640 media supplemented with 10% fetal bovine serum in a 37°C humidified incubator with 5% CO_2 and subcultured twice weekly. Only cultures exhibiting greater than 95% viability were used in any experiment (determined by trypan blue exclusion). Cells were seeded in 96-well standard assay microplates at a density of 5,000 cells/well for growth assays, then allowed to acclimate overnight before compound addition or stimulation with EGF.

Growth Assay

KB and H1975 cells were treated with 8 concentrations of inhibitors ranging from 50 µM to 8 nM (Specifially, the doses tested (in µM) were 50, 25, 10, 5, 1, 0.2, 0.04, and 0.008) followed by EGF stimulation (100 ng/mL) 1 h later. Cells were incubated for an additional 72 h at 37°C. Relative cell growth was determined by addition of Promega CellTiter Glo luciferase-based measure of ATP content, and the resulting luminescence was measured using a Molecular Devices Spectramax Paradigm microplate reader in luminescence mode. Growth inhibition data were analyzed using DMSO as a baseline (negative control equal to 0% growth inhibition) with GraphPad Prism curve fitting software. IC_{50} values are representative of the results at least two independent concentration-response experiments with three replicates per concentration.

EGFR kinase phosphorylation assay.

Phosphorylation assays were performed in a final volume of 20 µl containing 8 mM MOPS (pH 7.0), 0.2 mM EDTA, 10 mM $MnCl_2$, 200 µM substrate peptide, 0.25 mM DTT, 0.1 mg/ml BSA, 10 ng wild-type EGFR-Kinase (Cat. No. 40187, BPS Bioscience) or 30 ng mutant EGFR kinase (Cat. No. PV4879, Life Technologies), 10 mM magnesium acetate, 100 µM γ–[^{32}P]ATP, and inhibitors or DMSO control (1.25% v/v). For IC_{50} curves with the wild-type enzyme, the following concentrations of the compounds (in nM) were tested in triplicates: 150, 100, 50, 25, 15, 10, 7.5, 5, 2.5. In the case of the mutant enzyme, concentrations (in µM) of 10, 8, 4, 2, 1, 0.75, 0.5, 0.35, 0.2, and 0.1 were used. The assays were repeated at least once. Reactions were started by the addition of the magnesium acetate/ATP mixture. After 30 min incubation at 30°C, 5 µl of each reaction was spotted on phosphocellulose P81 paper (Whatman). The P81 paper was then washed 5 times with 50 mM phosphoric acid for 15 min, dried and exposed to a phosphorimager screen, which was scanned and densitometrically analyzed the next day. The sequence of the substrate peptide was derived from phospholipase C-γ1 and had the sequence "KHKKLAEGSAYEEV", according to Fry *et al.*[9]

Molecular modeling

The proteins used for the docking were downloaded from the protein data bank (PDB 2ITY and 3W2O). The proteins were first prepared for docking using MOE software in which the proteins were protonated and saved for docking. The ligands were drawn on MOE and energy minimized and then saved as “mol2” file. Docking was done using GOLD software, where the proteins were first prepared by deleting the water molecules and extracting the co-crystallized ligand. The docking was done for compounds **9a** and **11i** with 2ITY and compounds **6a**, **6b** and **10b** with 3W2O using CHEMPLP as the scoring function and Goldscore as a rescoring function. The viewing of the results was done using MOE and PyMOL softwares.

References

1. Holbro, T.; Hynes, N. E., ErbB receptors: directing key signaling networks throughout life. *Annu Rev Pharmacol Toxicol* **2004**, 44, 195-217.

2. Dancey, J. E., Predictive factors for epidermal growth factor receptor inhibitors--the bull's-eye hits the arrow. *Cancer Cell* **2004**, 5, (5), 411-5.

3. Sequist, L. V.; Lynch, T. J., EGFR tyrosine kinase inhibitors in lung cancer: an evolving story. *Annu Rev Med* **2008**, 59, 429-42.

4. Charpidou, A.; Blatza, D.; Anagnostou, V.; Syrigos, K. N., Review. EGFR mutations in non-small cell lung cancer--clinical implications. *In Vivo* **2008**, 22, (4), 529-36.

5. da Cunha Santos, G.; Shepherd, F. A.; Tsao, M. S., EGFR mutations and lung cancer. *Annu Rev Pathol* **2011**, 6, 49-69.

6. Sharma, S. V.; Bell, D. W.; Settleman, J.; Haber, D. A., Epidermal growth factor receptor mutations in lung cancer. *Nat Rev Cancer* **2007**, 7, (3), 169-81.

7. Pao, W.; Miller, V.; Zakowski, M.; Doherty, J.; Politi, K.; Sarkaria, I.; Singh, B.; Heelan, R.; Rusch, V.; Fulton, L.; Mardis, E.; Kupfer, D.; Wilson, R.; Kris, M.; Varmus, H., EGF receptor gene mutations are common in lung cancers from "never smokers" and are associated with sensitivity of tumors to gefitinib and erlotinib. *Proc Natl Acad Sci U S A* **2004**, 101, (36), 13306-11.

8. Bridges, A. J.; Zhou, H.; Cody, D. R.; Rewcastle, G. W.; McMichael, A.; Showalter, H. D.; Fry, D. W.; Kraker, A. J.; Denny, W. A., Tyrosine kinase inhibitors. 8. An unusually steep structure-activity relationship for analogues of 4-(3-bromoanilino)-6,7-dimethoxyquinazoline (PD 153035), a potent inhibitor of the epidermal growth factor receptor. *J Med Chem* **1996**, 39, (1), 267-76.

9. Fry, D. W.; Kraker, A. J.; McMichael, A.; Ambroso, L. A.; Nelson, J. M.; Leopold, W. R.; Connors, R. W.; Bridges, A. J., A specific inhibitor of the epidermal growth factor receptor tyrosine kinase. *Science* **1994**, 265, (5175), 1093-5.

10. Rewcastle, G. W.; Denny, W. A.; Bridges, A. J.; Zhou, H.; Cody, D. R.; McMichael, A.; Fry, D. W., Tyrosine kinase inhibitors. 5. Synthesis and structure-activity

relationships for 4-[(phenylmethyl)amino]- and 4-(phenylamino)quinazolines as potent adenosine 5'-triphosphate binding site inhibitors of the tyrosine kinase domain of the epidermal growth factor receptor. *J Med Chem* **1995**, 38, (18), 3482-7.

11. Wissner, A.; Berger, D. M.; Boschelli, D. H.; Floyd, M. B., Jr.; Greenberger, L. M.; Gruber, B. C.; Johnson, B. D.; Mamuya, N.; Nilakantan, R.; Reich, M. F.; Shen, R.; Tsou, H. R.; Upeslacis, E.; Wang, Y. F.; Wu, B.; Ye, F.; Zhang, N., 4-Anilino-6,7-dialkoxyquinoline-3-carbonitrile inhibitors of epidermal growth factor receptor kinase and their bioisosteric relationship to the 4-anilino-6,7-dialkoxyquinazoline inhibitors. *J Med Chem* **2000**, 43, (17), 3244-56.

12. Fry, D. W.; Bridges, A. J.; Denny, W. A.; Doherty, A.; Greis, K. D.; Hicks, J. L.; Hook, K. E.; Keller, P. R.; Leopold, W. R.; Loo, J. A.; McNamara, D. J.; Nelson, J. M.; Sherwood, V.; Smaill, J. B.; Trumpp-Kallmeyer, S.; Dobrusin, E. M., Specific, irreversible inactivation of the epidermal growth factor receptor and erbB2, by a new class of tyrosine kinase inhibitor. *Proc Natl Acad Sci U S A* **1998**, 95, (20), 12022-7.

13. Smaill, J. B.; Palmer, B. D.; Rewcastle, G. W.; Denny, W. A.; McNamara, D. J.; Dobrusin, E. M.; Bridges, A. J.; Zhou, H.; Showalter, H. D.; Winters, R. T.; Leopold, W. R.; Fry, D. W.; Nelson, J. M.; Slintak, V.; Elliot, W. L.; Roberts, B. J.; Vincent, P. W.; Patmore, S. J., Tyrosine kinase inhibitors. 15. 4-(Phenylamino)quinazoline and 4-(phenylamino)pyrido[d]pyrimidine acrylamides as irreversible inhibitors of the ATP binding site of the epidermal growth factor receptor. *J Med Chem* **1999**, 42, (10), 1803-15.

14. Carmi, C.; Lodola, A.; Rivara, S.; Vacondio, F.; Cavazzoni, A.; Alfieri, R. R.; Ardizzoni, A.; Petronini, P. G.; Mor, M., Epidermal growth factor receptor irreversible inhibitors: chemical exploration of the cysteine-trap portion. *Mini Rev Med Chem* **2011**, 11, (12), 1019-30.

15. Foucourt, A.; Dubouilh-Benard, C.; Chosson, E.; Corbière, C.; Buquet, C.; Iannelli, M.; Leblond, B.; Marsais, F.; Besson, T., Microwave-accelerated Dimroth rearrangement for the synthesis of 4-anilino-6-nitroquinazolines. Application to an efficient synthesis of a microtubule destabilizing agent. *Tetrahedron* **2010**, 66, (25), 4495-4502.

16. Wu, C. H.; Coumar, M. S.; Chu, C. Y.; Lin, W. H.; Chen, Y. R.; Chen, C. T.; Shiao, H. Y.; Rafi, S.; Wang, S. Y.; Hsu, H.; Chen, C. H.; Chang, C. Y.; Chang, T. Y.; Lien, T. W.; Fang, M. Y.; Yeh, K. C.; Chen, C. P.; Yeh, T. K.; Hsieh, S. H.; Hsu, J. T.; Liao, C. C.; Chao, Y. S.; Hsieh, H. P., Design and synthesis of tetrahydropyridothieno[2,3-d]pyrimidine scaffold based epidermal growth factor receptor (EGFR) kinase inhibitors: the role of side chain chirality and Michael acceptor group for maximal potency. *J Med Chem* **2010**, 53, (20), 7316-26.

17. Yun, C. H.; Boggon, T. J.; Li, Y.; Woo, M. S.; Greulich, H.; Meyerson, M.; Eck, M. J., Structures of lung cancer-derived EGFR mutants and inhibitor complexes: mechanism of activation and insights into differential inhibitor sensitivity. *Cancer Cell* **2007**, 11, (3), 217-27.

18. Sogabe, S.; Kawakita, Y.; Igaki, S.; Iwata, H.; Miki, H.; Cary, D. R.; Takagi, T.; Takagi, S.; Ohta, Y.; Ishikawa, T., Structure-Based Approach for the Discovery of Pyrrolo[3,2-d]pyrimidine-Based EGFR T790M/L858R Mutant Inhibitors. *ACS Medicinal Chemistry Letters* **2013**, 4, (2), 201-205.

19. Tsou, H. R.; Mamuya, N.; Johnson, B. D.; Reich, M. F.; Gruber, B. C.; Ye, F.; Nilakantan, R.; Shen, R.; Discafani, C.; DeBlanc, R.; Davis, R.; Koehn, F. E.; Greenberger, L. M.; Wang, Y. F.; Wissner, A., 6-Substituted-4-(3-bromophenylamino)quinazolines as putative irreversible inhibitors of the epidermal growth factor receptor (EGFR) and human epidermal growth factor receptor (HER-2) tyrosine kinases with enhanced antitumor activity. *J Med Chem* **2001**, 44, (17), 2719-34.

20. Madapa, S.; Tusi, Z.; Mishra, A.; Srivastava, K.; Pandey, S. K.; Tripathi, R.; Puri, S. K.; Batra, S., Search for new pharmacophores for antimalarial activity. Part II: synthesis and antimalarial activity of new 6-ureido-4-anilinoquinazolines. *Bioorg Med Chem* **2009**, 17, (1), 222-34.

3.III Targeting two pivotal cancer pathways with one molecule: first bispecific inhibitors of the Epidermal Growth factor receptor kinase and the NF-κB pathway

Major part of this chapter will be published in *Journal of Medicinal Chemistry*

Paper III

Abstract

Although, the use of clinically approved EGFR inhibitors, like Gefitinib, is well known in the treatment of cancer, yet they still suffer certain limitations such as emergence of resistance or presence of cancers being originally insensitive to the EGFR inhibitors. Therefore, treatment with a single, specific agent does not seem particularly promising because of the multigenic alterations of tumors. Hence, the use of a combination therapy during cancer treatment could sufficiently decrease the development of resistance and give at least an additive if not a synergistic effect. Accordingly, in this work we present new thiourea quinazoline derivatives which act as dual inhibitors towards the EGFR and the NF-κB activation pathway which are two complementary signaling pathways in cancer cells. This dual inhibitory activity proved to produce a synergistically potent inhibitory activity towards cells lines which are not very sensitive to Gefitinib. Starting from an identified hit compound **4b**, several modifications have been done to it resulting in highly potent compounds, such as **6c** and **6h**, towards both targets. The hit compound was found to inhibit the NF-κB pathway most likely through affecting the deubiquitination step. In addition, one of the most potent compounds **6c** showed much higher selectivity towards EGFR than Gefitinib.

Introduction

Inhibition of the EGF receptor kinase-mediated signaling is a well established strategy for the treatment of advanced stage non-small cell lung cancer. However, drugs used for the treatment, such as Gefitinib and Erlotinib respond more favorably if the tumor cells harbour a specific activating EGFR mutation which appear to preserve the ligand dependence of receptor activation but alter the pattern of downstream signaling.[1] This EGFR mutation includes mainly small, in-frame deletions in exon 19, or the single point mutation L858R,[1] and are found in ~10-50% of lung cancer patients, of which ~75% show a response to the TKI inhibitors compared to ~10% in wild-type case.[1, 2] Hence, only a minor proportion of lung cancer patients can actually profit from the treatment with EGFR inhibitors.

In addition, tumors responsive to initial treatment with EGFR inhibitors often become resistant due to acquisition of a mutation in the ATP binding pocket of EGFR (T790M) which mainly decreases the K_m for ATP, thus out-competing the binding of Gefitinib.[1, 3] Even within the same tumor, genetic heterogeneity[4] might account for a minor population of cells in which EGFR signaling is not essential for cell growth and/or survival, thus resuming cell growth after initial shrinking of the tumor volume. Alternatively, tumor cells might activate distinct pro-survival signaling pathways, as exemplified by the amplification of MET in lung cancers treated with epidermal growth factor receptor (EGFR) inhibitors.[5] Selective pressures that are exerted by cytotoxic therapy can lead to the expansion of resistant clones that either existed before the onset of treatment or that formed as a result of new alteration that were gained during the treatment. Whereas sampling and detection sensitivity issues often limit the ability to distinguish between these two possibilities, multiple reports have demonstrated that relapsed clones could be traced to variants present as minor clones before the start of therapy.[6-8] Therefore, the degree of genetic heterogeneity of a tumor might also contribute to the activation of alternative pro-survival pathways.[9] At any rate, clinical experience suggests that at least with advanced stage solid tumors, inhibition of only one cancer-relevant signaling pathway is not sufficient to achieve long term remission of the patients. It is generally accepted that simultaneous blocking of two major signaling pathways should have synergistic anti-tumor effects and might counteract the development of mutations.[10-13] In particular the NF-κB pathway represents another major signaling pathway active in many cancer types such as leukemia, lymphoma, colon cancer and ovarian cancer,[14, 15] where it induces anti-apoptotic proteins and mediates resistance to anticancer drugs and radiation.[16]

Importantly, in lung cancer cell lines, a large siRNA screen identified the NF-κB pathway activity as a key factor that determined the sensitivity towards EGFR inhibitors. Knock down of several components of the NF-κB pathway enhanced cell death induced by EGFR inhibition in cell lines such as EGFR-mutant lung cancer cells.[17] Validation studies confirmed that activation of NF-κB signaling conferred resistance to EGFR inhibitors in EGFR dependent tumor models and, conversely, that NF-κB inhibition enhanced sensitivity to EGFR inhibitors.[17] Therefore, co-inhibition of NF-κB signaling in NSCLC is expected to enhance response rates to EGFR inhibitors and extend the response duration.

While co-administration of anti-tumor therapeutics is a common strategy in several current cancer trials and has proven to be beneficial in some cases, toxic side effects could increase by the number of different agents.[18] Moreover, the individual pharmacokinetic properties render it difficult to deliver effective amounts of both therapeutics to the tumor cells in a concerted manner to achieve maximum efficacy.

Therefore, it would be a major advantage to combine in a single agent two distinct, but specific inhibitory activities which suppress two major, synergistic signaling pathways in cancer cells at the same time, such as EGFR/NF-κB in lung cancer cells.

In the following, we describe the development of dual EGFR and NF-κB signaling inhibitors based on the quinazoline-4-aminophenyl scaffold. We also provide evidence at least for one compound that suppression of NF-κB activation occurs most likely at the level of deubiquitinating (DUB) enzymes.

Results and Discussion

Strategy for Hit identification

With respect to EGFR kinase inhibition, it was known from previous studies that the quinazoline-4-aminophenyl motif is both essential and sufficient to mediate strong inhibition of the kinase in the nM range.[19, 20] On the other hand, the 6- and 7-positions of the quinazoline scaffold offered possibilities for substitutions without strongly compromising the EGFR-directed potency, because these positions pointed towards the outside of the ATP binding pocket (compare e.g., PDB 2ITY). Furthermore, the quinazoline heterocycle was successfully used as a scaffold for the synthesis of potent inhibitors for a range of enzymes beside protein kinases, including endothelin converting enzyme,[21] Thymidylate synthase,[22] trypanothione reductase,[23] Cyclic GMP phosphodiesterase inhibitors,[24] PDE7,[25] Pin1,[26] CDK,[27] NADH-ubiquinone oxidoreductase,[28] glucocerebrosidase,[29] and G9a-like protein lysine methyltransferase.[30]

The quinazoline system could therefore be considered a privileged scaffold, potentially suitable to serve as an affinity anchor for inhibitors of diverse enzymes – without evidence of promiscuous properties. Thus, our concept envisaged the expansion of the quinazoline core by suitable moieties in order to confer an additional pharmacologic activity to the resulting compounds while retaining EGFR kinase inhibitory activity. Accordingly, and to achieve the intended dual activity, several quinazoline derivatives with potential EGFR inhibitory activity prepared by us were screened for their inhibitory activity on the NF-κB activation pathway using a reporter gene assay. The compounds selected for screening featured at the 6-position different combinations of linkers, potentially acting as a H-bond donor/acceptor pair, and aliphatic or (hetero)aromatic moieties which may be accommodated in potential hydrophobic binding pockets of new target proteins. Furthermore, we included derivatives with variable substitutions at the 4-position of the quinazoline nucleus. The first group of screened compounds included variations in position 4 with an acrylamide moiety at position 6. The position 4 variations included substituents such as haloanilines, alkylanilines, alkoxyanilines, sulfonamide containing anilines and alicyclic amines **I-III** (Chart 1). The second group of screened compounds included variations at position 6 in presence of a *m*-bromoaniline at position 4. Position 6 variations included different substituents linked through several linkages to the quinazoline nucleus such as an imine **IV**, amide **V**, amino alkyl amide **VI** and thiourea **VII** (Chart 1).

Chart 1. General structures of the quinazoline derivatives selected for screening towards the NF-κB inhibitory activity.

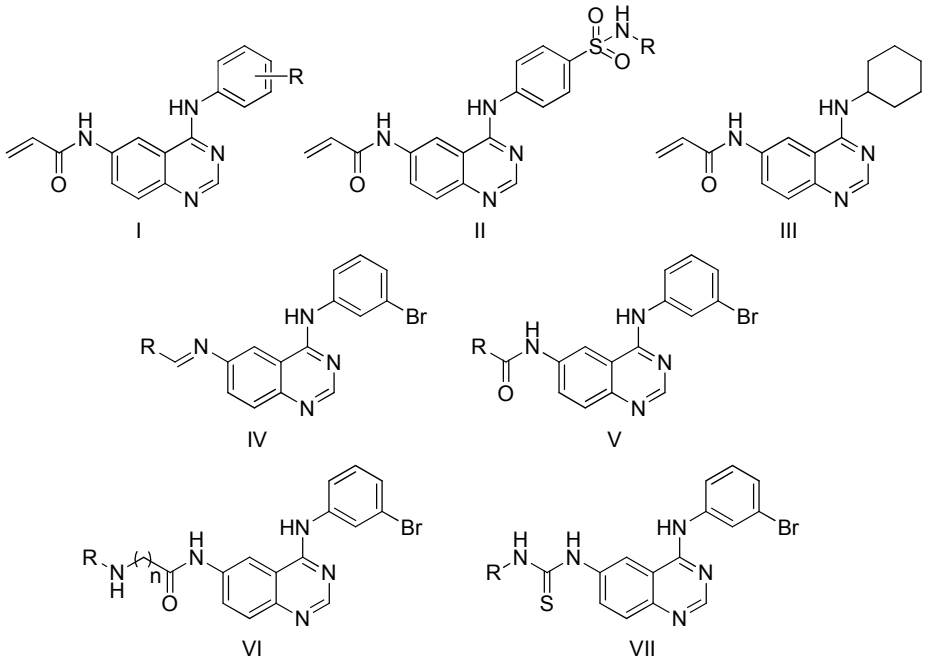

Screening of the quinazoline derivatives shown in Chart 1, resulted in several compounds which suppressed the NF-κB activation at 10 μM (e.g. in Table 1), while the most potent hit was the benzylthiourea derivative **4b**, exhibiting an almost 100 % reduction of the luciferase read out (Table 1). In comparison, the reference compound Gefitinib showed a considerably weaker inhibition of about 50 % at 10 μM, suggesting that the structural modifications had created a significant inhibitory activity on the NF-κB pathway. Importantly, **4b** still retained a nM activity with respect to EGFR inhibition, though it was about 4-times reduced compared with Gefitinib (Table 1).

Screening of hit compound (4b) against kinases directly involved in TNF-α Receptor signalling

To rule out that **4b** was a non-selective kinase inhibitor on the one hand, but also to test whether selective inhibition of one of the kinases specifically involved in NF-κB activation in U937 cells was responsible for the novel activity, the hit compound **4b** was screened against the panel of kinases shown in Table 2. Only one kinase, RIPK-2, was weakly inhibited by **4b**; however, with the estimated IC_{50} being above 10 μM, RIPK-2 was unlikely to be the actual target of this compound in the U937 cells, because the higher cellular ATP concentrations tend to reduce the potency further and the IC_{50} for the NF-κB suppression was 4.1 μM (Table 1). Thus we could conclude that compound **4b** did not affect a kinase which is directly involved in TNFα receptor signaling. Furthermore, the hit compound did not exhibit non-selective kinase inhibition, which encouraged us to carry out an optimization of the potency guided by the NF-κB reporter gene assay.

Table 1. Recombinant EGFR kinase IC_{50}, % inhibition and IC_{50} of U937 reporter gene assay at 10 μM concentration for some of the screened quinazoline derivatives that showed suppression of the NF-κB activation.

Comp.	Recombinant EGFR kinase	U937 reporter gene assay	
	IC_{50} (nM)	% inhibition at 10μM	IC_{50} (μM)
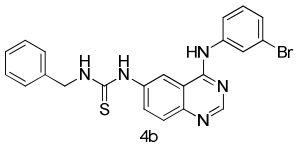 4b	17.2	97	4.1
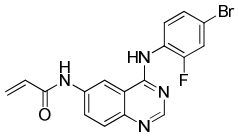 VIII	2.1	73.6	N.D.
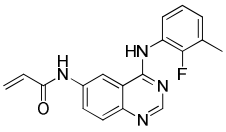 IX	1.5	70	N.D.
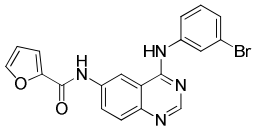 X	8.4	39.4	N.D.
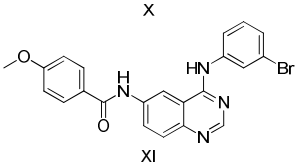 XI	N.D.	33.2	N.D.
Gefitinib	4.0	51.3	9.7

Table 2. Selectivity profiling of compound **4b** against the kinases associated with the TNF-α receptor complex in U937 cells.[31]

Kinase	% activity at 10 μM[a]	Kinase	% activity at 10 μM[a]
IKKα(h)	117	RIPK2(h)	54
IKKβ(h)	100	SAPK2a(h)	78
PKCι(h)	106	TAK1(h)	106
PKCζ(h)	92	TBK1(h)	92

[a] Values represent the mean of two experiments, S.D. < 5 %**.** All kinases were tested using ATP concentrations at the respective K_m values.

Chemistry

The identified hit compound **4b** was subjected to further optimization by a targeted synthesis of analogues. The optimization, using the following schemes, involved

modifications in the substituents at the 4 anilino ring, the side chain attached to the thiourea linker and the thiourea linker itself.

Synthesis of the quinazoline nucleus was done by refluxing of 5-nitro-2-aminobenzonitirile with triethyl orthoformate in presence of drops of acetic anhydride to yield the formimidate derivative **1**. Cyclization to form the quinazoline nucleus took place by refluxing of **1** with different anilines in acetic acid to yield the nitroquinazoline derivatives **2a-q**. Reduction of the nitro intermediates **2a-q** to their amino derivatives **3a-q** was done by refluxing the nitro derivatives with stannous chloride in methanol under nitrogen atmosphere. The benzyl thiourea derivatives **4a-4q** were obtained by stirring the aminoquinazoline derivatives **3a-q** with benzylisothiocyante in DMF. (Scheme 1)

Scheme 1.[a]

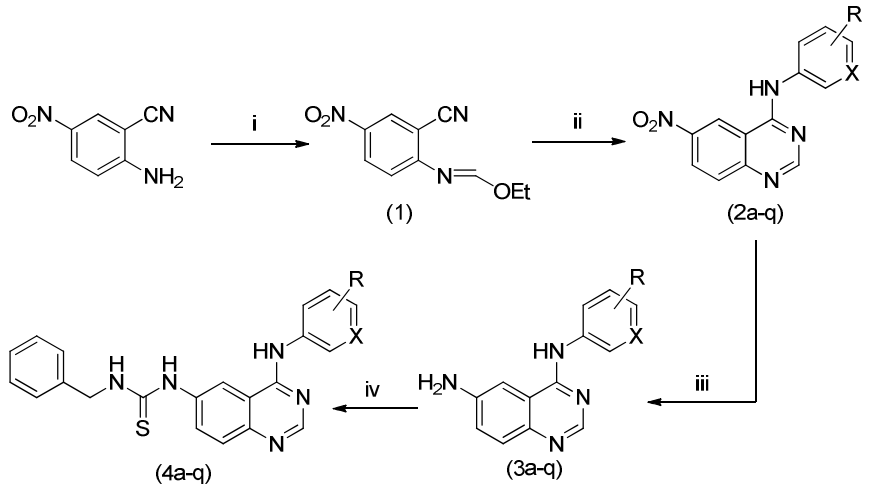

Comp.	X	R	Comp.	X	R
a	C	2-Br	**m**	C	4-OH
b	C	3-Br			
c	C	4-Br	**n**	C	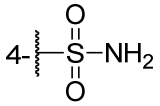
d	C	3-Cl			
e	C	3-Methyl			
f	C	2,3-Dimethyl	**o**	C	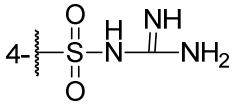
g	C	3-Ethyl			
h	C	4-isopropyl			
i	C	4-t-butyl	**p**	C	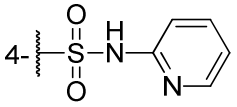
j	C	4-phenyl			
k	C	4-phenoxy	**q**	N	-
l	C	3-OH			

[a]Reagents and conditions: (i) TEOF, $(Ac)_2O$, reflux, 16h; (ii) R-NH_2, CH_3COOH, reflux, 1h; (iii) $SnCl_2$, MeOH, reflux, 30 min; (iv) $PhCH_2$-NCS, DMF, rt, 5h.

Reaction of compound **3b** with thiophosgene yielded the isothiocyanate derivative **5** which upon stirring with different amines in DMF gave the thiourea derivatives **6a-q** and **7a-e** (Scheme 2). The thiourea derivatives **6r-u** were obtained by reacting the

aminoquinazoline derivatives **3i-k** with the corresponding isothiocyanate derivatives in DMF at room temperature (Scheme 3). The urea derivatives **8a-b** were obtained by stirring compound **3b** with different isocyanate derivatives in DMF (Scheme 2).

Scheme 2.[a]

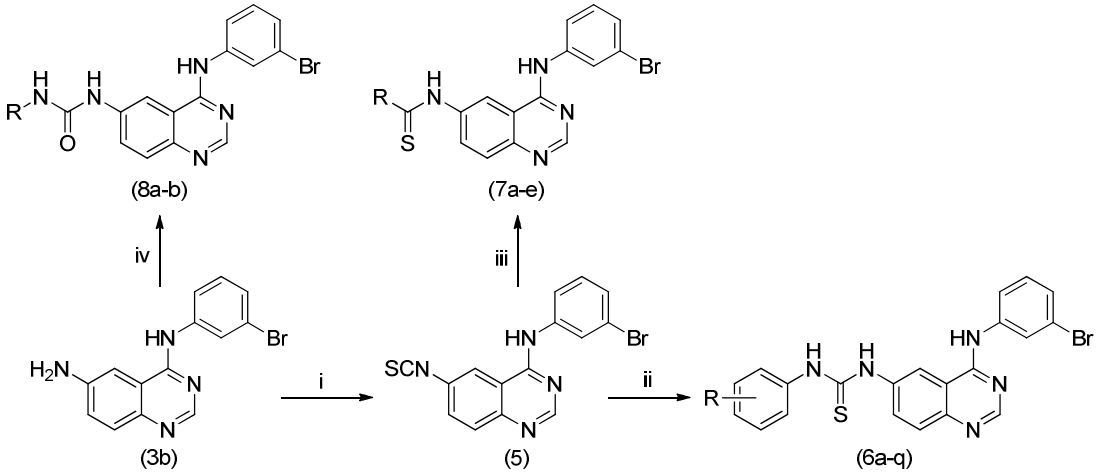

Comp.	R	Comp.	R
6a	H	**7a**	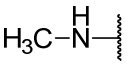
6b	2-Cl		
6c	3-Cl	**7b**	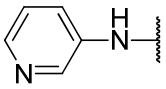
6d	4-Cl		
6e	2,4-dichloro		
6f	3,4-dichloro	**7c**	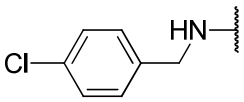
6g	3,5-dichloro		
6h	3-Cl,4-F		
6i	3-CF_3,4-Cl	**7d**	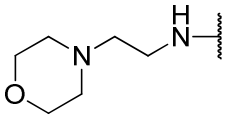
6j	2-F,3-CF_3		
6k	4-CF_3		
6l	3-CF_3	**7e**	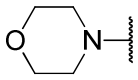
6m	3,5-di-trifluoromethyl		
6n	4-Br		
6o	4-OH		
6p	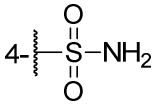	**8a**	Benzyl
6q	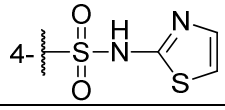	**8b**	4-Chlorophenyl

[a]Reagents and conditions: (i) $S=C(Cl)_2$, HCl (ii)Ar-NH_2, DMF, rt, 5h (iii) R-NH_2, DMF, rt, 5h (iv) R-NCO, DMF, rt, 5h

Scheme 3.

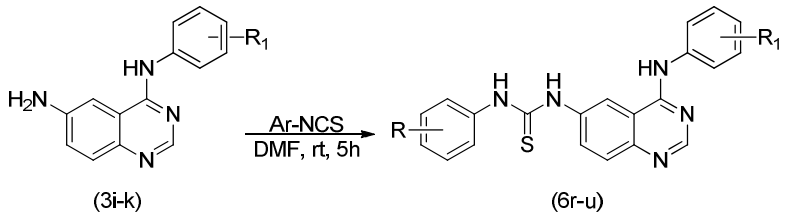

Comp.	R	R_1
6r	3-CF_3,4-Cl	4-t-butyl
6s	3-CF_3,4-Cl	4-phenoxy
6t	3-CF_3,4-Cl	4-phenyl
6u	3,5-di-trifluoromethyl	4-phenyl

Identification and validation of quinazoline derivatives displaying NF-κB inhibitory activity

To identify compounds endowed with new desired NF-κB inhibitory properties, we chose a reporter gene assay using the lymphoma cell line U937. Due to its origin from tissue macrophages,[32] this cell line responds with a strong activation of the NF-κB pathway after stimulation by LPS or TNFα. Inhibition of any of the essential components of the conserved classical (canonical) NF-κB pathway would be expected to result in a decrease of the final luciferase activity-based read out. As potential targets, protein kinases and adaptor proteins of the TNFα receptor complex, IκB kinase, and components of the ubiquitinylation and proteasome complex were conceivable. All of these stages of the NF-κB activation process had been proposed independently as potential targets for pharmacological intervention. Moreover, it was of importance that the U937 lymphoma cell type lacks expression of EGFR, thus excluding any interference due to the intrinsic EGFR inhibitory activity of the compounds.

Optimization of the hit compound (4b)

With respect to the optimization strategy of the hit compound **4b**, we hypothesized that the benzyl function might interact with a lipophilic binding pocket of a new target protein; thus, one strategy was to synthesize and test analogues with different hydrophobic substituents linked to the thiourea moiety while keeping the 3-bromoaniline at position 4. These substituents included halobenzyl, phenyl, substituted phenyl, heterocyclic and alkyl groups. In addition, the 4-anilino moiety at the quinazoline was considered as another adjustable position to optimize binding to a putative new target without compromising affinity toward EGFR kinase. Therefore we also decided to include several modifications in the substituents at position 4 while keeping the benzylthiourea part at position 6 of the quinazoline. Eventually, we planned to exchange the thiourea function by urea to investigate whether the thion sulfur played a major role. In the cell-based NF-κB reporter gene assay, a primary screening dose of 10 μM was

used, after which the IC_{50} was calculated for the compounds showing more than 80% inhibition (Table 3).

The optimization started by testing the importance of the methylene spacer between the thiourea and the aromatic ring, this was done by replacing the benzyl group as in (**4b** and **7c**) with their phenyl analogues (**6a** and **6d**). The results of this modification showed that the phenyl derivatives were more potent than their benzyl analogues. The next step was to confirm the importance of the thiourea group. Accordingly, the thiourea derivatives (**4b** and **6d**) were compared with their urea analogues (**8a** and **8b**). A direct comparison suggested that the presence of the thiourea moiety is important in order to retain the activity towards the NF-κB pathway. The following step was to know if the aromatic ring linked to the thiourea moiety was essential for activity. Therefore, the aromatic ring was replaced by a methyl group (**7a**), a morpholine (**7e**) and an ethyl morpholine (**7d**). As indicated by the loss of NF-κB suppression, the aromatic system was found to be essential for the activity (Table 3).

Next, several substituents were further added to the phenyl thiourea side chain to achieve an enhanced potency for the compounds. Firstly, we introduced several polar groups or heteroatoms on the phenyl ring as in (**6o**, **6p**, **6q** and **7b**) which resulted in a decrease in the activity towards the NF-κB pathway in the U973 cells. This was then followed by adding several lipophilic substituents on the phenyl thiourea side chain which resulted in variable potencies depending on the size and the position of the substituents. This finally resulted in compounds **6c** and **6h** which potently inhibited the activation of NF-κB in the reporter gene assay (Table 3).

Structure activity relationship for the NF-κB inhibitory activity

Concerning the modifications of the position 4 anilines in the presence of the benzyl thiourea at position 6, it was found that the aniline moiety should have lipophilic substituents as the presence of polar groups destroys the activity. This was clearly seen with polar substituents such as the hydroxy **4l** and **4m**, sulfonamide **4n**, substituted sulfonamide **4o** and **4p** or even heterocyclic **4q**, which all led to loss of activity (Table 3). Although the findings might be influenced by differences in cell permeability, the uniform reduction of activity by the more polar moieties suggests that the 4-aminophenyl is not only important for the affinity to EGFR kinase (see below) but also seemed to interact with the novel target(s) in the NF-κB pathway. Fortunately, the SAR for this position showed the same tendency for both targets (see below).

For the lipophilic *meta*-substituents on the aniline ring, it was found that the most potent were the halogens with the chlorine **4d** showing the best activity. This was followed by bromine **4b**, ethyl **4g**, methyl **4e** and finally the 2,3-dimethyl **4f**. For the Br substituent, it was found to be more tolerable and more potent when present in the *para* position **4c** followed by the *meta* **4b** and finally the *ortho* **4a**. For the *para* position, it was found that bulky groups are tolerated with the alkyl or aryl groups being less potent than

the halogens. The best group in the *para* position after the bromine was the isopropyl **4h** followed by phenyl **4j** then t-butyl **4i** and finally phenyloxy **4k** was the least active.

Modifications of the position 6 side chain in the presence of *m*-bromaniline in position 4, showed that the lipophilic substituents are optimal. Accordingly, any polar, heterocyclic or alkyl groups in this side chain such as sulfonamide **6p**, substituted sulfonamide **6q**, pyridyl **7b** or morpholine **7d** and **7e**; lead to loss of activity while the only tolerable group was the *p*-hydroxy **6o**.

Table 3. % inhibition, IC_{50} of Recombinant EGFR kinase and U937 reporter gene assay and IC_{50} for MDA-MB 231 cell growth inhibition.

Comp.	Recombinant EGFR Kinase		U937 reporter gene assay		MDA cell growth
	% inhibition at 150 nM	IC_{50} (nM)	% inhibition at 10µM	IC_{50} (µM)	IC_{50} (µM)
4a	13.1	>150	85.7	6.5	>30
4b	86.1	17.2	97	4.1	9.5
4c	47.7	>150	92.1	3.8	15.1
4d	84.8	11.4	89.7	3.7	7.3
4e	68.5	36.8	76.4	N.D.	19.5
4f	40.0	>150	71.5	N.D.	28.7
4g	41.7	>150	92.5	4.8	10.5
4h	4.2	>150	95.7	4.3	12.8
4i	0.9	>150	91.9	5.51	8.7
4j	14.5	>150	89.1	4.4	8.4
4k	21.9	>150	73.7	N.D.	6.8
4l	60.8	63.6	44.3	N.D.	>30
4m	44.1	>150	24.1	N.D.	27
4n	17.7	>150	19.2	N.D.	>30
4o	6.7	>150	21.7	N.D.	>30
4p	20.9	>150	6.6	N.D.	>30
4q	38.5	>150	7.7	N.D.	17.9

N.D.: Not Determined

Table 3. cont.

Comp.	Recombinant EGFR Kinase		U937 reporter gene assay		MDA cell growth
	% inhibition at 150 nM	IC_{50} (nM)	% inhibition at 10µM	IC_{50} (µM)	IC_{50} (µM)
6a	86.5	15.8	90.7	5.2	27.9
6b	84.3	15.8	95.8	3.5	8.5
6c	74.8	20.6	97.4	1.9	2.1
6d	79.6	19.5	89.5	4.9	>30
6e	66	48.9	93.1	2.9	12.2
6f	52.9	133.1	97.2	1.9	4.8
6g	50.9	146.3	99.6	1.8	3.0
6h	74.1	25.3	100	1.0	0.3
6i	44.0	>150	99.0	1.7	1.1
6j	55.6	112.4	98.0	1.3	0.4
6k	38.1	>150	94.8	1.7	12.2
6l	57.5	60.7	96.5	1.0	1.4
6m	32.3	>150	100	1.9	0.8
6n	70.4	35.4	96.7	2.0	>30
6o	91.5	8.9	85.3	6.4	>30
6p	92.3	9.5	29.0	N.D.	>30
6q	81.7	22.0	16.5	N.D.	>30
6r	8.7	>150	68.8	N.D.	2.1
6s	15.8	>150	100	0.97	0.2
6t	12.1	>150	74.1	N.D.	2.5
6u	10.2	>150	91.7	3.8	3.7
7a	92.2	9.1	3.0	N.D.	>30
7b	90.4	10.2	42.4	N.D.	>30
7c	77.5	28.3	78.6	N.D.	23
7d	91.8	10.7	20.9	N.D.	>30
7e	84.0	26.9	40.1	N.D.	>30
8a	89.9	8.9	42.6	N.D.	>30
8b	69.0	19.3	50.3	N.D.	<10
Gefitinib	93.2	4.0	51.3	9.7	14.2
Bortezomib			100% at 1µM; 84,4% at 0,2 µM		

N.D.: Not Determined

Structure activity relationship for the EGFR cell free assay

Since the goal of this study was to identify novel compounds that exhibited dual inhibitory activity both against EGFR and NF-κB signaling, we next determined the potencies of all compounds against recombinant EGFR kinase. A primary screening dose of 150 nM was done after which the IC_{50} for the compounds was calculated. Firstly, concerning the modifications in the aniline at position 4 in presence of the benzyl thiourea at position 6, it was clear that the nature, position and the size of the substituents

greatly affect the activity. It was found that *meta* position was the optimum for the substitution with a hydrophobic group. The groups which offered the most potent activity are the halogens especially medium sized halogen like chlorine **4d** which was more potent than the bromine **4b**. Replacing the halogen with alkyl group such as the methyl **4e** decreased the activity which further decreased with the polar hydroxy group **4l** and the least active was the more bulky ethyl **4g**. In addition, any substitutions in the *ortho*-position as in **4a** or **4f** resulted in significant decrease in activity. Furthermore, all the *para*-substitutions on the aniline also significantly decreased the activity irrespective to the nature of the substituent.

Replacing the thiourea linkage with a urea gave a more potent derivative in case of the benzyl substituent (**4b** with **8a**) while, the urea and thiourea were equipotent in case of the phenyl substituent (**6d** with **8b**).

Modifying the position 6 side chain in presence of *m*-bromoaniline at position 4 showed that several substituents are tolerable either lipophilic or hydrophilic with the hydrophilic or heterocyclic ones being more potent such as **6o**, **6p**, **7b** and **7d**. In addition, multiple and/or bulky lipophilic substituents on the phenyl ring (as in **6i**, **6m** and **6r-6u**) decreased or abolished the activity. The latter SAR were conflicting with the requirements for potent inhibition of NF-κB activation, thus it was not possible to optimize both biological activities in parallel to the same degree.

Cellular Effects on the MDA-MB-231 cells

To confirm that the dual inhibitory activity towards the EGFR and NF-κB activation pathway offers a synergistic effect and thus a potential advantage in the cancer therapy over the EGFR inhibitors alone, further testing was performed using the MDA-MB-231 cancer cell line which is known to be rather insensitive to the clinically approved EGFR inhibitor Gefitinib (literature: IC_{50}=15-20 μM)[33-35] (Table 3). As a general conclusion, it was observed that the potency towards the MDA cells was mainly controlled by the NF-κB inhibitory activity of the compounds (Table 3). This seemed reasonable since the potent EGFR inhibitor (Gefitinib) was not sensitive towards this cell line (IC_{50} = 14.2 μM). The correlation of the MDA cell growth inhibition with the activity of the reporter gene assay provided evidence that tumor cells which are non-responsive towards EGFR inhibition can successfully be defeated by the novel NF-κB suppressive activity.

Effects on A549 cell growth

The potency of the best compounds to inhibit the cell growth of the lung cancer cell line A549 was also tested. This assay was done to corroborate if the compounds with dual inhibitory activity still offer an advantage towards a cell line which is intermediately sensitive to the potent EGFR inhibitor (Gefitinib). The results showed that the dual inhibitors are more potent than Gefitinib in inhibiting the growth of A549 cancer cell line (Table 4).

Table 4. A549 cell growth inhibitory assay.

Comp.	IC_{50} (μM)[a] A549 cells
4b	2.1
6c	1.6
6h	1.0
Gefitinib	9.3

[a] S.D. ≤ 12%

In vitro kinase selectivity profile

Since the novel dual inhibitors were developed based on a kinase inhibitor scaffold, it was straightforward to test whether the suppression of the NF-κB activation was also due to inhibition of a kinase. To this end, an in vitro selectivity profile test on a panel of 106 protein kinase was performed. For the profiling we selected **6c**, an optimized compound which had shown potent inhibitory activity against both targets and a slightly stronger EGFR kinase inhibition than **6h**. The screening concentration was 5 μM, and the percentage of activity was calculated and shown in Table 5 (Supporting information). It was found that compound **6c** exhibited an excellent selectivity for the EGFR kinase, with only a weak inhibition towards two other kinases, namely Mnk2 and the Pim-1. The IC_{50}'s for these two kinases were further determined and are presented in Table 6 (Supporting information). It is clear from the IC_{50}'s that compound **6c** is a highly potent and selective EGFR kinase inhibitor. Compound **6c** was more selective than Gefitinib[36] and nearly 29-fold more potent against EGFR kinase than against the second most inhibited kinase, Pim-1.

Role of EGFR, Mnk2 and Pim-1 on the NF-κB pathway

In order to verify whether the additional targets identified for compound **6c** - though being affected only weakly - were the crucial targets for inhibition of NF-κB activation, three selective inhibitors (CGP 57380, SMI-4a and Gefitinib) of the three respective kinases were tested in the U937 reporter gene assay. They were assayed separately in 3 different concentrations "5, 2.5 and 1 μM" (Table 7, Supporting information), and also applied to the cells in different combinations "1μM compound each" (Table 8, Supporting information) to detect potential synergistic effects of the distinct inhibitory activities.

Testing of these specific inhibitors did not reveal any significant inhibition of NF-κB activation, either alone or in combination. In some cases, a weak inhibition was seen, however, without a clear concentration-dependency; thus it was rather a non-specific effect, maybe due to the lack of clear selectivity of the compounds used, so that several kinases in the TNFα signaling pathway might have been weakly affected. The combination of the inhibitors did not lead to additive or synergistic effects either. Thus,

these kinases could be excluded as potential new targets or a target combination in the U973 cell NF-κB activation pathway.

Given the remarkable selectivity of compound **6c**, it was rather unlikely that the new biological target was another protein kinase, although it could not be fully excluded since not the complete kinome was screened, only some representative kinases from each branch. However, if it was a kinase, then it would be from an unknown NF-κB activation pathway induced by TNFα, because all kinases identified as part of the TNF-α receptor complex[31] had been included in the kinase screen, also all other kinases which had been mentioned in literature before to play a role in NF-κB activation. In addition, all growth factor dependent kinase pathways were silenced in the U937 cells because of the serum starvation, e.g. the PI3 kinase pathway in which many NF-κB kinases are activated. Hence, targeting of such inactive kinases by our inhibitor **6c** would not have produced an effect in the reporter gene assay.

Elucidation of the mechanism of action responsible for NF-κB suppression

Having developed novel dual inhibitors, we aimed at investigating the cellular mechanism of action which was responsible for the observed suppression of NF-κB activation in the reporter gene assay, assuming that it was not the inhibition of another kinase. For this purpose we selected two different sets of test compounds. On the one hand, we included **6c** and **6h** displaying a markedly enhanced activity against the NF-κB and still potent EGFR inhibitory activity. On the other hand, the original hit compound **4b** possessed an advantageous potency towards EGFR kinase – probably due to the lack of lipophilic substituents at the benzyl residue (cf. SAR discussion above) – while it was less potent in the NF-κB reporter gene assay. Because of these somewhat distinct properties and the slightly different chemotype, both groups of compounds, **6c/6h** and **4b**, were selected for investigation of the new biological activity. The most obvious biological activity to test was the potential inhibition of the proteasome. The prototype of proteasome inhibitors, Bortezomib, inhibits two of the three distinct proteolytic activities and prevents the degradation of the IκB protein, thus blocking the release of the NF-κB dimer.[37]

For each of the three proteolytic activities, the trypsin-like, the chymotrypsin-like, and the caspase-like, we used a specific fluorigenic peptide and total protein extract from MDA-MB-231 cells as a source of proteasomal activities, basically as described.[38] However, whereas Bortezomib used as a positive control inhibited all three proteolytic activites, including the caspase-like activity at higher concentrations, none of the three test compounds showed any inhibitory activity even at 50 μM (data not shown). Thus, the three main proteolytic activities of the proteasome could be excluded as molecular targets.

NF-κB translocation assay

As an alternative approach to unravel the mechanism involved in NF-κB suppression, we analysed whether the translocation of the RelA subunit of NF-κB (p65) was inhibited by the compounds. To this end, we used a high-content screening system employing a CHO cell line stably expressing a GFP-p65 fusion protein. A cytoplasmic retention of this construct in the presence of the test compounds, as indicated by a diffuse cytoplasmic fluorescence, would signify an inhibition of the upstream NF-κB activation. The system automatically quantifies the ratio of cytoplasmic vs. nuclear fluorescence and provides microphotographs of each well. The cells were first stimulated for 30 min by 25 ng/ml IL-1β after which the translocation of the GFP-NFκB-p65 fusion protein from the cytoplasm to the nucleus was visualized; Bortezomib was used as a positive control, and Gefitinib was also included for comparison. Intriguingly, compound **4b** repeatedly showed a clear concentration-dependent inhibition of the NF-κB-p65 translocation (Figures 1 and 2). Since **4b** suffered from solubility problems in the serum-free F12 medium, Pluronic F-127 was added in some experiments to increase the solubility at higher concentrations, however, inhibition was noted already starting at 5 μM also in the absence of Pluronic F-127. In contrast, Gefitinib was inactive even at high concentrations (30μM), and so were the phenylthiourea derivatives **6c** and **6h**. Even in the presence of Pluronic F-127, which successfully prevented the precipitation that was observed before in the microphotographs, neither of the compounds prevented the migration of the NF-κB construct to the nucleus. This finding was unexpected given the high similarity of compounds **6c** and **6h** with compound **4b**.

Analysis of the compound´s effect on protein ubiquitinylation

To corroborate the results from the NF-κB translocation assay by a different experimental approach, we examined the effect of the test compounds on the polyubiquitinylation level of the cellular proteins. To this end, we incubated HeLa cells with our test compounds for 6 h, isolated the cellular proteins and analyzed the amount of polyubiquitinylated proteins by Western Blotting. Indeed, we observed that compound **4b** produced a significant accumulation of polyubiquitinylated proteins already at 7.5 μM (Figure 1B). The positive control compound Bortezomib caused the strongest increase, whereas Gefitinib was again completely ineffective in this assay. These results correlated well with the findings from the NF-κB translocation assay. We obtained similar results for compound **4b** in MDA-MB-231 cells (data not shown); however, in this cell type, Bortezomib was not suitable as a positive control, so that we used HeLa cells instead that were previously reported to show the desired polyubiquitinylation response when treated with Bortezomib.[39, 40] Also in this assay, compounds **6c** and **6h** failed to show any effect. Altogether, our results indicate that the benzylthiourea derivative **4b** and the two phenylthiourea analogues **6c** and **6h** have qualitatively distinct biological activities with respect to the suppression of the NF-κB activation. At least for compound **4b**, we could clearly show that this compound leads to an accumulation of polyubiquitinylated

proteins, which probably blocks the degradation step of the IκB proteins, so that NF-κB is retained in the cytoplasm. Deubiquitinating enzymes are a large family of enzymes that play essential roles at multiple levels of the proteasome degradation pathway, and dysregulation of the ubiquitin-proteasome system has been implicated in the pathogenesis of many human diseases, including cancer.[41] In particular the effectiveness of the proteasome inhibitor Bortezomib in the treatment of multiple myeloma validated the ubiquitin-proteasome system as a promising anti-cancer therapeutic target.[42] However, extended treatment with Bortezomib was associated with toxicity and drug resistance, limiting its efficacy.[43]

In contrast, therapeutic strategies that target specific aspects of the ubiquitin-proteasome pathway upstream of the proteasome, were discussed to have lower toxicity.[44] Therefore, our new compound **4b**, which interferes with the deubiquitinating enzyme level, might display lower mechanism-related toxicity than in the case of proteasome inhibition.

Since compounds **6c** and **6h** did not block the translocation of NF-κB-p65 to the nucleus, we wanted to verify that these compounds did not exhibit general cytotoxicity, e.g. via inhibition of the mRNA or protein synthesis machinery, which would have resulted in decreased luciferase read-out in the reporter gene assay as well. Therefore we tested our most potent compounds in another cytotoxicity assay using CHO cells as a non-tumor cell line, again comparing with Gefitinib. The IC_{50} values with this cell line were considerably higher than that obtained previously with either of the two cancer cell lines (Table 9). The selectivity factors calculated for the growth inhibition of the tumor cell vs. the non-tumor cell line were for all compounds, including **4b**, was substantially higher than for Gefitinib opening a large potential therapeutic window for this new class of compounds. Thus, a general cytotoxicity could clearly be ruled out. Rather, we were able to demonstrate a pronounced tumor-selectivity for the novel biological activity, although it could not be identified yet for compounds **6c** and **6h**. Future studies will show whether these compounds interfere with the NF-κB dimer directly or disturb the complexation with co-factors which are required for efficient transcriptional activity particularly in tumor cells.

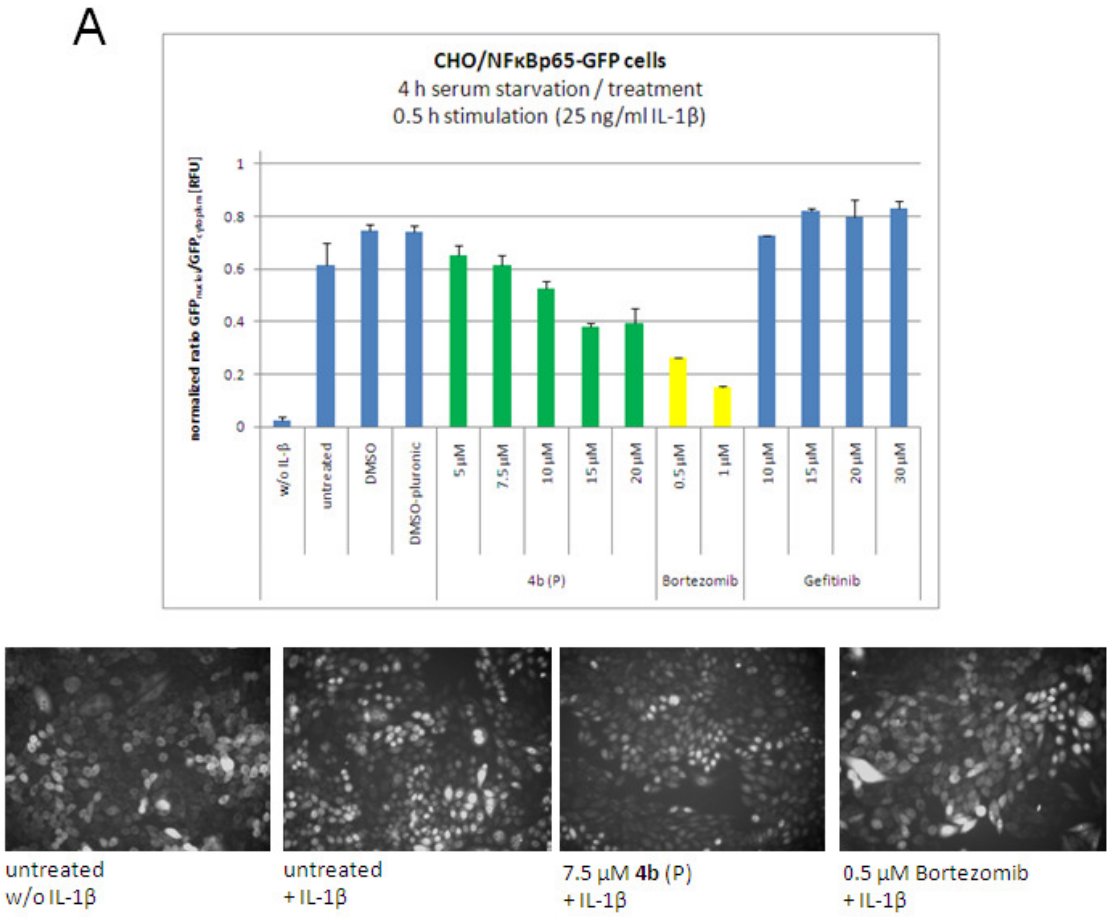

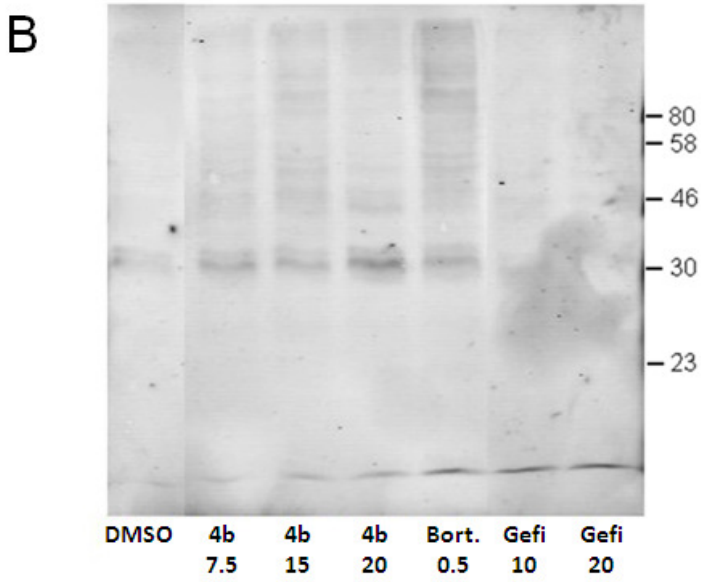

Figure 1. Results of the NF-κB translocation assay.

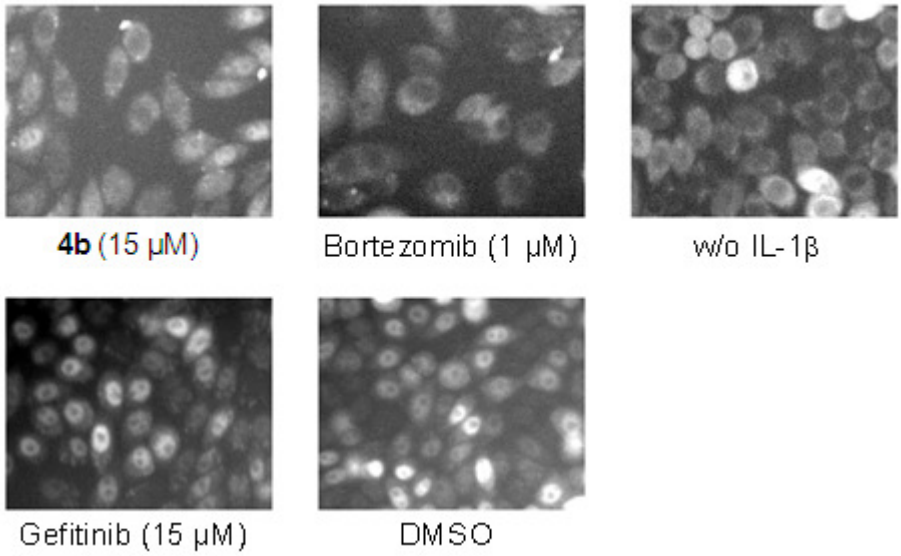

Figure 2. Images of the NF-κB translocation assay where a sharp fluorescent nucleus indicates translocation of the GFP-NFκB, while the diffuse cytosolic staining indicates that the GFP-NFκB resides in the cytoplasm.

Table 9. Cytotoxicity assay using CHO cells (non-tumor) and calculation of selectivity factor in comparison to the tumor cells A549.

Compound	IC_{50} (µM)[a] A549 cells	IC_{50} (µM) CHO-K1 cells	Fold selectivity non-tumor vs. tumor cell line
4b	2.1	34,8	16,6
6c	1.6	25,7	16,1
6h	1.0	52,1	52,1
Gefitinib	9.3	43,7	4,7
Bortezomib	0.07	< 0.06	N.A.

N.A.: not applicable.

Conclusion

A series of thiourea quinazoline derivatives have been synthesized in order to achieve a dual inhibitory activity towards the EGFR and NF-κB activation pathway. These two complementary pathways are essential for the growth and survival of the cancer cells. Therefore, the dual inhibitory activity would offer a synergistic effect that could be used for cancer cells that are not sensitive or intermediately sensitive to the clinically approved EGFR inhibitors alone. We have been able to identify compound **4b** as a good hit (among others that were weaker). Optimization of the hit compound resulted in **6c** and **6h** as best compounds for NF-κB inhibition with IC_{50}s in the low micromolar and submicromolar range, respectively. The best compounds **6c**, **6h** and **4b**

were investigated for their mechanism of NF-κB inhibition. For compound **4b** we identified a mechanism mainly involving the deubiquitination step, whereas for **6c** and **6h** it remains elusive. There is no inhibition of the proteasome nor do the compounds inhibit the translocation of NF-κB to the nucleus and they don't inhibit the deubiquitination step. However, we can exclude a general cytotoxicity; rather, the compounds display a tumor-cell selective cytotoxic effect, which was very promising. Compound **6c** also showed much higher selective towards EGFR kinase than Gefitinib.

Experimental

Chemistry

Solvents and reagents were obtained from commercial suppliers and used as received. 1H and 13C NMR spectra were recorded on a Bruker DRX 500 spectrometer. Chemical shifts are referenced to the residual protonated solvent signals. The purities of the tested compounds **4a-4q**, **6a-6u**, **7a-7e** and **8a-8b** were determined by HPLC coupled with mass spectrometry and were higher than 95% in all cases. Mass spectrometric analysis (HPLC-ESI-MS) was performed on a TSQ quantum (Thermo Electron Corporation) instrument equipped with an ESI source and a triple quadrupole mass detector (Thermo Finnigan). The MS detection was carried out at a spray voltage of 4.2 kV, a nitrogen sheath gas pressure of 4.0 x 105 Pa, an auxiliary gas pressure of 1.0 x 105 Pa, a capillary temperature of 400 ºC, a capillary voltage of 35 V, and a source CID of 10 V. All samples were injected by an autosampler (Surveyor, Thermo Finnigan) with an injection volume of 10 µL. An RP C18 NUCLEODUR 100-3 (125 x 3 mm) column (Macherey-Nagel) was used as the stationary phase. The solvent system consisted of water containing 0.1% TFA (A) and 0.1% TFA in acetonitrile (B). HPLC-Method: flow rate 400 µL/min. The percentage of B started at an initial of 5%, was increased up to 100% during 16 min, kept at 100% for 2 min, and flushed back to 5% in 2 min. Melting points are uncorrected and were determined on Buchi melting point apparatus (B-540). The IR spectra were measured on Nicolet 380 FT-IR spectrometer.

1-benzyl-3-(4-((3-bromophenyl)amino)quinazolin-6-yl)thiourea (4b). Yield 52%; 197-198; ^{1}H NMR (500 MHz, DMSO-d_6) δ 9.91 (s, 1H), 9.83 (s, 1H), 8.64 (s, 1H), 8.47 (d, J = 1.3 Hz, 1H), 8.42 (s, 1H), 8.25 (t, J = 1.9 Hz, 1H), 7.93 (ddd, J = 8.2, 1.9, 0.9 Hz, 1H), 7.85 (dd, J = 8.9, 2.1 Hz, 1H), 7.78 (d, J = 8.9 Hz, 1H), 7.38 – 7.31 (m, 5H), 7.30 (ddd, J = 7.9, 1.9, 1.0 Hz, 1H), 7.25 (t, J = 7.1 Hz, 1H), 4.79 (d, J = 5.1 Hz, 2H). ^{13}C NMR (126 MHz, DMSO-d_6) δ 181.56, 157.11, 153.66, 147.51, 141.07, 139.00, 136.98, 131.83, 131.80, 130.41, 128.21, 127.41, 126.83, 125.86, 123.89, 121.21, 120.43, 117.77, 115.26, 47.51. MS (+ESI): m/z = 464.09 (M + H).

1-(4-((3-bromophenyl)amino)quinazolin-6-yl)-3-(3-chlorophenyl)thiourea (6c). Yield 62%; m.p. 180-182°C; ^{1}H NMR (500 MHz, DMSO-d_6) δ 10.19 (s, 1H), 10.06 (s, 1H),

9.84 (s, 1H), 8.65 (s, 1H), 8.49 (d, *J* = 1.8 Hz, 1H), 8.23 (t, *J* = 1.8 Hz, 1H), 7.94 – 7.84 (m, 2H), 7.80 (d, *J* = 8.8 Hz, 1H), 7.70 (t, *J* = 2.0 Hz, 1H), 7.43 (d, *J* = 9.0 Hz, 1H), 7.36 (td, *J* = 8.0, 4.1 Hz, 2H), 7.30 (d, *J* = 8.7 Hz, 1H), 7.20 (ddd, *J* = 7.9, 2.0, 1.0 Hz, 1H). ^{13}C NMR (126 MHz, DMSO-*d*$_6$) δ 180.49, 157.15, 153.80, 147.66, 140.96, 140.89, 137.09, 132.49, 132.03, 130.40, 130.00, 128.10, 125.95, 124.34, 124.05, 123.52, 122.43, 121.18, 120.59, 118.36, 115.13. MS (+ESI): m/z = 483.34 (M + H).

1-(4-((3-bromophenyl)amino)quinazolin-6-yl)-3-(3-chloro-4-fluorophenyl)thiourea (6h). Yield 53%; m.p. 206-208°C; ^{1}H NMR (500 MHz, DMSO-*d*$_6$) δ 10.19 (s, 1H), 9.98 (s, 1H), 9.84 (s, 1H), 8.65 (s, 1H), 8.49 (d, *J* = 2.1 Hz, 1H), 8.24 (t, *J* = 2.0 Hz, 1H), 7.91 (ddd, *J* = 8.1, 2.0, 1.0 Hz, 1H), 7.86 (dd, *J* = 8.9, 2.2 Hz, 1H), 7.80 (d, *J* = 8.9 Hz, 1H), 7.77 (dd, *J* = 6.8, 2.5 Hz, 1H), 7.44 (ddd, *J* = 8.9, 4.6, 2.5 Hz, 1H), 7.41 (d, *J* = 9.0 Hz, 1H), 7.36 (dd, *J* = 14.2, 6.1 Hz, 1H), 7.30 (ddd, *J* = 8.0, 1.9, 1.0 Hz, 1H). ^{13}C NMR (126 MHz, DMSO-*d*$_6$) δ 180.77, 157.17, 154.42 (d, $^{1}J_{C\text{-}F}$ = 244.6 Hz), 153.87, 147.75, 140.98, 137.00, 136.59, 132.07, 130.41, 128.21, 126.43, 125.97, 125.20 (d, $^{3}J_{C\text{-}F}$ = 7.2 Hz), 124.05, 121.21, 120.59, 118.71 (d, $^{2}J_{C\text{-}F}$ = 18.6 Hz), 118.46, 116.47 (d, $^{2}J_{C\text{-}F}$ = 21.8 Hz), 115.18. MS (+ESI): m/z = 501.83 (M + H).

Biology screening

EGFR kinase phosphorylation assay. Phosphorylation assays were performed in a final volume of 20 µl containing 8 mM MOPS (pH 7.0), 0.2 mM EDTA, 10 mM $MnCl_2$, 200 µM substrate peptide, 0.25 mM DTT, 0.1 mg/ml BSA, 10 ng wild-type EGFR-Kinase (Cat. No. 40187, BPS Bioscience), 10 mM magnesium acetate, 100 µM γ–[^{32}P]ATP, and inhibitors or DMSO control (1.25% v/v). For IC_{50} curves with the wild-type enzyme, the following concentrations of the compounds (in nM) were tested in triplicates: 150, 100, 50, 25, 15, 10, 7.5, 5, 2.5. The assays were repeated at least once. Reactions were started by the addition of the magnesium acetate/ATP mixture. After 30 min incubation at 30°C, 5 µl of each reaction was spotted on phosphocellulose P81 paper (Whatman). The P81 paper was then washed 5 times with 50 mM phosphoric acid for 15 min, dried and exposed to a phosphorimager screen, which was scanned and densitometrically analyzed the next day. The sequence of the substrate peptide was derived from phospholipase C-γ1 and had the sequence "KHKKLAEGSAYEEV", according to Fry *et al.*[45]

Reporter Gene Assay. The NF-κB reporter gene assay was performed in U937 cells exactly as previously described.[46]

MDA-MB-231 and A549 cell growth assay. Cells were seeded in 96-well standard assay microplates at a density of 45,000 cells/well for growth assays, then allowed to acclimate overnight before compound addition. After 24 hours cells were treated with the different concentrations of the compounds. Cells were incubated for an additional 48 hours at 37 °C, after which 50µl of MTT reagent (prepared as 5mg/ml PBS) are added

and then incubated for additional 4 hours. After that 80µl SDS (prepared as 10% in 0.01N HCl) are then added and incubated for additional 1 hour. Absorbance is then measured at wavelength 570nm in a plate reader (PolarStar, BMG Labtech, Freiburg, Germany).

Cytotoxicity assay for CHO cells. CHO-K1 cells (ACC-110) were obtained from the from the German Collection of Microorganisms and Cell Cultures (*Deutsche Sammlung für Mikroorganismen und Zellkulturen, DSMZ*) and were cultured under conditions recommended by the depositor. Cells were seeded at 6 x 10^3 cells per well of 96-well plates in 180 µl complete medium (F12, 10% FBS) and treated with compounds at the indicated concentrations after 2 h of equilibration. Each compound was tested in duplicate. After 5 d incubation, 20 µl of 5 mg/ml MTT (Thiazolyl blue tetrazolium bromide) in PBS was added per well and it was further incubated for 2 h at 37°C. The medium was then discarded and cells were washed with 100 µl PBS before adding 100 µl 2-propanol/10 N HCl (250:1) in order to dissolve formazan granules. The absorbance at 570 nm was measured using a microplate reader (SpectraMax M5e, Molecular Devices) and cell viability was expressed as percentage relative to the control. IC_{50} values were determined by sigmoidal curve fitting.

High-Content Screening Analysis. The stable CHO/NFκBp65-GFP cell line was obtained from Affymetrix and cultivated as recommended by the distributor. For screening, cells were seeded into 96-well imaging plates (BD Falcon) at 5x10^3 cells/well in F12K medium (GIBCO, Invitrogen) containing 10% FBS Gold (v/v; PAA) and 100 µg/mL hygromycin B (Roche Applied Science) and were incubated for 2 days. The medium was exchanged to F12K medium containing 1% FBS. Cells were incubated with test compounds at the indicated concentrations for 3.5 h. For induction of NFκB translocation, 25 ng/mL IL-1β was added and the cells were further incubated for 0.5 h. Cells were washed twice with PBS and nuclei were stained with Hoechst33342 (5 µg/mL, 10 min). The translocation of NFκBp65 was analyzed by measuring the GFP fluorescence on an automated microscope (BD Pathway855). Nuclei and cytoplasmic segments were defined in subsequent analyses (AttoVision v1.6.2) and GFP fluorescence intensities were calculated within these segments. The ratio of GFP fluorescence intensity in nuclei and cytosplasm was used as a measure to describe the degree of NFκB nuclear translocation.

Kinase selectivity assay. All kinases were tested using ATP concentrations at the respective K_m values and was performed by Merck Millipore Kinase Profiler Service.

Polyubiquitinylation assay. HeLa cells were cultured in DMEM (10% FCS and antibiotics), seeded in 12 well plates, and after confluency starved overnight in DMEM containing 0,1% FCS. The next day, test compounds or DMSO control were added and the cells incubated for 6h at 37°C, 5% CO_2. Supernatants were then removed and the

cells lysed using 200 µL SDS PAGE buffer. The soluble fraction was subject to Western Blotting, and the membranes were incubated with anti-ubiquitin antibody (Cell Signaling, cat. #3933, dilution 1:250) as a primary antibody at 4°C overnight. The following day, the Blot was developed using RDY686 labeled goat anti-rabbit secondary antibody and the fluorescence signals detected in a LI-COR Odyssey apparatus.

Supporting information

Table 5. Kinase inhibition selectivity profile for compound **6c** at 5 µM concentration.

Kinase	% Activity	Kinase	% Activity	Kinase	% Activity
Abl(h)	142	IGF-1R(h)	77	PKA(h)	107
ACK1(h)	72	IKKα(h)	122	PKBα(h)	112
ALK(h)	71	IKKβ(h)	101	PKCα(h)	102
AMPKα1(h)	103	IRAK1(h)	96	PKCδ(h)	96
ASK1(h)	115	JAK2(h)	115	PKCθ(h)	86
Aurora-A(h)	83	JNK1α1(h)	96	PKCζ(h)	96
Axl(h)	93	JNK2α2(h)	103	PKD2(h)	99
Blk(h)	91	JNK3(h)	88	Plk1(h)	99
BRK(h)	89	KDR(h)	90	PRAK(h)	68
BrSK1(h)	39	Lck(h)	71	PRK2(h)	95
BTK(h)	99	LKB1(h)	75	RIPK2(h)	80
CaMKI(h)	82	LOK(h)	68	ROCK-II(h)	106
CDK2/cyclinA(h)	99	Lyn(h)	74	Rse(h)	90
CDK5/p25(h)	99	MAPK1(h)	82	Rsk1(h)	126
CDK9/cyclin T1(h)	95	MAPKAP-K2(h)	100	SAPK2a(h)	93
CHK1(h)	93	MEK1(h)	100	SAPK2b(h)	101
CHK2(h)	65	MARK1(h)	96	SAPK3(h)	95
CK1γ1(h)	72	Met(h)	96	SAPK4(h)	110
CK2(h)	93	MINK(h)	72	SGK(h)	100
CSK(h)	106	MKK4(m)	74	SRPK1(h)	89
c-RAF(h)	77	MKK6(h)	98	STK33(h)	100
cSRC(h)	96	MKK7β(h)	112	Syk(h)	99
DDR2(h)	85	MLCK(h)	83	TAK1(h)	99
DRAK1(h)	77	MLK1(h)	86	TAO1(h)	55
eEF-2K(h)	140	Mnk2(h)	22	TBK1(h)	91
EGFR(h)	-14	MSK1(h)	117	TGFBR1(h)	100
EphA5(h)	101	MSK2(h)	100	Tie2 (h)	115
EphB4(h)	90	MST1(h)	107	TLK2(h)	101
ErbB4(h)	46	MST2(h)	77	TrkA(h)	60
FGFR1(h)	65	NEK2(h)	97	Txk(h)	77
Flt1(h)	81	NEK6(h)	112	ULK2(h)	91
Flt3(h)	101	p70S6K(h)	61	VRK2(h)	103
Fyn(h)	82	PAK4(h)	96	Yes(h)	78
GCK(h)	56	PDGFRβ(h)	112	ZAP-70(h)	105
GSK3α(h)	82	PhKγ2(h)	101		
HIPK1(h)	95	Pim-1(h)	29		

Table 6. IC_{50} for compound **6c** against EGFR, Mnk2 and Pim-1.

Kinase	IC_{50} (µM)
EGFR (h)	0.041
Mnk2(h)	2.7
Pim-1(h)	1.2

Table 7. % inhibition of U937 reporter gene assay for CGP 57380, SIM-4a and Gefitinib at different concentrations

	% Inhibition		
Conc.	**CGP 57380**	**SIM-4a**	**Gefitinib**
5µM	40.4	-0.4	37.6
2,5µM	37.5	-6.2	32.6
1µM	30.3	17.5	24.8
0,5µM	N.D.	N.D.	21.2

N.D.: Not Determined

Table 8. % inhibition of U937 reporter gene assay using different combinations of CGP 57380, SIM-4a and Gefitinib at 1uM concentration.

Comp. Combination	% Inhibition
C+S	11.5
C+G	13.4
S+G	16.4
C+S+G	28.8

C= CGP 57380
S= SIM-4a
G= Gefitinib

Experimental
Chemistry

Ethyl *N*-(2-cyano-4-nitrophenyl)formimidate (1). 5g (30.6 mmol) of 2-amino-5-nitrobenzonitrile was refluxed in 50ml of triethyl orthoformate for 24 hours in the presence of 10 drops of acetic anhydride. The reaction was then concentrated under vacuum and the remaining residue was poured on ice water where a precipitate has been formed. The ppt. was filtered under vacuum and left to dry to give compound **1**. Yield 82%; IR: $\tilde{\nu}$ = 2228.6 cm^{-1} (C≡N); ^{1}H NMR (500 MHz, DMSO-d_6): δ 8.67 (d, *J* = 2.6 Hz, 1H), 8.43 (dd, *J* = 8.9, 2.7 Hz, 1H), 8.22 (s, 1H), 7.46 (s, *J* = 8.9 Hz, 1H), 4.36 (q, *J* = 7.0 Hz, 2H), 1.35 (t, *J* = 7.1 Hz, 3H). ^{13}C NMR (126 MHz, DMSO-d_6): δ 156.31, 156.08, 143.50, 130.58, 128.84, 122.20, 115.56, 114.95, 63.65, 13.87.

General procedure for the synthesis of *N*-(substituted)-6-nitroquinazolin-4-amine (2a-2q). Compound **1** (5 mmol) was refluxed for 1 hour with the respective amine derivative (5 mmol) in 8ml glacial acetic acid. A precipitate is formed during the reaction which is filtered on hot and the precipitate is then washed with diethyl ether to give the corresponding nitro quinazoline derivatives **(2a-2p)**. If a precipitate is not formed, the solution is poured on ice water and the formed precipitate is filtered followed by washing with diethyl ether to give the corresponding nitroquinazoline derivative.

N-(2-bromophenyl)-6-nitroquinazolin-4-amine (2a). Yield 71%; ^{1}H NMR (500 MHz, DMSO-d_6) δ 10.64 (s, 1H), 9.61 (s, 1H), 8.56 (d, *J* = 8.4 Hz, 2H), 7.94 (d, *J* = 8.0 Hz, 1H), 7.77 (d, *J* = 7.8 Hz, 1H), 7.60 – 7.43 (m, 2H), 7.31 (s, 1H). ^{13}C NMR (126 MHz, DMSO-d_6) δ 160.10, 157.89, 152.99, 144.50, 136.73, 132.95, 130.13, 129.47, 128.81, 128.44, 126.75, 122.11, 120.83, 113.79. MS (+ESI): m/z = 344.80 (M + H).

***N*-(3-bromophenyl)-6-nitroquinazolin-4-amine (2b)**
As reported.[1]

N-(4-bromophenyl)-6-nitroquinazolin-4-amine (2c). Yield 82%; ^{1}H NMR (300 MHz, DMSO-d_6) δ 10.48 (s, 1H), 9.64 (d, *J* = 2.4 Hz, 1H), 8.73 (s, 1H), 8.55 (dd, *J* = 9.2, 2.4 Hz, 1H), 7.93 (d, *J* = 9.2 Hz, 1H), 7.89 – 7.80 (m, 2H), 7.66 – 7.56 (m, 2H). ^{13}C NMR (75 MHz, DMSO-d_6) δ 159.09, 158.01, 153.50, 145.03, 138.33, 131.83, 130.04, 127.17, 125.08, 121.30, 116.77, 114.88. MS (+ESI): m/z = 344.79 (M + H).

N-(3-chlorophenyl)-6-nitroquinazolin-4-amine (2d). Yield 75%; ^{1}H NMR (300 MHz, DMSO-d_6) δ 10.43 (s, 1H), 9.61 (d, *J* = 2.2 Hz, 1H), 8.75 (s, 1H), 8.53 (dd, *J* = 9.2, 2.3 Hz, 1H), 8.05 (d, *J* = 1.8 Hz, 1H), 7.92 (d, *J* = 9.2 Hz, 1H), 7.84 (d, *J* = 8.2 Hz, 1H), 7.43 (t, *J* = 8.1 Hz, 1H), 7.22 (dd, *J* = 8.0, 1.1 Hz, 1H). ^{13}C NMR (75 MHz, DMSO-d_6) δ

159.13, 157.95, 153.47, 145.10, 140.49, 133.25, 130.64, 130.10, 127.20, 124.45, 122.47, 121.33, 121.25, 114.86. MS (+ESI): m/z = 300.94 (M + H).

6-nitro-N-(m-tolyl)quinazolin-4-amine (2e). Yield 70%; ^{1}H NMR (500 MHz, DMSO-d_6) δ 10.34 (s, 1H), 9.63 (d, *J* = 2.4 Hz, 1H), 8.68 (s, 1H), 8.51 (dd, *J* = 9.2, 2.4 Hz, 1H), 7.89 (d, *J* = 9.2 Hz, 1H), 7.66 (d, *J* = 8.0 Hz, 1H), 7.63 (s, 1H), 7.29 (t, *J* = 7.8 Hz, 1H), 7.00 (d, *J* = 7.5 Hz, 1H), 2.35 (s, 3H). ^{13}C NMR (126 MHz, DMSO-d_6) δ 158.77, 157.72, 153.07, 144.43, 138.29, 137.73, 129.42, 128.34, 126.49, 125.23, 123.32, 120.82, 120.05, 114.35, 21.13. MS (+ESI): m/z = 280.94 (M + H).

N-(2,3-dimethylphenyl)-6-nitroquinazolin-4-amine (2f). Yield 64%; ^{1}H NMR (300 MHz, DMSO-d_6) δ 10.42 (s, 1H), 9.60 (d, *J* = 2.4 Hz, 1H), 8.57 – 8.51 (m, 2H), 7.90 (d, *J* = 9.2 Hz, 1H), 7.19 – 7.12 (m, 3H), 2.31 (s, 3H), 2.07 (s, 3H). ^{13}C NMR (75 MHz, DMSO-d_6) δ 160.60, 158.63, 153.55, 144.78, 137.86, 136.78, 134.15, 129.80, 128.78, 126.97, 126.13, 125.73, 121.46, 114.42, 20.56, 14.84. MS (+ESI): m/z = 294.98 (M + H).

***N*-(3-ethylphenyl)-6-nitroquinazolin-4-amine (2g)** Yield 69%; ^{1}H NMR (500 MHz, $(CD_3)_2CO$) δ 9.70 (s, 1H), 9.37 (d, *J* = 2.3 Hz, 1H), 8.74 (s, 1H), 8.56 (dd, *J* = 9.2, 2.4 Hz, 1H), 7.96 (d, *J* = 9.2 Hz, 1H), 7.80 (dd, *J* = 8.1, 1.2 Hz, 1H), 7.75 (t, *J* = 1.6 Hz, 1H), 7.32 (t, *J* = 7.8 Hz, 1H), 7.05 (dd, *J* = 7.6, 0.6 Hz, 1H), 2.68 (q, *J* = 7.6 Hz, 2H), 1.25 (t, *J* = 7.6 Hz, 3H). ^{13}C NMR (126 MHz, $(CD_3)_2CO$): δ 159.95, 158.71, 154.53, 145.94, 145.60, 139.63, 130.90, 129.40, 127.13, 125.00, 122.80, 120.90, 120.67, 115.60, 29.48, 15.97.

N-(4-isopropylphenyl)-6-nitroquinazolin-4-amine (2h). Yield 65%; ^{1}H NMR (500 MHz, DMSO-d_6) δ 10.38 (s, 1H), 9.62 (d, *J* = 2.4 Hz, 1H), 8.65 (s, 1H), 8.51 (dd, *J* = 9.2, 2.4 Hz, 1H), 7.88 (d, *J* = 9.2 Hz, 1H), 7.75 – 7.66 (m, 2H), 7.33 – 7.21 (m, 2H), 2.90 (hept, *J* = 6.9 Hz, 1H), 1.23 (s, 3H), 1.22 (s, 3H). ^{13}C NMR (126 MHz, DMSO-d_6) δ 158.76, 157.74, 153.08, 144.74, 144.36, 135.99, 129.37, 126.45, 126.23, 123.02, 120.78, 114.30, 32.97, 23.90. MS (+ESI): m/z = 309.02 (M + H).

N-(4-(tert-butyl)phenyl)-6-nitroquinazolin-4-amine (2i). Yield 72%; ^{1}H NMR (300 MHz, DMSO-d_6) δ 10.38 (s, 1H), 9.62 (d, *J* = 2.4 Hz, 1H), 8.65 (s, 1H), 8.51 (dd, *J* = 9.2, 2.4 Hz, 1H), 7.88 (d, *J* = 9.2 Hz, 1H), 7.71 (d, *J* = 8.7 Hz, 2H), 7.42 (d, *J* = 8.7 Hz, 2H), 1.31 (s, 9H). ^{13}C NMR (75 MHz, DMSO-d_6) δ 159.27, 158.23, 153.58, 147.47, 144.87, 136.18, 129.88, 126.95, 125.63, 123.17, 121.29, 114.81, 34.64, 31.65. MS (+ESI): m/z = 323.00 (M + H).

N-([1,1'-biphenyl]-4-yl)-6-nitroquinazolin-4-amine (2j). Yield 68%; ^{1}H NMR (500 MHz, DMSO-d_6) δ 10.37 (s, 1H), 9.75 (d, *J* = 2.3 Hz, 1H), 8.74 (s, 1H), 8.51 (dd, *J* = 9.2, 2.4 Hz, 1H), 7.97 – 7.92 (m, 2H), 7.91 (d, *J* = 9.2 Hz, 1H), 7.67 – 7.60 (m, 4H), 7.47 –

7.42 (m, 2H), 7.34 (ddd, *J* = 8.5, 2.3, 1.1 Hz, 1H). ^{13}C NMR (126 MHz, DMSO-d_6) δ 158.31, 157.00, 152.66, 143.83, 139.41, 136.95, 136.24, 128.70, 127.96, 126.28, 126.13, 125.78, 125.34, 122.36, 120.20, 114.18. MS (+ESI): m/z = 342.90 (M + H).

6-nitro-N-(4-phenoxyphenyl)quinazolin-4-amine (2k). Yield 66%; ^{1}H NMR (300 MHz, DMSO-d_6) δ 10.48 (s, 1H), 9.65 (d, *J* = 2.4 Hz, 1H), 8.69 (s, 1H), 8.55 (dd, *J* = 9.2, 2.4 Hz, 1H), 7.92 (d, *J* = 9.2 Hz, 1H), 7.83 (d, *J* = 9.0 Hz, 2H), 7.41 (dd, *J* = 8.5, 7.5 Hz, 2H), 7.18 – 7.01 (m, 5H). ^{13}C NMR (75 MHz, DMSO-d_6) δ 159.24, 158.25, 157.46, 156.59, 153.57, 144.94, 134.39, 130.54, 129.94, 127.10, 125.20, 123.78, 121.31, 119.37, 118.77, 114.82. MS (+ESI): m/z = 358.87 (M + H).

3-((6-nitroquinazolin-4-yl)amino)phenol (2l). Yield 73%; ^{1}H NMR (300 MHz, DMSO-d_6) δ 10.30 (s, 1H), 9.64 (d, *J* = 2.4 Hz, 1H), 9.50 (s, 1H), 8.70 (s, 1H), 8.52 (dd, *J* = 9.2, 2.4 Hz, 1H), 7.90 (d, *J* = 9.2 Hz, 1H), 7.37 (t, *J* = 1.9 Hz, 1H), 7.22 (dt, *J* = 15.8, 8.1 Hz, 2H), 6.60 (ddd, *J* = 7.7, 2.2, 1.2 Hz, 1H). ^{13}C NMR (75 MHz, DMSO-d_6) δ 159.22, 158.15, 157.92, 153.56, 144.92, 139.84, 129.89, 129.59, 126.98, 121.36, 114.89, 114.05, 112.16, 110.45. MS (+ESI): m/z = 283.03 (M + H).

4-((6-nitroquinazolin-4-yl)amino)phenol (2m). Yield 79%; ^{1}H NMR (300 MHz, DMSO-d_6) δ 10.29 (s, 1H), 9.58 (d, *J* = 2.4 Hz, 1H), 9.41 (s, 1H), 8.59 (s, 1H), 8.50 (dd, *J* = 9.2, 2.4 Hz, 1H), 7.85 (d, *J* = 9.2 Hz, 1H), 7.60 – 7.48 (m, 2H), 6.84 – 6.78 (m, 2H). ^{13}C NMR (75 MHz, DMSO-d_6) δ 159.28, 158.42, 155.13, 153.58, 144.75, 130.01, 129.73, 126.84, 125.42, 121.23, 115.48, 114.76. MS (+ESI): m/z = 282.92 (M + H).

4-((6-nitroquinazolin-4-yl)amino)benzenesulfonamide (2n) Yield 78%; ^{1}H NMR (500 MHz, DMSO-d_6): δ 10.61 (s, 1H), 9.67 (d, *J* = 2.4 Hz, 1H), 8.78 (s, 1H), 8.57 (dd, *J* = 9.2, 2.4 Hz, 1H), 8.07 (d, *J* = 8.8 Hz, 2H), 7.96 (d, *J* = 9.2 Hz, 1H), 7.88 (d, *J* = 8.8 Hz, 2H), 7.32 (s, 2H). ^{13}C NMR (126 MHz, DMSO-d_6): δ 158.72, 157.40, 153.03, 144.68, 141.53, 139.28, 129.63, 126.76, 126.30, 122.17, 120.83, 114.44. MS (+ESI): m/z = 346.09 (M + H).

***N*-carbamimidoyl-4-((6-nitroquinazolin-4-yl)amino)benzenesulfonamide (2o)** Yield 75%; ^{1}H NMR (500 MHz, DMSO-d_6) δ 10.58 (s, 1H), 9.66 (d, *J* = 1.9 Hz, 1H), 8.77 (s, 1H), 8.56 (dd, *J* = 9.2, 2.5 Hz, 1H), 8.00 (d, *J* = 8.6 Hz, 2H), 7.95 (d, *J* = 9.2 Hz, 1H), 7.83 – 7.81 (m, 1H), 7.81 – 7.79 (m, 1H), 6.72 (s, 4H). ^{13}C NMR (126 MHz, DMSO-d_6) δ 158.71, 158.13, 157.47, 153.04, 144.66, 141.00, 139.86, 129.62, 126.77, 126.23, 122.07, 120.87, 114.46. MS (+ESI): m/z = 387.87 (M + H).

4-((6-nitroquinazolin-4-yl)amino)-*N*-(pyridin-2-yl)benzenesulfonamide (2p) Yield 75%; ^{1}H NMR (500 MHz, DMSO-d_6): δ 11.90 (s, 1H), 10.59 (s, 1H), 9.66 (d, *J* = 2.3 Hz, 1H), 8.78 (s, 1H), 8.56 (dd, *J* = 9.2, 2.4 Hz, 1H), 8.07 (d, *J* = 8.8 Hz, 2H), 8.03 (dd, *J* =

5.5, 1.1 Hz, 1H), 7.96 (d, *J* = 9.2 Hz, 1H), 7.95 – 7.91 (m, 2H), 7.73 (ddd, *J* = 8.9, 7.2, 1.9 Hz, 1H), 7.19 (d, *J* = 8.7 Hz, 1H), 6.88 (ddd, *J* = 7.0, 5.5, 0.9 Hz, 1H). ^{13}C NMR (126 MHz, DMSO-d_6): δ 158.64, 157.35, 153.03, 144.70, 141.98, 140.23, 140.21, 136.69, 136.67, 129.65, 127.35, 126.79, 121.94, 120.84, 115.72, 114.48, 113.65. MS (+ESI): m/z = 423.09 (M + H).

6-nitro-N-(pyridin-3-yl)quinazolin-4-amine (2q). Yield 60%; ^{1}H NMR (300 MHz, DMSO-d_6) δ 10.51 (s, 1H), 9.59 (d, *J* = 2.2 Hz, 1H), 8.99 (d, *J* = 2.2 Hz, 1H), 8.71 (s, 1H), 8.53 (dd, *J* = 9.2, 2.4 Hz, 1H), 8.38 (dd, *J* = 4.7, 1.4 Hz, 1H), 8.26 (d, *J* = 8.3 Hz, 1H), 7.91 (d, *J* = 9.2 Hz, 1H), 7.46 (dd, *J* = 8.3, 4.7 Hz, 1H). ^{13}C NMR (75 MHz, DMSO-d_6) δ 159.39, 157.96, 153.44, 145.62, 145.02, 144.57, 135.68, 130.37, 130.05, 127.17, 123.83, 121.22, 114.76. MS (+ESI): m/z = 268.01 (M + H).

General procedure for the synthesis of compunds (3a-3q).[2] A mixture of the respective nitroquinazoline derivative **(2a-2q)** (5 mmol) and stannous chloride (25 mmol) in MeOH (20 ml) was stirred at reflux for 1 h under nitrogen atmosphere. The excess MeOH was removed under reduced pressure; the remaining residue was dissolved in ethyl acetate (200 ml) and basified with aqueous $NaHCO_3$ solution. The resulting mixture was filtrated under vacuum followed by separation of the organic phase from the aqueous phase. The aqueous phase was extracted with ethyl acetate (2 x 20 ml), these organic fractions were combined, dried over anhydrous $MgSO_4$ and concentrated under reduced pressure to obtain the corresponding aminoquinazoline derivatives **(3a-3q)**.

***N*^{4}-(2-bromophenyl)quinazoline-4,6-diamine (3a).** Yield 80%; ^{1}H NMR (500 MHz, DMSO-d_6) δ 9.18 (s, 1H), 8.18 (d, *J* = 6.2 Hz, 1H), 7.71 (dd, *J* = 8.0, 1.3 Hz, 1H), 7.66 (dd, *J* = 7.9, 1.4 Hz, 1H), 7.55 – 7.51 (m, 1H), 7.44 (td, *J* = 7.7, 1.3 Hz, 1H), 7.27 – 7.18 (m, 3H), 5.62 (s, 2H). ^{13}C NMR (126 MHz, DMSO-d_6) δ 156.83, 149.98, 147.26, 142.46, 138.00, 132.66, 128.95, 128.61, 128.13, 127.20, 123.67, 121.14, 116.20, 100.69. MS (+ESI): m/z = 314.9 (M + H).

***N*^{4}-(3-bromophenyl)quinazoline-4,6-diamine(3b)**
As reported.[1]

***N*^{4}-(4-bromophenyl)quinazoline-4,6-diamine (3c).** Yield 83%; ^{1}H NMR (300 MHz, DMSO-d_6) δ 9.43 (s, 1H), 8.35 (s, 1H), 7.88 (d, *J* = 8.9 Hz, 2H), 7.57 – 7.52 (m, 2H), 7.52 – 7.49 (m, 1H), 7.35 (d, *J* = 2.3 Hz, 1H), 7.26 (dd, *J* = 8.9, 2.3 Hz, 1H), 5.60 (s, 2H). ^{13}C NMR (75 MHz, DMSO-d_6) δ 156.21, 150.09, 147.81, 143.13, 139.92, 131.56, 129.18, 124.23, 123.79, 117.19, 114.74, 101.41. MS (+ESI): m/z = 314.87 (M + H).

***N*^{4}-(3-chlorophenyl)quinazoline-4,6-diamine (3d).** Yield 81%; m.p. °C; ^{1}H NMR (300 MHz, DMSO-d_6) δ 9.45 (s, 1H), 8.39 (s, 1H), 8.12 (t, *J* = 1.9 Hz, 1H), 7.84 (dd, *J* = 8.2,

1.2 Hz, 1H), 7.56 (d, *J* = 8.9 Hz, 1H), 7.43 – 7.33 (m, 2H), 7.27 (dd, *J* = 8.9, 2.3 Hz, 1H), 7.09 (dd, *J* = 7.6, 1.7 Hz, 1H), 5.62 (s, 2H). ^{13}C NMR (75 MHz, DMSO-d_6) δ 156.17, 150.02, 147.87, 143.21, 142.09, 133.16, 130.41, 129.23, 124.33, 122.66, 121.06, 120.08, 117.20, 101.32. MS (+ESI): m/z = 270.89 (M + H).

***N*^{4}-(m-tolyl)quinazoline-4,6-diamine (3e).** Yield 75%; ^{1}H NMR (300 MHz, DMSO-d_6) δ 9.24 (s, 1H), 8.32 (s, 1H), 7.66 (d, *J* = 6.7 Hz, 2H), 7.52 (d, *J* = 8.9 Hz, 1H), 7.37 (d, *J* = 2.3 Hz, 1H), 7.28 – 7.17 (m, 2H), 6.88 (dd, *J* = 7.3, 0.5 Hz, 1H), 5.54 (s, 2H), 2.32 (s, 3H). ^{13}C NMR (75 MHz, DMSO-d_6) δ 156.53, 150.38, 147.64, 143.05, 140.33, 137.88, 129.09, 128.64, 124.07, 123.99, 122.70, 119.43, 117.16, 101.62, 21.73. MS (+ESI): m/z = 250.98 (M + H).

***N*^{4}-(3,4-dimethylphenyl)quinazoline-4,6-diamine (3f).** Yield 79%; ^{1}H NMR (300 MHz, DMSO-d_6) δ 9.15 (s, 1H), 8.10 (s, 1H), 7.49 (d, *J* = 8.8 Hz, 1H), 7.31 (d, *J* = 2.3 Hz, 1H), 7.21 (dd, *J* = 8.9, 2.3 Hz, 1H), 7.15 – 7.06 (m, 3H), 5.50 (s, 2H), 2.29 (s, 3H), 2.04 (s, 3H). ^{13}C NMR (75 MHz, DMSO-d_6) δ 157.52, 153.27, 150.45, 146.95, 142.34, 137.79, 136.91, 133.55, 128.46, 127.32, 125.32, 123.31, 116.18, 101.35, 20.16, 14.36. MS (+ESI): m/z = 264.8 (M + H).

***N*^{4}-(3-ethylphenyl)quinazoline-4,6-diamine (3g)** Yield 77%; ^{1}H NMR (300 MHz, DMSO-d_6) δ 9.27 (s, 1H), 8.32 (s, 1H), 7.73 (d, *J* = 8.1 Hz, 1H), 7.66 (s, 1H), 7.52 (d, *J* = 8.9 Hz, 1H), 7.37 (d, *J* = 2.3 Hz, 1H), 7.27 (d, *J* = 7.5 Hz, 1H), 7.22 (d, *J* = 2.4 Hz, 1H), 6.91 (d, *J* = 7.5 Hz, 1H), 5.57 (s, 2H), 2.62 (q, *J* = 7.6 Hz, 2H), 1.21 (t, *J* = 7.6 Hz, 3H). ^{13}C NMR (75 MHz, DMSO-d_6) δ 156.08, 149.93, 147.22, 143.85, 142.55, 139.93, 128.64, 128.24, 123.54, 122.42, 121.06, 119.27, 116.72, 101.16, 28.34, 15.63. MS (+ESI): m/z = 265.02 (M + H).

***N*^{4}-(4-isopropylphenyl)quinazoline-4,6-diamine (3h).** Yield 81%; ^{1}H NMR (500 MHz, DMSO-d_6) δ 9.26 (s, 1H), 8.29 (s, 1H), 7.78 – 7.69 (m, 2H), 7.52 (d, *J* = 8.8 Hz, 1H), 7.36 (d, *J* = 2.4 Hz, 1H), 7.25 – 7.21 (m, 2H), 7.21 – 7.20 (m, 1H), 5.54 (s, 2H), 2.86 (dq, *J* = 13.9, 7.1 Hz, 1H), 1.21 (d, *J* = 6.9 Hz, 6H). ^{13}C NMR (126 MHz, DMSO-d_6) δ 156.10, 149.95, 147.09, 142.99, 142.52, 137.56, 128.58, 126.01, 123.43, 121.96, 116.60, 101.13, 32.90, 23.99. MS (+ESI): m/z = 278.90 (M + H).

***N*^{4}-(4-(tert-butyl)phenyl)quinazoline-4,6-diamine (3i).** Yield 86%; ^{1}H NMR (500 MHz, DMSO-d_6) δ 9.27 (s, 1H), 8.29 (s, 1H), 7.77 – 7.70 (m, 2H), 7.52 (d, *J* = 8.8 Hz, 1H), 7.40 – 7.32 (m, 3H), 7.23 (dd, *J* = 8.8, 2.4 Hz, 1H), 5.54 (s, 2H), 1.29 (s, 9H). ^{13}C NMR (126 MHz, DMSO-d_6) δ 156.10, 149.94, 147.10, 145.22, 142.52, 137.24, 128.57, 124.91, 123.44, 121.62, 116.61, 101.13, 33.99, 31.24. MS (+ESI): m/z = 293.06 (M + H).

***N*^{4}-([1,1'-biphenyl]-4-yl)quinazoline-4,6-diamine (3j).** Yield 72%; ^{1}H NMR (300 MHz, DMSO-d_6) δ 9.44 (s, 1H), 8.37 (s, 1H), 8.06 – 7.93 (m, 2H), 7.72 – 7.62 (m, 4H), 7.55 (d, *J* = 8.9 Hz, 1H), 7.45 (t, *J* = 7.6 Hz, 2H), 7.40 (d, *J* = 2.3 Hz, 1H), 7.36 – 7.29 (m, 1H), 7.26 (dd, *J* = 8.9, 2.3 Hz, 1H), 5.59 (s, 2H). ^{13}C NMR (75 MHz, DMSO-d_6) δ 156.38, 150.30, 147.74, 143.16, 140.39, 140.01, 134.84, 129.36, 129.17, 127.37, 127.00, 126.70, 124.12, 122.29, 117.26, 101.55. MS (+ESI): m/z = 312.96 (M + H).

***N*^{4}-(4-phenoxyphenyl)quinazoline-4,6-diamine (3k).** Yield 74%; ^{1}H NMR (300 MHz, DMSO-d_6) δ 9.36 (s, 1H), 8.31 (s, 1H), 7.92 – 7.79 (m, 2H), 7.53 (d, *J* = 8.8 Hz, 1H), 7.42 – 7.34 (m, 3H), 7.24 (dd, *J* = 8.9, 2.3 Hz, 1H), 7.14 – 7.07 (m, 1H), 7.07 – 7.03 (m, 2H), 7.03 – 6.98 (m, 2H), 5.56 (s, 2H). ^{13}C NMR (75 MHz, DMSO-d_6) δ 157.95, 156.47, 152.00, 150.35, 147.64, 143.01, 136.25, 130.41, 129.10, 124.00, 123.94, 123.36, 119.58, 118.29, 117.06, 101.55. MS (+ESI): m/z = 328.93 (M + H).

3-((6-aminoquinazolin-4-yl)amino)phenol (3l). Yield 80%; ^{1}H NMR (300 MHz, DMSO-d_6) δ 9.34 (s, 1H), 9.18 (s, 1H), 8.33 (s, 1H), 7.52 (d, *J* = 8.8 Hz, 1H), 7.44 (t, *J* = 2.1 Hz, 1H), 7.36 (d, *J* = 2.3 Hz, 1H), 7.30 – 7.19 (m, 2H), 7.12 (t, *J* = 8.0 Hz, 1H), 6.54 – 6.41 (m, 1H), 5.54 (s, 2H). ^{13}C NMR (75 MHz, DMSO-d_6) δ 157.81, 156.46, 150.33, 147.63, 143.05, 141.44, 129.36, 129.09, 123.98, 117.20, 112.93, 110.49, 109.23, 101.66. MS (+ESI): m/z = 252.96 (M + H).

4-((6-aminoquinazolin-4-yl)amino)phenol (3m). Yield 84%; ^{1}H NMR (300 MHz, DMSO-d_6) δ 9.22 (s, 1H), 9.12 (s, 1H), 8.22 (s, 1H), 7.57 – 7.50 (m, 2H), 7.48 (d, *J* = 8.8 Hz, 1H), 7.32 (d, *J* = 2.3 Hz, 1H), 7.20 (dd, *J* = 8.8, 2.3 Hz, 1H), 6.81 – 6.71 (m, 2H), 5.47 (s, 2H). ^{13}C NMR (75 MHz, DMSO-d_6) δ 156.80, 153.99, 150.67, 147.43, 142.81, 131.63, 128.97, 124.62, 123.70, 116.94, 115.30, 101.72. MS (+ESI): m/z = 252.97 (M + H).

4-((6-aminoquinazolin-4-yl)amino)benzenesulfonamide (3n) Yield 82%; ^{1}H NMR (500 MHz, DMSO-d_6): δ 9.63 (s, 1H), 8.40 (s, 1H), 8.07 (d, *J* = 8.7 Hz, 2H), 7.80 (d, *J* = 8.8 Hz, 2H), 7.57 (d, *J* = 8.9 Hz, 1H), 7.37 (d, *J* = 2.2 Hz, 1H), 7.28 (dd, *J* = 8.9, 2.2 Hz, 1H), 7.23 (s, 2H), 5.64 (s, 2H). ^{13}C NMR (126 MHz, DMSO-d_6): δ 155.64, 149.45, 147.46, 143.17, 142.82, 137.43, 128.73, 126.24, 123.98, 120.52, 116.82, 100.81. MS (+ESI): m/z = 316.15 (M + H).

4-((6-aminoquinazolin-4-yl)amino)-N-carbamimidoylbenzenesulfonamide (3o) Yield 85%; ^{1}H NMR (500 MHz, DMSO-d_6): δ 9.56 (s, 1H), 8.39 (s, 1H), 8.00 (d, *J* = 8.8 Hz, 2H), 7.73 (d, *J* = 8.9 Hz, 2H), 7.56 (d, *J* = 8.9 Hz, 1H), 7.36 (d, *J* = 2.3 Hz, 1H), 7.27 (dd, *J* = 8.9, 2.4 Hz, 1H), 6.68 (s, 4H), 5.62 (s, 2H). ^{13}C NMR (126 MHz, DMSO-d_6): δ 158.04, 155.66, 149.52, 147.40, 142.82, 142.60, 138.03, 128.73, 126.12, 123.90, 120.41, 116.81, 100.86.

4-((6-aminoquinazolin-4-yl)amino)-N-(pyridin-2-yl)benzenesulfonamide (3p) Yield 83%; ^{1}H NMR (500 MHz, DMSO-d_6) δ 11.73 (s, 1H), 9.66 (s, 1H), 8.40 (s, 1H), 8.06 (d, *J* = 1.8 Hz, 1H), 8.05 (d, *J* = 5.2 Hz, 2H), 7.88 – 7.83 (m, 2H), 7.71 (ddd, *J* = 8.7, 7.2, 1.9 Hz, 1H), 7.56 (d, *J* = 8.9 Hz, 1H), 7.34 (d, *J* = 2.3 Hz, 1H), 7.28 (dd, *J* = 8.9, 2.4 Hz, 1H), 7.17 (dt, *J* = 8.6, 0.9 Hz, 1H), 6.88 (ddd, *J* = 7.1, 5.4, 0.9 Hz, 1H), 5.68 (s, 2H). ^{13}C NMR (126 MHz, DMSO-d_6) δ 155.56, 152.86, 149.34, 147.54, 143.71, 142.72, 139.89, 134.51, 128.66, 127.42, 124.07, 122.00, 120.39, 116.88, 116.06, 113.31, 100.79. MS (+ESI): m/z = 392.92 (M + H).

***N*^{4}-(pyridin-3-yl)quinazoline-4,6-diamine (3q).** Yield %; ^{1}H NMR (300 MHz, DMSO-d_6) δ 9.55 (s, 1H), 9.02 (d, *J* = 2.4 Hz, 1H), 8.35 (s, 1H), 8.33 – 8.28 (m, 1H), 8.26 (dd, *J* = 4.6, 1.3 Hz, 1H), 7.55 (d, *J* = 8.9 Hz, 1H), 7.38 (q, *J* = 5.1 Hz, 2H), 7.27 (dd, *J* = 8.9, 2.3 Hz, 1H), 5.63 (s, 2H). ^{13}C NMR (75 MHz, DMSO-d_6) δ 156.45, 150.08, 147.88, 144.01, 143.69, 143.16, 137.17, 129.18, 128.98, 124.36, 123.65, 117.13, 101.39. MS (+ESI): m/z = 238.05 (M + H).

General procedure for the synthesis of compounds (4a-4q). A mixture of the corresponding derivative (3a-3q) (1 mmol) and benzylisothiocyante (1.2 mmol) was stirred at room temperature in 10 ml DMF "Dimethylformamide". Excess solvent was then removed under reduced pressure and the remaining residue purified using column chromatography with ethylacetate as eluent.

1-benzyl-3-(4-((2-bromophenyl)amino)quinazolin-6-yl)thiourea (4a). Yield 53%; m.p. 207-209°C; ^{1}H NMR (500 MHz, DMSO-d_6) δ 9.86 (s, 1H), 9.75 (s, 1H), 8.41 (s, 1H), 8.37 (s, 2H), 7.88 (dd, *J* = 8.9, 2.1 Hz, 1H), 7.79 – 7.72 (m, 2H), 7.58 (dd, *J* = 7.9, 1.3 Hz, 1H), 7.47 (td, *J* = 7.6, 1.4 Hz, 1H), 7.39 – 7.31 (m, 4H), 7.29 – 7.22 (m, 2H), 4.78 (d, *J* = 4.8 Hz, 2H). ^{13}C NMR (126 MHz, DMSO-d_6) δ 181.63, 158.42, 154.06, 147.43, 138.96, 137.46, 136.99, 132.84, 131.73, 129.75, 128.27, 128.24, 128.03, 127.95, 127.40, 126.85, 121.81, 117.47, 114.74, 47.40. MS (+ESI): m/z = 463.76 (M + H).

1-benzyl-3-(4-((4-bromophenyl)amino)quinazolin-6-yl)thiourea (4c). Yield 59%; m.p. 210-212°C; ^{1}H NMR (500 MHz, DMSO-d_6) δ 9.86 (s, 1H), 9.81 (s, 1H), 8.59 (s, 1H), 8.46 (d, *J* = 1.6 Hz, 1H), 8.38 (s, 1H), 7.91 – 7.87 (m, 2H), 7.84 (dd, *J* = 8.9, 2.1 Hz, 1H), 7.77 (d, *J* = 8.8 Hz, 1H), 7.60 – 7.56 (m, 2H), 7.35 (dt, *J* = 15.1, 4.6 Hz, 4H), 7.24 (t, *J* = 7.1 Hz, 1H), 4.79 (d, *J* = 5.0 Hz, 2H). ^{13}C NMR (126 MHz, DMSO-d_6) δ 181.53, 157.12, 153.71, 147.51, 138.99, 138.75, 136.84, 131.74, 131.70, 131.23, 128.20, 127.38, 126.82, 123.74, 117.87, 115.27, 115.11, 47.50. MS (+ESI): m/z = 463.77 (M + H).

1-benzyl-3-(4-((3-chlorophenyl)amino)quinazolin-6-yl)thiourea (4d). Yield 61%; m.p. 200-202°C; ^{1}H NMR (500 MHz, DMSO-d_6) δ 9.87 (d, *J* = 11.7 Hz, 2H), 8.65 (s, 1H),

8.47 (s, 1H), 8.39 (s, 1H), 8.13 (s, 1H), 7.86 (dd, *J* = 8.9, 2.2 Hz, 2H), 7.79 (d, *J* = 8.8 Hz, 1H), 7.42 (t, *J* = 8.1 Hz, 1H), 7.38 – 7.30 (m, 4H), 7.25 (t, *J* = 7.1 Hz, 1H), 7.17 (ddd, *J* = 8.0, 2.1, 0.9 Hz, 1H), 4.79 (d, *J* = 5.0 Hz, 2H). ^{13}C NMR (126 MHz, DMSO-*d*$_6$) δ 181.53, 157.14, 153.59, 147.32, 140.87, 138.97, 136.99, 132.74, 131.81, 130.09, 128.20, 128.07, 127.39, 126.82, 123.00, 121.09, 120.05, 117.80, 115.23, 47.49. MS (+ESI): m/z = 419.69 (M + H).

1-benzyl-3-(4-(m-tolylamino)quinazolin-6-yl)thiourea (4e). Yield 49%; m.p. 191-193°C; ^{1}H NMR (500 MHz, DMSO-*d*$_6$) δ 10.13 (s, 1H), 9.76 (s, 1H), 8.65 (t, *J* = 5.6 Hz, 1H), 8.56 (s, 1H), 8.49 (d, *J* = 1.8 Hz, 1H), 7.87 (dd, *J* = 8.8, 2.0 Hz, 1H), 7.74 (d, *J* = 8.9 Hz, 1H), 7.67 (d, *J* = 7.2 Hz, 2H), 7.39 – 7.31 (m, 4H), 7.26 (ddd, *J* = 14.0, 10.1, 4.3 Hz, 2H), 6.95 (ddd, *J* = 3.3, 1.3, 0.7 Hz, 1H), 4.80 (d, *J* = 5.4 Hz, 2H), 2.34 (s, 3H). ^{13}C NMR (126 MHz, DMSO-*d*$_6$) δ 181.70, 157.44, 153.72, 146.97, 139.11, 139.02, 137.57, 137.03, 131.64, 128.27, 128.20, 127.59, 127.36, 126.79, 124.37, 122.71, 119.44, 117.69, 115.20, 47.31, 21.20. MS (+ESI): m/z = 399.81 (M + H).

1-benzyl-3-(4-((2,3-dimethylphenyl)amino)quinazolin-6-yl)thiourea (4f). Yield 55%; m.p. 161-163°C; ^{1}H NMR (500 MHz, DMSO-*d*$_6$) δ 9.82 (s, 1H), 9.63 (s, 1H), 8.36 (s, 1H), 8.35 (s, 1H), 8.33 (s, 1H), 7.82 (dd, *J* = 8.9, 2.2 Hz, 1H), 7.72 (d, *J* = 8.9 Hz, 1H), 7.38 – 7.31 (m, 4H), 7.27 – 7.23 (m, 1H), 7.17 – 7.10 (m, 3H), 4.78 (d, *J* = 4.8 Hz, 2H), 2.30 (s, 3H), 2.06 (s, 3H). ^{13}C NMR (126 MHz, DMSO-*d*$_6$) δ 181.61, 158.73, 154.42, 147.42, 139.02, 137.14, 137.06, 136.54, 133.61, 131.57, 128.21, 127.92, 127.75, 127.38, 126.82, 125.46, 125.37, 118.11, 114.84, 47.47, 20.12, 14.35. MS (+ESI): m/z = 413.84 (M + H).

1-benzyl-3-(4-((3-ethylphenyl)amino)quinazolin-6-yl)thiourea (4g). Yield 59%; m.p. 196-197°C; ^{1}H NMR (500 MHz, DMSO-*d*$_6$) δ 9.85 (s, 1H), 9.67 (s, 1H), 8.56 (s, 1H), 8.47 (d, *J* = 1.7 Hz, 1H), 8.36 (s, 1H), 7.82 (dd, *J* = 8.9, 2.1 Hz, 1H), 7.75 (d, *J* = 8.8 Hz, 2H), 7.67 (t, *J* = 1.7 Hz, 1H), 7.39 – 7.28 (m, 5H), 7.24 (t, *J* = 7.2 Hz, 1H), 6.98 (dd, *J* = 7.6, 0.6 Hz, 1H), 4.79 (d, *J* = 5.0 Hz, 2H), 2.64 (q, *J* = 7.6 Hz, 2H), 1.23 (t, *J* = 7.6 Hz, 3H). ^{13}C NMR (126 MHz, DMSO-*d*$_6$) δ 181.55, 157.37, 153.97, 147.52, 143.97, 139.23, 139.03, 136.64, 131.58, 128.31, 128.19, 128.12, 127.38, 126.79, 123.09, 121.38, 119.59, 118.11, 115.29, 47.50, 28.26, 15.55. MS (+ESI): m/z = 413.88 (M + H).

1-benzyl-3-(4-((4-isopropylphenyl)amino)quinazolin-6-yl)thiourea (4h). Yield 63%; m.p. 184-186°C; ^{1}H NMR (500 MHz, DMSO-*d*$_6$) δ 9.84 (s, 1H), 9.69 (s, 1H), 8.53 (s, 1H), 8.44 (d, *J* = 1.5 Hz, 1H), 8.35 (s, 1H), 7.81 (dd, *J* = 8.9, 2.1 Hz, 1H), 7.74 (dd, *J* = 8.8, 2.3 Hz, 3H), 7.38 – 7.30 (m, 4H), 7.28 – 7.22 (m, 3H), 4.79 (d, *J* = 5.1 Hz, 2H), 2.93 – 2.86 (m, 1H), 1.23 (s, 3H), 1.22 (s, 3H). ^{13}C NMR (126 MHz, DMSO-*d*$_6$) δ 181.57, 157.41, 154.02, 147.50, 143.78, 139.04, 136.88, 136.59, 131.59, 128.19, 128.09, 127.38,

126.80, 126.16, 122.35, 118.16, 115.24, 47.48, 32.94, 23.97. MS (+ESI): m/z = 427.87 (M^+).

1-benzyl-3-(4-((4-(tert-butyl)phenyl)amino)quinazolin-6-yl)thiourea (4i). Yield 51%; m.p. 173-175°C; ^{1}H NMR (500 MHz, DMSO-d_6) δ 9.84 (s, 1H), 9.70 (s, 1H), 8.53 (s, 1H), 8.44 (d, *J* = 1.6 Hz, 1H), 8.35 (s, 1H), 7.81 (dd, *J* = 8.9, 2.1 Hz, 1H), 7.78 – 7.71 (m, 3H), 7.43 – 7.39 (m, 2H), 7.38 – 7.30 (m, 4H), 7.24 (t, *J* = 7.1 Hz, 1H), 4.78 (d, *J* = 5.3 Hz, 2H), 1.31 (s, 9H). ^{13}C NMR (126 MHz, DMSO-d_6) δ 181.57, 157.41, 154.02, 147.53, 146.00, 139.03, 136.64, 136.57, 131.62, 128.19, 128.08, 127.38, 126.80, 125.06, 122.00, 118.15, 115.25, 47.49, 34.07, 31.22. MS (+ESI): m/z = 441.63 (M + H).

1-(4-([1,1'-biphenyl]-4-ylamino)quinazolin-6-yl)-3-benzylthiourea (4j). Yield 43%; m.p. 208-210°C; ^{1}H NMR (500 MHz, DMSO-d_6) δ 9.88 (s, 1H), 9.84 (s, 1H), 8.61 (s, 1H), 8.50 (s, 1H), 8.39 (s, 1H), 8.01 (d, *J* = 8.7 Hz, 2H), 7.84 (dd, *J* = 8.8, 2.0 Hz, 1H), 7.78 (d, *J* = 8.8 Hz, 1H), 7.71 (t, *J* = 8.6 Hz, 4H), 7.47 (t, *J* = 7.7 Hz, 2H), 7.35 (dt, *J* = 14.4, 7.5 Hz, 5H), 7.25 (t, *J* = 7.2 Hz, 1H), 4.80 (d, *J* = 4.8 Hz, 2H). ^{13}C NMR (126 MHz, DMSO-d_6) δ 181.54, 157.25, 153.90, 147.56, 139.76, 139.03, 138.81, 136.79, 136.74, 135.09, 131.67, 128.90, 128.20, 127.40, 127.03, 126.82, 126.62, 126.29, 122.23, 118.02, 115.36, 47.53. MS (+ESI): m/z = 461.91 (M + H).

1-benzyl-3-(4-((4-phenoxyphenyl)amino)quinazolin-6-yl)thiourea (4k). Yield 48%; m.p. 205-207°C; ^{1}H NMR (500 MHz, DMSO-d_6) δ 9.85 (s, 1H), 9.78 (s, 1H), 8.55 (s, 1H), 8.45 (s, 1H), 8.37 (s, 1H), 7.90 – 7.85 (m, 2H), 7.82 (dd, *J* = 8.9, 2.1 Hz, 1H), 7.75 (d, *J* = 8.8 Hz, 1H), 7.42 – 7.35 (m, 4H), 7.33 (t, *J* = 7.5 Hz, 2H), 7.25 (t, *J* = 7.1 Hz, 1H), 7.13 (tt, *J* = 7.6, 1.1 Hz, 1H), 7.10 – 7.06 (m, 2H), 7.05 – 7.01 (m, 2H), 4.79 (d, *J* = 4.8 Hz, 2H). ^{13}C NMR (126 MHz, DMSO-d_6) δ 181.56, 157.32, 157.28, 153.95, 152.17, 147.47, 139.02, 136.67, 134.99, 131.63, 129.97, 128.20, 128.11, 128.08, 127.39, 126.81, 123.88, 123.04, 119.07, 117.99, 115.21, 47.51. MS (+ESI): m/z = 477.70 (M + H).

1-benzyl-3-(4-((3-hydroxyphenyl)amino)quinazolin-6-yl)thiourea (4l). Yield 66%; m.p. 229-231°C; ^{1}H NMR (500 MHz, DMSO-d_6) δ 9.84 (s, 1H), 9.60 (s, 1H), 9.42 (s, 1H), 8.57 (s, 1H), 8.46 (s, 1H), 8.36 (s, 1H), 7.82 (dd, *J* = 8.9, 2.0 Hz, 1H), 7.75 (d, *J* = 8.8 Hz, 1H), 7.44 (t, *J* = 2.1 Hz, 1H), 7.39 – 7.30 (m, 4H), 7.30 – 7.22 (m, 2H), 7.16 (t, *J* = 8.1 Hz, 1H), 6.54 (ddd, *J* = 8.1, 2.3, 0.8 Hz, 1H), 4.79 (d, *J* = 4.9 Hz, 2H). ^{13}C NMR (126 MHz, DMSO-d_6) δ 181.51, 157.38, 157.30, 153.90, 147.51, 140.27, 139.02, 136.63, 131.55, 129.01, 128.19, 128.09, 127.38, 126.80, 118.08, 115.33, 112.79, 110.70, 109.13, 47.51. MS (+ESI): m/z = 401.73 (M + H).

1-benzyl-3-(4-((4-hydroxyphenyl)amino)quinazolin-6-yl)thiourea (4m). Yield 54%; m.p. 136-137°C; ^{1}H NMR (500 MHz, DMSO-d_6) δ 9.81 (s, 1H), 9.57 (s, 1H), 9.31 (s, 1H), 8.46 (s, 1H), 8.39 (s, 1H), 8.33 (s, 1H), 7.78 (dd, *J* = 8.9, 1.8 Hz, 1H), 7.71 (d, *J* =

8.8 Hz, 1H), 7.55 (d, *J* = 8.8 Hz, 2H), 7.34 (dt, *J* = 15.0, 7.4 Hz, 4H), 7.24 (t, *J* = 7.0 Hz, 1H), 6.79 (d, *J* = 8.8 Hz, 2H), 4.78 (d, *J* = 4.5 Hz, 2H). ^{13}C NMR (126 MHz, DMSO-d_6) δ 181.55, 157.50, 154.20, 153.97, 147.41, 139.04, 136.41, 131.40, 130.45, 128.19, 128.00, 127.37, 126.79, 124.35, 118.17, 115.16, 114.91, 47.47. MS (+ESI): m/z = 401.89 (M + H).

4-((6-(3-benzylthioureido)quinazolin-4-yl)amino)benzenesulfonamide (4n). Yield 40%; m.p. 238-240°C; ^{1}H NMR (500 MHz, DMSO-d_6) δ 10.01 (s, 1H), 9.89 (s, 1H), 8.66 (s, 1H), 8.50 (s, 1H), 8.41 (s, 1H), 8.10 (d, *J* = 8.8 Hz, 2H), 7.92 – 7.74 (m, 4H), 7.44 – 7.31 (m, 4H), 7.29 (s, 2H), 7.25 (t, *J* = 7.1 Hz, 1H), 4.79 (d, *J* = 4.6 Hz, 2H). ^{13}C NMR (126 MHz, DMSO-d_6) δ 181.53, 157.14, 153.58, 147.55, 142.44, 138.97, 138.25, 137.06, 131.90, 131.86, 128.20, 127.39, 126.83, 126.31, 121.14, 117.79, 115.34, 47.49. MS (+ESI): m/z = 464.88 (M + H).

4-((6-(3-benzylthioureido)quinazolin-4-yl)amino)-N-carbamimidoylbenzene sulfonamide (4o). Yield 38%; m.p. 231-233°C; ^{1}H NMR (500 MHz, DMSO-d_6) δ 9.95 (s, 1H), 9.89 (s, 1H), 8.63 (s, 1H), 8.49 (s, 1H), 8.40 (s, 1H), 8.06 – 7.97 (m, 2H), 7.86 (dd, *J* = 8.9, 2.1 Hz, 1H), 7.82 – 7.71 (m, 3H), 7.42 – 7.30 (m, 4H), 7.24 (t, *J* = 7.1 Hz, 1H), 6.70 (s, 4H), 4.79 (d, *J* = 4.5 Hz, 2H). ^{13}C NMR (126 MHz, DMSO-d_6) δ 181.55, 158.08, 157.15, 153.67, 147.62, 141.89, 138.99, 138.83, 137.01, 131.85, 128.33, 128.22, 127.40, 126.84, 126.22, 121.03, 117.85, 115.36, 47.50. MS (+ESI): m/z = 506.84 (M + H).

4-((6-(3-benzylthioureido)quinazolin-4-yl)amino)-N-(pyridin-3-yl)benzene sulfonamide (4p). Yield 46%; m.p. 163-165°C; ^{1}H NMR (500 MHz, DMSO-d_6) δ 11.80 (s, 1H), 9.98 (s, 1H), 9.89 (s, 1H), 8.64 (s, 1H), 8.47 (s, 1H), 8.40 (s, 1H), 8.10 – 8.06 (m, 2H), 8.04 (d, *J* = 4.5 Hz, 1H), 7.92 – 7.88 (m, 2H), 7.86 (dd, *J* = 8.9, 2.1 Hz, 1H), 7.80 (d, *J* = 8.9 Hz, 1H), 7.72 (ddd, *J* = 9.0, 7.2, 1.9 Hz, 1H), 7.33 (dt, *J* = 15.0, 7.3 Hz, 4H), 7.23 (t, *J* = 7.2 Hz, 1H), 7.18 (d, *J* = 8.6 Hz, 1H), 6.92 – 6.85 (m, 1H), 4.78 (d, *J* = 5.0 Hz, 2H). ^{13}C NMR (126 MHz, DMSO-d_6) δ 181.49, 170.30, 157.02, 153.52, 152.93, 147.61, 142.95, 139.99, 138.95, 137.07, 135.39, 131.86, 131.83, 128.24, 128.19, 127.43, 127.39, 126.81, 120.90, 117.70, 115.37, 113.51, 47.50. MS (+ESI): m/z = 541.83 (M + H).

1-benzyl-3-(4-(pyridin-3-ylamino)quinazolin-6-yl)thiourea (4q). Yield 40%; m.p. 146-148°C; ^{1}H NMR (500 MHz, DMSO-d_6) δ 9.90 (d, *J* = 9.5 Hz, 2H), 9.02 (d, *J* = 2.1 Hz, 1H), 8.60 (s, 1H), 8.47 (s, 1H), 8.40 (s, 1H), 8.32 (dt, *J* = 10.5, 5.2 Hz, 2H), 7.86 (dd, *J* = 8.9, 2.1 Hz, 1H), 7.79 (d, *J* = 8.9 Hz, 1H), 7.43 (dd, *J* = 8.1, 4.7 Hz, 1H), 7.39 – 7.30 (m, 4H), 7.25 (t, *J* = 7.2 Hz, 1H), 4.79 (d, *J* = 4.8 Hz, 2H). ^{13}C NMR (126 MHz, DMSO-d_6) δ 181.58, 157.41, 153.70, 147.51, 144.26, 143.48, 138.98, 136.99, 136.03, 131.87, 131.85, 129.02, 128.20, 127.39, 126.83, 123.30, 117.86, 115.20, 47.48. MS (+ESI): m/z = 386.83 (M + H).

***N*-(3-bromophenyl)-6-isothiocyanatoquinazolin-4-amine (5).** Yield 85%; ^{1}H NMR (500 MHz, DMSO-d_6) δ 11.29 (s, 1H), 8.95 (s, 1H), 8.88 (d, *J* = 2.0 Hz, 1H), 8.32 (dd, *J* = 9.0, 2.1 Hz, 1H), 8.06 (t, *J* = 1.9 Hz, 1H), 7.99 (d, *J* = 8.9 Hz, 1H), 7.78 (ddd, *J* = 8.0, 2.0, 1.1 Hz, 1H), 7.51 (ddd, *J* = 8.0, 1.9, 1.1 Hz, 1H), 7.46 (d, *J* = 8.0 Hz, 1H). ^{13}C NMR (126 MHz, DMSO-d_6) δ 181.28, 159.32, 150.55, 139.28, 138.59, 134.52, 130.64, 130.59, 128.96, 126.99, 123.39, 121.17, 120.53, 118.78, 113.97.

1-(4-((3-bromophenyl)amino)quinazolin-6-yl)-3-phenylthiourea (6a). Yield 68%; m.p. 167-169°C; ^{1}H NMR (500 MHz, DMSO-d_6) δ 10.01 (s, 1H), 9.97 (s, 1H), 9.85 (s, 1H), 8.64 (s, 1H), 8.49 (d, *J* = 2.0 Hz, 1H), 8.23 (s, 1H), 7.93 – 7.84 (m, 2H), 7.79 (d, *J* = 8.8 Hz, 1H), 7.50 (dd, *J* = 8.5, 1.0 Hz, 2H), 7.38 – 7.33 (m, 3H), 7.30 (ddd, *J* = 7.9, 1.9, 1.0 Hz, 1H), 7.19 – 7.12 (m, 1H). ^{13}C NMR (126 MHz, DMSO-d_6) δ 180.48, 157.14, 153.68, 147.50, 140.99, 139.24, 137.42, 132.18, 130.39, 128.47, 127.86, 125.92, 124.78, 124.14, 124.02, 121.18, 120.56, 118.26, 115.08. MS (+ESI): m/z = 449.41 (M + H).

1-(4-((3-bromophenyl)amino)quinazolin-6-yl)-3-(2-chlorophenyl)thiourea (6b). Yield 57%; m.p. 172-174°C; ^{1}H NMR (500 MHz, DMSO-d_6) δ 10.20 (s, 1H), 9.86 (s, 1H), 9.63 (s, 1H), 8.65 (s, 1H), 8.48 (d, *J* = 2.0 Hz, 1H), 8.25 (t, *J* = 1.9 Hz, 1H), 7.96 (dd, *J* = 8.9, 2.1 Hz, 1H), 7.91 (dd, *J* = 8.1, 1.0 Hz, 1H), 7.80 (d, *J* = 8.9 Hz, 1H), 7.65 (dd, *J* = 8.0, 1.5 Hz, 1H), 7.53 (dd, *J* = 8.0, 1.4 Hz, 1H), 7.39 – 7.34 (m, 2H), 7.32 – 7.25 (m, 2H). ^{13}C NMR (126 MHz, DMSO-d_6) δ 181.19, 157.16, 153.81, 147.73, 141.02, 137.16, 136.25, 132.35, 130.40, 130.20, 129.91, 129.48, 127.94, 127.75, 127.24, 125.90, 123.95, 121.19, 120.50, 118.41, 115.12. MS (+ESI): m/z = 483.65 (M + H).

1-(4-((3-bromophenyl)amino)quinazolin-6-yl)-3-(4-chlorophenyl)thiourea (6d). Yield 55%; m.p. 173-175°C; ^{1}H NMR (500 MHz, DMSO-d_6) δ 10.11 (s, 1H), 10.02 (s, 1H), 9.86 (s, 1H), 8.65 (s, 1H), 8.50 (d, *J* = 2.0 Hz, 1H), 8.23 (s, 1H), 7.90 (d, *J* = 8.0 Hz, 1H), 7.87 (dd, *J* = 8.9, 2.2 Hz, 1H), 7.79 (d, *J* = 8.9 Hz, 1H), 7.56 – 7.50 (m, 2H), 7.42 – 7.38 (m, 2H), 7.36 (dd, *J* = 9.7, 6.4 Hz, 1H), 7.30 (ddd, *J* = 8.0, 1.9, 1.1 Hz, 1H). ^{13}C NMR (126 MHz, DMSO-d_6) δ 180.55, 157.18, 153.71, 147.43, 140.94, 138.31, 137.24, 132.11, 130.40, 128.66, 128.32, 127.91, 125.99, 125.79, 124.07, 121.18, 120.61, 118.36, 115.10. MS (+ESI): m/z = 483.37 (M + H).

1-(4-((3-bromophenyl)amino)quinazolin-6-yl)-3-(2,4-dichlorophenyl)thiourea (6e). Yield 50%; m.p. 162-164°C; ^{1}H NMR (500 MHz, DMSO-d_6) δ 10.26 (s, 1H), 9.87 (s, 1H), 9.66 (s, 1H), 8.65 (s, 1H), 8.48 (d, *J* = 2.0 Hz, 1H), 8.24 (t, *J* = 1.9 Hz, 1H), 7.97 – 7.89 (m, 2H), 7.81 (d, *J* = 8.9 Hz, 1H), 7.70 (d, *J* = 2.4 Hz, 1H), 7.65 (d, *J* = 8.7 Hz, 1H), 7.46 (dd, *J* = 8.6, 2.4 Hz, 1H), 7.36 (t, *J* = 8.0 Hz, 1H), 7.30 (ddd, *J* = 8.0, 1.9, 1.0 Hz, 1H). ^{13}C NMR (126 MHz, DMSO-d_6) δ 181.21, 162.27, 157.18, 153.86, 147.75, 140.99,

137.03, 135.56, 132.33, 131.46, 131.18, 130.40, 128.96, 128.00, 127.43, 125.93, 123.98, 121.19, 120.52, 118.53, 115.12. MS (+ESI): m/z = 517.72 (M + H).

1-(4-((3-bromophenyl)amino)quinazolin-6-yl)-3-(3,4-dichlorophenyl)thiourea (6f). Yield 47%; m.p. 133-135°C; ^{1}H NMR (500 MHz, DMSO-d_6) δ 10.27 (s, 1H), 10.10 (s, 1H), 9.84 (s, 1H), 8.65 (s, 1H), 8.50 (d, *J* = 1.7 Hz, 1H), 8.23 (s, 1H), 7.92 – 7.88 (m, 2H), 7.86 (dd, *J* = 8.9, 2.1 Hz, 1H), 7.81 (d, *J* = 8.8 Hz, 1H), 7.60 (d, *J* = 8.7 Hz, 1H), 7.49 (dd, *J* = 8.8, 2.5 Hz, 1H), 7.36 (t, *J* = 8.0 Hz, 1H), 7.32 – 7.28 (m, 1H). ^{13}C NMR (126 MHz, DMSO-d_6) δ 180.49, 157.16, 153.87, 147.73, 140.94, 139.59, 136.92, 131.99, 130.43, 130.39, 130.16, 128.20, 126.38, 125.97, 125.39, 124.10, 124.06, 121.18, 120.59, 118.46, 115.15. MS (+ESI): m/z = 517.58 (M + H).

1-(4-((3-bromophenyl)amino)quinazolin-6-yl)-3-(3,5-dichlorophenyl)thiourea (6g). Yield 59%; m.p. 177-179°C; ^{1}H NMR (500 MHz, DMSO-d_6) δ 10.37 (s, 1H), 10.13 (s, 1H), 9.84 (s, 1H), 8.65 (s, 1H), 8.49 (d, *J* = 1.6 Hz, 1H), 8.23 (t, *J* = 1.8 Hz, 1H), 7.90 (d, *J* = 8.9 Hz, 1H), 7.85 (dd, *J* = 8.9, 2.0 Hz, 1H), 7.81 (d, *J* = 8.8 Hz, 1H), 7.64 (d, *J* = 1.8 Hz, 2H), 7.39 – 7.33 (m, 2H), 7.30 (d, *J* = 8.7 Hz, 1H). ^{13}C NMR (126 MHz, DMSO-d_6) δ 180.42, 157.16, 153.92, 147.79, 141.95, 140.93, 136.79, 133.41, 131.95, 130.40, 128.28, 125.99, 124.09, 123.65, 122.04, 121.18, 120.62, 118.48, 115.16. MS (+ESI): m/z = 517.71 (M + H).

1-(4-((3-bromophenyl)amino)quinazolin-6-yl)-3-(4-chloro-3-(trifluoromethyl) phenyl)thiourea (6i). Yield 42%; m.p. 128-130°C; ^{1}H NMR (500 MHz, DMSO-d_6) δ 10.37 (s, 1H), 10.18 (s, 1H), 9.84 (s, 1H), 8.66 (s, 1H), 8.53 (d, *J* = 1.8 Hz, 1H), 8.23 (t, *J* = 2.0 Hz, 1H), 8.10 (d, *J* = 2.5 Hz, 1H), 7.91 (ddd, *J* = 8.1, 2.0, 1.0 Hz, 1H), 7.87 – 7.80 (m, 3H), 7.69 (d, *J* = 8.7 Hz, 1H), 7.36 (t, *J* = 8.0 Hz, 1H), 7.30 (ddd, *J* = 8.0, 1.9, 1.0 Hz, 1H). ^{13}C NMR (126 MHz, DMSO-d_6) δ 180.55, 157.18, 153.95, 147.83, 140.95, 139.10, 136.73, 131.89, 131.52, 130.41, 129.05, 128.39, 126.19 (q, $^{2}J_{C\text{-}F}$ = 30.8 Hz), 126.00, 125.54, 124.08, 123.01, 122.70 (q, $^{1}J_{C\text{-}F}$ = 273.0 Hz), 121.20, 120.60, 118.51, 115.22. MS (+ESI): m/z = 551.59 (M + H).

1-(4-((3-bromophenyl)amino)quinazolin-6-yl)-3-(2-fluoro-3-(trifluoromethyl) phenyl)thiourea (6j). Yield 49%; m.p. 179-180°C; ^{1}H NMR (500 MHz, DMSO-d_6) δ 10.41 (s, 1H), 9.89 (s, 1H), 9.78 (s, 1H), 8.66 (s, 1H), 8.52 (d, *J* = 2.0 Hz, 1H), 8.24 (t, *J* = 1.8 Hz, 1H), 7.93 – 7.88 (m, 3H), 7.82 (d, *J* = 8.8 Hz, 1H), 7.65 (t, *J* = 6.6 Hz, 1H), 7.42 (t, *J* = 8.0 Hz, 1H), 7.36 (t, *J* = 8.0 Hz, 1H), 7.31 (ddd, *J* = 8.0, 1.9, 1.1 Hz, 1H). ^{13}C NMR (126 MHz, DMSO-d_6) δ MS (+ESI): m/z = 535.61 (M + H).

1-(4-((3-bromophenyl)amino)quinazolin-6-yl)-3-(4-(trifluoromethyl)phenyl)thiourea (6k). Yield 59%; m.p. 180-181°C; ^{1}H NMR (500 MHz, DMSO-d_6) δ 10.29 (s, 1H), 10.27 (s, 1H), 9.85 (s, 1H), 8.65 (s, 1H), 8.53 (d, *J* = 2.0 Hz, 1H), 8.23 (t, *J* = 1.9 Hz, 1H), 7.92

– 7.86 (m, 2H), 7.80 (dd, *J* = 12.4, 8.7 Hz, 3H), 7.71 (d, *J* = 8.7 Hz, 2H), 7.36 (t, *J* = 8.0 Hz, 1H), 7.30 (ddd, *J* = 8.0, 1.8, 1.0 Hz, 1H). ^{13}C NMR (126 MHz, DMSO-d_6) δ 180.58, 157.22, 153.80, 147.53, 143.24, 140.94, 137.14, 132.07, 130.42, 128.00, 126.03, 125.59, 124.34 (q, $^{1}J_{C-F}$ = 271.7 Hz), 124.13, 123.40, 123.03, 121.20, 120.66, 118.47, 115.14. MS (+ESI): m/z = 517.77 (M + H).

1-(4-((3-bromophenyl)amino)quinazolin-6-yl)-3-(3-(trifluoromethyl)phenyl)thiourea (6l). Yield 44%; m.p. 82-84°C; ^{1}H NMR (500 MHz, DMSO-d_6) δ 10.29 (s, 1H), 10.14 (s, 1H), 9.86 (s, 1H), 8.65 (s, 1H), 8.53 (d, *J* = 1.8 Hz, 1H), 8.23 (s, 1H), 7.97 (s, 1H), 7.91 (d, *J* = 8.1 Hz, 1H), 7.86 (dd, *J* = 8.9, 2.1 Hz, 1H), 7.83 – 7.78 (m, 2H), 7.58 (t, *J* = 7.9 Hz, 1H), 7.50 – 7.47 (m, 1H), 7.36 (t, *J* = 8.0 Hz, 1H), 7.30 (ddd, *J* = 8.0, 1.9, 1.0 Hz, 1H). ^{13}C NMR (126 MHz, DMSO-d_6) δ 180.65, 157.22, 153.82, 147.56, 140.94, 140.34, 136.97, 131.98, 130.42, 129.49, 128.98 (q, $^{2}J_{C-F}$ = 31.7 Hz), 128.15, 127.88, 126.04, 124.13, 124.06 (q, $^{1}J_{C-F}$ = 272.3 Hz), 121.21, 120.98, 120.65, 120.40, 118.44, 115.19. MS (+ESI): m/z = 517.68 (M + H).

1-(3,5-bis(trifluoromethyl)phenyl)-3-(4-((3-bromophenyl)amino)quinazolin-6-yl)thiourea (6m). Yield 49%; m.p. 142-144°C; ^{1}H NMR (500 MHz, DMSO-d_6) δ 10.57 (s, 1H), 10.32 (s, 1H), 9.84 (s, 1H), 8.66 (s, 1H), 8.55 (s, 1H), 8.29 (s, 2H), 8.23 (t, *J* = 2.0 Hz, 1H), 7.90 (ddd, *J* = 8.1, 2.0, 1.1 Hz, 1H), 7.84 (d, *J* = 1.9 Hz, 2H), 7.82 (s, 1H), 7.36 (t, *J* = 8.0 Hz, 1H), 7.30 (ddd, *J* = 8.0, 1.9, 1.1 Hz, 1H). ^{13}C NMR (126 MHz, DMSO-d_6) δ 180.51, 157.18, 154.02, 147.91, 141.70, 140.88, 136.39, 131.75, 130.39, 129.95 (q, $^{2}J_{C-F}$ = 33.0 Hz), 128.58, 126.03, 124.08, 124.05, 123.20 (q, $^{1}J_{C-F}$ = 272.7 Hz), 121.18, 120.61, 118.60, 117.27, 115.25. MS (+ESI): m/z = 585.56 (M + H).

1-(4-bromophenyl)-3-(4-((3-bromophenyl)amino)quinazolin-6-yl)thiourea (6n). Yield 62%; m.p. 173-175°C; ^{1}H NMR (500 MHz, DMSO-d_6) δ 10.12 (s, 1H), 10.01 (s, 1H), 9.84 (s, 1H), 8.64 (s, 1H), 8.50 (d, *J* = 1.9 Hz, 1H), 8.24 (t, *J* = 1.8 Hz, 1H), 7.93 – 7.83 (m, 2H), 7.80 (d, *J* = 8.9 Hz, 1H), 7.56 – 7.51 (m, 2H), 7.51 – 7.47 (m, 2H), 7.36 (t, *J* = 8.0 Hz, 1H), 7.30 (d, *J* = 8.7 Hz, 1H). ^{13}C NMR (126 MHz, DMSO-d_6) δ 180.48, 157.14, 153.78, 147.64, 140.98, 138.75, 137.19, 132.07, 131.24, 130.39, 128.05, 126.08, 125.93, 124.02, 121.18, 120.56, 118.36, 116.82, 115.13.MS (+ESI): m/z = 527.56 (M + H).

1-(4-((3-bromophenyl)amino)quinazolin-6-yl)-3-(4-hydroxyphenyl)thiourea (6o). Yield 58%; m.p. 208-210°C; ^{1}H NMR (500 MHz, DMSO-d_6) δ 9.81 (s, 1H), 9.72 (d, *J* = 15.7 Hz, 2H), 9.41 (s, 1H), 8.63 (s, 1H), 8.44 (s, 1H), 8.24 (t, *J* = 1.8 Hz, 1H), 7.95 – 7.84 (m, 2H), 7.76 (d, *J* = 8.9 Hz, 1H), 7.35 (t, *J* = 8.0 Hz, 1H), 7.29 (d, *J* = 8.0 Hz, 1H), 7.20 (d, *J* = 8.7 Hz, 2H), 6.75 (d, *J* = 8.7 Hz, 2H). ^{13}C NMR (126 MHz, DMSO-d_6) δ 180.61, 157.10, 155.16, 153.62, 147.50, 141.05, 137.63, 132.32, 130.38, 127.72, 126.67, 125.85,

123.95, 121.18, 120.50, 118.23, 117.55, 115.10, 115.03. MS (+ESI): m/z = 465.54 (M + H).

4-(3-(4-((3-bromophenyl)amino)quinazolin-6-yl)thioureido)benzenesulfonamide (6p). Yield 32%; m.p. 181-183°C; ^{1}H NMR (500 MHz, DMSO-d_6) δ 10.26 (d, J = 18.6 Hz, 2H), 9.93 (s, 1H), 8.67 (s, 1H), 8.54 (s, 1H), 8.22 (s, 1H), 7.89 (d, J = 7.9 Hz, 2H), 7.80 (dd, J = 13.6, 9.0 Hz, 3H), 7.73 (d, J = 8.6 Hz, 2H), 7.36 (t, J = 8.0 Hz, 1H), 7.31 (s, 3H). ^{13}C NMR (126 MHz, DMSO-d_6) δ 180.53, 162.27, 157.28, 153.67, 142.48, 140.83, 139.44, 137.24, 132.17, 130.42, 127.71, 126.13, 124.20, 123.18, 121.19, 120.73, 118.46, 117.19, 115.07. MS (+ESI): m/z = 528.30 (M + H).

4-(3-(4-((3-bromophenyl)amino)quinazolin-6-yl)thioureido)-*N*-(thiazol-2-yl)benzene sulfonamide (6q). Yield 28%; m.p. 158-160°C; ^{1}H NMR (500 MHz, DMSO-d_6) δ 12.69 (s, 1H), 10.24 (d, J = 11.5 Hz, 2H), 9.86 (s, 1H), 8.65 (s, 1H), 8.51 (d, J = 1.9 Hz, 1H), 8.22 (s, 1H), 7.91 – 7.85 (m, 2H), 7.80 (d, J = 8.9 Hz, 1H), 7.78 – 7.75 (m, 2H), 7.71 – 7.67 (m, 2H), 7.36 (t, J = 8.0 Hz, 1H), 7.30 (ddd, J = 8.0, 1.8, 1.0 Hz, 1H), 7.25 (d, J = 4.6 Hz, 1H), 6.83 (d, J = 4.6 Hz, 1H). ^{13}C NMR (126 MHz, DMSO-d_6) δ 180.43, 168.75, 167.50, 162.27, 157.17, 153.79, 147.57, 142.70, 140.94, 137.55, 137.16, 132.08, 130.40, 126.36, 125.98, 124.43, 124.08, 123.00, 121.18, 120.62, 118.42, 108.15. MS (+ESI): m/z = 611.22 (M + H).

1-(4-((4-(tert-butyl)phenyl)amino)quinazolin-6-yl)-3-(4-chloro-3-(trifluoromethyl) phenyl)thiourea (6r). Yield 43%; m.p. 114-116°C; ^{1}H NMR (500 MHz, DMSO-d_6) δ 10.34 (s, 1H), 10.15 (s, 1H), 9.73 (s, 1H), 8.54 (s, 1H), 8.50 (d, J = 2.0 Hz, 1H), 8.11 (d, J = 2.6 Hz, 1H), 7.85 – 7.79 (m, 2H), 7.77 (d, J = 8.8 Hz, 1H), 7.74 – 7.71 (m, 2H), 7.68 (d, J = 8.7 Hz, 1H), 7.42 – 7.39 (m, 2H), 1.30 (s, 9H). ^{13}C NMR (126 MHz, DMSO-d_6) δ 180.55, 157.50, 154.27, 147.76, 146.18, 139.14, 136.45, 136.41, 131.64, 131.50, 129.03, 128.21, 126.16 (q, $^{2}J_{C\text{-}F}$ = 30.9 Hz), 125.50, 125.10, 122.98, 122.71 (q, $^{1}J_{C\text{-}F}$ = 272.8 Hz), 122.19, 118.72, 115.22, 34.10, 31.22. MS (+ESI): m/z = 529.69 (M + H).

1-(4-chloro-3-(trifluoromethyl)phenyl)-3-(4-((4-phenoxyphenyl)amino)quinazolin-6-yl)thiourea (6s). Yield 40%; m.p. 129-131°C; ^{1}H NMR (500 MHz, MeOD) δ 8.45 (s, 1H), 8.45 (s, 1H), 8.38 – 8.34 (m, 1H), 8.04 (d, J = 2.6 Hz, 1H), 7.88 (dd, J = 8.9, 2.3 Hz, 1H), 7.78 – 7.72 (m, 2H), 7.67 – 7.63 (m, 2H), 7.54 (d, J = 8.7 Hz, 1H), 7.37 – 7.32 (m, 3H), 7.12 – 7.08 (m, 1H), 7.05 – 6.99 (m, 5H). ^{13}C NMR (126 MHz, MeOD) δ 182.75, 159.87, 158.95, 155.80, 155.37, 148.31, 140.06, 138.53, 135.10, 132.80, 132.74, 130.88, 129.87, 129.06 (q, $^{2}J_{C\text{-}F}$ = 31.6 Hz), 128.62, 126.40, 126.28, 124.47, 124.33, 124.17 (q, $^{1}J_{C\text{-}F}$ = 272.4 Hz), 120.24, 119.64, 119.03, 116.73. MS (+ESI): m/z = 565.98 (M + H).

1-(4-([1,1'-biphenyl]-4-ylamino)quinazolin-6-yl)-3-(4-chloro-3-(trifluoromethyl) phenyl)thiourea (6t). Yield 38%; m.p. 168-170°C; ^{1}H NMR (500 MHz, DMSO-d_6) δ

10.37 (s, 1H), 10.18 (s, 1H), 9.87 (s, 1H), 8.63 (s, 1H), 8.56 (d, *J* = 1.7 Hz, 1H), 8.11 (d, *J* = 2.5 Hz, 1H), 7.99 (d, *J* = 8.7 Hz, 2H), 7.85 (dd, *J* = 8.8, 2.2 Hz, 2H), 7.81 (d, *J* = 8.8 Hz, 1H), 7.73 – 7.72 (m, 1H), 7.72 – 7.67 (m, 4H), 7.51 – 7.43 (m, 2H), 7.38 – 7.30 (m, 1H). ^{13}C NMR (126 MHz, DMSO-d_6) δ 180.56, 157.35, 154.15, 147.77, 139.76, 139.13, 138.67, 136.57, 135.28, 131.77, 131.52, 129.06, 128.91, 128.26, 127.07, 126.66, 126.32, 126.06, 125.53, 122.71 (q, $^{1}J_{C-F}$ = 272.9 Hz), 123.00, 122.44, 118.68, 115.32. MS (+ESI): m/z = 549.73 (M + H).

1-(4-([1,1'-biphenyl]-4-ylamino)quinazolin-6-yl)-3-(3,5-bis(trifluoromethyl) phenyl)thiourea (6u). Yield 48%; m.p. 143-145°C; ^{1}H NMR (500 MHz, DMSO-d_6) δ 10.57 (s, 1H), 10.33 (s, 1H), 9.88 (s, 1H), 8.64 (s, 1H), 8.59 (s, 1H), 8.30 (s, 2H), 7.98 (d, *J* = 8.6 Hz, 2H), 7.89 – 7.80 (m, 3H), 7.75 – 7.66 (m, 4H), 7.47 (t, *J* = 7.7 Hz, 2H), 7.35 (t, *J* = 7.4 Hz, 1H). ^{13}C NMR (126 MHz, DMSO-d_6) δ 180.54, 157.36, 154.23, 147.85, 141.74, 139.72, 138.60, 136.24, 135.31, 131.66, 129.95 (q, $^{2}J_{C-F}$ = 32.9 Hz), 128.89, 128.44, 127.06, 126.63, 126.30, 124.05, 123.21 (q, $^{1}J_{C-F}$ = 272.7 Hz), 122.46, 118.79, 117.25, 115.35. MS (+ESI): m/z = 583.79 (M + H).

1-(4-((3-bromophenyl)amino)quinazolin-6-yl)-3-methylthiourea (7a). Yield 39%; m.p. 207-209°C; ^{1}H NMR (500 MHz, DMSO-d_6) δ 9.80 (s, 2H), 8.63 (s, 1H), 8.43 (s, 1H), 8.24 (s, 1H), 7.92 (d, *J* = 8.2 Hz, 1H), 7.89 (s, 1H), 7.77 (s, 2H), 7.36 (t, *J* = 8.0 Hz, 1H), 7.30 (d, *J* = 8.0 Hz, 1H), 2.96 (d, *J* = 4.1 Hz, 3H). ^{13}C NMR (126 MHz, DMSO-d_6) δ 181.48, 157.06, 153.60, 147.41, 141.02, 136.81, 131.31, 130.38, 128.43, 125.87, 123.94, 121.18, 120.50, 117.53, 115.30, 31.58. MS (+ESI): m/z = 387.43 (M + H).

1-(4-((3-bromophenyl)amino)quinazolin-6-yl)-3-(pyridin-3-yl)thiourea (7b). Yield %; m.p. 152-153°C; ^{1}H NMR (500 MHz, DMSO-d_6) δ 10.28 (s, 1H), 10.03 (s, 1H), 9.87 (s, 1H), 8.68 – 8.61 (m, 2H), 8.53 (d, *J* = 2.0 Hz, 1H), 8.35 (dd, *J* = 4.7, 1.5 Hz, 1H), 8.23 (s, 1H), 7.95 (ddd, *J* = 8.3, 2.5, 1.5 Hz, 1H), 7.92 – 7.84 (m, 2H), 7.81 (d, *J* = 8.9 Hz, 1H), 7.41 – 7.37 (m, 1H), 7.35 (d, *J* = 8.0 Hz, 1H), 7.30 (ddd, *J* = 8.0, 1.9, 1.1 Hz, 1H). ^{13}C NMR (126 MHz, DMSO) δ 181.10, 157.19, 153.80, 147.58, 145.84, 145.56, 140.93, 137.00, 136.20, 132.07, 131.92, 130.41, 128.08, 126.00, 124.07, 123.15, 121.18, 120.62, 118.48, 115.15. MS (+ESI): m/z = 450.59 (M + H).

1-(4-((3-bromophenyl)amino)quinazolin-6-yl)-3-(4-chlorobenzyl)thiourea (7c). Yield 47%; m.p. 140-142°C; ^{1}H NMR (500 MHz, DMSO-d_6) δ 9.93 (s, 1H), 9.82 (s, 1H), 8.64 (s, 1H), 8.46 (s, 1H), 8.41 (s, 1H), 8.25 (t, *J* = 1.9 Hz, 1H), 7.96 – 7.88 (m, 1H), 7.83 (dd, *J* = 8.9, 2.1 Hz, 1H), 7.79 (d, *J* = 8.8 Hz, 1H), 7.39 (d, *J* = 5.4 Hz, 4H), 7.35 (d, *J* = 8.1 Hz, 1H), 7.30 (ddd, *J* = 8.0, 1.8, 1.0 Hz, 1H), 4.77 (d, *J* = 5.6 Hz, 2H). ^{13}C NMR (126 MHz, DMSO) δ 181.57, 157.12, 153.71, 147.57, 141.05, 138.17, 136.82, 131.76, 131.33, 130.41, 129.25, 128.25, 128.10, 125.88, 123.88, 121.22, 120.42, 117.92, 115.29, 46.78. MS (+ESI): m/z = 497.80 (M + H).

1-(4-((3-bromophenyl)amino)quinazolin-6-yl)-3-(2-morpholinoethyl)thiourea (7d). Yield 52%; 149-151; ^{1}H NMR (500 MHz, $(CD_3)_2CO$) δ 9.15 (s, 2H), 8.68 (s, 1H), 8.41 – 8.32 (m, 2H), 7.95 (ddd, *J* = 8.0, 1.8, 1.0 Hz, 1H), 7.89 – 7.83 (m, 2H), 7.44 (s, 1H), 7.34 (t, *J* = 8.0 Hz, 1H), 7.29 (ddd, *J* = 7.9, 1.6, 1.1 Hz, 1H), 3.71 (s, 2H), 3.47 (s, 4H), 2.58 (s, 2H), 2.41 (s, 4H). ^{13}C NMR (126 MHz, DMSO-*d*$_6$) δ 180.71, 157.04, 153.64, 147.40, 141.01, 136.92, 131.49, 130.39, 128.33, 125.87, 123.90, 121.18, 120.44, 117.13, 115.21, 66.14, 56.34, 53.06, 40.94. MS (+ESI): m/z = 487.16 (M + H).

***N*-(4-((3-bromophenyl)amino)quinazolin-6-yl)morpholine-4-carbothioamide (7e).** Yield 54%; m.p. 240-242°C; ^{1}H NMR (500 MHz, DMSO-*d*$_6$) δ 9.82 (s, 1H), 9.73 (s, 1H), 8.64 (s, 1H), 8.35 (d, *J* = 1.9 Hz, 1H), 8.26 (t, *J* = 2.0 Hz, 1H), 7.93 (ddd, *J* = 8.2, 2.0, 1.0 Hz, 1H), 7.79 (dd, *J* = 8.9, 2.1 Hz, 1H), 7.75 (d, *J* = 8.8 Hz, 1H), 7.35 (t, *J* = 8.0 Hz, 1H), 7.29 (ddd, *J* = 8.0, 1.9, 1.0 Hz, 1H), 3.98 – 3.92 (m, 4H), 3.72 – 3.66 (m, 4H). ^{13}C NMR (126 MHz, DMSO-*d*$_6$) δ 182.06, 157.10, 153.64, 147.56, 141.08, 139.19, 133.41, 130.37, 127.45, 125.83, 123.93, 121.18, 120.44, 118.71, 114.89, 65.80, 48.41. MS (+ESI): m/z = 443.47 (M + H).

1-benzyl-3-(4-((3-bromophenyl)amino)quinazolin-6-yl)urea (8a). Yield 68%; m.p. 235-237°C; ^{1}H NMR (500 MHz, DMSO-*d*$_6$) δ 9.79 (s, 1H), 8.88 (s, 1H), 8.53 (s, 1H), 8.42 (d, *J* = 2.2 Hz, 1H), 8.18 (t, *J* = 2.0 Hz, 1H), 7.91 – 7.82 (m, 2H), 7.73 (d, *J* = 9.0 Hz, 1H), 7.35 (d, *J* = 1.9 Hz, 2H), 7.34 (s, 2H), 7.32 (d, *J* = 8.0 Hz, 1H), 7.28 – 7.23 (m, 2H), 6.89 (t, *J* = 6.0 Hz, 1H), 4.37 (d, *J* = 5.9 Hz, 2H). ^{13}C NMR (126 MHz, DMSO-*d*$_6$) δ 156.91, 155.15, 152.14, 145.53, 141.32, 140.20, 138.53, 130.25, 128.33, 128.31, 127.11, 126.75, 126.35, 125.61, 124.07, 121.10, 120.66, 115.69, 109.13, 42.81. MS (+ESI): m/z = 447.42 (M + H).

1-(4-((3-bromophenyl)amino)quinazolin-6-yl)-3-(4-chlorophenyl)urea (8b). Yield 65%; m.p. 255-257°C; ^{1}H NMR (500 MHz, DMSO-*d*$_6$) δ 9.84 (s, 1H), 9.02 (d, *J* = 12.9 Hz, 2H), 8.57 (s, 1H), 8.51 (d, *J* = 2.0 Hz, 1H), 8.20 (t, *J* = 1.8 Hz, 1H), 7.88 (dd, *J* = 9.1, 1.9 Hz, 2H), 7.78 (d, *J* = 8.9 Hz, 1H), 7.55 (d, *J* = 8.9 Hz, 2H), 7.34 (t, *J* = 8.5 Hz, 3H), 7.28 (d, *J* = 8.6 Hz, 1H). ^{13}C NMR (126 MHz, DMSO-*d*$_6$) δ 156.98, 152.53, 152.50, 145.95, 141.22, 138.53, 137.51, 130.27, 128.65, 128.51, 126.65, 125.73, 125.58, 124.16, 121.11, 120.74, 119.87, 115.60, 110.30. MS (+ESI): m/z = 467.51 (M + H).

References of the supporting information

1. Tsou, H. R.; Mamuya, N.; Johnson, B. D.; Reich, M. F.; Gruber, B. C.; Ye, F.; Nilakantan, R.; Shen, R.; Discafani, C.; DeBlanc, R.; Davis, R.; Koehn, F. E.; Greenberger, L. M.; Wang, Y. F.; Wissner, A., 6-Substituted-4-(3-bromophenylamino)quinazolines as putative irreversible inhibitors of the epidermal

growth factor receptor (EGFR) and human epidermal growth factor receptor (HER-2) tyrosine kinases with enhanced antitumor activity. *J Med Chem* **2001**, 44, (17), 2719-34.

2. Madapa, S.; Tusi, Z.; Mishra, A.; Srivastava, K.; Pandey, S. K.; Tripathi, R.; Puri, S. K.; Batra, S., Search for new pharmacophores for antimalarial activity. Part II: synthesis and antimalarial activity of new 6-ureido-4-anilinoquinazolines. *Bioorg Med Chem* **2009**, 17, (1), 222-34.

References of the manuscript

1. Sequist, L. V.; Lynch, T. J., EGFR tyrosine kinase inhibitors in lung cancer: an evolving story. *Annu Rev Med* **2008**, 59, 429-42.

2. da Cunha Santos, G.; Shepherd, F. A.; Tsao, M. S., EGFR mutations and lung cancer. *Annu Rev Pathol* **2011**, 6, 49-69.

3. Godin-Heymann, N.; Ulkus, L.; Brannigan, B. W.; McDermott, U.; Lamb, J.; Maheswaran, S.; Settleman, J.; Haber, D. A., The T790M "gatekeeper" mutation in EGFR mediates resistance to low concentrations of an irreversible EGFR inhibitor. Mol *Cancer Ther* **2008**, 7, (4), 874-9.

4. Jiang, S. X.; Yamashita, K.; Yamamoto, M.; Piao, C. J.; Umezawa, A.; Saegusa, M.; Yoshida, T.; Katagiri, M.; Masuda, N.; Hayakawa, K.; Okayasu, I., EGFR genetic heterogeneity of nonsmall cell lung cancers contributing to acquired gefitinib resistance. *Int J Cancer* **2008**, 123, (11), 2480-6.

5. Engelman, J. A.; Zejnullahu, K.; Mitsudomi, T.; Song, Y.; Hyland, C.; Park, J. O.; Lindeman, N.; Gale, C. M.; Zhao, X.; Christensen, J.; Kosaka, T.; Holmes, A. J.; Rogers, A. M.; Cappuzzo, F.; Mok, T.; Lee, C.; Johnson, B. E.; Cantley, L. C.; Janne, P. A., MET amplification leads to gefitinib resistance in lung cancer by activating ERBB3 signaling. *Science* **2007**, 316, (5827), 1039-43.

6. Ding, L.; Ley, T. J.; Larson, D. E.; Miller, C. A.; Koboldt, D. C.; Welch, J. S.; Ritchey, J. K.; Young, M. A.; Lamprecht, T.; McLellan, M. D.; McMichael, J. F.; Wallis, J. W.; Lu, C.; Shen, D.; Harris, C. C.; Dooling, D. J.; Fulton, R. S.; Fulton, L. L.; Chen, K.; Schmidt, H.; Kalicki-Veizer, J.; Magrini, V. J.; Cook, L.; McGrath, S. D.; Vickery, T. L.; Wendl, M. C.; Heath, S.; Watson, M. A.; Link, D. C.; Tomasson, M. H.; Shannon, W. D.; Payton, J. E.; Kulkarni, S.; Westervelt, P.; Walter, M. J.; Graubert, T. A.; Mardis, E. R.; Wilson, R. K.; DiPersio, J. F., Clonal evolution in relapsed acute myeloid leukaemia revealed by whole-genome sequencing. *Nature* **2012**, 481, (7382), 506-10.

7. Mullighan, C. G.; Phillips, L. A.; Su, X.; Ma, J.; Miller, C. B.; Shurtleff, S. A.; Downing, J. R., Genomic analysis of the clonal origins of relapsed acute lymphoblastic leukemia. *Science* **2008**, 322, (5906), 1377-80.

8. Roche-Lestienne, C.; Lai, J. L.; Darre, S.; Facon, T.; Preudhomme, C., A mutation conferring resistance to imatinib at the time of diagnosis of chronic myelogenous leukemia. *N Engl J Med* **2003**, 348, (22), 2265-6.

9. Marusyk, A.; Almendro, V.; Polyak, K., Intra-tumour heterogeneity: a looking glass for cancer? *Nat Rev Cancer* **2012**, 12, (5), 323-34.

10. Chiu, C. W.; Nozawa, H.; Hanahan, D., Survival benefit with proapoptotic molecular and pathologic responses from dual targeting of mammalian target of rapamycin and epidermal growth factor receptor in a preclinical model of pancreatic neuroendocrine carcinogenesis. *J Clin Oncol* **2010**, 28, (29), 4425-33.

11. Faivre, S.; Djelloul, S.; Raymond, E., New paradigms in anticancer therapy: targeting multiple signaling pathways with kinase inhibitors. *Semin Oncol* **2006**, 33, (4), 407-20.

12. Jin, N.; Jiang, T.; Rosen, D. M.; Nelkin, B. D.; Ball, D. W., Dual inhibition of mitogen-activated protein kinase kinase and mammalian target of rapamycin in differentiated and anaplastic thyroid cancer. *J Clin Endocrinol Metab* **2009**, 94, (10), 4107-12.

13. Xu, H.; Stabile, L. P.; Gubish, C. T.; Gooding, W. E.; Grandis, J. R.; Siegfried, J. M., Dual blockade of EGFR and c-Met abrogates redundant signaling and proliferation in head and neck carcinoma cells. *Clin Cancer Res* **2011**, 17, (13), 4425-38.

14. Rayet, B.; Gelinas, C., Aberrant rel/nfkb genes and activity in human cancer. *Oncogene* **1999**, 18, (49), 6938-47.

15. Lin, A.; Karin, M., NF-kappaB in cancer: a marked target. *Semin Cancer Biol* **2003**, 13, (2), 107-14.

16. Luo, J. L.; Kamata, H.; Karin, M., IKK/NF-kappaB signaling: balancing life and death--a new approach to cancer therapy. *J Clin Invest* **2005**, 115, (10), 2625-32.

17. Bivona, T. G.; Hieronymus, H.; Parker, J.; Chang, K.; Taron, M.; Rosell, R.; Moonsamy, P.; Dahlman, K.; Miller, V. A.; Costa, C.; Hannon, G.; Sawyers, C. L., FAS and NF-kappaB signalling modulate dependence of lung cancers on mutant EGFR. *Nature* **2011**, 471, (7339), 523-6.

18. Shimizu, T.; Tolcher, A. W.; Papadopoulos, K. P.; Beeram, M.; Rasco, D. W.; Smith, L. S.; Gunn, S.; Smetzer, L.; Mays, T. A.; Kaiser, B.; Wick, M. J.; Alvarez, C.; Cavazos, A.; Mangold, G. L.; Patnaik, A., The clinical effect of the dual-targeting strategy involving PI3K/AKT/mTOR and RAS/MEK/ERK pathways in patients with advanced cancer. *Clin Cancer Res* **2012**, 18, (8), 2316-25.

19. Rewcastle, G. W.; Denny, W. A.; Bridges, A. J.; Zhou, H.; Cody, D. R.; McMichael, A.; Fry, D. W., Tyrosine kinase inhibitors. 5. Synthesis and structure-activity relationships for 4-[(phenylmethyl)amino]- and 4-(phenylamino)quinazolines as potent adenosine 5'-triphosphate binding site inhibitors of the tyrosine kinase domain of the epidermal growth factor receptor. *J Med Chem* **1995**, 38, (18), 3482-7.

20. Smaill, J. B.; Rewcastle, G. W.; Loo, J. A.; Greis, K. D.; Chan, O. H.; Reyner, E. L.; Lipka, E.; Showalter, H. D.; Vincent, P. W.; Elliott, W. L.; Denny, W. A., Tyrosine kinase inhibitors. 17. Irreversible inhibitors of the epidermal growth factor receptor: 4-

(phenylamino)quinazoline- and 4-(phenylamino)pyrido[3,2-d]pyrimidine-6-acrylamides bearing additional solubilizing functions. *J Med Chem* **2000**, 43, (7), 1380-97.

21. Ahn, K.; Sisneros, A. M.; Herman, S. B.; Pan, S. M.; Hupe, D.; Lee, C.; Nikam, S.; Cheng, X. M.; Doherty, A. M.; Schroeder, R. L.; Haleen, S. J.; Kaw, S.; Emoto, N.; Yanagisawa, M., Novel selective quinazoline inhibitors of endothelin converting enzyme-1. *Biochem Biophys Res Commun* **1998**, 243, (1), 184-90.

22. Jones, T. R.; Thornton, T. J.; Flinn, A.; Jackman, A. L.; Newell, D. R.; Calvert, A. H., Quinazoline antifolates inhibiting thymidylate synthase: 2-desamino derivatives with enhanced solubility and potency. *J Med Chem* **1989**, 32, (4), 847-52.

23. Cavalli, A.; Lizzi, F.; Bongarzone, S.; Brun, R.; Luise Krauth-Siegel, R.; Bolognesi, M. L., Privileged structure-guided synthesis of quinazoline derivatives as inhibitors of trypanothione reductase. *Bioorg Med Chem Lett* **2009**, 19, (11), 3031-5.

24. Takase, Y.; Saeki, T.; Watanabe, N.; Adachi, H.; Souda, S.; Saito, I., Cyclic GMP phosphodiesterase inhibitors. 2. Requirement of 6-substitution of quinazoline derivatives for potent and selective inhibitory activity. *J Med Chem* **1994**, 37, (13), 2106-11.

25. Sanchez, A. I.; Martinez-Barrasa, V.; Burgos, C.; Vaquero, J. J.; Alvarez-Builla, J.; Terricabras, E.; Segarra, V., Synthesis and evaluation of quinazoline derivatives as phosphodiesterase 7 inhibitors. *Bioorg Med Chem* **2013**, 21, (8), 2370-8.

26. Zhu, L.; Jin, J.; Liu, C.; Zhang, C.; Sun, Y.; Guo, Y.; Fu, D.; Chen, X.; Xu, B., Synthesis and biological evaluation of novel quinazoline-derived human Pin1 inhibitors. *Bioorg Med Chem* **2011**, 19, (9), 2797-807.

27. Brasca, M. G.; Amboldi, N.; Ballinari, D.; Cameron, A.; Casale, E.; Cervi, G.; Colombo, M.; Colotta, F.; Croci, V.; D'Alessio, R.; Fiorentini, F.; Isacchi, A.; Mercurio, C.; Moretti, W.; Panzeri, A.; Pastori, W.; Pevarello, P.; Quartieri, F.; Roletto, F.; Traquandi, G.; Vianello, P.; Vulpetti, A.; Ciomei, M., Identification of N,1,4,4-tetramethyl-8-{[4-(4-methylpiperazin-1-yl)phenyl]amino}-4,5-dihydro-1H-py razolo[4,3-h]quinazoline-3-carboxamide (PHA-848125), a potent, orally available cyclin dependent kinase inhibitor. *J Med Chem* **2009**, 52, (16), 5152-63.

28. Murai, M.; Sekiguchi, K.; Nishioka, T.; Miyoshi, H., Characterization of the inhibitor binding site in mitochondrial NADH-ubiquinone oxidoreductase by photoaffinity labeling using a quinazoline-type inhibitor. *Biochemistry* **2009**, 48, (4), 688-98.

29. Marugan, J. J.; Zheng, W.; Motabar, O.; Southall, N.; Goldin, E.; Westbroek, W.; Stubblefield, B. K.; Sidransky, E.; Aungst, R. A.; Lea, W. A.; Simeonov, A.; Leister, W.; Austin, C. P., Evaluation of quinazoline analogues as glucocerebrosidase inhibitors with chaperone activity. *J Med Chem* **2011**, 54, (4), 1033-58.

30. Chang, Y.; Zhang, X.; Horton, J. R.; Upadhyay, A. K.; Spannhoff, A.; Liu, J.; Snyder, J. P.; Bedford, M. T.; Cheng, X., Structural basis for G9a-like protein lysine methyltransferase inhibition by BIX-01294. *Nat Struct Mol Biol* **2009**, 16, (3), 312-7.

31. Haas, T. L.; Emmerich, C. H.; Gerlach, B.; Schmukle, A. C.; Cordier, S. M.; Rieser, E.; Feltham, R.; Vince, J.; Warnken, U.; Wenger, T.; Koschny, R.; Komander, D.; Silke, J.; Walczak, H., Recruitment of the linear ubiquitin chain assembly complex stabilizes the TNF-R1 signaling complex and is required for TNF-mediated gene induction. *Mol Cell* **2009**, 36, (5), 831-44.

32. Passmore, J. S.; Lukey, P. T.; Ress, S. R., The human macrophage cell line U937 as an in vitro model for selective evaluation of mycobacterial antigen-specific cytotoxic T-cell function. *Immunology* **2001**, 102, (2), 146-56.

33. Ferrer-Soler, L.; Vazquez-Martin, A.; Brunet, J.; Menendez, J. A.; De Llorens, R.; Colomer, R., An update of the mechanisms of resistance to EGFR-tyrosine kinase inhibitors in breast cancer: Gefitinib (Iressa) -induced changes in the expression and nucleo-cytoplasmic trafficking of HER-ligands (Review). *Int J Mol Med* **2007**, 20, (1), 3-10.

34. Corkery, B.; Crown, J.; Clynes, M.; O'Donovan, N., Epidermal growth factor receptor as a potential therapeutic target in triple-negative breast cancer. *Ann Oncol* **2009**, 20, (5), 862-7.

35. Moasser, M. M.; Basso, A.; Averbuch, S. D.; Rosen, N., The tyrosine kinase inhibitor ZD1839 ("Iressa") inhibits HER2-driven signaling and suppresses the growth of HER2-overexpressing tumor cells. *Cancer Res* **2001**, 61, (19), 7184-8.

36. Emanuel, S. L.; Hughes, T. V.; Adams, M.; Rugg, C. A.; Fuentes-Pesquera, A.; Connolly, P. J.; Pandey, N.; Moreno-Mazza, S.; Butler, J.; Borowski, V.; Middleton, S. A.; Gruninger, R. H.; Story, J. R.; Napier, C.; Hollister, B.; Greenberger, L. M., Cellular and in vivo activity of JNJ-28871063, a nonquinazoline pan-ErbB kinase inhibitor that crosses the blood-brain barrier and displays efficacy against intracranial tumors. *Mol Pharmacol* **2008**, 73, (2), 338-48.

37. Montagut, C.; Rovira, A.; Mellado, B.; Gascon, P.; Ross, J. S.; Albanell, J., Preclinical and clinical development of the proteasome inhibitor bortezomib in cancer treatment. *Drugs Today (Barc)* **2005**, 41, (5), 299-315.

38. Berkers, C. R.; Verdoes, M.; Lichtman, E.; Fiebiger, E.; Kessler, B. M.; Anderson, K. C.; Ploegh, H. L.; Ovaa, H.; Galardy, P. J., Activity probe for in vivo profiling of the specificity of proteasome inhibitor bortezomib. *Nat Methods* **2005**, 2, (5), 357-62.

39. Bazzaro, M.; Anchoori, R. K.; Mudiam, M. K.; Issaenko, O.; Kumar, S.; Karanam, B.; Lin, Z.; Isaksson Vogel, R.; Gavioli, R.; Destro, F.; Ferretti, V.; Roden, R. B.; Khan, S. R., alpha,beta-Unsaturated carbonyl system of chalcone-based derivatives is responsible for broad inhibition of proteasomal activity and preferential killing of human papilloma virus (HPV) positive cervical cancer cells. *J Med Chem* **2011**, 54, (2), 449-56.

40. Issaenko, O. A.; Amerik, A. Y., Chalcone-based small-molecule inhibitors attenuate malignant phenotype via targeting deubiquitinating enzymes. *Cell Cycle* **2012**, 11, (9), 1804-17.

41. Reverdy, C.; Conrath, S.; Lopez, R.; Planquette, C.; Atmanene, C.; Collura, V.; Harpon, J.; Battaglia, V.; Vivat, V.; Sippl, W.; Colland, F., Discovery of specific inhibitors of human USP7/HAUSP deubiquitinating enzyme. *Chem Biol* **2012**, 19, (4), 467-77.

42. Cohen, P.; Tcherpakov, M., Will the ubiquitin system furnish as many drug targets as protein kinases? *Cell* **2010**, 143, (5), 686-93.

43. Chauhan, D.; Catley, L.; Li, G.; Podar, K.; Hideshima, T.; Velankar, M.; Mitsiades, C.; Mitsiades, N.; Yasui, H.; Letai, A.; Ovaa, H.; Berkers, C.; Nicholson, B.; Chao, T. H.; Neuteboom, S. T.; Richardson, P.; Palladino, M. A.; Anderson, K. C., A novel orally active proteasome inhibitor induces apoptosis in multiple myeloma cells with mechanisms distinct from Bortezomib. *Cancer Cell* **2005**, 8, (5), 407-19.

44. Goldenberg, S. J.; McDermott, J. L.; Butt, T. R.; Mattern, M. R.; Nicholson, B., Strategies for the identification of novel inhibitors of deubiquitinating enzymes. *Biochem Soc Trans* **2008**, 36, (Pt 5), 828-32.

45. Fry, D. W.; Kraker, A. J.; McMichael, A.; Ambroso, L. A.; Nelson, J. M.; Leopold, W. R.; Connors, R. W.; Bridges, A. J., A specific inhibitor of the epidermal growth factor receptor tyrosine kinase. *Science* **1994**, 265, (5175), 1093-5.

46. Frohner, W.; Lopez-Garcia, L. A.; Neimanis, S.; Weber, N.; Navratil, J.; Maurer, F.; Stroba, A.; Zhang, H.; Biondi, R. M.; Engel, M., 4-benzimidazolyl-3-phenylbutanoic acids as novel PIF-pocket-targeting allosteric inhibitors of protein kinase PKCzeta. *J Med Chem* **2011**, 54, (19), 6714-23.

4 Overall Discussion

This chapter summarizes the main results and the best compounds obtained from the whole work as well as the future improvements that could be implemented. The aim of the present thesis was the development of a novel group of potent anticancer compounds that are effective towards cancers that are insensitive or resistant to the clinically approved EGFR inhibitors. This was done using 2 strategies: firstly by doing several structural modifications in the compounds that were expected to enhance the activity against the mutant EGFR which causes resistance towards the EGFR inhibitors (Chapters **3.I** and **3.II**). The second strategy (Chapter **3.III**) was by synthesizing compounds having dual inhibitory activity towards the EGFR kinase and the NF-κB activation pathway. This would result in a synergistic anticancer activity that would be effective towards a wide range of cancer cells that are less sensitive or resistant towards the clinically approved EGFR inhibitors such as Gefitinib and Erlotinib. To reach our goal we started from the 6-substituted 4-anilinoquinazoline scaffold **(I)** which was known to possess potent EGFR inhibitory activity.

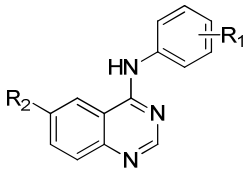

(I)

The first strategy included two parts of modifications that were expected to enhance the activity towards the mutant EGFR. Chapter **3.I** deals with the first part of these modifications which included several diverse variations taking place in position 4 of the quinazoline scaffold **(I)** while using a Michael acceptor group in position 6 such as the acrylamide group (**II**). The acrylamide group is added to form a covalent interaction with the Cys 797 of the ATP binding pocket of the EGFR enzyme (Figure 21). This covalent, irreversible binding with the EGFR enzyme may increase effectiveness by prolonging the inhibition of EGFR signaling to the entire lifespan of the drug-bound receptor molecule. In cell culture models, irreversibly binding EGFR inhibitors can produce potent anticancer activity that would be effective towards cells that have acquired resistance to reversible EGFR inhibitors.

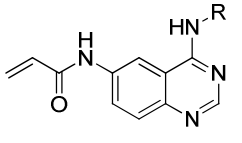

(II)

The resistance caused by the T790M mutation takes place at the gatekeeper amino acid that is near the deep pocket within which the 4-anilino moiety accommodates (Figure 21). Therefore, we managed to make modifications in the portion of the molecule

which is directed towards this point mutation site in a trial to increase the chance of finding such a mutant EGFR-selective ligand. Accordingly, we tested the effect of the modifications of the position 4 substituents - in presence of a Michael acceptor group - on the inhibitory activity of the wild-type and mutant EGFR containing cancer cell lines.

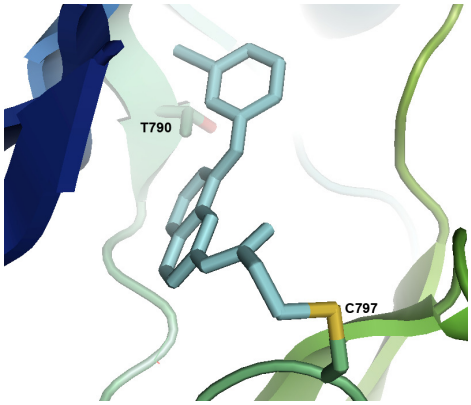

Figure 21: Cocrystal structure of wt EGFR complexed with an irreversible inhibitor which forms a covalent interaction with Cys797 of the enzyme (PDB 2J5F).

The modifications firstly included variable substituents on the aniline ring such as with different dihalo, alkyl halo, alkoxy halo, dialkoxy and alkyl groups **(III)**. This was then followed with the use of free sulfonamide or substituted sulfonamide groups **(IV)**. The last modification in position 4 was replacing the aniline ring with the alicyclic cyclohexyl group **(V)**.

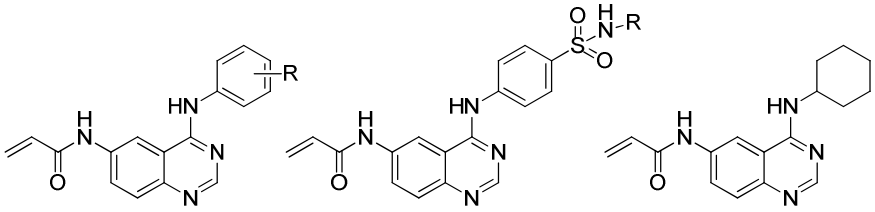

(III) **(IV)** **(V)**

The synthesized compounds were tested for their inhibitory activity towards the purified EGFR kinase and towards cancer cell lines with wild-type EGFR (SKBR3 cells) and double mutated EGFR$^{T790M/L858R}$ (H1975) (Table 2). The modifications resulted in two compounds **I.4e**[*] and **I.4i** -with alkyl substituents- showing about 4 fold selectivity towards the mutant EGFR containing cell line than the wild-type. The results also showed that the presence of a Michael acceptor group alone -to form an irreversible covalent interaction- is not enough to achieve potent inhibitory activity towards the mutant as well as the wild-type EGFR containing cell lines. And it was clear that the position 4

[*] For the sake of clarity, all compounds that are referred to in chapter 4 are presented as a combination of a Roman numeral (**I-III**) and an Arabic numeral with an alphabetical letter. The Roman numeral indicates in which result part they are enclosed and the Arabic numeral with alphabetical letter corresponds to the compound number in the chapter. (e.g. **I.4a** is compound 4a described in chapter I of the results).

substituents have a significant role in modulating the activity of these compounds especially for the cellular activity. Among the conclusions that were obtained from the modifications done in position 4, was that larger more bulky residues such as the pyridyl sulfonamide aniline in **I.4n** seemed to be accepted better by the cells growing dependent on wild-type (wt) EGFR than those dependent on double mutated (DM) EGFR. The di-substituted anilines at position 4 -especially with halogens- are the most potent. Compounds **I.4a**, **I.4b** and **I.4f** were the best compromise showing potent growth inhibitory activities towards both cancer cells with mutant or wt EGFR kinase. Also, among the new findings was that substituents like the cyclohexyl amine in **I.4o** resulted in an active and potent compound towards the wt EGFR while was not as active towards the mutant EGFR. Further modifications such as introducing different alkyl substituents to the phenyl ring could result in a more shifting of the selectivity towards the mutant cell lines. In addition, further testing against the purified mutant enzyme would exclude any role for off-targets in the cellular activity.

Table 2. Influence of the modifications at the ring in 4-position of the quinazoline nucleus on EGFR inhibitory potency and cell growth.

Comp.	Fm	R	Recombinant EGFR Kinase	IC_{50} (μM) Cell Growth inhibition	
			IC_{50} (nM)	SKBR3	H1975
I.4a	III	2-Br, 6-F	2.2	0.23	0.26
I.4b	III	4-Br, 2-F	2.1	0.51	0.28
I.4e	III	2F, 3Me	1.5	1.86	0.39
I.4f	III	4-Br, 3-OMe	2.5	0.36	0.40
I.4i	III	3-Et	2.7	2.82	0.68
I.4n	IV	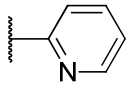	9.8	0.39	>40
I.4o	V	-	3.4	0.40	>40
Gefitinib	-	-	4	5.36	11.39

Chapter **3.I** also covered the modification taking place in the main scaffold by replacing the quinazoline nucleus with the tetrahydropyridothieno[2,3-*d*]pyrimidine nucleus (**VI**). The same acrylamido group was present at position 7 while using in position 4 the most potent substituents that were obtained with the quinazoline derivatives (**I.4a-I.4o**). The results of this modification didn't show significant improvement in the activity over the quinazoline nucleus towards the wt or mutant EGFR containing cell lines. Further trials with smaller scaffolds rather than the big ones could result in an enhanced activity.

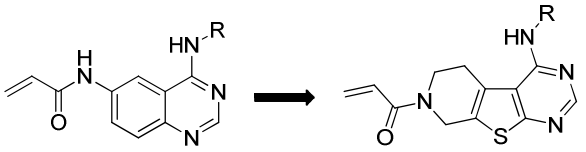

(VI)

Chapter **3.II** deals with the second part of modifications which include the variations taking place at position 6 of compound **(I)** -with non-reactive moieties- while using a *m*-bromoaniline in position 4. These modifications were done with an aim to offer chances for extra possible interactions that could take place with the mutant enzyme without covalent binding, in addition to the chance of modulating the cellular activity.

The modifications in the position 6 side chain included several aryl and heterocyclic substituents attached through different linkers to the quinazoline core. The linkers included an imine **(VII)**, amide **(VIII)**, amino alkyl amide **(IX)** and a thiourea **(X)** linkage.

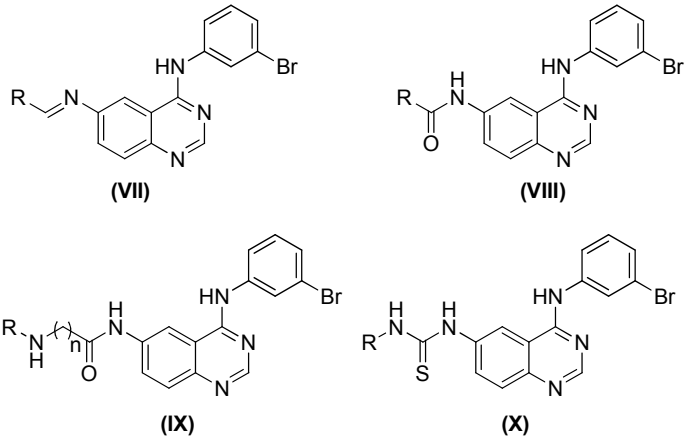

(VII) (VIII) (IX) (X)

All the compounds were tested for their inhibitory activity towards the recombinant wt and DM (L858R/T790M) EGFR as well as towards cancer cell lines with wt (KB cells) and double mutated EGFR (H1975) (Table 3). Interestingly, the results confirmed that the presence of aryl or heterocylic rings in the side chain at position 6 of the quinazoline is essential in modulating the activity especially towards the mutant EGFR and also for the cellular activity. Most of the compounds showed significant potency towards the wt EGFR, while only some compounds such as **II.6a**, **II.6b**, **II.10b** only showed potent activity towards the EGFR double mutant which functioned as a highly stringent filter, clearly identifying the most promising modifications of the quinazoline scaffold. Several compounds showed enhanced cellular activity than Gefitinib towards both cell lines. This was clearly observed with the amide derivatives having heterocyclic rings such as **II.11i** and the benzylthiourea derivative **II.6a.** The benzylthiourea derivative **II.6a** retained potent cellular activity in addition to the potent activity towards wt and the DM purified enzymes, representing the most promising lead compound of this study. The furyl derivative **II.11i** also retained the highest activity in cells beside the potent activity towards only the wt purified enzyme, suggesting that inhibition of H1975

cell growth by **II.11i** and some other compounds is due to off-target effects. As a major achievement of our study, we were able to identify compounds that show potent inhibition of the mutant enzyme without covalent binding. In addition, we were also able to identify combinations which led to efficient growth inhibition of both cell lines. Further optimization of the aryl substituents at position 6 by replacing the benzyl in **II.6a** by substituted derivatives or five- and six-membered heterocycles would likely result in optimized EGFR kinase inhibitors which are equally potent towards the wild-type enzyme and Gefitinib-resistant mutants.

Table 3. Influence of the modifications at the position 6 of the quinazoline nucleus on EGFR inhibitory potency and cell growth.

Comp.	Fm	R	EGFR enzyme assay IC_{50} (nM)		Cell Growth inhibition IC_{50} (µM)	
			Wt	DM	KB	H1975
II.11i	VII	2-furyl	8.4	N.D.	12.3	14.3
II.9a	VIII n=1	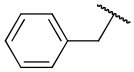	5.2	N.D.	14.6	27.9
II.10b	VIII n=2	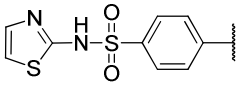	23.1	480	33.6	20.8
II.6a	IX	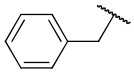	17.2	290	8.5	18.0
II.6b	IX	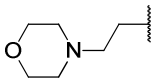	10.7	1020	29.8	35.0
Gefitinib	-	-	4	7000	17.5	30

N.D.: Not Determined

Chapter **3.III** deals mainly with a second strategy to treat cancers that are originally insensitive or resistant to the clinically approved EGFR inhibitors. This is done through the dual inhibition of two complementary pathways involved in cancer such as the EGFR and NF-κB using a single molecule. In order to achieve this dual inhibitory activity we started by screening most of our previously synthesized compounds -that originally showed an EGFR inhibition- for an NF-κB inhibitory activity using a U937 cells reporter gene assay. The screening resulted in a Hit compound (**III.4b**) which showed potent activity towards both EGFR and NF-κB, in addition to some other compounds but with lower potencies towards the NF-κB. The Hit compound was the benzylthiourea derivative (**III.4b**), showing a 97% inhibition for the NF-κB at 10 µM, in addition to an IC_{50} of 17.2 nM for the wt EGFR.

The Hit compound was further subjected to optimization which was mainly guided by the NF-κB activity. The optimization of the Hit compound included three parts. The first part was concerned with the modifications of the substituents on the 4-anilino ring

while keeping the benzylthiourea at position 6 of the quinazoline (**XI**). The second part was to make modifications in the side chain linked to the thiourea moiety while keeping the 3-bromoaniline at position 4 of the quinazoline (**XII**). The last part was to confirm the importance of the thiourea group by replacing it with the urea moiety (**XIII**). Chapter **3.III** deals also with the different trials done to identify the molecular target with which these compounds inhibit the NF-κB pathway.

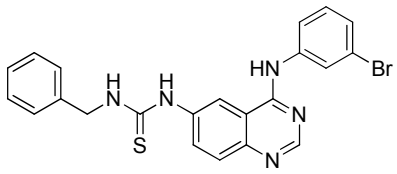

(III.4b)
Hit compound

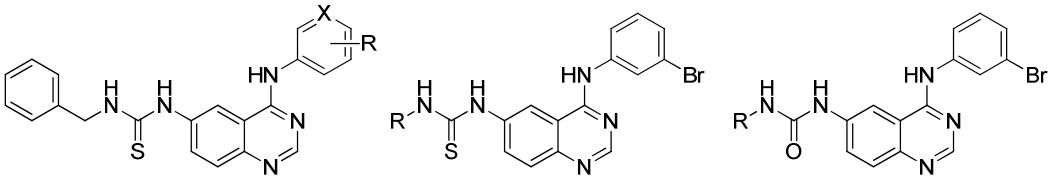

(XI) **(XII)** **(XIII)**

All the newly optimized compounds were then tested for their inhibitory activity towards the recombinant EGFR kinase and the NF-κB pathway. In addition, to test the effectiveness of the dual inhibitory activity on the anticancer potency, all the compounds were further tested for their cellular growth inhibitory activity towards the MDA-MB-23l cell line. This cell line was chosen as it overexpresses the EGFR and is not highly sensitive to the clinically approved EGFR inhibitor "Gefitinib" and so would be a good model to prove that the enhanced anticancer activity of the synthesized compounds is due to the dual activity.

A clear structure activity relationship was observed from the modifications taking place at the 4-anilino ring of the quinazoline. The SAR showed that the optimum substituents for the EGFR activity were the lipophilic groups at the *meta* position. And it was also clear that the presence of polar hetero atoms on the 4-anilino ring significantly decrease the activity towards the NF-κB pathway. Accordingly, the compounds that are able to show dual inhibitory activity should have a medium sized halogen in the *meta* position of the 4-anilino ring such as in compound **III.4d**.

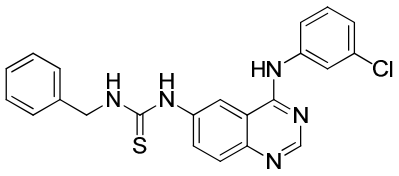

(III.4d)

Recombinant EGFR Kinase		**U937 reporter gene assay**	
% inhibition at 150 nM	IC_{50} (nM)	% inhibition at 10µM	IC_{50} (µM)
84.8	11.4	89.7	3.7

The next step was to confirm the importance of the presence of the methylene spacer between the thiourea linker and the aromatic ring. This was done by replacing the benzyl

side chain by a phenyl side chain where it was found that the phenyl derivatives are better than their benzyl analogues (Table 4).

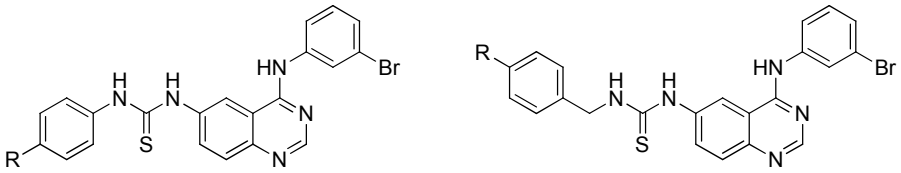

(III.6a) R = H
(III.6d) R = Cl

(III.4b) R = H
(III.7c) R = Cl

Table 4. Influence of the methylene spacer on the EGFR and NF-κB inhibitory potencies.

Comp.	Recombinant EGFR Kinase		U937 reporter gene assay	
	% inhibition at 150 nM	IC_{50} (nM)	% inhibition at 10µM	IC_{50} (µM)
III.4b	86.1	17.2	97	4.1
III.6a	86.5	15.8	90.7	5.2
III.7c	77.5	28.3	78.6	N.D.
III.6d	79.6	19.5	89.5	4.9

N.D.: Not Determined

This was followed by testing the importance of the thiourea linker by replacing it with a urea moiety. It was significantly clear from the results that the thiourea was essential to retain the activity towards the NF-κB pathway (Table 5).

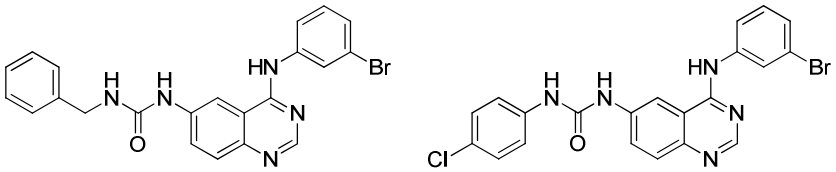

(III.8a)

(III.8b)

Table 5. Influence of the replacement of the thiourea linker by a urea, on the EGFR and NF-κB inhibitory potencies.

Comp.	Recombinant EGFR Kinase		U937 reporter gene assay	
	% inhibition at 150 nM	IC_{50} (nM)	% inhibition at 10µM	IC_{50} (µM)
III.4b	86.1	17.2	97	4.1
III.8a	89.9	8.9	42.6	N.D.
III.6d	79.6	19.5	89.5	4.9
III.8b	69.0	19.3	50.3	N.D.

N.D.: Not Determined

After that it was to confirm the importance of the presence of an aromatic ring in the side chain. This was done by replacing it with a methyl, morpholine and an ethyl

morpholine. The results showed that an aromatic ring is essential in the side chain for retaining the activity towards the NF-κB (Table 6).

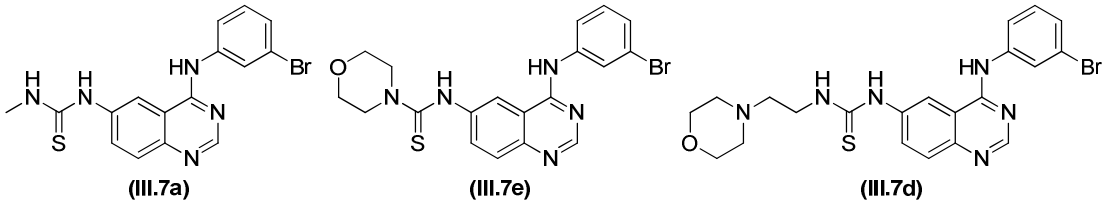

Table 6. Influence of the presence of aromatic ring in the side chain on the EGFR and NF-κB inhibitory potencies.

Comp.	Recombinant EGFR Kinase		U937 reporter gene assay	
	% inhibition at 150 nM	IC_{50} (nM)	% inhibition at 10μM	IC_{50} (μM)
III.4b	86.1	17.2	97	4.1
III.7a	92.2	9.1	3.0	N.D.
III.7e	84.0	26.9	40.1	N.D.
III.7d	91.8	10.7	20.9	N.D.

N.D.: Not Determined

Next, several substituents were further added to the phenyl thiourea side chain to achieve an enhanced potency for the compounds..

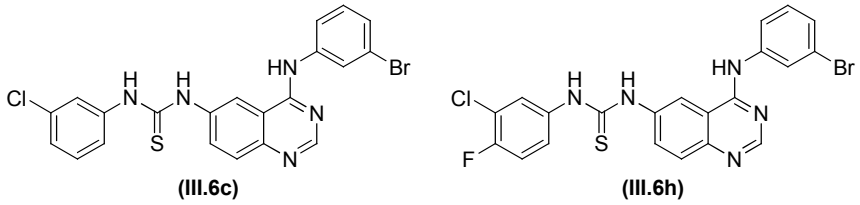

Table 7. Most potent derivatives obtained from the modifications on the phenyl ring of the position 6 side chain.

Comp.	Recombinant EGFR Kinase		U937 reporter gene assay		MDA cell growth
	% inhibition at150 nM	IC_{50} (nM)	% inhibition at 10μM	IC_{50} (μM)	IC_{50} (μM)
III.6c	74.8	20.6	97.4	1.9	2.1
III.6h	74.1	25.3	100	1.0	0.3
Gef.	93.2	4.0	51.3	9.7	14.2

The modifications of the position 6 side chain in presence of *m*-bromoaniline at position 4 showed that several substituents are tolerable either lipophilic or hydrophilic with the hydrophilic or heterocyclic ones being more potent towards the EGFR kinase. This was the opposite in case of the NF-κB activity which showed that the lipophilic substituents are the optimum ones. And any polar groups or heterocyclic rings in this side

chain lead to loss of activity. So in order to keep the dual activity, a lipophilic substituent is essential in this side chain. Several compounds showed variable significant activities against both targets with compounds **III.6c** and **III.6h** being the most potent against both targets (Table 7).

The best compounds **III.6c, III.6h** and **III.4b** were investigated for their mechanism of NF-κB inhibition. For **III.4b** we were able to identify a mechanism which is mainly affecting the deubiquitination step, whereas for the other 2 compounds it still remains elusive. There is was no inhibition of the proteasome nor do the compounds inhibit the translocation of NF-κB to the nucleus and they don't inhibit the deubiquitination step. However, we can exclude a general cytotoxicity; rather, the compounds display a tumor-cell selective cytotoxic effect, which was very promising. Further testing to identify the molecular target of the other compounds is to be implemented. In addition, some modifications that would result in better solubility of the compounds, such as replacing the aromatic ring in the side chain by heteroaryl rings, are to be tested.

Conclusion

Finally, as a general conclusion we have been able to achieve the intended goals by synthesizing compounds effective against cancers that are originally insensitive or resistant to the clinically approved EGFR inhibitors. Chapter **3.I** showed that the irreversible inhibitors are effective towards the wild-type and mutant EGFR containing cancer cell lines and that position-4 substituents were important to possibly shift the selectivity towards the mutant EGFR containing cancer cell lines. A higher degree of selectivity might attenuate toxic effects that may be attributed to the irreversible blockage also of the wild type EGFR. Chapter **3.II** also represents a success of being able to identify compounds that are potent inhibitors for the mutant EGFR without the requirement for covalent binding. Hence, the modifications done in Chapters **3.I** and **3.II** have achieved the intended aim of being able to overcome the cancers that are resistant to the EGFR inhibitors. Chapter **3.III** also represents a highly successful outcome being able to identify first group of compounds with dual inhibitory activity -towards the EGFR and NF-κB- that is expected to significantly increase efficacy towards cancers that are less sensitive or resistant to the present generation of EGFR inhibitors.

5 References

1. Kasture, V. S.; Musmade, D. S.; Aher, S. J.; Patil, P. P., Tyrosine Kinases: promising targets for cancer chemotherapy. *Medicinal chemistry & Drug Discovery* **2012,** 3, (1), 37-51.

2. Lehninger, A. L.; Nelson, D. L.; Cox, M. M., *Lehninger principles of biochemistry*. 5th ed.; W.H. Freeman: New York, 2008; p 1 v. (various pagings).

3. Blume-Jensen, P.; Hunter, T., Oncogenic kinase signalling. *Nature* **2001,** 411, (6835), 355-65.

4. Kontzias, A.; Laurence, A.; Gadina, M.; O'Shea, J. J., Kinase inhibitors in the treatment of immune-mediated disease. *F1000 Med Rep* **2012,** 4, 5.

5. Novel Protein Kinase D inhibitors. www.medchemblog.blogspot.com/2010/06/novel-protein-kinase-d-inhibitors_19.html (Accessed on March 17 2013),

6. Manning, G.; Whyte, D. B.; Martinez, R.; Hunter, T.; Sudarsanam, S., The protein kinase complement of the human genome. *Science* **2002,** 298, (5600), 1912-34.

7. Lander, E. S.; Linton, L. M.; Birren, B.; Nusbaum, C.; Zody, M. C.; Baldwin, J.; Devon, K.; Dewar, K.; Doyle, M.; FitzHugh, W.; Funke, R.; Gage, D.; Harris, K.; Heaford, A.; Howland, J.; Kann, L.; Lehoczky, J.; LeVine, R.; McEwan, P.; McKernan, K.; Meldrim, J.; Mesirov, J. P.; Miranda, C.; Morris, W.; Naylor, J.; Raymond, C.; Rosetti, M.; Santos, R.; Sheridan, A.; Sougnez, C.; Stange-Thomann, N.; Stojanovic, N.; Subramanian, A.; Wyman, D.; Rogers, J.; Sulston, J.; Ainscough, R.; Beck, S.; Bentley, D.; Burton, J.; Clee, C.; Carter, N.; Coulson, A.; Deadman, R.; Deloukas, P.; Dunham, A.; Dunham, I.; Durbin, R.; French, L.; Grafham, D.; Gregory, S.; Hubbard, T.; Humphray, S.; Hunt, A.; Jones, M.; Lloyd, C.; McMurray, A.; Matthews, L.; Mercer, S.; Milne, S.; Mullikin, J. C.; Mungall, A.; Plumb, R.; Ross, M.; Shownkeen, R.; Sims, S.; Waterston, R. H.; Wilson, R. K.; Hillier, L. W.; McPherson, J. D.; Marra, M. A.; Mardis, E. R.; Fulton, L. A.; Chinwalla, A. T.; Pepin, K. H.; Gish, W. R.; Chissoe, S. L.; Wendl, M. C.; Delehaunty, K. D.; Miner, T. L.; Delehaunty, A.; Kramer, J. B.; Cook, L. L.; Fulton, R. S.; Johnson, D. L.; Minx, P. J.; Clifton, S. W.; Hawkins, T.; Branscomb, E.; Predki, P.; Richardson, P.; Wenning, S.; Slezak, T.; Doggett, N.; Cheng, J. F.; Olsen, A.; Lucas, S.; Elkin, C.; Uberbacher, E.; Frazier, M.; Gibbs, R. A.; Muzny, D. M.; Scherer, S. E.; Bouck, J. B.; Sodergren, E. J.; Worley, K. C.; Rives, C. M.; Gorrell, J. H.; Metzker, M. L.; Naylor, S. L.; Kucherlapati, R. S.; Nelson, D. L.; Weinstock, G. M.; Sakaki, Y.; Fujiyama, A.; Hattori, M.; Yada, T.; Toyoda, A.; Itoh, T.; Kawagoe, C.; Watanabe, H.; Totoki, Y.; Taylor, T.; Weissenbach, J.; Heilig, R.; Saurin, W.; Artiguenave, F.; Brottier, P.; Bruls, T.; Pelletier, E.; Robert, C.; Wincker, P.; Smith, D. R.; Doucette-Stamm, L.; Rubenfield, M.; Weinstock, K.; Lee, H. M.; Dubois, J.; Rosenthal, A.; Platzer, M.; Nyakatura, G.; Taudien, S.; Rump, A.; Yang, H.; Yu, J.; Wang, J.; Huang, G.; Gu, J.; Hood, L.; Rowen, L.; Madan, A.; Qin, S.; Davis, R. W.; Federspiel, N. A.; Abola, A. P.; Proctor, M. J.; Myers, R. M.; Schmutz, J.; Dickson, M.; Grimwood, J.; Cox, D. R.; Olson, M. V.; Kaul, R.; Shimizu, N.; Kawasaki, K.; Minoshima, S.; Evans, G. A.; Athanasiou, M.; Schultz, R.; Roe, B. A.; Chen, F.; Pan, H.; Ramser, J.; Lehrach, H.; Reinhardt, R.; McCombie, W. R.; de la Bastide, M.; Dedhia, N.; Blocker, H.; Hornischer, K.; Nordsiek, G.; Agarwala, R.; Aravind, L.; Bailey, J. A.; Bateman, A.; Batzoglou, S.;

Birney, E.; Bork, P.; Brown, D. G.; Burge, C. B.; Cerutti, L.; Chen, H. C.; Church, D.; Clamp, M.; Copley, R. R.; Doerks, T.; Eddy, S. R.; Eichler, E. E.; Furey, T. S.; Galagan, J.; Gilbert, J. G.; Harmon, C.; Hayashizaki, Y.; Haussler, D.; Hermjakob, H.; Hokamp, K.; Jang, W.; Johnson, L. S.; Jones, T. A.; Kasif, S.; Kaspryzk, A.; Kennedy, S.; Kent, W. J.; Kitts, P.; Koonin, E. V.; Korf, I.; Kulp, D.; Lancet, D.; Lowe, T. M.; McLysaght, A.; Mikkelsen, T.; Moran, J. V.; Mulder, N.; Pollara, V. J.; Ponting, C. P.; Schuler, G.; Schultz, J.; Slater, G.; Smit, A. F.; Stupka, E.; Szustakowski, J.; Thierry-Mieg, D.; Thierry-Mieg, J.; Wagner, L.; Wallis, J.; Wheeler, R.; Williams, A.; Wolf, Y. I.; Wolfe, K. H.; Yang, S. P.; Yeh, R. F.; Collins, F.; Guyer, M. S.; Peterson, J.; Felsenfeld, A.; Wetterstrand, K. A.; Patrinos, A.; Morgan, M. J.; de Jong, P.; Catanese, J. J.; Osoegawa, K.; Shizuya, H.; Choi, S.; Chen, Y. J., Initial sequencing and analysis of the human genome. *Nature* **2001,** 409, (6822), 860-921.

8. Manning, G.; Plowman, G. D.; Hunter, T.; Sudarsanam, S., Evolution of protein kinase signaling from yeast to man. *Trends Biochem Sci* **2002,** 27, (10), 514-20.

9. Rubin, G. M.; Yandell, M. D.; Wortman, J. R.; Gabor Miklos, G. L.; Nelson, C. R.; Hariharan, I. K.; Fortini, M. E.; Li, P. W.; Apweiler, R.; Fleischmann, W.; Cherry, J. M.; Henikoff, S.; Skupski, M. P.; Misra, S.; Ashburner, M.; Birney, E.; Boguski, M. S.; Brody, T.; Brokstein, P.; Celniker, S. E.; Chervitz, S. A.; Coates, D.; Cravchik, A.; Gabrielian, A.; Galle, R. F.; Gelbart, W. M.; George, R. A.; Goldstein, L. S.; Gong, F.; Guan, P.; Harris, N. L.; Hay, B. A.; Hoskins, R. A.; Li, J.; Li, Z.; Hynes, R. O.; Jones, S. J.; Kuehl, P. M.; Lemaitre, B.; Littleton, J. T.; Morrison, D. K.; Mungall, C.; O'Farrell, P. H.; Pickeral, O. K.; Shue, C.; Vosshall, L. B.; Zhang, J.; Zhao, Q.; Zheng, X. H.; Lewis, S., Comparative genomics of the eukaryotes. *Science* **2000,** 287, (5461), 2204-15.

10. Venter, J. C.; Adams, M. D.; Myers, E. W.; Li, P. W.; Mural, R. J.; Sutton, G. G.; Smith, H. O.; Yandell, M.; Evans, C. A.; Holt, R. A.; Gocayne, J. D.; Amanatides, P.; Ballew, R. M.; Huson, D. H.; Wortman, J. R.; Zhang, Q.; Kodira, C. D.; Zheng, X. H.; Chen, L.; Skupski, M.; Subramanian, G.; Thomas, P. D.; Zhang, J.; Gabor Miklos, G. L.; Nelson, C.; Broder, S.; Clark, A. G.; Nadeau, J.; McKusick, V. A.; Zinder, N.; Levine, A. J.; Roberts, R. J.; Simon, M.; Slayman, C.; Hunkapiller, M.; Bolanos, R.; Delcher, A.; Dew, I.; Fasulo, D.; Flanigan, M.; Florea, L.; Halpern, A.; Hannenhalli, S.; Kravitz, S.; Levy, S.; Mobarry, C.; Reinert, K.; Remington, K.; Abu-Threideh, J.; Beasley, E.; Biddick, K.; Bonazzi, V.; Brandon, R.; Cargill, M.; Chandramouliswaran, I.; Charlab, R.; Chaturvedi, K.; Deng, Z.; Di Francesco, V.; Dunn, P.; Eilbeck, K.; Evangelista, C.; Gabrielian, A. E.; Gan, W.; Ge, W.; Gong, F.; Gu, Z.; Guan, P.; Heiman, T. J.; Higgins, M. E.; Ji, R. R.; Ke, Z.; Ketchum, K. A.; Lai, Z.; Lei, Y.; Li, Z.; Li, J.; Liang, Y.; Lin, X.; Lu, F.; Merkulov, G. V.; Milshina, N.; Moore, H. M.; Naik, A. K.; Narayan, V. A.; Neelam, B.; Nusskern, D.; Rusch, D. B.; Salzberg, S.; Shao, W.; Shue, B.; Sun, J.; Wang, Z.; Wang, A.; Wang, X.; Wang, J.; Wei, M.; Wides, R.; Xiao, C.; Yan, C.; Yao, A.; Ye, J.; Zhan, M.; Zhang, W.; Zhang, H.; Zhao, Q.; Zheng, L.; Zhong, F.; Zhong, W.; Zhu, S.; Zhao, S.; Gilbert, D.; Baumhueter, S.; Spier, G.; Carter, C.; Cravchik, A.; Woodage, T.; Ali, F.; An, H.; Awe, A.; Baldwin, D.; Baden, H.; Barnstead, M.; Barrow, I.; Beeson, K.; Busam, D.; Carver, A.; Center, A.; Cheng, M. L.; Curry, L.; Danaher, S.; Davenport, L.; Desilets, R.; Dietz, S.; Dodson, K.; Doup, L.; Ferriera, S.; Garg, N.; Gluecksmann, A.; Hart, B.; Haynes, J.; Haynes, C.; Heiner, C.; Hladun, S.; Hostin, D.; Houck, J.; Howland, T.; Ibegwam, C.; Johnson, J.; Kalush, F.; Kline, L.; Koduru, S.; Love, A.; Mann, F.; May, D.; McCawley, S.; McIntosh, T.; McMullen, I.; Moy, M.; Moy, L.; Murphy, B.; Nelson,

K.; Pfannkoch, C.; Pratts, E.; Puri, V.; Qureshi, H.; Reardon, M.; Rodriguez, R.; Rogers, Y. H.; Romblad, D.; Ruhfel, B.; Scott, R.; Sitter, C.; Smallwood, M.; Stewart, E.; Strong, R.; Suh, E.; Thomas, R.; Tint, N. N.; Tse, S.; Vech, C.; Wang, G.; Wetter, J.; Williams, S.; Williams, M.; Windsor, S.; Winn-Deen, E.; Wolfe, K.; Zaveri, J.; Zaveri, K.; Abril, J. F.; Guigo, R.; Campbell, M. J.; Sjolander, K. V.; Karlak, B.; Kejariwal, A.; Mi, H.; Lazareva, B.; Hatton, T.; Narechania, A.; Diemer, K.; Muruganujan, A.; Guo, N.; Sato, S.; Bafna, V.; Istrail, S.; Lippert, R.; Schwartz, R.; Walenz, B.; Yooseph, S.; Allen, D.; Basu, A.; Baxendale, J.; Blick, L.; Caminha, M.; Carnes-Stine, J.; Caulk, P.; Chiang, Y. H.; Coyne, M.; Dahlke, C.; Mays, A.; Dombroski, M.; Donnelly, M.; Ely, D.; Esparham, S.; Fosler, C.; Gire, H.; Glanowski, S.; Glasser, K.; Glodek, A.; Gorokhov, M.; Graham, K.; Gropman, B.; Harris, M.; Heil, J.; Henderson, S.; Hoover, J.; Jennings, D.; Jordan, C.; Jordan, J.; Kasha, J.; Kagan, L.; Kraft, C.; Levitsky, A.; Lewis, M.; Liu, X.; Lopez, J.; Ma, D.; Majoros, W.; McDaniel, J.; Murphy, S.; Newman, M.; Nguyen, T.; Nguyen, N.; Nodell, M.; Pan, S.; Peck, J.; Peterson, M.; Rowe, W.; Sanders, R.; Scott, J.; Simpson, M.; Smith, T.; Sprague, A.; Stockwell, T.; Turner, R.; Venter, E.; Wang, M.; Wen, M.; Wu, D.; Wu, M.; Xia, A.; Zandieh, A.; Zhu, X., The sequence of the human genome. *Science* **2001,** 291, (5507), 1304-51.

11. Cohen, P., Protein kinases--the major drug targets of the twenty-first century? *Nat Rev Drug Discov* **2002,** 1, (4), 309-15.

12. Hunter, T., Signaling--2000 and beyond. *Cell* **2000,** 100, (1), 113-27.

13. Grant, S. K., Therapeutic protein kinase inhibitors. *Cell Mol Life Sci* **2009,** 66, (7), 1163-77.

14. Johnson, L. N., Protein kinase inhibitors: contributions from structure to clinical compounds. *Q Rev Biophys* **2009,** 42, (1), 1-40.

15. Miranda-Saavedra, D.; Barton, G. J., Classification and functional annotation of eukaryotic protein kinases. *Proteins* **2007,** 68, (4), 893-914.

16. Mora, A.; Komander, D.; van Aalten, D. M.; Alessi, D. R., PDK1, the master regulator of AGC kinase signal transduction. *Semin Cell Dev Biol* **2004,** 15, (2), 161-70.

17. Zhu, G.; Fujii, K.; Liu, Y.; Codrea, V.; Herrero, J.; Shaw, S., A single pair of acidic residues in the kinase major groove mediates strong substrate preference for P-2 or P-5 arginine in the AGC, CAMK, and STE kinase families. *J Biol Chem* **2005,** 280, (43), 36372-9.

18. Klimecka, M.; Muszynska, G., Structure and functions of plant calcium-dependent protein kinases. *Acta Biochim Pol* **2007,** 54, (2), 219-33.

19. Knippschild, U.; Gocht, A.; Wolff, S.; Huber, N.; Lohler, J.; Stoter, M., The casein kinase 1 family: participation in multiple cellular processes in eukaryotes. *Cell Signal* **2005,** 17, (6), 675-89.

20. Cohen, P.; Goedert, M., GSK3 inhibitors: development and therapeutic potential. *Nat Rev Drug Discov* **2004,** 3, (6), 479-87.

21. Malumbres, M.; Barbacid, M., Mammalian cyclin-dependent kinases. *Trends Biochem Sci* **2005,** 30, (11), 630-41.

22. Malumbres, M.; Barbacid, M., Cell cycle kinases in cancer. *Curr Opin Genet Dev* **2007,** 17, (1), 60-5.

23. Sundaram, M. V., RTK/Ras/MAPK signaling. *WormBook* **2006**, 1-19.

24. Aparicio, J. G.; Applebury, M. L., The photoreceptor guanylate cyclase is an autophosphorylating protein kinase. *J Biol Chem* **1996,** 271, (43), 27083-9.

25. Mishra, N. S.; Tuteja, R.; Tuteja, N., Signaling through MAP kinase networks in plants. *Arch Biochem Biophys* **2006,** 452, (1), 55-68.

26. Tibes, R.; Trent, J.; Kurzrock, R., Tyrosine kinase inhibitors and the dawn of molecular cancer therapeutics. *Annu Rev Pharmacol Toxicol* **2005,** 45, 357-84.

27. Wolf, D.; Tilg, H.; Rumpold, H.; Gastl, G.; Wolf, A. M., The kinase inhibitor imatinib--an immunosuppressive drug? *Curr Cancer Drug Targets* **2007,** 7, (3), 251-8.

28. Parkinson Study Group PRECEPT Investigators, Mixed lineage kinase inhibitor CEP-1347 fails to delay disability in early Parkinson disease. *Neurology* **2007,** 69, (15), 1480-90.

29. Scharpfenecker, M.; van Dinther, M.; Liu, Z.; van Bezooijen, R. L.; Zhao, Q.; Pukac, L.; Lowik, C. W.; ten Dijke, P., BMP-9 signals via ALK1 and inhibits bFGF-induced endothelial cell proliferation and VEGF-stimulated angiogenesis. *J Cell Sci* **2007,** 120, (Pt 6), 964-72.

30. Drennan, D.; Ryazanov, A. G., Alpha-kinases: analysis of the family and comparison with conventional protein kinases. *Prog Biophys Mol Biol* **2004,** 85, (1), 1-32.

31. Abraham, R. T., PI 3-kinase related kinases: 'big' players in stress-induced signaling pathways. *DNA Repair (Amst)* **2004,** 3, (8-9), 883-7.

32. Mayers, R. M.; Leighton, B.; Kilgour, E., PDH kinase inhibitors: a novel therapy for Type II diabetes? *Biochem Soc Trans* **2005,** 33, (Pt 2), 367-70.

33. LaRonde-LeBlanc, N.; Wlodawer, A., The RIO kinases: an atypical protein kinase family required for ribosome biogenesis and cell cycle progression. *Biochim Biophys Acta* **2005,** 1754, (1-2), 14-24.

34. Hidaka, H.; Sasaki, Y.; Tanaka, T.; Endo, T.; Ohno, S.; Fujii, Y.; Nagata, T., N-(6-aminohexyl)-5-chloro-1-naphthalenesulfonamide, a calmodulin antagonist, inhibits cell proliferation. *Proc Natl Acad Sci U S A* **1981,** 78, (7), 4354-7.

35. Tamaoki, T.; Nomoto, H.; Takahashi, I.; Kato, Y.; Morimoto, M.; Tomita, F., Staurosporine, a potent inhibitor of phospholipid/Ca++dependent protein kinase. *Biochem Biophys Res Commun* **1986,** 135, (2), 397-402.

36. Davies, S. P.; Reddy, H.; Caivano, M.; Cohen, P., Specificity and mechanism of action of some commonly used protein kinase inhibitors. *Biochem J* **2000,** 351, (Pt 1), 95-105.

37. Alessi, D. R., The protein kinase C inhibitors Ro 318220 and GF 109203X are equally potent inhibitors of MAPKAP kinase-1beta (Rsk-2) and p70 S6 kinase. *FEBS Lett* **1997,** 402, (2-3), 121-3.

38. Fischer, P. M.; Lane, D. P., Inhibitors of cyclin-dependent kinases as anti-cancer therapeutics. *Curr Med Chem* **2000,** 7, (12), 1213-45.

39. Glab, N.; Labidi, B.; Qin, L. X.; Trehin, C.; Bergounioux, C.; Meijer, L., Olomoucine, an inhibitor of the cdc2/cdk2 kinases activity, blocks plant cells at the G1 to S and G2 to M cell cycle transitions. *FEBS Lett* **1994,** 353, (2), 207-11.

40. Aklilu, M.; Kindler, H. L.; Donehower, R. C.; Mani, S.; Vokes, E. E., Phase II study of flavopiridol in patients with advanced colorectal cancer. *Ann Oncol* **2003,** 14, (8), 1270-3.

41. Benson, C.; White, J.; De Bono, J.; O'Donnell, A.; Raynaud, F.; Cruickshank, C.; McGrath, H.; Walton, M.; Workman, P.; Kaye, S.; Cassidy, J.; Gianella-Borradori, A.; Judson, I.; Twelves, C., A phase I trial of the selective oral cyclin-dependent kinase inhibitor seliciclib (CYC202; R-Roscovitine), administered twice daily for 7 days every 21 days. *Br J Cancer* **2007,** 96, (1), 29-37.

42. Backes, A. C.; Zech, B.; Felber, B.; Klebl, B.; ller, G., Small-molecule inhibitors binding to protein kinases. Part I: exceptions from the traditional pharmacophore approach of type I inhibition. *Expert Opinion on Drug Discovery* **2008,** 3, (12), 1409-1425.

43. Backes, A. C.; Zech, B.; Felber, B.; Klebl, B.; ller, G., Small-molecule inhibitors binding to protein kinase. Part II: the novel pharmacophore approach of type II and type III inhibition. *Expert Opinion on Drug Discovery* **2008,** 3, (12), 1427-1449.

44. Liu, Y.; Gray, N. S., Rational design of inhibitors that bind to inactive kinase conformations. *Nat Chem Biol* **2006,** 2, (7), 358-64.

45. Klebl, B.; Müller, G.; Hamacher, M., *Protein kinases as drug targets*. Wiley-VCH: Weinheim, 2011; p xxi, 373 p.

46. Traxler, P. M., Protein tyrosine kinase inhibitors in cancer treatment. *Expert Opinion on Therapeutic Patents* **1997,** 7, (6), 571-588.

47. Regan, J.; Breitfelder, S.; Cirillo, P.; Gilmore, T.; Graham, A. G.; Hickey, E.; Klaus, B.; Madwed, J.; Moriak, M.; Moss, N.; Pargellis, C.; Pav, S.; Proto, A.; Swinamer, A.; Tong, L.; Torcellini, C., Pyrazole urea-based inhibitors of p38 MAP kinase: from lead compound to clinical candidate. *J Med Chem* **2002,** 45, (14), 2994-3008.

48. Atwell, S.; Adams, J. M.; Badger, J.; Buchanan, M. D.; Feil, I. K.; Froning, K. J.; Gao, X.; Hendle, J.; Keegan, K.; Leon, B. C.; Muller-Dieckmann, H. J.; Nienaber, V. L.; Noland, B. W.; Post, K.; Rajashankar, K. R.; Ramos, A.; Russell, M.; Burley, S. K.; Buchanan, S. G., A novel mode of Gleevec binding is revealed by the structure of spleen tyrosine kinase. *J Biol Chem* **2004,** 279, (53), 55827-32.

49. Adrian, F. J.; Ding, Q.; Sim, T.; Velentza, A.; Sloan, C.; Liu, Y.; Zhang, G.; Hur, W.; Ding, S.; Manley, P.; Mestan, J.; Fabbro, D.; Gray, N. S., Allosteric inhibitors of Bcr-abl-dependent cell proliferation. *Nat Chem Biol* **2006,** 2, (2), 95-102.

50. Lindsley, C. W.; Zhao, Z.; Leister, W. H.; Robinson, R. G.; Barnett, S. F.; Defeo-Jones, D.; Jones, R. E.; Hartman, G. D.; Huff, J. R.; Huber, H. E.; Duggan, M. E., Allosteric Akt (PKB) inhibitors: discovery and SAR of isozyme selective inhibitors. *Bioorg Med Chem Lett* **2005,** 15, (3), 761-4.

51. Ohren, J. F.; Chen, H.; Pavlovsky, A.; Whitehead, C.; Zhang, E.; Kuffa, P.; Yan, C.; McConnell, P.; Spessard, C.; Banotai, C.; Mueller, W. T.; Delaney, A.; Omer, C.; Sebolt-Leopold, J.; Dudley, D. T.; Leung, I. K.; Flamme, C.; Warmus, J.; Kaufman, M.; Barrett, S.; Tecle, H.; Hasemann, C. A., Structures of human MAP kinase kinase 1 (MEK1) and MEK2 describe novel noncompetitive kinase inhibition. *Nat Struct Mol Biol* **2004,** 11, (12), 1192-7.

52. Pytel, D.; Sliwinski, T.; Poplawski, T.; Ferriola, D.; Majsterek, I., Tyrosine kinase blockers: new hope for successful cancer therapy. *Anticancer Agents Med Chem* **2009,** 9, (1), 66-76.

53. Hubbard, S. R.; Till, J. H., Protein tyrosine kinase structure and function. *Annu Rev Biochem* **2000,** 69, 373-98.

54. http://bio1151b.nicerweb.com/Locked/media/ch11/11_07bTyrosineKinases.jpg (Accessed on May 01 2013),

55. Schlessinger, J., Cell signaling by receptor tyrosine kinases. *Cell* **2000,** 103, (2), 211-25.

56. van der Geer, P.; Hunter, T.; Lindberg, R. A., Receptor protein-tyrosine kinases and their signal transduction pathways. *Annu Rev Cell Biol* **1994,** 10, 251-337.

57. Zwick, E.; Bange, J.; Ullrich, A., Receptor tyrosine kinase signalling as a target for cancer intervention strategies. *Endocr Relat Cancer* **2001,** 8, (3), 161-73.

58. Ullrich, A.; Schlessinger, J., Signal transduction by receptors with tyrosine kinase activity. *Cell* **1990,** 61, (2), 203-12.

59. Ullrich, A.; Coussens, L.; Hayflick, J. S.; Dull, T. J.; Gray, A.; Tam, A. W.; Lee, J.; Yarden, Y.; Libermann, T. A.; Schlessinger, J.; et al., Human epidermal growth factor receptor cDNA sequence and aberrant expression of the amplified gene in A431 epidermoid carcinoma cells. *Nature* **1984,** 309, (5967), 418-25.

60. Alroy, I.; Yarden, Y., The ErbB signaling network in embryogenesis and oncogenesis: signal diversification through combinatorial ligand-receptor interactions. *FEBS Lett* **1997,** 410, (1), 83-6.

61. Riese, D. J., 2nd; Stern, D. F., Specificity within the EGF family/ErbB receptor family signaling network. *Bioessays* **1998,** 20, (1), 41-8.

62. Burden, S.; Yarden, Y., Neuregulins and their receptors: a versatile signaling module in organogenesis and oncogenesis. *Neuron* **1997,** 18, (6), 847-55.

63. Cooper, O.; Vlotides, G.; Fukuoka, H.; Greene, M. I.; Melmed, S., Expression and function of ErbB receptors and ligands in the pituitary. *Endocr Relat Cancer* **2011,** 18, (6), R197-211.

64. Herbst, R. S., Review of epidermal growth factor receptor biology. *Int J Radiat Oncol Biol Phys* **2004,** 59, (2 Suppl), 21-6.

65. Arora, A.; Scholar, E. M., Role of tyrosine kinase inhibitors in cancer therapy. *J Pharmacol Exp Ther* **2005,** 315, (3), 971-9.

66. Harari, P. M., Epidermal growth factor receptor inhibition strategies in oncology. *Endocr Relat Cancer* **2004,** 11, (4), 689-708.

67. Carpenter, G.; Cohen, S., Epidermal growth factor. *Annu Rev Biochem* **1979,** 48, 193-216.

68. Salomon, D. S.; Brandt, R.; Ciardiello, F.; Normanno, N., Epidermal growth factor-related peptides and their receptors in human malignancies. *Crit Rev Oncol Hematol* **1995,** 19, (3), 183-232.

69. Franklin, W. A.; Veve, R.; Hirsch, F. R.; Helfrich, B. A.; Bunn, P. A., Jr., Epidermal growth factor receptor family in lung cancer and premalignancy. *Semin Oncol* **2002,** 29, (1 Suppl 4), 3-14.

70. Sequist, L. V.; Lynch, T. J., EGFR tyrosine kinase inhibitors in lung cancer: an evolving story. *Annu Rev Med* **2008,** 59, 429-42.

71. Paez, J. G.; Janne, P. A.; Lee, J. C.; Tracy, S.; Greulich, H.; Gabriel, S.; Herman, P.; Kaye, F. J.; Lindeman, N.; Boggon, T. J.; Naoki, K.; Sasaki, H.; Fujii, Y.; Eck, M. J.; Sellers, W. R.; Johnson, B. E.; Meyerson, M., EGFR mutations in lung cancer: correlation with clinical response to gefitinib therapy. *Science* **2004,** 304, (5676), 1497-500.

72. Pao, W.; Miller, V.; Zakowski, M.; Doherty, J.; Politi, K.; Sarkaria, I.; Singh, B.; Heelan, R.; Rusch, V.; Fulton, L.; Mardis, E.; Kupfer, D.; Wilson, R.; Kris, M.; Varmus, H., EGF receptor gene mutations are common in lung cancers from "never smokers" and are associated with sensitivity of tumors to gefitinib and erlotinib. *Proc Natl Acad Sci U S A* **2004,** 101, (36), 13306-11.

73. Sequist, L. V.; Bell, D. W.; Lynch, T. J.; Haber, D. A., Molecular predictors of response to epidermal growth factor receptor antagonists in non-small-cell lung cancer. *J Clin Oncol* **2007,** 25, (5), 587-95.

74. Pham, D.; Kris, M. G.; Riely, G. J.; Sarkaria, I. S.; McDonough, T.; Chuai, S.; Venkatraman, E. S.; Miller, V. A.; Ladanyi, M.; Pao, W.; Wilson, R. K.; Singh, B.; Rusch, V. W., Use of cigarette-smoking history to estimate the likelihood of mutations in epidermal growth factor receptor gene exons 19 and 21 in lung adenocarcinomas. *J Clin Oncol* **2006,** 24, (11), 1700-4.

75. Mitsudomi, T.; Kosaka, T.; Endoh, H.; Horio, Y.; Hida, T.; Mori, S.; Hatooka, S.; Shinoda, M.; Takahashi, T.; Yatabe, Y., Mutations of the epidermal growth factor receptor gene predict prolonged survival after gefitinib treatment in patients with non-small-cell lung cancer with postoperative recurrence. *J Clin Oncol* **2005,** 23, (11), 2513-20.

76. Shigematsu, H.; Lin, L.; Takahashi, T.; Nomura, M.; Suzuki, M.; Wistuba, II; Fong, K. M.; Lee, H.; Toyooka, S.; Shimizu, N.; Fujisawa, T.; Feng, Z.; Roth, J. A.; Herz, J.; Minna, J. D.; Gazdar, A. F., Clinical and biological features associated with epidermal growth factor receptor gene mutations in lung cancers. *J Natl Cancer Inst* **2005,** 97, (5), 339-46.

77. Ono, M.; Hirata, A.; Kometani, T.; Miyagawa, M.; Ueda, S.; Kinoshita, H.; Fujii, T.; Kuwano, M., Sensitivity to gefitinib (Iressa, ZD1839) in non-small cell lung cancer cell lines correlates with dependence on the epidermal growth factor (EGF) receptor/extracellular signal-regulated kinase 1/2 and EGF receptor/Akt pathway for proliferation. *Mol Cancer Ther* **2004,** 3, (4), 465-72.

78. Sordella, R.; Bell, D. W.; Haber, D. A.; Settleman, J., Gefitinib-sensitizing EGFR mutations in lung cancer activate anti-apoptotic pathways. *Science* **2004,** 305, (5687), 1163-7.

79. Lynch, T. J.; Bell, D. W.; Sordella, R.; Gurubhagavatula, S.; Okimoto, R. A.; Brannigan, B. W.; Harris, P. L.; Haserlat, S. M.; Supko, J. G.; Haluska, F. G.; Louis, D. N.; Christiani, D. C.; Settleman, J.; Haber, D. A., Activating mutations in the epidermal growth factor receptor underlying responsiveness of non-small-cell lung cancer to gefitinib. *N Engl J Med* **2004,** 350, (21), 2129-39.

80. Yun, C. H.; Boggon, T. J.; Li, Y.; Woo, M. S.; Greulich, H.; Meyerson, M.; Eck, M. J., Structures of lung cancer-derived EGFR mutants and inhibitor complexes:

mechanism of activation and insights into differential inhibitor sensitivity. *Cancer Cell* **2007,** 11, (3), 217-27.

81. Irmer, D.; Funk, J. O.; Blaukat, A., EGFR kinase domain mutations - functional impact and relevance for lung cancer therapy. *Oncogene* **2007,** 26, (39), 5693-701.

82. Kobayashi, S.; Boggon, T. J.; Dayaram, T.; Janne, P. A.; Kocher, O.; Meyerson, M.; Johnson, B. E.; Eck, M. J.; Tenen, D. G.; Halmos, B., EGFR mutation and resistance of non-small-cell lung cancer to gefitinib. *N Engl J Med* **2005,** 352, (8), 786-92.

83. Kosaka, T.; Yatabe, Y.; Endoh, H.; Yoshida, K.; Hida, T.; Tsuboi, M.; Tada, H.; Kuwano, H.; Mitsudomi, T., Analysis of epidermal growth factor receptor gene mutation in patients with non-small cell lung cancer and acquired resistance to gefitinib. *Clin Cancer Res* **2006,** 12, (19), 5764-9.

84. Weinstein, I. B., Cancer. Addiction to oncogenes--the Achilles heal of cancer. *Science* **2002,** 297, (5578), 63-4.

85. Weinstein, I. B.; Joe, A. K., Mechanisms of disease: Oncogene addiction--a rationale for molecular targeting in cancer therapy. *Nat Clin Pract Oncol* **2006,** 3, (8), 448-57.

86. Sharma, S. V.; Gajowniczek, P.; Way, I. P.; Lee, D. Y.; Jiang, J.; Yuza, Y.; Classon, M.; Haber, D. A.; Settleman, J., A common signaling cascade may underlie "addiction" to the Src, BCR-ABL, and EGF receptor oncogenes. *Cancer Cell* **2006,** 10, (5), 425-35.

87. Pao, W.; Miller, V. A.; Politi, K. A.; Riely, G. J.; Somwar, R.; Zakowski, M. F.; Kris, M. G.; Varmus, H., Acquired resistance of lung adenocarcinomas to gefitinib or erlotinib is associated with a second mutation in the EGFR kinase domain. *PLoS Med* **2005,** 2, (3), e73.

88. Carter, T. A.; Wodicka, L. M.; Shah, N. P.; Velasco, A. M.; Fabian, M. A.; Treiber, D. K.; Milanov, Z. V.; Atteridge, C. E.; Biggs, W. H., 3rd; Edeen, P. T.; Floyd, M.; Ford, J. M.; Grotzfeld, R. M.; Herrgard, S.; Insko, D. E.; Mehta, S. A.; Patel, H. K.; Pao, W.; Sawyers, C. L.; Varmus, H.; Zarrinkar, P. P.; Lockhart, D. J., Inhibition of drug-resistant mutants of ABL, KIT, and EGF receptor kinases. *Proc Natl Acad Sci U S A* **2005,** 102, (31), 11011-6.

89. Michalczyk, A.; Kluter, S.; Rode, H. B.; Simard, J. R.; Grutter, C.; Rabiller, M.; Rauh, D., Structural insights into how irreversible inhibitors can overcome drug resistance in EGFR. *Bioorg Med Chem* **2008,** 16, (7), 3482-8.

90. Stamos, J.; Sliwkowski, M. X.; Eigenbrot, C., Structure of the epidermal growth factor receptor kinase domain alone and in complex with a 4-anilinoquinazoline inhibitor. *J Biol Chem* **2002,** 277, (48), 46265-72.

91. Engelman, J. A.; Zejnullahu, K.; Mitsudomi, T.; Song, Y.; Hyland, C.; Park, J. O.; Lindeman, N.; Gale, C. M.; Zhao, X.; Christensen, J.; Kosaka, T.; Holmes, A. J.; Rogers, A. M.; Cappuzzo, F.; Mok, T.; Lee, C.; Johnson, B. E.; Cantley, L. C.; Janne, P. A., MET amplification leads to gefitinib resistance in lung cancer by activating ERBB3 signaling. *Science* **2007,** 316, (5827), 1039-43.

92. Camp, E. R.; Summy, J.; Bauer, T. W.; Liu, W.; Gallick, G. E.; Ellis, L. M., Molecular mechanisms of resistance to therapies targeting the epidermal growth factor receptor. *Clin Cancer Res* **2005,** 11, (1), 397-405.

93. Rubin, B. P.; Duensing, A., Mechanisms of resistance to small molecule kinase inhibition in the treatment of solid tumors. *Lab Invest* **2006,** 86, (10), 981-6.

94. Ennis, B. W.; Lippman, M. E.; Dickson, R. B., The EGF receptor system as a target for antitumor therapy. *Cancer Invest* **1991,** 9, (5), 553-62.

95. Kondapaka, S. B.; Fridman, R.; Reddy, K. B., Epidermal growth factor and amphiregulin up-regulate matrix metalloproteinase-9 (MMP-9) in human breast cancer cells. *Int J Cancer* **1997,** 70, (6), 722-6.

96. Herbst, R. S.; Langer, C. J., Epidermal growth factor receptors as a target for cancer treatment: the emerging role of IMC-C225 in the treatment of lung and head and neck cancers. *Semin Oncol* **2002,** 29, (1 Suppl 4), 27-36.

97. Ethier, S. P., Signal transduction pathways: the molecular basis for targeted therapies. *Semin Radiat Oncol* **2002,** 12, (3 Suppl 2), 3-10.

98. Fujino, S.; Enokibori, T.; Tezuka, N.; Asada, Y.; Inoue, S.; Kato, H.; Mori, A., A comparison of epidermal growth factor receptor levels and other prognostic parameters in non-small cell lung cancer. *Eur J Cancer* **1996,** 32A, (12), 2070-4.

99. Pavelic, K.; Banjac, Z.; Pavelic, J.; Spaventi, S., Evidence for a role of EGF receptor in the progression of human lung carcinoma. *Anticancer Res* **1993,** 13, (4), 1133-7.

100. Velu, T. J., Structure, function and transforming potential of the epidermal growth factor receptor. *Mol Cell Endocrinol* **1990,** 70, (3), 205-16.

101. Tang, C. K.; Gong, X. Q.; Moscatello, D. K.; Wong, A. J.; Lippman, M. E., Epidermal growth factor receptor vIII enhances tumorigenicity in human breast cancer. *Cancer Res* **2000,** 60, (11), 3081-7.

102. Hsieh, E. T.; Shepherd, F. A.; Tsao, M. S., Co-expression of epidermal growth factor receptor and transforming growth factor-alpha is independent of ras mutations in lung adenocarcinoma. *Lung Cancer* **2000,** 29, (2), 151-7.

103. Seth, D.; Shaw, K.; Jazayeri, J.; Leedman, P. J., Complex post-transcriptional regulation of EGF-receptor expression by EGF and TGF-alpha in human prostate cancer cells. *Br J Cancer* **1999,** 80, (5-6), 657-69.

104. Grandis, J. R.; Chakraborty, A.; Zeng, Q.; Melhem, M. F.; Tweardy, D. J., Downmodulation of TGF-alpha protein expression with antisense oligonucleotides inhibits proliferation of head and neck squamous carcinoma but not normal mucosal epithelial cells. *J Cell Biochem* **1998,** 69, (1), 55-62.

105. Gschwind, A.; Zwick, E.; Prenzel, N.; Leserer, M.; Ullrich, A., Cell communication networks: epidermal growth factor receptor transactivation as the paradigm for interreceptor signal transmission. *Oncogene* **2001,** 20, (13), 1594-600.

106. Prenzel, N.; Fischer, O. M.; Streit, S.; Hart, S.; Ullrich, A., The epidermal growth factor receptor family as a central element for cellular signal transduction and diversification. *Endocr Relat Cancer* **2001,** 8, (1), 11-31.

107. Huang, S. M.; Harari, P. M., Epidermal growth factor receptor inhibition in cancer therapy: biology, rationale and preliminary clinical results. *Invest New Drugs* **1999,** 17, (3), 259-69.

108. Overholser, J. P.; Prewett, M. C.; Hooper, A. T.; Waksal, H. W.; Hicklin, D. J., Epidermal growth factor receptor blockade by antibody IMC-C225 inhibits growth of a human pancreatic carcinoma xenograft in nude mice. *Cancer* **2000,** 89, (1), 74-82.

109. Prewett, M.; Rothman, M.; Waksal, H.; Feldman, M.; Bander, N. H.; Hicklin, D. J., Mouse-human chimeric anti-epidermal growth factor receptor antibody C225 inhibits the growth of human renal cell carcinoma xenografts in nude mice. *Clin Cancer Res* **1998,** 4, (12), 2957-66.

110. Levitzki, A., Tyrphostins: tyrosine kinase blockers as novel antiproliferative agents and dissectors of signal transduction. *FASEB J* **1992,** 6, (14), 3275-82.

111. Noonberg, S. B.; Benz, C. C., Tyrosine kinase inhibitors targeted to the epidermal growth factor receptor subfamily: role as anticancer agents. *Drugs* **2000,** 59, (4), 753-67.

112. Ciardiello, F.; Caputo, R.; Bianco, R.; Damiano, V.; Pomatico, G.; De Placido, S.; Bianco, A. R.; Tortora, G., Antitumor effect and potentiation of cytotoxic drugs activity in human cancer cells by ZD-1839 (Iressa), an epidermal growth factor receptor-selective tyrosine kinase inhibitor. *Clin Cancer Res* **2000,** 6, (5), 2053-63.

113. Pawar, V. G.; Sos, M. L.; Rode, H. B.; Rabiller, M.; Heynck, S.; van Otterlo, W. A.; Thomas, R. K.; Rauh, D., Synthesis and biological evaluation of 4-anilinoquinolines as potent inhibitors of epidermal growth factor receptor. *J Med Chem* **2010,** 53, (7), 2892-901.

114. Rewcastle, G. W.; Denny, W. A.; Bridges, A. J.; Zhou, H.; Cody, D. R.; McMichael, A.; Fry, D. W., Tyrosine kinase inhibitors. 5. Synthesis and structure-activity relationships for 4-[(phenylmethyl)amino]- and 4-(phenylamino)quinazolines as potent adenosine 5'-triphosphate binding site inhibitors of the tyrosine kinase domain of the epidermal growth factor receptor. *J Med Chem* **1995,** 38, (18), 3482-7.

115. Wissner, A.; Berger, D. M.; Boschelli, D. H.; Floyd, M. B., Jr.; Greenberger, L. M.; Gruber, B. C.; Johnson, B. D.; Mamuya, N.; Nilakantan, R.; Reich, M. F.; Shen, R.; Tsou, H. R.; Upeslacis, E.; Wang, Y. F.; Wu, B.; Ye, F.; Zhang, N., 4-Anilino-6,7-dialkoxyquinoline-3-carbonitrile inhibitors of epidermal growth factor receptor kinase and their bioisosteric relationship to the 4-anilino-6,7-dialkoxyquinazoline inhibitors. *J Med Chem* **2000,** 43, (17), 3244-56.

116. Wissner, A.; Mansour, T. S., The development of HKI-272 and related compounds for the treatment of cancer. *Arch Pharm (Weinheim)* **2008,** 341, (8), 465-77.

117. Kwak, E. L.; Sordella, R.; Bell, D. W.; Godin-Heymann, N.; Okimoto, R. A.; Brannigan, B. W.; Harris, P. L.; Driscoll, D. R.; Fidias, P.; Lynch, T. J.; Rabindran, S. K.; McGinnis, J. P.; Wissner, A.; Sharma, S. V.; Isselbacher, K. J.; Settleman, J.; Haber, D. A., Irreversible inhibitors of the EGF receptor may circumvent acquired resistance to gefitinib. *Proc Natl Acad Sci U S A* **2005,** 102, (21), 7665-70.

118. Sequist, L. V., Second-generation epidermal growth factor receptor tyrosine kinase inhibitors in non-small cell lung cancer. *Oncologist* **2007,** 12, (3), 325-30.

119. Xu, L.; Russu, W. A., Molecular docking and synthesis of novel quinazoline analogues as inhibitors of transcription factors NF-kappaB activation and their anti-cancer activities. *Bioorg Med Chem* **2013,** 21, (2), 540-6.

120. Hayden, M. S.; Ghosh, S., NF-kappaB in immunobiology. *Cell Res* **2011,** 21, (2), 223-44.

121. Kieran, M.; Blank, V.; Logeat, F.; Vandekerckhove, J.; Lottspeich, F.; Le Bail, O.; Urban, M. B.; Kourilsky, P.; Baeuerle, P. A.; Israel, A., The DNA binding subunit of NF-kappa B is identical to factor KBF1 and homologous to the rel oncogene product. *Cell* **1990,** 62, (5), 1007-18.

122. Baeuerle, P. A.; Baltimore, D., A 65-kappaD subunit of active NF-kappaB is required for inhibition of NF-kappaB by I kappaB. *Genes Dev* **1989,** 3, (11), 1689-98.

123. Tsai, K. C.; Teng, L. W.; Shao, Y. M.; Chen, Y. C.; Lee, Y. C.; Li, M.; Hsiao, N. W., The first pharmacophore model for potent NF-kappaB inhibitors. *Bioorg Med Chem Lett* **2009,** 19, (19), 5665-9.

124. Baeuerle, P. A.; Baltimore, D., I kappa B: a specific inhibitor of the NF-kappa B transcription factor. *Science* **1988,** 242, (4878), 540-6.

125. Alkalay, I.; Yaron, A.; Hatzubai, A.; Orian, A.; Ciechanover, A.; Ben-Neriah, Y., Stimulation-dependent I kappa B alpha phosphorylation marks the NF-kappa B inhibitor for degradation via the ubiquitin-proteasome pathway. *Proc Natl Acad Sci U S A* **1995,** 92, (23), 10599-603.

126. Berkowitz, B.; Huang, D. B.; Chen-Park, F. E.; Sigler, P. B.; Ghosh, G., The x-ray crystal structure of the NF-kappa B p50.p65 heterodimer bound to the interferon beta -kappa B site. *J Biol Chem* **2002,** 277, (27), 24694-700.

127. Brown, K.; Gerstberger, S.; Carlson, L.; Franzoso, G.; Siebenlist, U., Control of I kappa B-alpha proteolysis by site-specific, signal-induced phosphorylation. *Science* **1995,** 267, (5203), 1485-8.

128. Phelps, C. B.; Sengchanthalangsy, L. L.; Malek, S.; Ghosh, G., Mechanism of kappa B DNA binding by Rel/NF-kappa B dimers. *J Biol Chem* **2000,** 275, (32), 24392-9.

129. Scherer, D. C.; Brockman, J. A.; Chen, Z.; Maniatis, T.; Ballard, D. W., Signal-induced degradation of I kappa B alpha requires site-specific ubiquitination. *Proc Natl Acad Sci U S A* **1995,** 92, (24), 11259-63.

130. Van Antwerp, D. J.; Martin, S. J.; Kafri, T.; Green, D. R.; Verma, I. M., Suppression of TNF-alpha-induced apoptosis by NF-kappaB. *Science* **1996,** 274, (5288), 787-9.

131. Nishikori, M., Classical and Alternative NF-κB Activation Pathways and Their Roles in Lymphoid Malignancies. *Journal of Clinical and Experimental Hematopathology* **2005,** 45, (1), 15-24.

132. Bonizzi, G.; Karin, M., The two NF-kappaB activation pathways and their role in innate and adaptive immunity. *Trends Immunol* **2004,** 25, (6), 280-8.

133. Ghosh, S.; May, M. J.; Kopp, E. B., NF-kappa B and Rel proteins: evolutionarily conserved mediators of immune responses. *Annu Rev Immunol* **1998,** 16, 225-60.

134. Li, Q.; Verma, I. M., NF-kappaB regulation in the immune system. *Nat Rev Immunol* **2002,** 2, (10), 725-34.

135. Li, Q.; Yu, Y. Y.; Zhu, Z. G.; Ji, Y. B.; Zhang, Y.; Liu, B. Y.; Chen, X. H.; Lin, Y. Z., Effect of NF-kappaB constitutive activation on proliferation and apoptosis of gastric cancer cell lines. *Eur Surg Res* **2005,** 37, (2), 105-10.

136. Chen, X.; Kandasamy, K.; Srivastava, R. K., Differential roles of RelA (p65) and c-Rel subunits of nuclear factor kappa B in tumor necrosis factor-related apoptosis-inducing ligand signaling. *Cancer Res* **2003,** 63, (5), 1059-66.

137. Lin, A.; Karin, M., NF-kappaB in cancer: a marked target. *Semin Cancer Biol* **2003,** 13, (2), 107-14.

138. Sun, S. C.; Xiao, G., Deregulation of NF-kappaB and its upstream kinases in cancer. *Cancer Metastasis Rev* **2003,** 22, (4), 405-22.

139. Gilston, V.; Jones, H. W.; Soo, C. C.; Coumbe, A.; Blades, S.; Kaltschmidt, C.; Baeuerle, P. A.; Morris, C. J.; Blake, D. R.; Winyard, P. G., NF-kappa B activation in human knee-joint synovial tissue during the early stage of joint inflammation. *Biochem Soc Trans* **1997,** 25, (3), 518S.

140. Keates, S.; Hitti, Y. S.; Upton, M.; Kelly, C. P., Helicobacter pylori infection activates NF-kappa B in gastric epithelial cells. *Gastroenterology* **1997,** 113, (4), 1099-109.

141. Schwartz, M. D.; Moore, E. E.; Moore, F. A.; Shenkar, R.; Moine, P.; Haenel, J. B.; Abraham, E., Nuclear factor-kappa B is activated in alveolar macrophages from patients with acute respiratory distress syndrome. *Crit Care Med* **1996,** 24, (8), 1285-92.

142. Gilmore, T. D., Introduction to NF-kappaB: players, pathways, perspectives. *Oncogene* **2006,** 25, (51), 6680-4.

143. Karin, M., How NF-kappaB is activated: the role of the IkappaB kinase (IKK) complex. *Oncogene* **1999,** 18, (49), 6867-74.

144. Scheidereit, C., IkappaB kinase complexes: gateways to NF-kappaB activation and transcription. *Oncogene* **2006,** 25, (51), 6685-705.

145. Tergaonkar, V., NFkappaB pathway: a good signaling paradigm and therapeutic target. *Int J Biochem Cell Biol* **2006,** 38, (10), 1647-53.

146. Chen, Z. J., Ubiquitin signalling in the NF-kappaB pathway. *Nat Cell Biol* **2005,** 7, (8), 758-65.

147. Oeckinghaus, A.; Hayden, M. S.; Ghosh, S., Crosstalk in NF-kappaB signaling pathways. *Nat Immunol* **2011,** 12, (8), 695-708.

148. Hayden, M. S.; Ghosh, S., Signaling to NF-kappaB. *Genes Dev* **2004,** 18, (18), 2195-224.

149. Love, K. R.; Catic, A.; Schlieker, C.; Ploegh, H. L., Mechanisms, biology and inhibitors of deubiquitinating enzymes. *Nat Chem Biol* **2007,** 3, (11), 697-705.

150. Deng, L.; Wang, C.; Spencer, E.; Yang, L.; Braun, A.; You, J.; Slaughter, C.; Pickart, C.; Chen, Z. J., Activation of the IkappaB kinase complex by TRAF6 requires a dimeric ubiquitin-conjugating enzyme complex and a unique polyubiquitin chain. *Cell* **2000,** 103, (2), 351-61.

151. Wang, C.; Deng, L.; Hong, M.; Akkaraju, G. R.; Inoue, J.; Chen, Z. J., TAK1 is a ubiquitin-dependent kinase of MKK and IKK. *Nature* **2001,** 412, (6844), 346-51.

152. Wertz, I. E.; Dixit, V. M., Signaling to NF-kappaB: regulation by ubiquitination. *Cold Spring Harb Perspect Biol* **2010,** 2, (3), a003350.

153. Yang, J. M., Emerging roles of deubiquitinating enzymes in human cancer. *Acta Pharmacol Sin* **2007,** 28, (9), 1325-30.

154. Kowalski, J. R.; Juo, P., The role of deubiquitinating enzymes in synaptic function and nervous system diseases. *Neural Plast* **2012,** 2012, 892749.

155. Clague, M. J.; Coulson, J. M.; Urbe, S., Cellular functions of the DUBs. *J Cell Sci* **2012,** 125, (Pt 2), 277-86.

156. Hussain, S.; Zhang, Y.; Galardy, P. J., DUBs and cancer: the role of deubiquitinating enzymes as oncogenes, non-oncogenes and tumor suppressors. *Cell Cycle* **2009,** 8, (11), 1688-97.

157. Lipkowitz, S., The role of the ubiquitination-proteasome pathway in breast cancer: ubiquitin mediated degradation of growth factor receptors in the pathogenesis and treatment of cancer. *Breast Cancer Res* **2003,** 5, (1), 8-15.

158. Amit, S.; Ben-Neriah, Y., NF-kappaB activation in cancer: a challenge for ubiquitination- and proteasome-based therapeutic approach. *Semin Cancer Biol* **2003,** 13, (1), 15-28.

159. Oeckinghaus, A.; Ghosh, S., The NF-kappaB family of transcription factors and its regulation. *Cold Spring Harb Perspect Biol* **2009,** 1, (4), a000034.

160. Chen, F.; Castranova, V.; Shi, X.; Demers, L. M., New insights into the role of nuclear factor-kappaB, a ubiquitous transcription factor in the initiation of diseases. *Clin Chem* **1999,** 45, (1), 7-17.

161. Lim, J. W.; Kim, H.; Kim, K. H., Nuclear factor-kappaB regulates cyclooxygenase-2 expression and cell proliferation in human gastric cancer cells. *Lab Invest* **2001,** 81, (3), 349-60.

162. Suh, J.; Rabson, A. B., NF-kappaB activation in human prostate cancer: important mediator or epiphenomenon? *J Cell Biochem* **2004,** 91, (1), 100-17.

163. Wang, W.; Abbruzzese, J. L.; Evans, D. B.; Larry, L.; Cleary, K. R.; Chiao, P. J., The nuclear factor-kappa B RelA transcription factor is constitutively activated in human pancreatic adenocarcinoma cells. *Clin Cancer Res* **1999,** 5, (1), 119-27.

164. Karin, M.; Yamamoto, Y.; Wang, Q. M., The IKK NF-kappa B system: a treasure trove for drug development. *Nat Rev Drug Discov* **2004,** 3, (1), 17-26.

165. Karin, M.; Lin, A., NF-kappaB at the crossroads of life and death. *Nat Immunol* **2002,** 3, (3), 221-7.

166. Pommier, Y.; Sordet, O.; Antony, S.; Hayward, R. L.; Kohn, K. W., Apoptosis defects and chemotherapy resistance: molecular interaction maps and networks. *Oncogene* **2004,** 23, (16), 2934-49.

167. Yamamoto, Y.; Gaynor, R. B., Therapeutic potential of inhibition of the NF-kappaB pathway in the treatment of inflammation and cancer. *J Clin Invest* **2001,** 107, (2), 135-42.

168. Kobayashi, T.; Yoshimori, A.; Kino, K.; Komori, R.; Miyazawa, H.; Tanuma, S. I., A new small molecule that directly inhibits the DNA binding of NF-kappaB. *Bioorg Med Chem* **2009,** 17, (14), 5293-7.

169. Pande, V.; Sharma, R. K.; Inoue, J.; Otsuka, M.; Ramos, M. J., A molecular modeling study of inhibitors of nuclear factor kappa-B (p50)--DNA binding. *J Comput Aided Mol Des* **2003,** 17, (12), 825-36.

170. Tobe, M.; Isobe, Y.; Tomizawa, H.; Nagasaki, T.; Takahashi, H.; Fukazawa, T.; Hayashi, H., Discovery of quinazolines as a novel structural class of potent inhibitors of NF-kappa B activation. *Bioorg Med Chem* **2003,** 11, (3), 383-91.

171. Adams, J.; Stein, R.; James, A. B., Chapter 28. Novel Inhibitors of the Proteasome and Their Therapeutic Use in Inflammation. In *Annual Reports in Medicinal Chemistry*, Academic Press: 1996; Vol. Volume 31, pp 279-288.

172. Fiedler, M. A.; Wernke-Dollries, K.; Stark, J. M., Inhibition of TNF-alpha-induced NF-kappaB activation and IL-8 release in A549 cells with the proteasome inhibitor MG-132. *Am J Respir Cell Mol Biol* **1998,** 19, (2), 259-68.

173. Pierce, J. W.; Schoenleber, R.; Jesmok, G.; Best, J.; Moore, S. A.; Collins, T.; Gerritsen, M. E., Novel inhibitors of cytokine-induced IkappaBalpha phosphorylation and endothelial cell adhesion molecule expression show anti-inflammatory effects in vivo. *J Biol Chem* **1997,** 272, (34), 21096-103.

174. Natarajan, K.; Singh, S.; Burke, T. R., Jr.; Grunberger, D.; Aggarwal, B. B., Caffeic acid phenethyl ester is a potent and specific inhibitor of activation of nuclear transcription factor NF-kappa B. *Proc Natl Acad Sci U S A* **1996,** 93, (17), 9090-5.

175. Lyss, G.; Knorre, A.; Schmidt, T. J.; Pahl, H. L.; Merfort, I., The anti-inflammatory sesquiterpene lactone helenalin inhibits the transcription factor NF-kappaB by directly targeting p65. *J Biol Chem* **1998,** 273, (50), 33508-16.

176. Rungeler, P.; Castro, V.; Mora, G.; Goren, N.; Vichnewski, W.; Pahl, H. L.; Merfort, I.; Schmidt, T. J., Inhibition of transcription factor NF-kappaB by sesquiterpene lactones: a proposed molecular mechanism of action. *Bioorg Med Chem* **1999,** 7, (11), 2343-52.

177. Zahorowska, B.; Crowe, P. J.; Yang, J. L., Combined therapies for cancer: a review of EGFR-targeted monotherapy and combination treatment with other drugs. *J Cancer Res Clin Oncol* **2009,** 135, (9), 1137-48.

178. Caraglia, M.; Tassone, P.; Marra, M.; Budillon, A.; Venuta, S.; Tagliaferri, P., Targeting Raf-kinase: molecular rationales and translational issues. *Ann Oncol* **2006,** 17 Suppl 7, vii124-7.

179. Yang, J. L.; Qu, X. J.; Russell, P. J.; Goldstein, D., Interferon-alpha promotes the anti-proliferative effect of gefitinib (ZD 1839) on human colon cancer cell lines. *Oncology* **2005,** 69, (3), 224-38.

180. Diao, Y.; Tian, X. H.; Huang, Y. L.; Chen, L. K.; Lin, X. N.; Zhuang, Z. W., Enhanced cancer therapy with the combination of EGFR and VEGFR-2 targeting in an orthotopic glioblastoma model. *J Chemother* **2010,** 22, (6), 407-12.

181. Quesada, A. R.; Medina, M. A.; Alba, E., Playing only one instrument may be not enough: limitations and future of the antiangiogenic treatment of cancer. *Bioessays* **2007,** 29, (11), 1159-68.

182. Xu, L.; Kikuchi, E.; Xu, C.; Ebi, H.; Ercan, D.; Cheng, K. A.; Padera, R.; Engelman, J. A.; Janne, P. A.; Shapiro, G. I.; Shimamura, T.; Wong, K. K., Combined EGFR/MET or EGFR/HSP90 inhibition is effective in the treatment of lung cancers codriven by mutant EGFR containing T790M and MET. *Cancer Res* **2012,** 72, (13), 3302-11.

183. Biswas, D. K.; Iglehart, J. D., Linkage between EGFR family receptors and nuclear factor kappaB (NF-kappaB) signaling in breast cancer. *J Cell Physiol* **2006,** 209, (3), 645-52.

184. Le Page, C.; Koumakpayi, I. H.; Lessard, L.; Saad, F.; Mes-Masson, A. M., Independent role of phosphoinositol-3-kinase (PI3K) and casein kinase II (CK-2) in EGFR and Her-2-mediated constitutive NF-kappaB activation in prostate cancer cells. *Prostate* **2005,** 65, (4), 306-15.

185. Le Page, C.; Koumakpayi, I. H.; Lessard, L.; Mes-Masson, A. M.; Saad, F., EGFR and Her-2 regulate the constitutive activation of NF-kappaB in PC-3 prostate cancer cells. *Prostate* **2005,** 65, (2), 130-40.

186. Galati, R., *The Role of Cyclooxygenase-2, Epidermal Growth Factor Receptor and Aromatase in Malignant Mesothelioma*. 2012.

187. El-Rayes, B. F.; Ali, S.; Ali, I. F.; Philip, P. A.; Abbruzzese, J.; Sarkar, F. H., Potentiation of the effect of erlotinib by genistein in pancreatic cancer: the role of Akt and nuclear factor-kappaB. *Cancer Res* **2006,** 66, (21), 10553-9.